Ph.D. CHEMISTRY

Allan David Adley

STEREOCHEMISTRY OF SOME GROUP IVb TETRAFLUORIDE ADDUCTS

ABSTRACT

$MF_4 \cdot 2L$ and $MF_4 \cdot LL$ adducts (M = Si, Ge and Sn) with various oxygen donors (e.g. lactams) and nitrogen donors (e.g. dipyridyl) were prepared and characterized. Molecular symmetries were assigned on the basis of infrared, Raman, ^{19}F NMR and ^{1}H NMR spectra. Solid state vibrational spectra of adducts with bidentate donors were interpreted in terms of the expected cis structure and this was confirmed by their ^{19}F spectra in chloroacetonitrile. For $MF_4 \cdot 2L$ adducts only tentative conclusions were made on the basis of solid state vibrational spectra, while ^{19}F NMR measurements in chloroacetonitrile indicated the presence of cis and trans isomers. On the basis of these physical measurements it was concluded that for $MF_4 \cdot 2L$ adducts: (1) the factors which determine stereochemistry in the solid state and solution are not necessarily the same, and (2) symmetry effects, steric factors, and π-bonding are not singularly effective in determining stereochemistry.

Stereochemistry of Some Group IVb Tetrafluoride Adducts

STEREOCHEMISTRY OF SOME GROUP IVb TETRAFLUORIDE ADDUCTS

by

Allan David Adley, B.Sc. (McGill) M.S. (Minnesota)

A thesis submitted to the Faculty of Graduate Studies and Research of McGill University in partial fulfilment of the requirements for the degree of Doctor of Philosophy

From the Inorganic Chemistry Laboratory
under the supervision of
Dr. M. Onyszchuk

McGill University
Montreal, Quebec.

November, 1970

ACKNOWLEDGEMENTS

The author wishes to thank Dr. M. Onyszchuk for his assistance and encouragement during the course of this work.

The author thanks Dr. D.F.R. Gilson for his assistance in recording the NMR spectra and for many valuable discussions on various aspects of this thesis. The author is grateful to Dr. I. Wharf for his help in interpreting certain infrared and NMR data.

The author wishes to thank the following members of the Chemistry Department at Sir George Williams University; Dr. R. Verschingel for the use of certain instruments within the department, Dr. P. Bird who provided X-ray data on the dipyridyl series, and Dr. T.J. Adley who did the mass spectral measurements.

The author is grateful to his colleagues at Dawson College for their consideration during the completion of this study.

The author thanks the Faculty of Graduate Studies and Research for a fellowship (1967-68).

To Nina, Allyson Sarah, Mom and Dad

ABBREVIATIONS

py	pyridine
Dipy	dipyridyl
HMPA	hexamethylphosphoramide
DMP	2,6-dimethyl-γ-pyrone
PYROL	pyrrolidinone
CAP	caprolactam
CAP-D	N-deuterated caprolactam
AZA-NON	azacyclononanone
AZA-NON-D	N-deuterated azacyclononanone
AZA-OCT	azacyclo-octanone
AZA-OCT-D	N-deuterated azacyclo-octanone
VAL	valerolactam
VAL-D	N-deuterated valerolactam
TMU	tetramethylurea
TMEN	tetramethylethylenediamine
ISOQ	Isoquinoline

TABLE OF CONTENTS

Table of Contents (cont'd.) page

Table of Contents (cont'd.)

Table of Contents (cont'd.)

Table of Contents (cont'd.)

INDEX OF TABLES

Index of Tables (cont'd.)

INDEX OF FIGURES

Index of Figures (cont'd.)

Index of Figures (cont'd.)

Index of Figures (cont'd.)

Index of Figures (cont'd.)

Index of Figures (cont'd.)

Index of Figures (cont'd.)

Index of Figures (cont'd.)

Index of Figures (cont'd.)

Index of Figures (cont'd.)

Index of Figures (cont'd.)

Index of Figures (cont'd.)

I. INTRODUCTION

Hundreds of co-ordination compounds of Group IV elements have been prepared and characterized. Of considerable interest are the six co-ordinate addition compounds of the metal tetrahalides which fall on the basis of stoichiometry metry into two categories:

(1) $MX_4 \cdot 2L$ in which M = Si, Ge, Sn or Ti;

X = F, Cl, Br or I;

(2) $MX_4 \cdot LL$ L = monodentate Lewis base;

LL = bidentate Lewis base.

Until recently little has been known about their structures and the thermodynamics of their formation. Beattie (1) has reviewed the literature up to the beginning of 1963 emphasizing the physical and chemical properties of co-ordination compounds of Si, Ge or Sn as well as their relative stability and stereochemistry. His main conclusions were:

1. The formation of co-ordination compounds by the tetrahalides of silicon, germanium and tin appear to follow the sequence of stability: Sn>>Ge>Si and F>Cl>Br>I.
2. The occurrence of cis-trans isomers can be interpreted in terms of steric effects and π-bonding. The latter involves the capacity of the lone pairs on the halogen or ligand to π-bond with the appropriate empty metal d-orbitals.
3. Reliable thermochemical data for the interaction of Group IVb tetrahalides with ligands are lacking.

These conclusions have become the basis of further

work and study by many investigators. Progress in this field of research has been rapid due mainly to the application of the following physical techniques:

(1) X-Ray Diffraction

(2) Dipole Moments

(3) Infrared and Raman Spectroscopy

(4) NMR Spectroscopy

(5) Mössbauer Spectroscopy.

The main object of this Introduction will be to illustrate how these measurements have been used to determine stereochemistry and bonding in octahedral Group IVb complexes: each is described separately in order to provide a background for the present work. A summary of the compounds, technique used, and the conclusion as to their structure is given in Appendix A.

X-Ray Diffraction

Three-dimensional X-ray diffraction measurements on single crystals represent one of the most powerful tools for obtaining information on crystal and molecular structure. Only a few adducts of Group IVb tetrahalides have so far been studied in detail by this method. These compounds and their structures are summarized below:

Compound	Structure	Reference
$SnCl_4 \cdot 2POCl_3$	Cis molecular	2
$SnCl_4 \cdot 2SeOCl_2$	" "	3
$SnCl_4 \cdot 2CH_3C{\equiv}N$	" "	4

Compound	Structure	Reference
$SnCl_4 \cdot 2DMSO$	Cis molecular	5
$SnCl_4 \cdot CN(CH_2)_3CN$	Cis polymeric	6
$SiF_4 \cdot 2py$	Trans molecular	7
$SiCl_4 \cdot 2py$	" "	7
$GeCl_4 \cdot 2py$	" "	8
$SnCl_4 \cdot 2py$	" "	9
$SnBr_4 \cdot 2py$	" "	9

It is interesting to note that $SiCl_4 \cdot 2py$, which was shown to be trans by X-ray (7), had been previously (10,11) thought to be cis on the basis of infrared and Raman spectroscopy.

Because of the difficulty in obtaining single crystals and the long time involved in the solution of structures, progress in this field has been slow. With the development of new techniques for growing crystals and the use of computers to facilitate calculations, rapid progress in this field is anticipated. X-ray diffraction measurements usually give unambiguous proof of molecular structure in the solid state, but not in the molten state or in solution, in which the molecular structure of a compound may or may not be different.

Dipole Moments

The dipole moment of polyatomic molecules can ideally

be obtained by the addition of the vectors of the individual bond moments. As a result, these moments can be helpful in distinguishing between cis and trans geometrical isomers of $MX_4 \cdot 2L$ in solution.

In his review of dipole moment measurements, Beattie (1) pointed out that because of the limited solubility of silicon and germanium tetrahalide complexes, most work has been on adducts of tin (IV) chloride. Brown and Kubota (12) studied the equilibrium interaction of $SnCl_4$ with benzonitrile using benzene as the solvent. They found that the 1:1 complex was the primary species present together with some 2:1. Dipole moment measurements on the latter were so uncertain that no conclusion could be drawn regarding its structure. As these authors and Beattie pointed out, the results and the interpretation of such data are of questionable value when one considers the following factors:

1. A six co-ordinate trans adduct of the type $MX_4 \cdot 2L$ could have an appreciable moment if L is not aligned ideally.
2. Dissociation of the addition compound can occur giving any one of a number of misleading effects.
3. The possibility that both cis and trans isomers can co-exist in solution.

More recently, Curran and Mullin (13) reported dipole moments for $(C_4H_9)_2SnX_2 \cdot L$ (X = Cl, Br or I; L = o-phenanthroline and dipyridyl) and compared them with moments calculated for trans and cis configurations of butyl groups:

Compound	μ* obs.	μ* calc. cis	μ* calc. trans
$(C_4H_9)_2SnCl_2 \cdot$o-phen.	11.3	10.2	11.6
$(C_4H_9)_2SnBr_2 \cdot$o-phen.	12.7	10.0	11.4
$(C_4H_9)_2SnI_2 \cdot$o-phen.	12.9	9.7	11.0

*in Debye units.

They concluded that the structures are trans, in accord with infrared results obtained on complexes of the type $R_2SnCl_2 \cdot$Dipy (R = CH_3, C_2H_5, C_4H_9) by Clark and Wilkins (14).

Nelson (15) used dipole moment measurements in benzene to show that six co-ordinate tin complexes of the type SnX_2L_2 (where X = Cl, Br or I and L was either the anion of acetylacetone or dibenzoylmethane) have a cis configuration. He confirmed this by studying their ^1H NMR spectra.

In their respective studies Curran and Mullins (13), and Nelson (15) neglected the possibility of non-ideal structures which might make their results misleading. Schlemper (16) studied the crystal and molecular structure of dimethyl tin bis(8-hydroxyquinolate). This compound was purposely chosen because of the dispute in the literature regarding the displacement of the methyl groups. The structure is a highly distorted octahedron with a C-Sn-C angle of 107.8°, very close to tetrahedral. In an infrared and NMR study Tanaka et al. (17), concluded that in dimethyl tin bis (kojato) the C-Sn-C angle is between tetrahedral and dihedral rather than linear as is generally found in similar compounds. They postulated a dis-

torted trans structure with the two Sn-C bonds inclined to the side where both C=O groups co-ordinate.

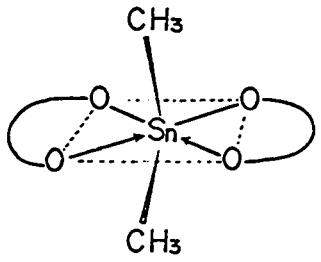

The distortion in these molecules illustrates the inherent danger in drawing firm conclusions from dipole moment measurements in hexaco-ordinate dialkyl systems.

Infrared and Raman Spectroscopy

The use of Infrared and Raman spectroscopy in correlating fundamental metal-halogen stretching and bending vibrations with molecular symmetry of $MX_4 \cdot 2L$ adducts has been recognized for some time (1). The octahedral 1:2 complexes may have a D_{4h} or C_{2v} symmetry, depending on whether the ligands are arranged trans or cis to each other. Based on group theoretical assignments the ideal trans 1:2 complexes are expected to have one infrared active and two Raman active M-X vibrations while the corresponding cis complexes are expected to have four infrared active and four Raman active M-X vibrations. With increased availability of infra-

red and Raman spectrometers capable of recording spectra at low wavenumbers, a combination of these measurements has become a powerful tool for examining stereochemistry, particularly for complexes of the non-transition elements where the lack of partially filled d-shells renders many other spectroscopic techniques inapplicable.

In their studies of the infrared spectra of $SnCl_4 \cdot 2L$ compounds (L = monodentate, oxygen or nitrogen Lewis base) Beattie and Rule (18) concluded that the adduct with acetone had a cis structure but as the ligands became more sterically hindered, as was the case with trimethylamine, ether, tetrahydrofuran and tetrahydrothiophen, the resulting complexes were trans. They also concluded that the adduct with tetramethylenediamine was bridged and not chelated.

Their results (19) using Raman spectroscopy on the same set of compounds were less revealing because of the weak intensity of certain modes. They concluded that on the basis of these measurements alone they would have made incorrect assignments. Beattie and his co-workers have also studied extensively (10,20) the infrared spectra of many silicon and germanium complexes and tentatively assigned structures on the basis of the number of M-X stretching bands observed:

Compound	Structure	Reference
$SiCl_4 \cdot 2py$	Cis	10
$SiBr_4 \cdot 2py$	Cis	10
$GeCl_4 \cdot 2py$	Trans	20

The danger in this approach was obvious when X-ray measurements (7) proved that crystalline $SiCl_4 \cdot 2py$ is trans molecular rather than cis as had been indicated by its infrared spectrum. Calculations (21) on cis- and trans-$SiX_4 \cdot 2L$, $GeCl_4 \cdot 2L$ and $SnCl_4 \cdot 2L$ suggest that in each of the trans isomers the single IR active ν(M-X) mode occurs in the same frequency region as three of the four IR active ν(M-X) modes of the corresponding cis compound.

Clark and Wilkins' (22) assignment of a cis structure for $SnBr_4 \cdot 2py$ and $SnCl_4 \cdot 2py$ on the basis of a vibrational analysis was later proved to be incorrect by Beattie et al. (9), whose single crystal X-ray analysis showed that both molecules are trans.

Fowles et al. (23), studied the Raman and infrared spectra of chelated adducts of $SnCl_4$ and TiX_4 (where X = Cl or Br) and had difficulty in assigning vibrational modes. They pointed out that the spectra may be simplified by the occurrence of accidental band degeneracies or one of these vibrational modes may give rise to bands of very low intensity which escape detection. In the case of $SnCl_4 \cdot 2py$ they assigned a trans structure on the basis of lack of infrared and Raman coincidences which is anticipated for a centrosymmetric structure. However the IR shows three assignable Sn-Cl modes (one is predicted for trans). One of the additional bands was rationalized in terms of solid state effects while the other was unexplained.

Although he had a similar difficulty in assigning

the Sn-X stretching vibrations Tanaka (24) postulated a cis structure for $SnX_4 \cdot 2DMSO$ where X = Cl, Br, or I and DMSO is dimethylsulphoxide. He was apparently unaware that an X-ray determination had shown that $SnCl_4 \cdot 2DMSO$ was cis (5). The IR of $(CH_3)_2SeO$ complexes with SnX_4 also indicated a cis formulation (24).

The infrared spectra of complexes of germanium tetraiodide and germanium tetrabromide with phenylhydrazine and p-nitrophenylhydrazine indicated that the compounds were six co-ordinated with an octahedral trans-configuration (25):

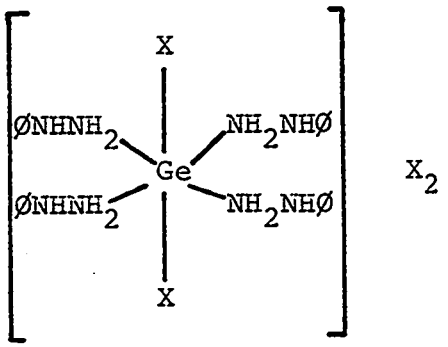

Haendler and Wilkins (26) studied the infrared spectra of a series of octahedral tin (IV) fluoride complexes with various ligands. They concluded that ligands having polarizable π-bond linkages at the co-ordinate site (e.g. $CH_3C{\equiv}N$, $CH_3\overset{\overset{O}{\|}}{C}CH_3$ or $(C_6H_5)_3P{=}O$) gave cis complexes but in all other cases the trans isomer is formed. Apparently, overlap of the π-bonding charge cloud with an empty d-orbital plays an important part in the linkage. Rivest and Jain (27) prepared a variety of TiX_4 and SnX_4 (X = Cl or Br) with such ligands as:

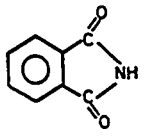

(L_A)

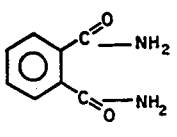

(L_B)

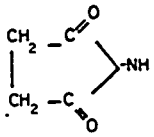

(L_C)

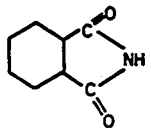

(L_D)

From their infrared spectra $2TiCl_4 \cdot L_A$ complexes were characterized as having co-ordination number six about titanium with bridging halide and the ligand acting as a bidentate donor co-ordinated to two metal atoms through the C=O groups. However, for the $MX_4 \cdot 2L_A$ (MX_4 = $TiBr_4$ and $SnCl_4$) complexes the ligand functions as a monodentate donor giving a cis structure. Compounds of the type $MX_4 \cdot L_B$ were found to be cis molecular with the ligand acting as a bidentate donor. $MX_4 \cdot L_C$ and $MX_4 \cdot L_D$ were believed to be cyclic polynuclear compounds in which the C=O groups co-ordinated to different metal atoms. Molecular weight and infrared studies on $SnBr_4 \cdot 2$(triphenylarsine) by Rivest et al. (28), indicated a trans structure while $SnCl_4 \cdot$triphenylphosphine was believed to be a dimer at high concentrations in methylene chloride (infrared evidence indicates bridging halide) which breaks into monomers at low concentrations.

Clark et al. (29), prepared a variety of the mixed-

halo species $MX_4Y_2^{2-}$ (M = Ti or Sn; X = Cl, Br or I) as the tetraethylammonium salts and examined their infrared and Raman spectra. They concluded that most and possibly all of the mixed anions possess the cis configuration in the solid state. The preponderance of the cis configuration over the more sterically favourable trans structure was suggested to be the result of π-donor ability of the halogens to the t_{2g} metal orbitals.

The far infrared spectra of some compounds of Group IV tetrahalides with 8-quinolinol, salicaldehyde, and acetylacetone have been studied by Douek et al. (30). Complexes were of the type MX_2OX_2, $MX_4 \cdot 2HOX$ and $MX_4 \cdot HOX$ (M = Ti, Zr, Ge or Sn; X = F, Cl, Br or I; HOX = 8-quinolinol etc.). Vibrational modes due to M-X stretching were assigned and suggestions made as to the likely stereochemistry of the complexes. However, due to the complexity of the spectra it was not possible to establish configurations unequivocally.

Douek et al. (30), recognized the limitations of correlating the number of infrared active bands with the disposition of metal-halogen bands (cis and trans). However, as these and other workers have pointed out, infrared measurements should ideally be made in dilute solutions, using a non-polar solvent to avoid intermolecular forces, or else the splitting of degenerate modes and/or activation of otherwise infrared inactive vibrations may occur, increasing the number of observed ν(M-X) absorptions. They note that even in solution, stereochemical assignments are not unequivocal because

ν(M-X) bands arising from a particular isomer may occur over a narrow frequency range, often separated by less than 15 cm^{-1} so that the actual number of ν(M-X) may be in doubt. Raman measurements including accurate polarization data are necessary together with infrared spectra in order to avoid ambiguities.

Crystal field effects (20) have been thought to be of significance in $BaSiF_6$ where a triply degenerate fundamental of the symmetrical SiF_6^{2-} is split into two peaks, due presumably to elongation of the octahedron along the three-fold axis causing a lowering of symmetry from O_h to D_{3d}. No such splitting was observed in K_2SiF_6 or $(NH_4)_2SiF_6$ (20). Beattie (1) has also questioned postulates on geometry based on vibrational band splitting associated with the ligand at the site of co-ordination. For example a single sulphoxide absorption band ν(S=O) in $SiF_4 \cdot 2DMSO$ and $GeF_4 \cdot 2DMSO$ has been taken to indicate a trans-formulation while in $SnF_4.2DMSO$ a splitting of this band suggested a cis structure. If the coupling of the two ligand molecules is weak for the cis molecule no splitting may be observed. Conversely solid state effects could cause splitting of a single band in a trans complex.

With the use of the laser as a light source, improved resolution of Raman spectra has been made feasible thereby enhancing the possibility of observing isotope splitting for totally symmetric vibrations. A different isotope splitting

would be anticipated (31) for the A_g and A_1 stretching mode of trans- and cis-$SiCl_4 \cdot 2py$, respectively, due to presence of ^{35}Cl and ^{37}Cl isotopes. The former would be predicted to split fivefold and the latter threefold. This could not be verified experimentally because of the intrinsic broadness of the absorptions (31).

Nuclear Magnetic Resonance Spectroscopy

A. ^{19}F NMR

^{19}F nuclear magnetic resonance spectroscopy was used by Muetterties (32) to study the stereochemistry of Group IV fluoride adducts involving a variety of mono- and bidentate ligands.

Differences in environment of fluorine nuclei caused by differences in bonding and geometry are revealed by this technique. Thus in the case of trans-$MF_4 \cdot 2L$, where all ^{19}F nuclei are equivalent, one resonance is expected, while in the case of cis-$MF_4 \cdot 2L$ where there are two pairs of ^{19}F nuclei having different environments, spin-spin splitting causes two triplet resonances. The ^{19}F spectra of all the SiF_4 and GeF_4 complexes studied by Muetterties (32) consisted of single resonances from the freezing point of the solution to well above room temperature. Although these results were inconclusive since the absence of fine structure could be the result of fast ligand exchange, Muetterties concluded that SiF_4 and GeF_4

have a lesser tendency than SnF_4 to expand their valence shell. If this were true, one would anticipate easy dissociation of $SiF_4 \cdot 2L$ and $GeF_4 \cdot 2L$ complexes for which Muetterties obtained no evidence.

Solutions of SnF_4 complexes in ethers, nitriles or excess base were studied by Muetterties from +15° down to the freezing point and the spectra consisted of two resonances of approximately equal intensity each of which was split into a triplet. He concluded that the cis isomer was the only structure consistent with this result. Molecular models (type not indicated) of the compounds showed no significant differences in terms of steric repulsions for the cis and trans arrangements. No details were given of chemical shifts, metal-fluorine or fluorine-fluorine coupling constants for any of the Si, Ge or Sn complexes.

Ragsdale and Stewart (33) found that the ^{19}F spectrum of the stannic fluoride-ethanol complex consisted of an A_2B_2 multiplet which proves that the complex is cis octahedral. They also observed a single line resonance and assigned it to the trans-isomer. At 50° the cis and trans isomers were in approximately the same concentration, but as the temperature increased, the concentration of the trans isomer decreased.

Dean and Evans (34) characterized approximately 100 anions of the type $SnF_{6-n}X_n^{2-}$ where X was either a mono- or half a bidentate ligand. In many cases, geometrical isomerism was observed and was studied closely for $SnF_4X_2^{2-}$, $SnF_3X_3^{2-}$ and

$SnF_2X_4^{2-}$ systems. Of particular significance was the observation that the equilibrium constant for the cis to trans ratio did not vary in the series $SnF_4X_2^{2-}$ where X = Cl, Br or I, confirming Muetterties (32) previous ideas that ligand repulsion was not of great significance.

Downing and Ragsdale (35) studied complexes of TiF_4 with substituted pyridines such as 4-methyl-, 2-methyl-, 2,6-dimethyl-, 3-chloro-, 2-chloro-, 3-bromo- and 2-bromo-pyridine. Of these only the 2-chloro and 2-bromo were soluble upon addition to a TiF_4-dimethoxyethane solution. The others were insoluble in a wide range of solvents. Each of the two complexes gave a F^{19} NMR consisting of two triplets indicating a cis configuration. This result was rationalized in terms of the π-acceptor ability of the pyridine which would in turn strengthen the Ti-F bond.

For the case of $TiF_4 \cdot 2EtOH$ (32,36) evidence has been found for only the cis structure whereas for $SnF_4 \cdot 2EtOH$ (33) both isomers were found. The latter was explained (37) in terms of reduced dπ-pπ interaction for tin because it has a d^{10} electronic configuration. Recognizing that steric factors might be involved, Dyer and Ragsdale (38) also studied the ^{19}F NMR spectra for a series of TiF_4-substituted pyridine-N-oxide adducts. The results can be summarized as follows:

Complex	Isomer
$TiF_4 \cdot 2C_5H_5NO$	Cis
$TiF_4 \cdot 2(2\text{-}CH_3C_5H_4NO)$	Cis and Trans
$TiF_4 \cdot 2[2,6(CH_3)_2C_5H_3NO]$	Trans

Ragsdale and Dyer (37) proposed that trans-$TiF_4 \cdot 2L$ were only formed when there was sufficient steric interaction to overcome symmetry effects and the tendency to maximize π-bonding. In the case of the last complex molecular models (Fischer-Hirschfelder-Taylor) indicated considerable steric-hindrance between the methyl groups and the fluorines. In turn this would cause steric interaction between the fluorines themselves which could only be relieved by isomerization to the trans structure. Their models also indicated that the donor molecules did not interact with each other in the equilibrium configuration and therefore donor induced repulsions between the fluorines in the cis isomer caused formation of the trans isomer. Steric repulsions between the fluorines, if present, would be expected to favour the trans configuration. If one considered only nearest neighbour interactions there are five such F-F repulsions in a cis but only four for a trans complex.

The importance of symmetry effects was also recognized. The symmetry for an $MF_4 \cdot 2L$ complex is higher for the trans isomer than for the cis isomer, so that

$$\underline{\text{Trans}}\text{-}MF_4 \cdot 2L \rightleftarrows \underline{\text{Cis}}\text{-}MF_4 \cdot 2L$$

in the absence of steric effects ΔF for the above equilibrium would be positive. Since $\Delta F = \Delta H - T\Delta S$, as the temperature is raised the equilibrium would be shifted to the right and ΔF would become more negative. This is in fact observed in the case of $SnF_4 \cdot 2EtOH$ where the concentration of the cis isomer

increased as the temperature was raised.

Dyer and Ragsdale (39) considered the significance of π-bonding in more detail by measuring the ^{19}F resonances of $TiF_4 \cdot DD'$ (D = substituted pyridine-1-oxide and D' = dimethylacetamide (DMA)). Their results were interpreted on the basis of changes in the fluorine π donation to the titanium d-orbitals which could result from competition between the pyridine-1-oxide donor oxygen and fluorine for the available d-orbitals of proper symmetry on the metal. The more O-N π-bonding that exists, the less successfully can the oxygen compete with fluorine for the available metal d-orbitals. As fluorine to titanium pπ-dπ donation increases, the F^{19} NMR signal shifts downfield. Changes in the shift of the F (identified as $F_{\beta'}$) trans to the <u>para</u>-substituted (identified as Z) pyridine-1-

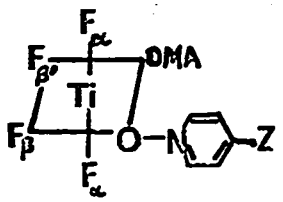

oxide were attributed to changes at Z which are transmitted through the conjugated π system as Z is varied from a strong

electron donor (CH_3O-) to a strong electron acceptor ($-NO_2$). This in turn would change in succession the N-O, Ti-O, Ti-F bonding interactions. The chemical shift for F_β, shows a 27 ppm change over this range. However, corresponding measurements were not made on complexes containing meta-substituted pyridine-1-oxides where changes in Z would not be transmitted to the oxygen through the π system as they are in the para-substituted case. Such measurements should provide a strong test of the π theory invoked by Ragsdale.

The existence of trans-TiF_4 [(tetramethylurea)(4-CH_3-C_5H_4NO)] when no trans-TiF_4 [(tetramethylurea)(4-$NO_2C_5H_4NO$)] could be found was rationalized as follows (37). A strongly basic ligand would have the effect of reducing π bonding between F and Ti so that a factor favouring a cis configuration would be lost.

B. ^1H Nuclear Magnetic Resonance

Proton nuclear magnetic resonance spectroscopy has also been used with some success in the study of isomerism in octahedral complexes. Bradley and Holloway (40,41) showed that $Ti(acac)_2X_2$ (where X was an alkoxy of varying complexity) adopted the cis configuration. The preference for this configuration was interpreted in terms of ligand to metal π-electron donation.

Similarly other workers showed that a number of structurally related dihalogeno-bis-(β-diketonato) derivatives $M(acac)_2X_2$ (M = Ge, Ti or Sn; X = F, Cl or Br) were also cis (42,

43,44,45). A reinvestigation of dichloro-bis(β-diketonato) germanium complexes using ^1H NMR showed that both cis and trans isomers were present (46). Only the dimethyl derivatives $Me_2Sn(acac)_2$ (47) and $Me_2Pb(acac)_2$ (48) have been found in the trans configuration, whilst $Si(acac)_2(OAc)_2$ (49) appears to be trans in the solid state but slowly converts to cis in solution. Two independent workers have thus shown the value of NMR in establishing differences in protonic environment for cis and trans formulations. For the case of $Si(acac)_2(OAc)_2$, the authors (44) proposed that the isomerization in solution reflected the higher dipole moment of the cis isomer. They considered that the fairly polar solvents used would tend to shift the cis-trans equilibrium toward the cis isomer. In contrast to this, Dean and Evans (34) reported that the cis-trans ratio for $SnF_4Cl_2^{2-}$ stayed approximately constant in $CHCl_3$, MeOH, $HCNH_2$ (O) and as a result they concluded that solvent effects were not very important.

Tobias and McGrady (47) have summarized the proton spectra of acetylacetonato complexes involving C, Si and Sn. In $CDCl_3$ the signal for hydrogen on the central carbon appears at δ = 5.24 ppm in $Me_2Sn(acac)_2$ and at δ = 5.38 ppm for $\emptyset_2Sn(acac)_2$. In $Si(acac)_3[HCl_2]$, where appreciable π bonding would be anticipated, δ = 6.26 ppm was observed.

C. ^{29}Si and ^{119}Sn Nuclear Magnetic Resonance

Recently Hunter and Reeves (50) have studied the ^{29}Si NMR spectra of the series R_3SiX where R = CH_3 and

X = H, CH_3, I, Br, Cl. They postulated that the tetrahedral hybridization in this series is conserved and that the ^{29}Si chemical shift shows a linear dependence on the electronegativity of X. Abnormally large shifts to high field were observed when X = O, N or F and this added shielding was interpreted in terms of (p→d)π-bonding, but they were unable to estimate its magnitude. ^{119}Sn chemical shifts were also measured for $(CH_3)_3SnX$ and a gross linear dependence on the electronegativity was observed over the limited variation X = Sn, C, Br, Cl. Some shielding due to (p→d)π-bonding in the series $(n\text{-butyl})_nSnCl_{4-n}$ was suggested. Although they studied some equilibria of the type

$$Me_3SnX + D \rightleftarrows Me_3SnX{:}D,$$

the ^{119}Sn chemical shift observed was the time average of the complexed and free forms. No evidence was found for more than one ^{119}Sn resonance.

Mössbauer Spectroscopy

Mössbauer spectroscopy has recently been used in studies of octahedral tin complexes. The isomer shift obtained from the spectra can be related to changes in s-electron density at the tin nucleus while the quadrupole splitting is of interest because it is a measure of the deviation from cubic symmetry of the p and d electron distribution in the bonds to tin. Greenwood and Ruddick (51) studied a series of compounds which were classified into four main groups:

(1) SnX_6^{2-} where X = Cl, Br or I

(2) SnX_4L L = bidentate donor (neutral)

(3) SnX_2L_2 L = anionic bidentate donor such as acetylacetonate

(4) $(CH_3)_2SnL_2$ L is the same as above.

The most prominent feature of the results was the absence of quadrupole splitting from nearly all of the hexa-co-ordinate tin compounds even when the six atoms bonded to tin were not all the same, provided that all six had non-bonding p_π-electrons. As the authors pointed out, this is not unexpected for compounds containing SnX_6^{2-}, since these ions have cubic symmetry (O_h) and any electric field gradient arising from the non-symmetric distribution of cations in the lattice is expected to be small. Quadrupole splitting is only observed when one of the groups attached to the tin atom is of the alkyl type. Tin tetrafluoride seems to be anomalous - even though it exhibits O_h symmetry, it nevertheless is reported to give quadrupole splitting. The authors reasoned that the lack of quadrupole splitting for the cases where true O_h symmetry no longer exists can be rationalized in terms of the σ and π-bonding interactions. The coefficients involving the σ-bonding molecular orbitals appear to be averaged and differences in ligand electronegativity or radial bond distance do not lead to an electric field gradient at the tin atom which sees a true O_h array of σ bonding orbitals. Similarly, π interactions involving filled p_π-orbitals with

vacant 5d-orbitals on tin, do not cause sufficient deviation from O_h symmetry to produce a detectable electric field gradient at the tin nucleus. Only when some of the ligands have no p_π-electron density available for subsidiary π-bonding is a quadrupole interaction observed. Where doubt exists as to the co-ordination number of tin, Mössbauer spectroscopy has proved to be useful. For example the 1:1 adduct of tin (IV) chloride with 8-hydroxyquinoline had been considered to be pentaco-ordinate. Greenwood and Ruddick (51) pointed out that if this were true there would be a large quadrupole splitting. The absence of the latter led them to conclude that the compound is truly six co-ordinate. Also of interest are the two forms α- and β-$SnX_2(Ø_2PO)_2N$ where X = Br or Cl and the ligand is the anion of the weak acid $Ø_2P(O)\overset{H}{N}P(O)Ø_2$. The structural differences of these forms are not evident from their Mossbauer spectra. The similarity of their infrared spectra led Greenwood and Ruddick (51) to reject cis-trans isomerism and postulate a difference in degree of aggregation.

Drago et al. (52) have recently studied the Mössbauer spectra of Lewis base adducts with $(CH_3)_3SnCl$. The literature concerning π-bonding in tin adducts is reviewed in this paper. In independent studies of compounds such as $(alkyl)_3SnOC_6H_5$ and $(CH_3)_3Sn\overset{H}{N}-C_6H_5$ there was no evidence for (p→d)π-bonding. Consequently, the authors believe that Greenwood's and Ruddick's (51) interpretation of their Mössbauer data on tetrahedral Sn was inconsistent since it invoked large π-bonding effects.

Drago et al. correlated the quadrupole splitting with $J_{Sn^{119}-C-H}$ which led them to conclude that the splitting was due to an imbalance in the electron density in the p-orbitals. They postulated that a similar non-uniform electron distribution in octahedral complexes exists in the p_x, p_y and p_z orbitals causing the quadrupole splitting for the case when the metal is bound to carbon.

Parish and Platt (53) came to a similar conclusion for a range of substituted alkyl- and aryl-tin (IV) compounds with tetrahedral geometry.

$SnCl_4 \cdot 2L$ (54) complexes (L = mono- and bidentate oxygen-donor molecules of the type SO, SO_2, PO, CO) showed a larger quadrupole splitting than for similar complexes formed by nitrogen donors (51). X-ray data on some of these adducts was given to support the idea that this splitting was caused by a weak donor-acceptor bond or by steric hindrance due to bulky ligand groups. Either of these led to an imbalance of electrons in the orbitals around tin and a quadrupole splitting.

In contrast to this, Nelson (15) interpreted his results on the dipole moment and ^1H NMR spectra for SnX_2L_2 complexes (where L = acetylacetonate or dibenzoylmethanate; X = Cl, Br or I) as indicating that the tin halogen bonds were stronger than those of other six co-ordinate adducts because of enhanced (p→d)π-bonding.

Mullins and Curran (13,55) correlated dipole moment

measurements and quadrupole splitting values (ΔE_Q) obtained from Mössbauer spectra. The relatively small moments obtained for the phenanthroline (o-phen) and dipyridyl (Dipy) complexes of $(C_6H_5)_2Sn(NCS)_2$ indicate that the phenyl groups are cis in these complexes. The theoretical moments calculated when the NCS group are placed trans to each other gave values close to the experimental ones.

Recent calculations (56,57) have suggested that for compounds of the type R_2SnX_4 the quadrupole splitting for the trans isomer ΔE_Q(R trans) is approximately twice that for ΔE_Q(R cis). On this basis Curran et al. interpreted their quadrupole data on $\emptyset_2Sn(NCS)_2 \cdot$Dipy and $\emptyset_2Sn(NCS)_2 \cdot$(o-phen) in terms of a cis arrangement of the phenyl groups in agreement with solution dipole results. Contrasting this was the fact that dipole moment and Mössbauer measurements indicated that for $Bu_2Sn(NCS)_2 \cdot$(o-phen) and $Bu_2(NCS)_2 \cdot$Dipy the butyl groups were trans to each other. The authors could not give a reason for the difference. Mössbauer measurements alone indicated in $\emptyset_2SnCl_2 \cdot$(o-phen) and $\emptyset_2SnCl_2 \cdot$Dipy the phenyl groups were trans.

Zuckerman (58) has criticized the direct correlation of Mössbauer isomer shifts and ligand electronegativity (or % ionic character). He argues that changes in the density of electrons at the tin nucleus have been interpreted solely in terms of the 5s electrons and the effect of p, d or f electrons have been neglected. His results show that on oxidation

($Sn^{o} \rightarrow Sn^{+4}$) the isomer shift is also affected by:

1. A decrease in screening by the inner s electrons
2. The resultant shrinkage of the tin atom when electrons are lost from the valence shell.

The correlation is also criticized because of the unknown factor involved when (p→d)π-bonding occurs for tin. Because there is no evidence to suggest that such bonding varies directly with the electronegativity of the atoms, it is difficult to estimate the magnitude of this effect.

The series $[C_2H_5N]_2[SnX_4Y_2]$ (where X = Cl, Br or I; Y = F, Cl, Br or I) have been studied by Mössbauer spectroscopy (59). The isomer shift showed a linear decrease with increasing electronegativity (Mulliken electronegativity values) of the halides bonded to the tin. Therefore, suggest the authors, it is possible that separate contributions of the s, p, d electrons to the isomer shift are independently linear with halide electronegativities.

II. STATEMENT OF THE PROBLEM

The preceding survey of the literature reveals that although the ^{19}F NMR of titanium (IV) fluoride complexes (32, 35,36,34,38,39,60) have been studied intensively, little has been done on Group IVb metal tetrafluoride adducts. Although Muetterties (39) studied the ^{19}F spectra of several $MF_4 \cdot 2L$ complexes (M = Si, Ge or Sn), his results were vague and incomplete. No detailed information was given on chemical shifts, coupling constants or the particular solvent used to dissolve the complexes. In contrast to the report by Muetterties (32) that ^{19}F NMR spectra of tin tetrafluoride in organic bases always consisted of two triplets of equal intensity, indicating that only the cis isomer is present, Ragsdale and Stewart (33) obtained ^{19}F NMR data which proved that tin tetrafluoride in ethanol forms both the cis and trans isomers. Ragsdale et al. (34) also found evidence for cis- and trans-$TiF_4 \cdot 2$(tetramethylurea) while Muetterties indicated that only the cis isomer existed. In view of the questionable nature of Muetterties data, a more detailed examination of the ^{19}F NMR spectra of $MF_4 \cdot 2L$ (M = Si, Ge and Sn) was undertaken. It was anticipated that such measurements would also test tentative structural assignments that had been made on the basis of infrared measurements by Hickie (11) for $SiF_4 \cdot 2L$ and $GeF_4 \cdot 2L$ complexes and by Haendler and Wilkins (26) for $SnF_4 \cdot 2L$ complexes.

There is no information about the infrared spectra of $MF_4 \cdot 2L$ complexes in solution apparently because of the poor solubility of the complexes. The ligands previously used to co-ordinate Group IVb tetrafluorides were not always chosen to overcome this handicap. Accordingly, we chose to use ligands not only with strong co-ordinating ability but also with a large amount of organic character in the hope that their complexes would be soluble. A series of lactam donors with the formula 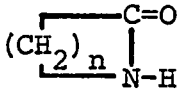 where n = 3, 4, 5, 6 and 7 satisfied these requirements. The Lewis base character of this ligand is enhanced by the ability of the lone electron pair on the nitrogen to delocalize into a π-molecular orbital involving oxygen, carbon and nitrogen:

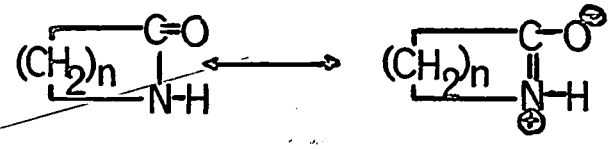

Similarly, 2,6 dimethyl-γ-pyrone (DMP), tetramethylurea (TMU) and hexamethylphosphoramide (HMPA) were chosen.

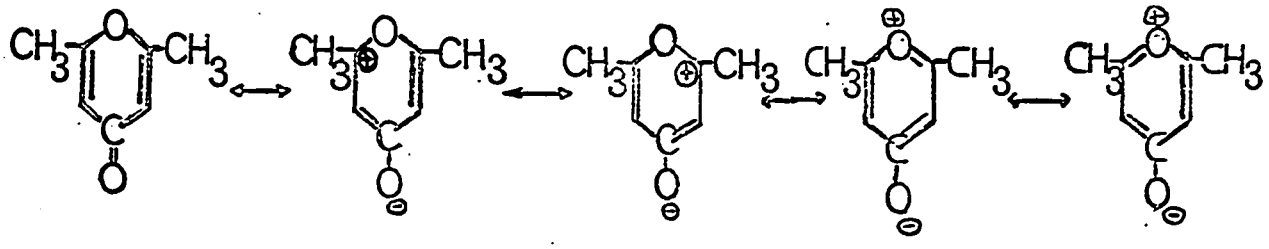

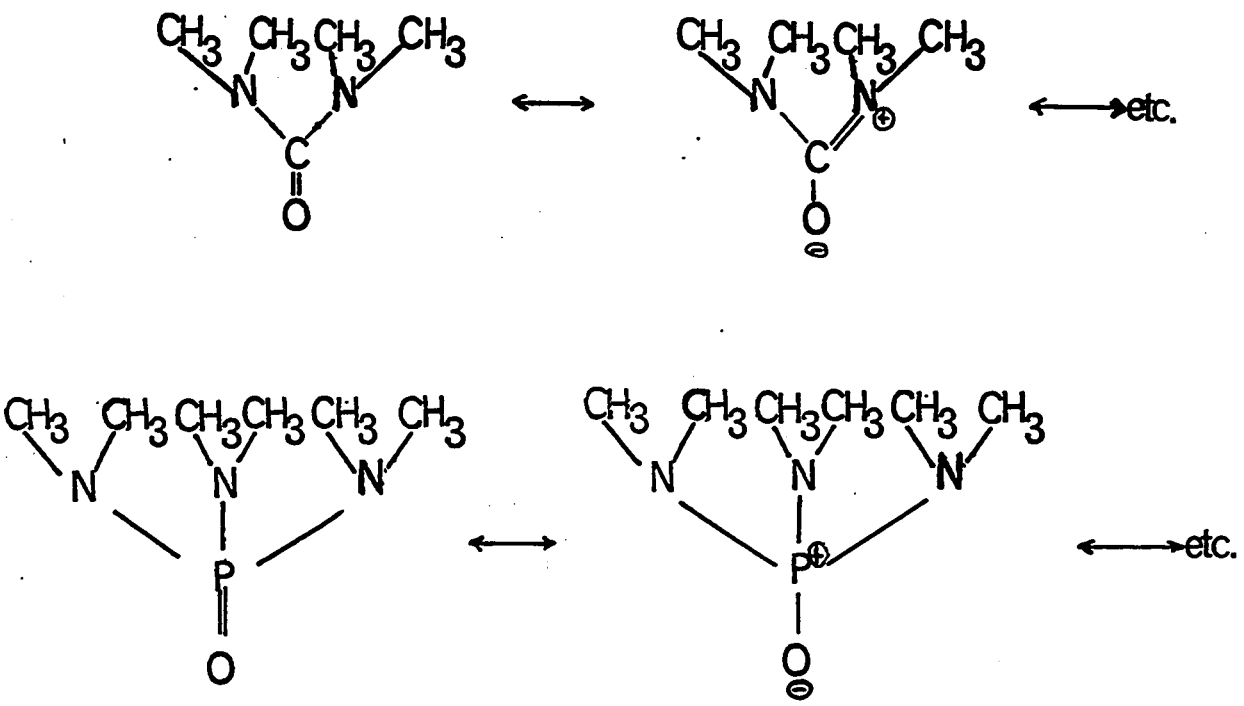

The main objects of this work were:

1. To prepare and characterize octahedral complexes of SiF_4, GeF_4 and SnF_4 with ligands chosen to enhance the solubility.
2. To study and compare the solid state and solution infrared and Raman spectra of $MF_4 \cdot 2L$ and $MF_4 \cdot LL$ complexes (M = Si, Ge and Sn; L = monodentate ligand, LL = bidentate ligand).
3. To measure ^{19}F and ^{1}H NMR spectra of $MF_4 \cdot 2L$ and $MF_4 \cdot LL$ complexes over as wide a temperature range as possible so as to define splitting patterns, chemical shifts, coupling constants and stereochemistry.

III. Experimental

III.A. Purification of Materials

In table 1, the sources, methods of purification, and purities of materials are listed.

III.B. Preparation of Complexes

III.B.1. Preparation of SiF_4 and GeF_4 Adducts

Silicon tetrafluoride and germanium tetrafluoride adducts (tables 2 and 3) were prepared as described by Guertin (70) and Hickie (11).

For the adducts $SiF_4 \cdot 2py$, $SiF_4 \cdot Dipy$, $SiF_4 \cdot TMEN$ and $SiF_4 \cdot 2HMPA$, approximately 2-3 g of each ligand was dissolved in 50 ml of CCl_4 and then SiF_4 was bubbled into the solution. The resulting precipitates were filtered in a glove bag under a nitrogen atmosphere. For the preparation of $SiF_4 \cdot 2CAP$, $SiF_4 \cdot 2AZA\text{-}NON$, $SiF_4 \cdot 2DMP$ and $SiF_4 \cdot 2PYROL$, the same amount of ligand was first dissolved in 5 ml of CH_2Cl_2 and then 50 ml of CCl_4 was added.

Adducts of GeF_4 were prepared by bubbling GeF_4 into solutions of the base (3-4 g) in CH_2Cl_2, CCl_4, or a mixture of the two as shown below:

100 ml CH_2Cl_2	33 ml CH_2Cl_2 + 67 ml CCl_4	100 ml CCl_4
$GeF_4 \cdot S_4N_4$	$GeF_4 \cdot CAP$	$GeF_4 \cdot 2HMPA$
$GeF_4 \cdot 2DMP$	$GeF_4 \cdot 2VAL$	$GeF_4 \cdot 2PYROL$
$GeF_4 \cdot 2AZA\text{-}OCT$	$GeF_4 \cdot 2AZA\text{-}NON$	
	$GeF_4 \cdot Dipy$	

$$\frac{33 \text{ ml } CH_2Cl_2 + 67 \text{ ml } CCl_4}{\begin{array}{l} GeF_4 \cdot 2py \\ GeF_4 \cdot TMEN \\ GeF_4 \cdot 2TMU \end{array}}$$

the precipitates obtained were treated just like the SiF_4 adducts. $GeF_4 \cdot 2CAP$ was prepared by heating $GeF_4 \cdot CAP$ *in vacuo* at 70°

III.B.2. Preparation of $GeF_4 \cdot 2L\text{-}D$ Adducts

Deuterated complexes of the type $GeF_4 \cdot 2$ 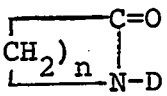 where n = 4, 5, 6 and 7, were prepared by dissolving the corresponding protonated species in D_2O. Each solution was evaporated to dryness on a vacuum line and the remaining solid was manipulated in a nitrogen filled glove bag. Although the isotopic purity of these complexes was not established the IR spectra showed strong absorptions in the region 2400 cm^{-1} due to ν(N-D) and only weak bands in the region 3300 cm^{-1} due to ν(N-H). A comparison of the mass spectrum of $GeF_4 \cdot 2CAP$ with that of the deuterated species confirmed that the identity of the latter was $GeF_4 \cdot 2CAP\text{-}D$. This series of complexes was prepared to assist in the assignment of bands in the IR spectra of lactam adducts.

III.B.3. Preparation of SnF_4 Adducts

The tin tetrafluoride complexes were prepared according to the procedure described by Haendler (26). All operations were carried out in a dry box under a nitrogen atmosphere. Approximately 1 g of tin tetrafluoride was added

Table 1. Purification of Materials

Compound	Source	Method of Purification	Purity Check
azacyclo-octanone	Aldrich	sublimed[A]	^{1}H NMR[B]
δ-valerolactam	Chemical Procurement		^{1}H NMR[B]
caprolactam	Eastman	recrystallized from CH_2Cl_2	IR (61), NMR (61)
azacyclononane	Chemical Procurement		^{1}H NMR[B]
2,6-dimethyl-γ-pyrone	Aldrich		IR (62)
pyridine	Eastman	fractional distillation from CaH_2, under vacuum	IR (63)
hexamethylphosphoramide	Eastman		IR (64)
pyrrolidinone	Aldrich		IR (65)
isoquinoline	Fisher		IR (11)
tetrahydrofuran	Fisher	fractional distillation from sodium and benzo-quinone, nitrogen atmosphere	B.P. 65° Lit. (71) 65-66°

[A]compound hygroscopic: handled in glove bag.

[B]assignment made by comparison with caprolactam.

(cont'd.)

Table 1 (cont'd.) - Purification of Materials

Compound	Source	Method of Purification	Purity Check
1,1,3,3-tetramethylurea	Aldrich	fractional distillation from CaH_2, nitrogen atmosphere	IR (66)
N,N,N',N'-tetramethyl-ethylenediamine	Eastman		B.P. 120° Lit. (71)120-122°
chloroacetonitrile	Eastman		B.P. 123° Lit. (71)124-126°
dipropylamine	Eastman		B.P. 109-110° Lit. (71)108-110°
methylene chloride	Fisher		B.P. 40-41° Lit. (71) 40-41°
carbon tetrachloride	Fisher		B.P. 77° Lit. (71) 76.8°
2,2'-dipyridyl	Fisher	used as received	IR (63,67,68)
tetrasulphur tetranitride	under-graduate preparation		IR (69)
silicon tetrafluoride	Matheson		-
germanium tetrafluoride	Ozark-Mahoning		-
tin tetrafluoride	Ozark-Mahoning		-
deuterium oxide	Merck, Sharp and Dohme		-

Table 2. Elemental Analyses of SiF_4 Adducts

		Elements present %				
		Si	F	C	H	N
$SiF_4 \cdot 2PYROL^C$	Calc.	7.97	21.57	47.71	4.59	10.21
	Found	7.74	19.70	46.16	4.91	-
			21.50	46.22	5.10	-
			21.63			
$SiF_4 \cdot 2CAP^{B,C}$	Calc.	8.50	23.00	43.61	6.72	8.48
	Found	-	20.14	41.23	6.82	-
			21.98	42.30	7.08	-
$SiF_4 \cdot 2AZA\text{-}NON^{B,C}$	Calc.	7.26	19.66	49.71	7.84	7.25
	Found	-	15.30	48.64	8.63	-
			15.80			
			16.94			
$SiF_4 \cdot 2HMPA^A$	Not analyzed					
$SiF_4 \cdot 2DMP^C$	Calc.	7.97	21.57	47.71	4.59	-
	Found	7.74	19.70	46.16	4.91	-
			21.50	46.22	5.10	-
			21.63			
$SiF_4 \cdot 2py^C$	Calc.	10.71	28.97	45.79	3.85	10.68
	Found	10.09	32.90	38.87	3.88	9.03
		9.50	28.94	41.88	4.88	
			28.64	36.47	3.87	
			28.67			
$SiF_4 \cdot Dipy$	Calc.	10.79	29.20	46.14	3.40	10.76
	Found	10.20	28.72	46.21	3.26	-
			27.70	46.18		
			29.01			
$SiF_4 \cdot TMEN^C$	Calc.	12.75	34.49	32.71	7.33	12.72
	Found		34.18	25.11	7.05	-
			35.09	26.80		

[A] decomposed rapidly

[B] decomposed slowly

[C] moisture sensitive

Table 3. Elemental Analyses of GeF_4 Adducts

		Elements present %				
		Ge	F	C	H	N
$GeF_4 \cdot 2PYROL$	Calc.	22.77	23.84	30.14	4.43	8.79
	Found	23.11	22.00	29.30	4.81	8.81
$GeF_4 \cdot 2VAL$	Calc.	20.93	21.91	34.62	5.24	8.08
	Found	18.35 20.63	22.30	35.45	5.76	8.42
$GeF_4 \cdot 2CAP$	Calc.	19.36	20.27	38.44	5.93	7.47
	Found	19.67	19.99	38.31	6.02	7.34
$GeF_4 \cdot 2AZA\text{-}OCT$	Calc.	18.01	18.86	41.72	6.52	6.95
	Found	20.65 18.14	18.24	40.96	6.40	6.63
$GeF_4 \cdot 2AZA\text{-}NON$	Calc.	16.84	17.63	44.58	7.03	6.50
	Found	15.87	18.42	43.95	7.10	6.72
$GeF_4 \cdot 2TMU$[C]	Calc.	19.05	19.95	31.53	6.36	14.71
	Found	19.48	19.86	31.05	6.43	-
$GeF_4 \cdot 2HMPA$[B,C]	Calc.	14.32	28.42	14.99	7.17	16.58
	Found	15.06	28.73	15.25	7.31	16.36 16.60
$GeF_4 \cdot 2DMP$	Calc.	18.29	19.15	42.36	4.07	-
	Found	18.30	19.05 19.15	42.65 39.32	3.98 4.38	-
$GeF_4 \cdot TMEN$[C]	Calc.	27.41	28.70	27.21	6.10	10.58
	Found	25.38	28.46	27.13	6.63	-
$GeF_4 \cdot Dipy$	Calc.	23.82	24.94	39.40	2.65	9.19
	Found	-	25.14	39.30	2.67	-

[B] decomposed slowly

[C] moisture sensitive

(cont'd.)

Table 3 (cont'd.) - Elemental Analyses of GeF_4 Adducts

		Elements present %					
		Ge	F	C	H	N	S
$GeF_4 \cdot CAP$[C]	Calc.	27.73	29.03	27.83	4.24	5.35	-
	Found	27.01	29.12	27.41	4.52	5.61	-
$GeF_4 \cdot S_4N_4$[B,C]	Calc.	21.81	22.83			16.83	38.53
	Found	23.01	22.56			15.82	35.00
						15.34	34.74
						15.31	30.97
						16.88	
$GeF_4 \cdot 2py$[C]	Calc.	23.66	24.77	39.14	3.39	9.13	
	Found	-	24.22	37.57	3.42	-	
				38.28	3.27		
$(CH_3CH_2CH_2NH_2)_2GeF_6$	Calc.	18.58	29.15	36.85	8.26	7.17	
	Found	18.82	27.40	37.11	8.29	7.33	

[B] decomposed slowly

[C] moisture sensitive

to 200 ml of tetrahydrofuran and the magnetically stirred solution was heated to boiling. The solution was filtered to remove undissolved SnF_4. The SnF_4-THF solution was then added to 2 g of ligand in 25 ml of THF. The resulting precipitate was filtered and dried. In the case of the HMPA complex it was necessary to evaporate the solution to approximately 10 ml before precipitation began.

III.B.4. Preparation of the Hexafluorometallates

Salts of the type $[(CH_3CH_2CH_2)_2NH_2]_2MF_6$ (M = Ge or Sn) were prepared according to a procedure described by Dean et al. (72)

$$2(CH_3CH_2CH_2)_2NH + (NH_4)_2MF_6 \rightarrow [(CH_3CH_2CH_2)_2NH_2]_2MF_6 + 2NH_3\uparrow$$

Dipropylamine was refluxed with the appropriate ammonium hexafluorometallate overnight. Excess amine was pumped off and the crude product was then dissolved in methanol and the unreacted $(NH_4)_2MF_6$ was removed by filtration. The complex was precipitated by adding an excess of ether.

III.C. Analyses

Analyses were performed by Schwartzkopf Microanalytical Laboratory of Woodside, New York. The results are summarized in Tables 2, 3 and 4.

III.D. Infrared and Raman Spectra

The infrared spectra of all solids were obtained

Table 4. Elemental Analyses of SnF_4 Adducts

		Elements present %				
		Sn	F	C	H	N
$SnF_4 \cdot 2PYROL$	Calc.	32.52	20.83	26.33	3.87	7.68
	Found	32.36	20.73	26.07	4.21	-
$SnF_4 \cdot 2CAP$	Calc.	28.19	18.05	34.23	5.28	6.65
	Found	28.10	17.91	33.84	5.27	-
$SnF_4 \cdot 2AZA\text{-}NON$	Calc.	24.87	15.93	40.27	6.35	5.87
	Found	24.55	16.04	40.05	6.40	-
$SnF_4 \cdot 2HMPA$[C]	Calc.	21.46	13.74	26.05	6.57	15.20
	Found	21.23	14.04	26.06	5.87	-
$SnF_4 \cdot 2DMP$	Calc.	26.79	17.16	37.96	3.65	-
	Found	27.15	17.04	37.95	3.70	-
$SnF_4 \cdot TMEN$[C]	Calc.	38.17	24.44	23.18	5.20	9.01
	Found	-	20.31	17.64	5.38	-
			24.04	17.96		
				18.07		
$SnF_4 \cdot Dipy$	Calc.	33.83	21.66	34.23	2.30	7.99
	Found	33.36	21.26	33.94	2.47	-
$SnF_4 \cdot 2py$[C]	Calc.	33.63	21.54	34.03	3.17	7.94
	Found	34.51	21.24	33.50	2.90	-
			22.06	29.78		
$SnF_4 \cdot 2ISOQ$[C]	Calc.	26.20	16.78	47.72	3.12	6.19
	Found	26.39	16.46	47.52	3.37	-
$(CH_3CH_2CH_2NH_2)_2SnF_6$	Calc.	27.15	26.08	32.97	7.39	6.41
	Found	-	24.45	33.27	7.52	-
			24.72			

[C] moisture sensitive

as Nujol mulls between cesium bromide or potassium bromide plates. The instrument used was a Perkin Elmer Model 521 dual grating infrared spectrometer. Spectra were run between 4,000 and 300 cm^{-1} Calibration of the instrument was checked using standard polystyrene film.

Spectra of the adducts in chloroacetonitrile solution were recorded using 0.1 mm cells on the Perkin Elmer Model 337 instrument. Solutions were prepared in a glove bag in a nitrogen atmosphere and were adjusted so that the concentration was 0.25 to 0.5 moles $l.^{-1}$

Raman spectra were recorded on a Cary 81 Raman spectrometer coupled to either a He-Ne or an argon ion laser. The spectra were recorded on solid samples in glass ampoules.

III.E. Nuclear Magnetic Resonance Measurements

^{19}F nuclear magnetic resonance spectra were obtained with a Varian 56.4 Mc high resolution spectrometer model 4311 equipped with variable temperature accessories. The spectra were calibrated in terms of displacements in Hz. from the fluorine resonance of trichlorofluoromethane (external). Calibration was accomplished by superimposing an audio frequency on the sweep field to produce side band peaks on the trichlorofluoromethane resonance. All shifts were calculated by means of the formula $\left[\frac{\nu_S - \nu_R}{\nu_o}\right]10^6$ where the quantity $(\nu_S - \nu_R)$ is the difference

between the resonance frequencies of the sample and reference and ν_o refers to constant probe frequency 56.4 Mc. employed for fluorine. All measurements proved to be to high field. In most cases six spectra were recorded for each complex and the average shift computed. Coupling constants generally showed some variation due to low solubility and a resulting low signal to noise ratio which made it difficult to assign the centre of peaks accurately. All complexes were studied as saturated solutions in chloroacetonitrile and were prepared in glove bags under a nitrogen atmosphere; the majority of the complexes had solubilities in the range 1 to 2 moles l^{-1}. $GeF_4 \cdot 2HMPA$ and $SnF_4 \cdot 2HMPA$ were soluble to the extent of 4 moles l^{-1}.

Proton NMR spectra were measured on a Varian A-60 high resolution spectrometer equipped with variable temperature accessories. The complexes were studied as saturated solutions in chloroacetonitrile and chemical shifts were measured with respect to internal tetramethylsilane (TMS).

III.F. Magnitude and Sources of Error

The magnitude and sources of error for the spectroscopic techniques used in this study are shown in Table 5.

Table 5. Magnitude and Sources of Error

No.	Measurement	Magnitude	Sources of Error
1.	^{19}F NMR		
	A. Chemical shift	Variable see Table E, Appendix	Variation in sweep rate Pen readability Calibration error
	B. Coupling constant		
2.	^{1}H NMR Chemical shift	$\pm$ 0.1 ppm	Pen readability Calibration error
3.	Infrared spectra		
	P.E. 521 (4,000-2,000 cm^{-1})	$\pm$ 5.0 cm^{-1}	Pen readability Calibration error
	" " (2,000-250 cm^{-1})	$\pm$ 2.0 cm^{-1}	
	P.E. 337 (700-400 cm^{-1})	$\pm$ 2.0 cm^{-1}	
4.	Raman spectra Cary 81	$\pm$ 1.0 cm^{-1}	Pen readability Calibration error

IV. Results and Interpretation.

A symmetry analysis for $MX_4 \cdot 2L$ appears in Appendix B. For each molecular geometry the number and type of metal-halogen stretching and bending vibrations are described. Subsequent discussion will be based on this description.

IV.A. Vibrational Spectra of Pyridine (py) Adducts

The infrared spectra of $SiF_4 \cdot 2py$, $GeF_4 \cdot 2py$, and $SnF_4 \cdot 2py$ (see figures 10 to 13, Appendix C and table 6) agree favourably with previous data (11,26,105,119) which were interpreted in terms of an idealized trans-D_{4h} symmetry. The assignments in table 6 are based on comparison with pyridine (63) and follow those previously reported (11,26,105,119).

IV.A.1. $SiF_4 \cdot 2py$

The results for $SiF_4 \cdot 2py$ must now be reinterpreted in the light of its recently reported crystal structure (7) and Raman spectrum (31). This complex, which is molecular with a centrosymmetric trans octahedral configuration, belongs to space group $P\bar{1}$ ($z = 1$). The factor group for this is C_i^1 and the site symmetry corresponds to C_i. Although the molecular symmetry is

Table 6. Infrared Spectra* of Pyridine Adducts

$SnF_4 \cdot 2py$		$GeF_4 \cdot 2py$		$SiF_4 \cdot 2py$		py		Assignment
ν, $cm.^{-1}$	Int.	ν, $cm.^{-1}$	Int.	ν, $cm.^{-1}$	Int.	ν, $cm.^{-1}$	Int.	
3055	w	3060	w	3240	w	3042	m	ν(C-H)
				3170	m	3070	s	
				3120	m	3050	s	
				3105	m	3020	s	
						2954	m	
						2930	m	
						2908	m	
Nujol		Nujol		Nujol		Nujol		ν(CC)
1611	s	1618	s	1630	sh	1585	sbr	
1580	w	1578	w	1617	s			
				1537	m			
1485	sh	1486	m	1484	s	1481	s	ν(CC,CN)
Nujol		Nujol		Nujol		1435	s,br	
						1372	w	
1340	w	1340	w	1341	w	1355	w	
1300	w	1305	w	1308	w	1290	w	
1250	w	1258	w	1251	m	1215	w	δ(C-H) in-plane
1202	m	1202	m	1205	s	1145	s	
1063	s	1159	w	1158	m	1066	s	
1047	m	1070	s	1109	w			
		1052	m	1100	w			
				1072	s			
				1051	m			

*Fundamental vibrational frequencies

(cont'd.)

Table 6 (cont'd.) - Infrared Spectra* of Pyridine Adducts

$SnF_4 \cdot 2py$		$GeF_4 \cdot 2py$		$SiF_4 \cdot 2py$		py		Assignment
ν, cm^{-1}	Int.	ν, cm^{-1}	Int.	ν, cm^{-1}	Int.	ν, cm^{-1}	Int.	
1018	m	1022	m	1021	m	1029	s	ring breathing and/or ν_{12} for py
1011	sh	1008	w	1002	w			
961	w	970	w	988	w	991	s	δ(C-H) out-of-plane
		950	w	967	m	939	w	
		888	w	950	sh	881	w	
				883	w			
				798	s			ν(M-F)
763	s	767	s	760	s	742	m	ϕ(CC)
Nujol		Nujol				698	m	
688	s	687	s	680	s			
650	s	657	s	657	s			α(CCC)
647	sh	652	m	649	sh			
				635	sh			ν(M-F)
		621	s					ν(M-F)
				607	w	602	w	X sens.
568	s							ν(M-F)
				485	s,br			δ(M-F)
430	m	454	m					X sens.
				388	m			ϕ(CC)
		328	sh					δ(M-F)
		315	s					
		305	sh					

*Fundamental vibrational frequencies

the same because there is only one molecule per unit cell the distortion from D_{2h} is only slight.

The correlation between the D_{2h} symmetry of the free molecule, the C_i site symmetry, and C_i^1 symmetry of the crystal given in table 7 shows that the number of infrared or Raman active bands does not change under these conditions:

Table 7. Correlation Between the Various Symmetries Associated with $SiF_4 \cdot 2py$

Molecular Symmetry	Site Symmetry	Factor Group
D_{2h}	C_i	C_i^1
$a_g(R)$	$a_g(R)$	$a_g(R)$
$b_{1g}(R)$		
$b_{2u}(IR)$	$a_u(IR)$	$a_u(IR)$
$b_{3u}(IR)$		

Two bands at 664 cm^{-1} and 656 cm^{-1} in the Raman spectrum of $SiF_4 \cdot 2py$ have been assigned respectively to the a_g and b_{1g} modes for D_{2h} (31). Although a weak ligand vibration appears in $GeF_4 \cdot 2py$ at 656 cm^{-1}, it is not observed in $SiF_4 \cdot 2py$ (31). Ozin made no assignments for the infrared active ν(Si-F) modes b_{2u} and b_{3u}. The strong band at 798 cm^{-1} (table 6) is definitely one of these and it is conceivable that the second band is the shoulder at 635 cm^{-1} in the same region as that of a ligand vibration. Thus the infrared and

Raman data are consistent with the near D_{2h} symmetry indicated by the X-ray data.

IV.A.2. $GeF_4 \cdot 2py$

The Raman active modes a_g and b_{1g} for $GeF_4 \cdot 2py$ are reported to occur at 658 cm^{-1} and 580 cm^{-1} respectively (31) in agreement with our spectrum (see figure 83, Appendix D). One IR active ν(Ge-F) occurs at 621 cm^{-1}, but the second one expected for D_{2h} cannot be assigned. It might be coincident with the ligand vibrations occurring at 652 and 657 $cm.^{-1}$ The three bands at 328, 315 and 305 cm^{-1} which appear in the region $\nu_4(t_{2u})$ for GeF_6^{2-}, are probably the in- and out-of-plane deformation modes b_{1u}, b_{2u}, b_{3u} for D_{2h} symmetry. Although the current infrared and Raman data for $GeF_4 \cdot 2py$ are not inconsistent with <u>trans</u>-D_{2h} symmetry, single crystal X-ray measurements are required to confirm its exact structure.

IV.A.3. $SnF_4 \cdot 2py$

The infrared spectrum of $SnF_4 \cdot 2py$ is practically the same as that of $GeF_4 \cdot 2py$ with the exception that only a single M-F stretch is found at 568 $cm.^{-1}$ The infrared data are thus consistent with a <u>trans</u> structure.

A recent X-ray study of $SnBr_4 \cdot 2py$ shows it to be trans (9); only gross features of the structure were given and since there is no information on the atomic co-ordinates

the exact molecular symmetry is not known. The factor group is C_{2h}^3 with z = 2 giving a site symmetry corresponding to C_{2h}. A normal co-ordinate analysis and IR investigation revealed two Sn-Br modes (9). This was rationalized in terms of splitting of the e type stretching mode in the idealized D_{4h} planar unit due to the presence of py ligands. Since four other bands have partial ν(Sn-Br) contributions, it would seem that the infrared results are too complex to be interpreted with such an over-simplification.

IV.B. Vibrational Spectra of Dipyridyl (Dipy) Adducts

The infrared spectra of the dipyridyl adducts of SiF_4, GeF_4 and SnF_4 (see figures 14 to 19, appendix C and table 8) and their Raman spectra (see figures 86 to 88, appendix D) agree favourably with earlier measurements (11, 26). Bands are assigned on the basis of comparisons with those of dipyridyl (63,73) and other adducts (14,67,68). Previous assignments (11,26) were based on a cis-C_{2v} symmetry without a knowledge of their crystal structure. Now that the following three-dimensional X-ray data are available (74), it is necessary to re-examine band assignments. Since the axial $\hat{FMF}$ angle is distorted from 180° in each case by only about 6 to 10°, the deviation from molecular symmetry C_{2v} is not significantly large.

The correlation between the C_{2v} symmetry of the free

Table 8. Infrared Spectra of Dipyridyl Adducts

SnF_4·Dipy		GeF_4·Dipy		SiF_4·Dipy		Dipy		Assignment
ν, cm^{-1}	Int.	ν, cm^{-1}	Int.	ν, cm^{-1}	Int.	ν, cm^{-1}	Int.	
3145	w	3150	sh	3138	m	3055	w	ν(C-H)
3122	w	3130	w	3118	w			
3080	m	3087	m	3102	m			
3073	sh			3080	m			
				3055	w			
Nujol		Nujol		Nujol		Nujol		
1613	m	1617	m					ν(CC)
1599	s	1603	s	1623	m	1584	m	
1574	w	1576	m	1613	s	1563	sh	
1567	w	1569	m	1580	m	1560	m	
1559	w	1558	w	1570	m	1548	sh	
1497	m	1500	m	1509	sh			
				1502	w			
Nujol		Nujol		Nujol		Nujol		
						1420	m	ν(CC,CN)
				1332	w			
1321†	m	1317†	m	1324†	m			

†Unassigned band which also appears in rare earth complexes (68).

(cont'd.)

Table 8 (cont'd.) - Infrared Spectra of Dipyridyl Adducts

SnF_4·Dipy		GeF_4·Dipy		SiF_4·Dipy		Dipy		Assignment
ν, cm^{-1}	Int.	ν, cm^{-1}	Int.	ν, cm^{-1}	Int.	ν, cm^{-1}	Int.	
1261	m	1272	w	1289	w	1252	m	δ(C-H) in-plane
1255	sh	1260	m	1257	m	1140	w	
1221	w	1182	w	1235	w	1092	m	
1188	w	1165	m	1200	w	1087	m	
1168	m	1110	w	1179	m	1066	w	
1108	w	1061	m	1165	s	1042	m	
1072	sh	1050	w	1131	w			
1062	m	1042	m	1116	w			
1048	sh			1096	w			
1041	w			1081	sh			
				1070	s			
				1054	m			
				1045	s			
				1035	m			
1025	m	1025	m	1025	m	997	sh	ring breathing
980	w	975	w	1015	sh	995	m	
				1005	w			
				918	w	897	w	unassigned
				850	w			
804	w	800	w					δ(C-H) out-of-plane
				802	s			ν(M-F)
				780	s			ν(M-F)

(cont'd.)

Table 8 (cont'd.) - Infrared Spectra of Dipyridyl Adducts

SnF_4·Dipy		GeF_4·Dipy		SiF_4·Dipy		Dipy		Assignment
ν, cm^{-1}	Int.	ν, cm^{-1}	Int.	ν, cm^{-1}	Int.	ν, cm^{-1}	Int.	
763	s	773	s	770	s	755	s	δ(C-H) out-of-plane
				748	s			ν(M-F)
728	m	744	w	738	s	740	m	δ(C-H) out-of-plane
		729	m					
668	m	670	m	651	w	655	m	α(CCC)
655	m	655	m	643	w	622	m	
				637	sh			
591		635	s	588	m			ν(M-F)
580		625	s					
570		610	s					
518		530	w					
				548	w			unassigned
				495	m			δ(M-F)

(cont'd.)

Table 8 (cont'd.) - Infrared Spectra of Dipyridyl Adducts

SnF_4·Dipy		GeF_4·Dipy		SiF_4·Dipy		Dipy		Assignment
ν, cm^{-1}	Int.	ν, cm^{-1}	Int.	ν, cm^{-1}	Int.	ν, cm^{-1}	Int.	
				458	s			X sens. δ(M-F)
				455	sh			
				429	m			
				424	sh			
				420	sh			
				395	m			
443	w	462	m			402	m	X sens. Ø(CC)
415	w	414	w					
				375	w			Unassigned
		375	sh					δ(M-F) Ø(CC)
		355	sh					
		335	sh					
		325	s,br					
				325	sh			ligand vib.
				305	sh			

Compound	Space Group	Factor Group	No. of Molecules per Unit Cell	Site Symmetry	Molecular Symmetry
SiF_4·Dipy	$P2_{1/c}$	C_{2h}^5	2	C_i	C_{2v}
GeF_4·Dipy	$P2_{1/m}$	C_{2h}^2	4	C_i	C_{2v}
SnF_4·Dipy	$P2_{1/c}$	C_{2h}^5	2	C_i	C_{2v}

molecule, the C_i site symmetry and the C_{2h}^x (x = 2 or 5) symmetry of the crystal is shown in table 9 together with spectroscopic activities. The factor group C_{2h}^x (x = 5 or 2) is isomorphous with the corresponding point group C_{2h}. It is apparent from the diagram that each mode in the free MF_4·Dipy molecule could be split into four in the crystal. However, if we consider only the IR stretching modes in the region of $a_{1g}(\nu_1)$ and t_{1u} for MF_6^{2-} (M=Si, Ge or Sn) there should be two and six stretches, respectively.

IV.B.1. <u>SiF_4·Dipy</u>

The solid state infrared and Raman spectra in the ν(Si-F) region for SiF_4·Dipy are compared in the following table:

SiF_4·Dipy (805-700 cm^{-1})

IR Solid State	Raman Solid State	Ligand IR Solid State
802 s	811 s	
780 s	777 s	
770 s		
748 s	748 m	755 s
738 s		740 m

Of the five infrared bands in the 805-700 cm^{-1} region two are probably ligand bands (11) leaving three to be correlated with $t_{1u}(\nu_3)$ for SiF_6^{2-}. The band corresponding to $a_{1g}(\nu_1)$ occurs at 588 cm^{-1}. Since only three bands appear in the region of t_{1u}, there is no evidence for correlation splitting in the solid state; this indicates that either the splitting is too small to be observed or that the correlation effects are negligible so that the IR results may be interpreted in terms of molecular geometry C_{2v}.

IV.B.2. GeF_4·Dipy

Comparison of vibrational spectra of GeF_4·Dipy in solid state and in $ClCH_2CN$ solution are shown in the following table:

Table 9. Correlation Between the Various Symmetries Associated with the $MF_4 \cdot$Dipy Molecule

Molecular Group	Site Group	Factor Group
C_{2v}	C_i	C_{2h}^5 or C_{2h}^2

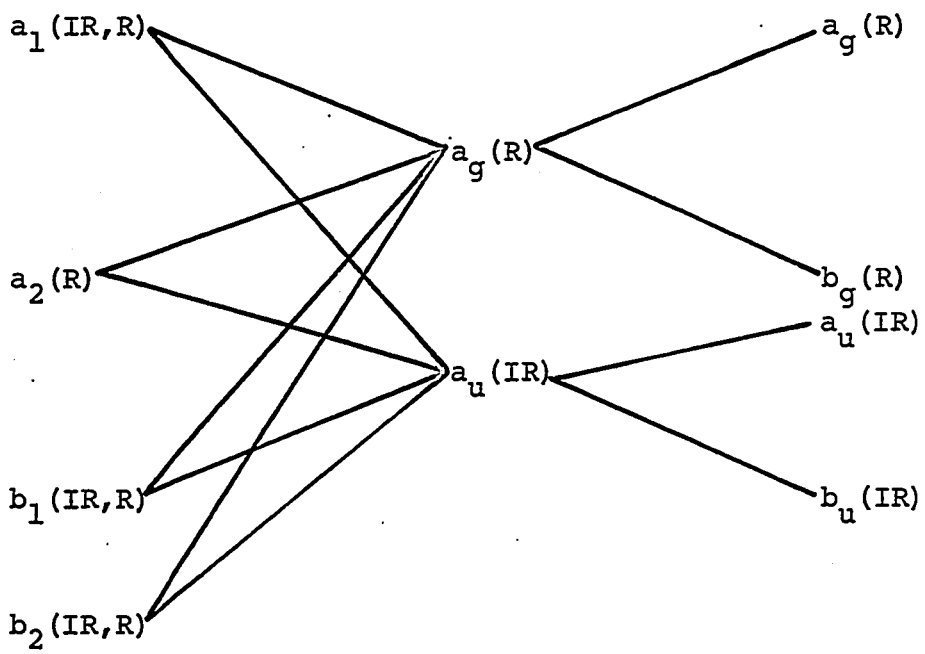

$GeF_4 \cdot Dipy$ (700-500 cm^{-1})

IR Solid State	Raman Solid State	IR Solution	Ligand IR Solid	Ligand IR Solution
670 m		672 s		
655 m		660 s	655 m	657 m
635 s	636 s	638 s		
625 s		625 sh	622 m	622 s
610 s				
530 w	534 m	538 w		

Although the ligand has a strong band at 622 cm^{-1} it does not appear in this region for $SiF_4 \cdot Dipy$ or $SnF_4 \cdot Dipy$ and so the three infrared bands in the region of 600 cm^{-1} are assigned to ν(Ge-F) and are correlated with $a_{1g}(\nu_1)$ and $t_{1u}(\nu_3)$ for GeF_6^{2-}.

The fourth band of type a_1 anticipated for C_{2v} is expected to be weak and should occur at a very much lower frequency than the other three. It is probably the band at 530 cm^{-1}. The bands at 670 and 655 cm^{-1} in $GeF_4 \cdot Dipy$ also occur in the same region for $SnF_4 \cdot Dipy$ and are therefore assigned to ligand vibrations.

The Raman spectrum of $GeF_4 \cdot Dipy$ shows a single peak at 636 cm^{-1}. Fluorides are poor scatterers and this combined with fluorescence of these compounds in the laser beam makes it impossible to detect the overlap of bands because of the resulting poor signal to noise ratio. Because there is no similar band in $SiF_4 \cdot Dipy$, the 636 cm^{-1} band is assigned to

ν(Ge-F). Since it is coincident with a Ge-F band in the IR, there does not appear to be a centre of symmetry.

The solution IR results are similar to the solid state results with one exception. The band at 610 cm^{-1} in the latter does not appear in the former. The band could be hidden in the broad solution band at 638 cm^{-1}. The IR and Raman data are consistent with a cis-C_{2v} molecular symmetry of the complex.

IV.B.3. $SnF_4 \cdot Dipy$

The results for $SnF_4 \cdot Dipy$ are summarized in the following table:

$SnF_4 \cdot Dipy$ (600-500 cm^{-1})

IR Solid State	Raman Solid State	Ligand IR Solid
591 s		
580 s	586 s	No bands in this region
570 s		
518 w	516 w	
	507 w	

The four bands between 600 and 500 cm^{-1} in the IR are assigned to ν(Sn-F). As in the case of $GeF_4 \cdot Dipy$, the Raman spectrum suggests that there is no centre of symmetry. Therefore, the results strongly point to a cis-

C_{2v} molecular structure.

IV.C. Vibrational Spectra of Hexamethylphosphoramide (HMPA) Adducts

Although transition metal and rare earth complexes of HMPA have been studied by various authors (75,76,77,78, 79) there are no previous reports of group (IV)b adducts with this ligand. Except for the assignment of the P=O stretching frequency, the infrared of these complexes have not been examined. Bands for $SiF_4 \cdot 2HMPA$, $GeF_4 \cdot 2HMPA$ and $SnF_4 \cdot 2HMPA$ (see spectra in figures 20 to 26, appendix C) are assigned in table 10 on the basis of comparisons with those of the pure ligand (64).

IV.C.1. $SiF_4 \cdot 2HMPA$

The poor crystallinity of $SiF_4 \cdot 2HMPA$ combined with its instability make a detailed analysis of its IR spectrum suspect. The P=O stretching frequency is lowered by 62 cm^{-1} relative to unco-ordinated HMPA, indicating that oxygen is the donor site of the ligand. The bands at 910 cm^{-1} and 870 cm^{-1} are assigned to Si-F stretches as no bands appear in this region for HMPA, $GeF_4 \cdot 2HMPA$ or $SnF_4 \cdot 2HMPA$. However, the broadness and complexity in the region 785-722 cm^{-1} when compared with the same region for the Sn and Ge complex suggest that there are additional ν(Si-F) modes besides the P-N stretching modes that normally occur in this region.

Table 10. Infrared Spectra of HMPA Adducts

$SnF_4 \cdot 2HMPA$		$GeF_4 \cdot 2HMPA$		$SiF_4 \cdot 2HMPA$		HMPA		Assignment
ν, cm^{-1}	Int.	ν, cm^{-1}	Int.	ν, cm^{-1}	Int.	ν, cm^{-1}	Int.	
Nujol		Nujol		Nujol		2990	s	$\nu(CH_3)$
						2875	s	
						2838	s	
						2795	s	
Nujol		Nujol		Nujol		1492	sh	$\delta(CH_3)$
						1483	s	
						1460	s	
						1440	sh	
1298	s	1297	s	1306	s	1292	s	CH_3 rocking
1193	m	1195	m	1188	s			
1165	m	1167	m	1165	s			
						1212	s	$\nu(P=O)$
						1170	s	CH_3 rocking
						1150	sh	
						1105	w	unassigned
1118	s	1127	s	1140	s			$\nu(P=O)$
1073	w	1075	m	1072	m	1067	m	$\nu(CN)$ anti-symmetric
1059	w	1059	m					

(cont'd.)

Table 10 (cont'd.) - Infrared Spectra of HMPA Adducts

$SnF_4 \cdot 2HMPA$		$GeF_4 \cdot 2HMPA$		$SiF_4 \cdot 2HMPA$		HMPA		Assignment
ν, cm^{-1}	Int.	ν, cm^{-1}	Int.	ν, cm^{-1}	Int.	ν, cm^{-1}	Int.	
985	s	990	s	996	s	980	s	ν(CN) symmetric
				910	s			ν(M-F)
				870	m			ν(M-F)
				785	sh			ν(P-N) ν(M-F)?
				760	s			
				742	s			
				722	s			
760	s	762	s			738	s	ν(P-N)
751	s	752	s					
720*	sh	720*	sh					
				640	m			ν(M-F)?
652	w	655	w			630	w	unassigned
633	w							
575	s	629	s					ν(M-F)
				500	sh			ν(M-F) + ligand vib.
				489	sh			
				478	m			

*Nujol

(cont'd.)

Table 10 (cont'd.) - Infrared Spectra of HMPA Adducts

$SnF_4 \cdot 2HMPA$		$GeF_4 \cdot 2HMPA$		$SiF_4 \cdot 2HMPA$		HMPA		Assignment
ν, cm	Int.	ν, cm	Int.	ν, cm	Int.	ν, cm	Int.	
529	w	534	m	436	s	481	s	ligand vib.
471	m	485	sh			375	w	
		475	m			345	w	
		412	w					
		389	w					
		313	sh					δ(M-F)
		303	s					
		278	sh					

The band at 640 cm^{-1} could be either a ν(Si-F) mode or ligand vibration. Thus the infrared spectrum is compatible with at least two completely different structures, trans-C_1 or cis-C_{2v}.

IV.C.2. $GeF_4 \cdot 2HMPA$

The infrared and Raman spectra in the ν(Ge-F) region of $GeF_4 \cdot 2HMPA$ are summarized in the table below:

$GeF_4 \cdot 2HMPA$ (700-500 cm^{-1})

IR Solid State	Raman Solid State	IR Solution	Ligand IR Solution	Ligand IR neat liquid
	657 s			
	637 m	632 s	632 w	630 w
629 s		600 m		
	587 s	582 sh		
534 m		547 w		
	524 m			

The P=O stretch in $GeF_4 \cdot 2HMPA$ showed a lowering of approximately 85 cm^{-1} compared to HMPA. The strong infrared band in the solid state at 629 cm^{-1} is assigned to ν(Ge-F). Although the assignments for the four Raman bands (see figure 89, appendix D) cannot be made, a comparison with the IR shows that a centre of symmetry probably exists and therefore the geometry is trans in the solid state. The

three bands assignable to ν(Ge-F) indicate a cis structure may be present in solution.

IV.C.3. $SnF_4 \cdot 2HMPA$

Infrared bands of $SnF_4 \cdot 2HMPA$ in the region of 650-500 cm^{-1} are compared in the table below:

$SnF_4 \cdot 2HMPA$ (650-500 cm^{-1})

IR Solid State	IR Solution	Ligand IR Solution	Ligand IR neat
		632 w	630 w
575 s	578 s		
	545 m		
529 w	532 w		

The phosphoryl stretching frequency changes by 94 cm^{-1} on co-ordination. The solid state spectrum of $SnF_4 \cdot 2HMPA$ is virtually the same as that of $GeF_4 \cdot 2HMPA$ except for the change in the lone M-F stretch which appears at 575 cm^{-1}. As in the case of solid $GeF_4 \cdot 2HMPA$, this is interpreted in terms of a trans geometry. The solution spectrum shows an additional band which might be an Sn-F stretch making it difficult to assign a structure.

The changes in the P=O frequency in the three complexes are summarized below. Transition metal complexes (76,77,78) show only 10 to 20 cm^{-1} shifts as do the rare earth complexes (75). Brown et al. (79), on the other hand,

	ν(P=O)	
HMPA	1212	Δν(P=O)
$SiF_4 \cdot 2HMPA$	1140	72
$GeF_4 \cdot 2HMPA$	1127	85
$SnF_4 \cdot 2HMPA$	1118	94

reported a ν(P=O) shift of 277 cm^{-1} for $NbCl_5 \cdot HMPA$. One possible explanation for this large difference is that in the former cases the metal centres have relatively low positive charge and partially or completely filled d-orbitals while in the latter case the Nb has a high positive charge and empty d-orbitals which might increase its acidic character. The ν(P=O) shifts observed in this work could be interpreted in terms of a Lewis acid order of SnF_4 > GeF_4 > SiF_4.

IV.D. Vibrational Spectra of 2,6-Dimethyl-γ-pyrone (DMP) Adducts

The assignment of bands in the infrared spectra of the complexes $SiF_4 \cdot 2DMP$, $GeF_4 \cdot 2DMP$ and $SnF_4 \cdot 2DMP$ (see figures 27 to 33 , appendix C) given in table 11 are based on Cook's (62) assignment for DMP and some of its complexes. DMP is considered to be a resonance hybrid of the following structures.

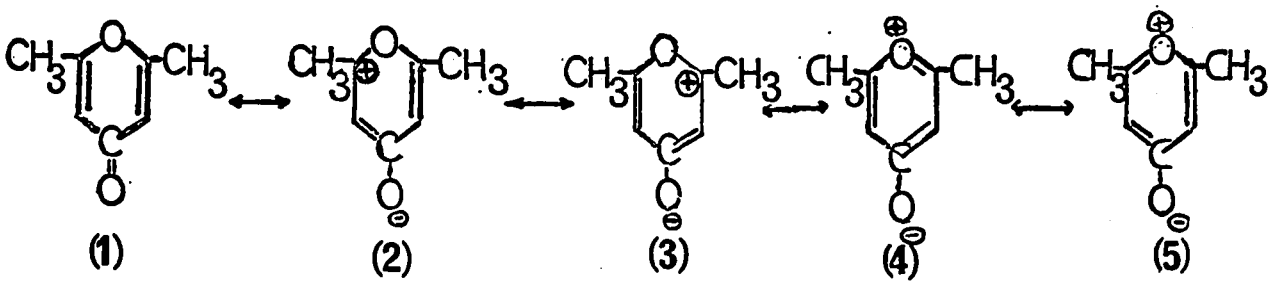

(1) (2) (3) (4) (5)

The carbonyl frequencies in $SiF_4 \cdot 2DMP$, $GeF_4 \cdot 2DMP$ and $SnF_4 \cdot 2DMP$ are lowered and split, parallelling Cook's observation in other Lewis acid-base complexes (62). This supports the idea that co-ordination enhances the contributions of structures (2) to (5).

IV.D.1. $SiF_4 \cdot 2DMP$

The solid state IR spectrum of $SiF_4 \cdot 2DMP$ shows three bands at 808, 800 and 655 cm^{-1} which are assigned to ν(Si-F) stretches based on comparisons with the Sn and Ge analogs. The Raman spectrum has no bands in the region 850-650 cm^{-1}. The infrared spectrum alone indicates the possibility of a cis structure.

Table 11. Infrared Spectra of DMP Adducts

$SnF_4 \cdot 2DMP$		$GeF_4 \cdot 2DMP$		$SiF_4 \cdot 2DMP$		DMP		Assignment
ν, cm^{-1}	Int.	ν, cm^{-1}	Int.	ν, cm^{-1}	Int.	ν, cm^{-1}	Int.	
3095	w	3195	w	3200	w	3060	w	ν(C-H)
3075	w	3142	m	3160	w	3045	w	
		3120	sh	3075	sh	3028	w	
		3055	m	3065	w			
		3035	sh	3030	w			
Nujol		Nujol		Nujol		Nujol		
1653	sh	1645	s	1652	s	1685	sh	ν(C=C)
1647	s			1639	sh	1670	sh	
						1665	s	
						1655	sh	
1558	s	1559	s	1567	s	1610	s	ν(C=O)
1507	s	1514	s	1562	sh	1596	s	
1497	sh	1497	sh	1542	sh			
1490	sh	1489	sh	1506	w			
				1493	w			
Nujol		Nujol		Nujol		Nujol		
		1432	m	1423	m			ν(C=O)
		1425	sh	1400	w			
		Nujol		Nujol				
1332	s	1335	s	1340	m	1338	m	ν(C=O)

(cont'd.)

Table 11 (cont'd.) - Infrared Spectra of DMP Adducts

$SnF_4 \cdot 2DMP$		$GeF_4 \cdot 2DMP$		$SiF_4 \cdot 2DMP$		DMP		Assignment
ν, cm	Int.	ν, cm	Int.	ν, cm	Int.	ν, cm	Int.	
1194	s	1196	s	1201	s	1193	m	δ(C-H)
1170	m	1171	m	1175	m	1159	s	
1032	m	1051	sh	1050	m	1035	m	
962	m	1042	m	1041	m	952	m	
		961	m	964	m			
913	s	915	s	920	s	933	m	γ(C-H)
887	s	885	s	900	sh	897	s	
		852	m	885	s	890	sh	
		800	w	859	s			
		765	w					unassigned
				808	s			ν(M-F)
				800	s			
		Nujol		Nujol		Nujol		
		637	s	655	m			ν(M-F) ligand vib.
				635	sh	620	w	
		585	m					ν(M-F)? ligand vib.?
		534	m					
636	m							ν(M-F) ligand vib.
586	s							
577	s							
565	m							
529	m							

(cont'd.)

Table 11 (cont'd.) - Infrared Spectra of DMP Adducts

$SnF_4 \cdot 2DMP$		$GeF_4 \cdot 2DMP$		$SiF_4 \cdot 2DMP$		DMP		Assignment
ν, cm^{-1}	Int.	ν, cm^{-1}	Int.	ν, cm^{-1}	Int.	ν, cm^{-1}	Int.	
				597	m			δ(M-F)
				545	m	537	m	ligand vib.
						510	w	
430	w	445	w	435	s			unassigned
		411	w					

IV.D.2. $GeF_4 \cdot 2DMP$

Solid state and solution spectra are summarized in the table below:

$GeF_4 \cdot 2DMP$ (700-500 cm^{-1})

IR Solid State	Ligand IR Solid State	IR Solution	Ligand IR Solution
637 s	620 w	638 s	
		622 s	605 w
		598 m	
585 m		580 m	
		550 w	555 w
534 m	537 m	533 w	
		525 w	525 m
	510 w		508 w

The solid state IR of $GeF_4 \cdot 2DMP$ shows a band at 637 cm^{-1} which is most probably a Ge-F stretching vibration. On the basis of a comparison with $SiF_4 \cdot 2DMP$, the two bands at 585 and 534 cm^{-1} might be ligand vibrations although one cannot preclude that they are due to ν(Ge-F). However, the solution IR shows four bands at 638, 622, 598 and 580 cm^{-1} which are probably ν(Ge-F). Thus while the solid state results are inconclusive, the solution spectra indicate the presence of a cis structure.

IV.D.3. $SnF_4 \cdot 2DMP$

A summary of infrared bands in the solid state and

solution spectra of $SnF_4 \cdot 2DMP$ is given below:

$SnF_4 \cdot 2DMP$ (700-500 cm^{-1})

IR Solid State	Ligand IR Solid State	IR Solution	Ligand IR Solution
636 m	620 w	639 m	
586 s		583 s	
577 s		568 s	
565 m		550 sh,m	555 w
529 m	537 m	532 m	525 m
	510 w		508 m

A comparison of the solid state IR spectrum of $SnF_4 \cdot 2DMP$ with that of $SiF_4 \cdot 2DMP$ indicates that of the five bands appearing in the 650-500 cm^{-1} region of the former, three could be ligand bands. A comparison of the solution IR for this compound with that of $GeF_4 \cdot 2DMP$ in solution indicates that the bands at 568, 550 and 532 are due to ν(Sn-F). Assignments for ν(M-F) in these complexes are uncertain because of interference by ligand vibrations. Thus while solid state results for $SnF_4 \cdot 2DMP$ are inconclusive, its spectrum in solution points to the presence of the cis isomer.

IV.E. Vibrational Spectra of Pyrrolidinone (PYROL) Adducts

Assignments for bands in the infrared spectra of

$SiF_4 \cdot 2PYROL$, $GeF_4 \cdot 2PYROL$ and $SnF_4 \cdot 2PYROL$ (see figures 34 to 40, appendix C) are given in table 12 on the basis of comparisons with spectra of pyrrolidinone and some of its Co(II) complexes (65).

The carbonyl stretching frequency at 1680 cm^{-1} in pyrrolidinone splits into two bands in $SiF_4 \cdot 2PYROL$, one of medium intensity at 1691 cm^{-1} and the other is a very strong broad band centred at 1642 cm^{-1}. This splitting might be due to the cis isomer or solid state effects. The lowering of the carbonyl frequency is attributed to co-ordination through oxygen thereby enhancing the contribution of structure (2):

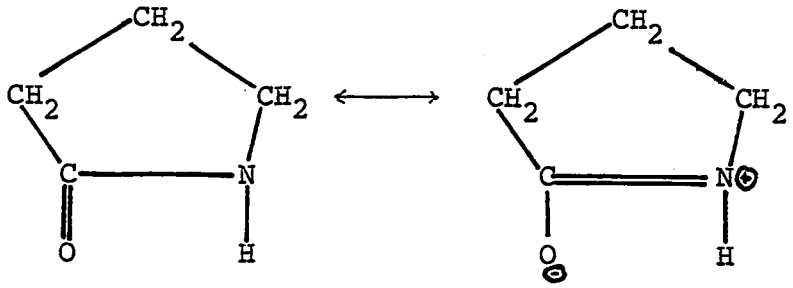

(1) (2)

The N-H stretch in pyrrolidinone appears at 3230 cm^{-1} and is assigned to a hydrogen bonded ν(N-H) frequency. By comparison the free ν(N-H) occurs at 3440 cm^{-1} (65). In $SiF_4 \cdot 2PYROL$, ν(N-H) appears at 3230 cm^{-1}. This lowering of ν(N-H) compared to the free ν(N-H) is attributed to increased contribution of resonance structure (2) when co-ordination occurs through oxygen. The shift may also be caused by inter- or intra-molecular hydrogen bonding.

Table 12. Infrared Spectra of PYROL Adducts

$SnF_4 \cdot 2PYROL$		$GeF_4 \cdot 2PRYOL$		$SiF_4 \cdot 2PYROL$		PYROL		Assignment
ν, cm^{-1}	Int.	ν, cm^{-1}	Int.	ν, cm^{-1}	Int.	ν, cm^{-1}	Int.	
3322 3235		3355		3383 3360 3180				ν(N-H)
						3230		ν(N-H) hydrogen bonded
Nujol		Nujol		Nujol		2960 2940		$\nu(CH_2)$
1670 1636	s s,br	1675 1652 1648 1637	sh sh sh s,br	1691 1642	m s,br	1680		ν(C=O)
1497 1490	sh	1490	m	1505 1495	sh m	1489 1459 1438	m s sh	(CH_2) sciss. δ(N-H)
Nujol 1423	m	Nujol 1423	m	Nujol		1430 1420	sh s	
Nujol		Nujol		Nujol				
1312	s	1308	s	1309	s	1375 1303	m sh	ν(CN)+ δ(NH)
						1285	s,br	ν(CN)

(cont'd.)

Table 12 (cont'd.) - Infrared Spectra of PYROL Adducts

$SnF_4 \cdot 2PYROL$		$GeF_4 \cdot 2PYROL$		$SiF_4 \cdot 2PYROL$		PYROL		Assignment
ν, cm	Int.	ν, cm	Int.	ν, cm	Int.	ν, cm	Int.	
1225	w	1225	w	1226	w	1265 1225	sh w	CH_2 wagging
						1165	w	$\nu(CH_2-N)+$ $\delta(N-H)$
1082	w	1083	w	1082	w	1064	s	
1061	w	1061	w	1065	w	991	s	CH_2 rocking
992	m	991	m	992	m			
930	w	926	w	920	w			
897	m	897	m	900	m	915 882	w w,br	unassigned
				825				$\nu(M-F)$
				755	sh			$\gamma(N-H)$
				740	s			$\nu(M-F)$?
				710	s			
750	s	749	s			725	s,br	$\gamma(N-H)$
711	m	709	m			675	s	$\delta(C=O)$
650	m			642	w	635	m	$\gamma(C=O)$
579	s	621	s	609	m			
560	s	597	m					$\nu(M-F)$
		572	m					

(cont'd.)

Table 12 (cont'd.) - Infrared Spectra of PYROL Adducts

$SnF_4 \cdot 2PYROL$		$GeF_4 \cdot 2PYROL$		$SiF_4 \cdot 2PYROL$		PYROL		Assignment
ν, cm^{-1}	Int.	ν, cm^{-1}	Int.	ν, cm^{-1}	Int.	ν, cm^{-1}	Int.	
552	s	550	m	575	m			γ (C=O)
546	s							ν (M-F)
				472	s			δ (M-F)
475	w					472	s	skeletal
		322	s					δ (M-F)
		300	sh					

IV.E.1. $SiF_4 \cdot 2PYROL$

$SiF_4 \cdot 2PYROL$ (850-650 cm^{-1})

IR Solid State	Ligand IR Neat Liquid
825 s	
755 sh	
740 s	725 s,br
710 s	
	675 s

From a comparison of the spectrum of $SiF_4 \cdot 2PYROL$ with that of $GeF_4 \cdot 2PYROL$ and $SnF_4 \cdot 2PYROL$ it is concluded that the 825 cm^{-1} band in the IR of the solid is due to ν(Si-F). In the region of 755-710 cm^{-1} there are three bands for $SiF_4 \cdot 2PYROL$ compared to two for each of the other complexes. The additional one is possibly an Si-F stretch, either at 755 cm^{-1} or 740 cm^{-1}. It is difficult to make definitive assignments in this region because the ligand has an extremely broad band centred at 725 cm^{-1}, presumably an N-H rocking band with some contribution from a C=O bending mode. The band at 609 cm^{-1} is probably an Si-F stretch because no band appears in this region in $SnF_4 \cdot 2PYROL$. Thus, the three Si-F stretches might be due to a cis-C_{2v} structure with the fourth band missing presumably because of its weak intensity. This conclusion is of course based on the assump-

tion that the ligands are behaving as point masses and that there are no correlation effects.

IV.E.2. $GeF_4 \cdot 2PYROL$

The results from Raman (see figure 90, appendix D) and IR spectra of $GeF_4 \cdot 2PYROL$ in the region of 700 to 500 cm^{-1} are summarized below:

$GeF_4 \cdot 2PYROL$ (700-500 cm^{-1})

IR Solid State	Raman Solid State	IR Solution	Ligand IR Neat	Ligand IR Solution
		638 s	675 s	
621 s	624 s		635 m	642 m
597 m		605 m		590 m
572 m	571 m	577 m		
550 m		555 w		
	520 w			

By comparing the solid state IR spectrum of $GeF_4 \cdot 2PYROL$ with that of $SiF_4 \cdot 2PYROL$ and $SnF_4 \cdot 2PYROL$, the three bands at 621, 597 and 572 cm^{-1} are probably Ge-F stretches although this is by no means definite since ligand vibrations also occur in this region. The band at 550 cm^{-1} is assigned to a ligand vibration. If the two Raman active bands at 624 cm^{-1} and 571 cm^{-1} are due to ν(Ge-F) and because they are coincidental with IR bands, there is no centre of

symmetry. In the solution IR of the complex there is no change in the number of bands, although they are slightly shifted in position from the solid state. On the basis of these results, a cis-C_{2v} structure seems to be present in both the solid and solution.

IV.E.3. $SnF_4 \cdot 2PYROL$

$SnF_4 \cdot 2PYROL$ (700-500 cm^{-1})

IR Solid State	Raman Solid State	IR Solution	Ligand IR Neat Liquid	Ligand IR Solution
			675 s	
650 m		640 m	635 m	642 m
579 s		590 s		590 m
560 s	562 s	560 sh		
552 s				
546 s	547 m			

Comparisons of the solid state IR spectra of $SnF_4 \cdot 2PYROL$ with the other complexes and pyrrolidinone itself indicate that three of the bands in the region 579-546 cm^{-1} are due to ν(Sn-F). The two Raman bands (see figure 91, appendix D) due to ν(Sn-F) are coincidental with IR bands indicating that there is no centre of symmetry. The solution results cannot be unambiguously interpreted. Although there are fewer bands in the solution spectrum than in the solid

state spectrum, the bands in the former are much broader and could be the composite of several Sn-F stretches. These results suggest that the cis isomer is present but it is not possible to exclude the presence of the trans isomer.

IV.F. Vibrational Spectra of Caprolactam (CAP) Adducts

Assignment of the bands in the infrared spectra of $SiF_4 \cdot 2CAP$, $GeF_4 \cdot 2CAP$ and $SnF_4 \cdot 2CAP$ (see figures 41 to 47, appendix C) are given in table 13. These are based on a comparison with caprolactam whose bands in turn were assigned by comparison with its homologue pyrrolidinone. The carbonyl stretching frequency in CAP is shifted downfield in all of the complexes indicating co-ordination through the C=O.

IV.F.1. $SiF_4 \cdot 2CAP$

The strong broad symmetrical band at 835 cm^{-1} in the solid state IR of $SiF_4 \cdot 2PYROL$, which does not appear in either the SnF_4 or GeF_4 analogue, is assigned to ν(Si-F) and it may be the composite of more than one band. A second ν(Si-F) is assigned to a strong band at 612 cm^{-1} because it is not present in the specimen of $SnF_4 \cdot 2CAP$. Another Si-F band might be present in the ligand vibration region 760-740 cm^{-1}. On the basis of these limited results, a cis structure is tentatively assigned to the solid complex.

Table 13. Infrared Spectra of CAP Adducts

$SnF_4 \cdot 2CAP$		$GeF_4 \cdot 2CAP$		$SiF_4 \cdot 2CAP$		CAP		Assignment
ν, cm^{-1}	Int.	ν, cm^{-1}	Int.	ν, cm^{-1}	Int.	ν, cm^{-1}	Int.	
3267	s	3308	s	3345	sh	3285	m	ν(N-H)
3220	sh	3218	m	3338	s	3200	s	
				3240	m	3055	s,br	
Nujol		Nujol		Nujol		Nujol		
1615	s,br	1630	s,br	1630	s,br	1659	s,br	ν(C=O)
1490	s	1502	m	1509	s	1481	s	CH_2 sciss.
Nujol		Nujol		Nujol		Nujol		
1400	m	1409	m	1413	m	1421	s	CH_2 sciss. or δ(N-H)
Nujol		Nujol		Nujol		Nujol		
1350	m	1350	m	1371	s	1349	m	δ(N-H)+ ν(CN)
1331	m	1336	w	1361	w	1330	m	
1310	w	1326	w	1351	s	1312	m	
		1315	w	1330	w			
1285	s	1290	m	1293		1287	m	ν(CN)

(cont'd.)

Table 13 (cont'd.) - Infrared Spectra of CAP Adducts

$SnF_4 \cdot 2CAP$		$GeF_4 \cdot 2CAP$		$SiF_4 \cdot 2CAP$		CAP		Assignment
ν, cm	Int.	ν, cm	Int.	ν, cm	Int.	ν, cm	Int.	
1258	m	1259	m	1260	m	1253	m	CH_2 wagging
1237	w	1241	w	1240	w	1234	m	$\nu(CH_2-N)+$
1188	s	1196	s	1196	s	1195	s	δ(N-H)
1162	m	1169	w	1172	w	1162	w	
1105	m	1118	sh	1115	m	1120	s	
		1111	w					
1084	m	1085	m	1090	m	1082	m	CH_2 rocking
1069	sh	1070	w	1072	w	1070	sh	
1018	m	1027	w	1031	w	1015	w	
978	m	980	m	982	m	995	w	
970	sh	968	w	969	w	979	s	
		959	vw	894	m	960	m	
881	m	892	m	874	m	878	m	
865	w	870	w			862	m	
		845	w					
		829	m					
				835	s,br			ν(M-F)
811	s	790	s	760	sh	843	sh	CH_2 rocking
749	w	750	w	740	s	835	sh	γ(N-H)
719	w	730	w			818	s	
						800	s	
						736	w	
						715	sh	

(cont'd.)

Table 13 (cont'd.) - Infrared Spectra of CAP Adducts

$SnF_4 \cdot 2CAP$		$GeF_4 \cdot 2CAP$		$SiF_4 \cdot 2CAP$		CAP		Assignment
ν, cm^{-1}	Int.	ν, cm^{-1}	Int.	ν, cm^{-1}	Int.	ν, cm^{-1}	Int.	
700	m	692	w	685	m	685	m	δ(C=O)
		660	w			665	sh	
		640	s					ν(M-F)
		610	s	612	s			ν(M-F)
		589	s	582	s	582	s	γ(C=O)
		570	m					ν(M-F)
		555	sh					ν(M-F)
573	s							ν(M-F) or γ(C=O) ν(M-F)
553	s							ν(M-F)
519	sh							
494	w	507	sh	508	s	502	s	γ(C=O)
		500	m	465	s,br	495	sh	
		490	sh					
320	w	421	w	432	s	395	m	skeletal
		390	w	420	sh	325	sh	
		390	m			318	m	
		335	s					δ(M-F)+ skeletal
		312	s					
		297	s					

IV.F.2. $GeF_4 \cdot 2CAP$

The following table shows that there are five bands in the region of ν(Ge-F) in the infrared spectrum, one of which is a ligand vibration.

$GeF_4 \cdot 2CAP$ (650-550 cm^{-1})

IR Solid State	Raman Solid State	IR Solution	Ligand IR Solid	Ligand IR Solution
640 s	650 w	630 s		
610 s	610 s			599 m,br
589 s		582 s	582 s	
570 m				
555 sh				555 m,br

The Raman spectrum (see figure 92, appendix D) confirms coincidence for only two bands. These results alone suggest a cis structure in the solid. The solution spectrum shows at most two bands assignable to ν(Ge-F) making any conclusion uncertain.

IV.F.3. $SnF_4 \cdot 2CAP$

The IR and Raman spectra are summarized in the table below:

$SnF_4 \cdot 2CAP$ (700-500 cm^{-1})

IR Solid State	Raman Solid State	IR Solution	Ligand IR Solid State	Ligand IR Solution
573 s	574 s	593 sh,s	582 s	599 m,br
553 s		580 s		
519 s		560 s		555 m,br

A comparison of the solid state IR spectrum of $SnF_4 \cdot 2CAP$ with that of $SiF_4 \cdot 2CAP$ indicates that of the three bands in the region of ν(M-F) of the former, one may be a ligand vibration. The band at 553 cm^{-1} could be the composite of more than one ν(Sn-F) stretch. The Raman spectrum (see figure 93, appendix D) shows a single strong band at 574 cm^{-1} coincidental with one in the IR. Although the current vibrational spectra for $SnF_4 \cdot 2CAP$ are not inconsistent with a cis-C_{2v} structure, single crystal X-ray measurements are necessary to obtain its exact structure. A comparison of the solution spectra of caprolactam and $SnF_4 \cdot 2CAP$ indicates that there may be only a single ν(Sn-F) suggesting the presence of trans-$SnF_4 \cdot 2CAP$.

IV.F.4. $GeF_4 \cdot 2CAP$-D

The vibrational assignments for $GeF_4 \cdot 2CAP$-D and CAP-D (see IR spectra in figures 48 and 49, appendix C), given in table 14 are based on comparisons with CAP and $GeF_4 \cdot 2CAP$.

Table 14. Infrared Spectra of CAP-D and $GeF_4 \cdot 2CAP-D$

$GeF_4 \cdot 2CAP-D$		CAP-D		Assignment
ν, cm^{-1}	Int.	ν, cm^{-1}	Int.	
Nujol		Nujol		ν(N-H)
2463	s	2467	m	
2440	s	2415	m	
2395	w	2370	sh	ν(N-D)
		2345	s	
		2335	sh	
		2325	sh	
		2268	m	
1606		1640	s,br	ν(C=O)
1488		1470	sh	CH_2 sciss.
Nujol		Nujol		
1353	m	1354	m	
1338	w	1346	m	
1330	w	1336	w	
1299	m	1292	m	
1261	m	1257		δ(N-D) + ν(CN)
1244	w	1239	m	ν(CN)
1239	m	1230		δ(N-D)
1200	w	1199	w	CH_2 wagging
1175	m	1172	s	$\nu(CH_2\text{-}N)$ + δ(N-D)
1167	sh	1161	m	
1124	w	1123	w	
1095	sh	1099	m	
1090	m	1088	m	
1039	w	1040	w	$\nu(CH_2\text{-}N)$ + δ(N-D)
975	m	994	m	CH_2 rocking
950	w	974	s	
899	w	953	w	δ(N-D)
862	w	887	s	δ(N-D) + ν(CN)
849	w	860	w	
812	m	840	m	
751	w	808	w	
724	s	741	m	δ(C=O)
		710	s	ν(N-D)

(cont'd.)

Table 14 (cont'd.)

Infrared Spectra of CAP-D and $GeF_4 \cdot 2CAP-D$

$GeF_4 \cdot 2CAP-D$		CAP-D		Assignment
ν, cm^{-1}	Int.	ν, cm^{-1}	Int.	
649				ν(M-F)
615				ν(M-F)
592		595	s	γ(C=O)
		570	m	γ(N-D)
575				ν(M-F), γ(C=O),
569				γ(N-D)
492	w			
420		392	m	skeletal
		318	m	
343	sh			
337	s			
316	s			γ(Ge-F)
300	s			skeletal
290	sh			
277	m			

The series of seven bands in the region of 2467-2268 cm^{-1} in CAP-D is assigned to ν(N-D) and in $GeF_4 \cdot 2CAP$-D these occur at 2463, 2440 and 2395 cm^{-1}. The ratio of the most intense frequencies ν(N-D) and ν(N-H) in $GeF_4 \cdot 2CAP$-D and $GeF_4 \cdot 2CAP$, respectively, is 1.36 which is close to the value of 1.38 if the mass effect alone is assumed to cause the isotopic shift. The carbonyl stretching frequency at 1640 cm^{-1} in CAP-D is lowered to 1606 cm^{-1} in $GeF_4 \cdot 2CAP$-D in agreement with the previous conclusion that co-ordination is most likely through oxygen.

Comparison of CAP-D and $GeF_4 \cdot 2CAP$-D indicates there are five bands for the latter in the region 649-569 cm^{-1} two of which could be ligand bands. Thus three are tentatively assigned to ν(Ge-F) modes and therefore the compound probably has a cis structure in the solid state. Spectra of $GeF_4 \cdot 2CAP$ and $GeF_4 \cdot 2CAP$-D are similar in the 650-550 cm^{-1} region.

IV.G. Vibrational Spectra of Azacyclononanone (AZA-NON) Adducts

Bands in the infrared spectrum of $SiF_4 \cdot 2AZA$-NON, $GeF_4 \cdot 2AZA$-NON and $SnF_4 \cdot 2AZA$-NON (see figures 50 to 56, appendix C) are assigned in table 15 on the basis of a comparison with AZA-NON. Since there is no detailed information about the IR of AZA-NON, bands for it were assigned by comparison with its homologue pyrrolidinone. Because of the

Table 15. Infrared Spectra of AZA-NON Adducts

$SnF_4 \cdot 2AZA\text{-}NON$		$GeF_4 \cdot 2AZA\text{-}NON$		$SiF_4 \cdot 2AZA\text{-}NON$		AZA-NON		Assignment
ν, cm^{-1}	Int.	ν, cm^{-1}	Int.	ν, cm^{-1}	Int.	ν, cm^{-1}	Int.	
3255	m	3280	m	3317	s	3310	s,br	ν(N-H)
3195	s	3219	m	3240	m	3195	sh	
		3213	sh					
						3060	m	ν(C-H)
Nujol		Nujol		Nujol		Nujol		
1612	s,br	1625	s,br	1631	s	1640	s,br	ν(C=O)
		1491	m	1500	m	1545	m	CH_2 sciss.
						1525	m	
						1490	m	
Nujol		Nujol		Nujol		Nujol		
1405	s	1406	m	1412	m			CH_2 sciss. or δ(NH)
1395	sh							CH_2 sciss. or δ(NH)
Nujol		Nujol		Nujol		Nujol		
1352	w	1353	w	1357	w	1355	m	δ(N-H)+ν(CN)
1338	w	1341	m	1342	m	1341	m	
1323	w	1330	sh	1332	w	1327	m	
1295	w	1325	w	1328	w	1312	w	
		1295	sh	1294	w			

(cont'd.)

Table 15 (cont'd.) - Infrared Spectra of AZA-NON Adducts

$SnF_4 \cdot 2AZA\text{-}NON$		$GeF_4 \cdot 2AZA\text{-}NON$		$SiF_4 \cdot 2AZA\text{-}NON$		AZA-NON		Assignment
ν, cm^{-1}	Int.	ν, cm^{-1}	Int.	ν, cm^{-1}	Int.	ν, cm^{-1}	Int.	
1280	m	1285	m	1288	m	1285	m	ν(CN)
1250	s	1254	m	1255	m	1264	w	
1240	sh	1243	m	1245	m	1234	m	
1215	m	1218	m	1219	m	1230	m	CH_2 wagging
1181	w	1182	w	1182	w	1199	m	
1159	w	1170	w	1172	w	1176	w	$\nu(CH_2\text{-}N)$+
1114	w	1118	w	1120	w	1150	s	δ(N-H)
						1100	w	
1094	w	1097	w	1097	w	1090	w	
1050	w	1054	w	1056	w	1065	w	
1021	m	1019	w	1020	w	1055	vw	CH_2 rocking
968	w	1010	w	1010	w	1030	s	
943	w	974	w	973	w	1029	sh	
		949	w	950	w	972	m	
		938	w	937	w	944	m	
		900	m	902	m	885	w	
895	m	846	s	850	s	868	m	
851	s	837	sh	839	m	848	m	CH_2 rocking
835	m	819	w	820	m	794	s	δ(N-H)
811	m	773	w	800	w			
771	w	762	w					
760	w							
		Nujol						
				772	m			ν(M-F) or ligand vib.

(cont'd.)

Table 15 (cont'd.) - Infrared Spectra of AZA-NON Adducts

$SnF_4 \cdot 2AZA\text{-}NON$		$GeF_4 \cdot 2AZA\text{-}NON$		$SiF_4 \cdot 2AZA\text{-}NON$		AZA-NON		Assignment
ν, cm^{-1}	Int.	ν, cm^{-1}	Int.	ν, cm^{-1}	Int.	ν, cm^{-1}	Int.	
				760	sh			ν(M-F) or ligand vib.
				735	s			ν(M-F)
710	w	714	m	720	sh	735	sh	γ(N-H) or δ(CO)
690	m	691	m	695	m	739	s	
						715	s	
		652	s					ν(M-F)
		622	sh	625	sh			ν(M-F) or γ(CO)
621	w							γ(CO)
		611	m	618	m			ν(M-F) or γ(CO)
610	sh					605	m	γ(CO)
595	s	590	s					ν(M-F)
590	sh							ν(M-F)
545	s	553	s	565	s			γ(CO)
505	w	515	w	525	m	512	s	γ(CO) or skeletal

(cont'd.)

Table 15 (cont'd.) - Infrared Spectra of AZA-NON Adducts

$SnF_4 \cdot 2AZA\text{-}NON$		$GeF_4 \cdot 2AZA\text{-}NON$		$SiF_4 \cdot 2AZA\text{-}NON$		AZA-NON		Assignment
ν, cm^{-1}	Int.	ν, cm^{-1}	Int.	ν, cm^{-1}	Int.	ν, cm^{-1}	Int.	
				460	s	465	w	skeletal
				447	s	438	m	
						378	m	
						365	m	
		345	s					skeletal
		325	sh					δ(M-F)
		317	s					
		301	sh					

complexity of the spectrum and the possibility of overlap of different types of bands, a number of frequencies cannot be identified with certainty.

Although the strong broad N-H stretching band at 3310 cm^{-1} (with a shoulder at 3195 cm^{-1}) changes to sharp bands in all of the complexes, examination of table 15 shows no identifiable pattern involved in the slight frequency shift. However, the C=O stretching frequency for AZA-NON is lowered in all three cases. As in the case of the other lactam complexes, this is attributed to co-ordination through the carbonyl oxygen.

IV.G.1. $SiF_4 \cdot 2$AZA-NON

Comparisons of the solid state infrared spectrum of $SiF_4 \cdot 2$AZA-NON with its tin and germanium analogs show that the bands at 772, 735 and one of the two bands at 625 and 618 cm^{-1} are probably Si-F stretches. Bands appear at approximately 770 cm^{-1} in both $SnF_4 \cdot 2$AZA-NON and $GeF_4 \cdot 2$AZA-NON but they are considerably weaker than the 722 cm^{-1} band of $SiF_4 \cdot 2$AZA-NON. Results from the Raman (see figure 94, appendix D) and infrared spectra are summarized below:

$SiF_4 \cdot 2AZA\text{-}NON$ (800-500 cm^{-1})

IR	Raman
772 m	
760 sh	756 m
735 s	730 s
720 sh	
695 m	
	672 s
	651 s
625 sh	623 w
618 m	
	603 w
	584 m
565 s	
525 m	

From the coincidences in the IR and Raman frequencies it appears that the band at 760 cm^{-1} might be an Si-F stretch instead of the one at 772 cm^{-1}. Coincidences are observed for the other probable Si-F stretches at 625 and 730 cm^{-1}. On the basis of these results, $SiF_4 \cdot 2AZA\text{-}NON$ is tentatively assigned a cis structure in the solid state.

IV.G.2. $GeF_4 \cdot 2AZA\text{-}NON$

A comparison of the solid state infrared spectrum

of $GeF_4 \cdot 2AZA\text{-}NON$ with that of $SiF_4 \cdot 2AZA\text{-}NON$ shows that of the five bands in the region 650-550 cm^{-1} three are probably ligand vibrations leaving two Ge-F stretching bands. Therefore any conclusion about symmetry is uncertain. In the solution spectrum there is a strong band at 633 cm^{-1} together with a broad band centred at 580 cm^{-1}. However, it is impossible to ascertain how many bands are contained in this broad envelope so that the solution results, like those in the solid state, are inconclusive.

IV.G.3. $SnF_4 \cdot 2AZA\text{-}NON$

The vibrational bands for $SnF_4 \cdot 2AZA\text{-}NON$ are summarized below:

$SnF_4 \cdot 2AZA\text{-}NON$ (650-500 cm^{-1})

IR Solid State	Raman Solid State	IR Solution	Ligand IR Solid State	Ligand IR Solution
621 vw				
610 sh	608		605 m	
595 s		590 s		
590 sh	582			
		575		565 w
	563	557		560 w
545 s				
			512 s	

A comparison of the solid state IR of $SnF_4 \cdot 2AZA\text{-}NON$ with that of $SiF_4 \cdot 2AZA\text{-}NON$ indicates that of the five bands in the 621-545 cm^{-1} region three are possibly ligand vibrations. Coincidences in the Raman (see figure 95, appendix D) and IR spectra are observed for only two bands. The Raman spectrum was of poor quality due to fluorescence. On the basis of the two coincidences it is tentatively concluded that the complex is cis octahedral in the solid state, although the possibility of its being trans-C_1 cannot be ruled out.

IV.G.4. $GeF_4 \cdot 2AZA\text{-}NON\text{-}D$

The assignments for bands in the solid state infrared spectrum of $GeF_4 \cdot 2AZA\text{-}NON\text{-}D$ given in table 16 are based on a comparison with that of AZA-NON-D (both spectra are shown in figures 57 and 58, appendix C). Assignments for the latter were derived by comparison with AZA-NON. Although the pattern and number of N-D stretches change in going from the ligand to its complex, no significant frequency shift is observed. The C=O frequency shifts downward in the complex indicating co-ordination through the oxygen. There are five bands in the region 670 to 551 cm^{-1} for $GeF_4 \cdot 2AZA\text{-}NON\text{-}D$ and by comparison with AZA-NON-D it is evident that three of these could be ligand vibrations leaving two Ge-F stretching vibrations. These results are not sufficiently complete to permit even a tentative conclusion

Table 16. Infrared Spectra of AZA-NON-D and GeF_4·2AZA-NON-D

GeF_4·2AZA-NON-D		AZA-NON-D		Assignment
ν, cm^{-1}	Int.	ν, cm^{-1}	Int.	
3285	w	3318	w	ν(N-H)
3028	w	3250	w	
Nujol		Nujol		
2480	w	2460	s	ν(N-D)
2428	s	2440	s	
2412	sh	2404	m	
2375	m	2350	sh	
2330	sh			
1600	s,br	1632	s,br	ν(C=O)
		1542	w	CH_2 sciss.
Nujol		Nujol		
1357	w	1348	m	
1342	m	1345	sh	
1338	w	1324	w	
1328	m	1320	m	
1302	m	1313	w	δ(N-D) + ν(CN)
1289	m	1303	w	ν(CN)
1272	w	1265	m	δ(N-D)
1247	m	1248	m	CH_2 wagging
1218	m	1218	w	
1208	m	1168	m	$\nu(CH_2\text{-}N)$ + δ(N-D)
1172	m	1159	s	
1162	w	1129	m	
1125	w			
1112	w			
1096	m	1063	w	
1065	m	1058	w	
1037	m	1031	m	
1021	m	1020	w	
998	w	981	m	
970	m	972	m	$\nu(CH_2\text{-}N)$ + δ(N-D)
953	m	934	m	CH_2 rocking
942	m	882	m	δ(N-D)
900	sh	860	m	δ(N-D) + ν(CN)
895	m	842	w	
836	m			
817	m			

(cont'd.)

Table 16 (cont'd.)

Infrared Spectra of AZA-NON-D and $GeF_4 \cdot 2$AZA-NON-D

$GeF_4 \cdot 2$AZA-NON-D		AZA-NON-D		Assignment
ν, cm^{-1}	Int.	ν, cm^{-1}	Int.	
		795	m	δ(C=O)
		744	m	γ(N-D)
		730	m	
		720	m	
670	sh			ν(M-F)
660	s			γ(N-D)
612	s			γ(C=O)
588	s			
551	s			
		627	sh	γ(N-D)
		619	s	γ(C=O)
		574	s	
510	m	504	s	γ(C=O)
425		465	w	skeletal
375		436	w	
		375	sh	
		364	m	
		290	m	
346	s			δ(M-F)
320	s			skeletal
305	sh			

about its structure in the solid state.

IV.H. Infrared Spectra of Azacyclo-octanone (AZA-OCT) Adducts

IV.H.1. $GeF_4 \cdot 2AZA\text{-}OCT$

Assignment for bands in the solid state infrared spectrum of $GeF_4 \cdot 2AZA\text{-}OCT$ given in table 17 are based on a comparison with that of AZA-OCT (both spectra are shown in figures 59 and 60, appendix C) and pyrrolidinone. As was the case with AZA-NON there is some uncertainty in these assignments. There is no appreciable shift in the N-H stretching frequency in going from the ligand to its complex. However, the C=O stretch in AZA-OCT is split into two bands at 1665 cm^{-1} (m) and 1620 cm^{-1} (s,br), suggesting that a cis structure may be present. Of the five bands in the region of 625 to 549 cm^{-1} only one appears to be a ligand vibration leaving four as Ge-F stretching vibrations. On the basis of this infrared data, this compound is tentatively assigned a cis structure.

IV.H.2. $GeF_4 \cdot 2AZA\text{-}OCT\text{-}D$

Assignment for bands in the solid state infrared spectra of $GeF_4 \cdot 2AZA\text{-}OCT\text{-}D$ are based on comparison with that of AZA-OCT-D (see figures 61 and 62, appendix C and table 18). Of the five bands that appear in the region 621 to 541 cm^{-1} for the former three are possibly ligand vibra-

Table 17. Infrared Spectra of AZA-OCT and GeF_4·2AZA-OCT

GeF_4·2AZA-OCT		AZA-OCT		Assignment
ν, cm^{-1}	Int.	ν, cm^{-1}	Int.	
3280	s	3300	sh	ν(N-H)
3212	m	3215	s,br	
		3080	s	
Nujol		Nujol		
1665	m	1670	s,br	ν(C=O)
1620	s,br			
1491	s			CH_2 sciss.
1487	s			
Nujol		Nujol		
1429	m	1406	m	CH_2 sciss.
1400	m	1399	sh	
		1395	sh	δ(N-H)
Nujol		Nujol		
1341	m	1340	w	
1320	w	1310	sh	
1315	w	1301	m	δ(N-H) + ν(CN)
1301	w	1274	w	ν(CN)
1292	w			
1270	w			
1241	s	1255	m	
1235	sh	1240	m	
1199	m	1228	w	CH_2 wagging
1161	m	1215	w	
1102	m	1180	m	$\nu(CH_2\text{-}N)$ + δ(N-H)
		1160	s	
		1114	w	
1077	w	1099	s	
1031	w	1075	m	
1022	m	1025	m	CH_2 rocking
1005	w	995	m	
960	m	896	m	
910	w			

(cont'd.)

Table 17 (cont'd.)

Infrared Spectra of AZA-OCT and $GeF_4 \cdot 2AZA\text{-}OCT$

$GeF_4 \cdot 2AZA\text{-}OCT$		AZA-OCT		Assignment
ν, cm^{-1}	Int.	ν, cm^{-1}	Int.	
884	w	872	m	γ(N-H) CH_2 rocking
854	m	835	m	
841	s	801	m	
810	w	795	m	
767	m	755	m	γ(N-H) δ(C=O)
750	w	735	m	
Nujol		Nujol		
684	w			γ(N-H) or δ(C=O)
		663	w	δ(C=O)
625	s			ν(M-F)
606	s			ν(M-F)
591	s			ν(M-F)
570	m	568	s	γ(C=O)
549	m			ν(M-F)
520	m	498	s	γ(C=O)
470	w	450	w	skeletal
400	w	380	w	
395	w	375	sh	
375	w	305	w	
337	s			skeletal δ(Ge-F)
325	s			
315	sh			
290	w			

Table 18. Infrared Spectra of AZA-OCT-D and GeF_4·2AZA-OCT-D

GeF_4·2AZA-OCT-D		AZA-OCT-D		Assignment
ν, cm^{-1}	Int.	ν, cm^{-1}	Int.	
Nujol		Nujol		
2448	m	2710	sh	
2425	s	2670	sh	
2380	m	2580	m,br	ν(N-D)
		2460	sh	
		2365	s	
		2340	sh	
1595	s,br	1638	s,br	ν(C=O)
1485	sh			CH_2 scissors
Nujol		Nujol		
1423	m	1420	s	
Nujol		Nujol		
1340	m	1342	w	
1318	w	1319	w	
1295	w	1290	sh	
1270	w	1278	m	
1257	w	1258	m	
1235	w	1234	m	δ(N-D) + ν(CN)
1188	m	1198	w	ν(CN)
1152	m	1194	w	δ(N-D)
1125	m	1180	w	CH_2 wagging
1105	w	1173	sh	
		1145	s	$\nu(CH_2\text{-}N)$ + δ(N-D)
		1105	w	
1095	w	1090	m	
1005	w	1050	w	
975	m	1021	w	
917	w	997	m	
902	w	985	m	$\nu(CH_2\text{-}N)$ + δ(N-D)
880	w	920	w	CH_2 rocking
847	w	895	m	
		875	w	δ(N-D)
		840	w	δ(N-D) + ν(CN)
		835	w	

(cont'd.)

Table 18 (cont'd.)

Infrared Spectra of AZA-OCT-D and $GeF_4 \cdot 2AZA\text{-}OCT\text{-}D$

$GeF_4 \cdot 2AZA\text{-}OCT\text{-}D$		AZA-OCT-D		Assignment
ν, cm^{-1}	Int.	ν, cm^{-1}	Int.	
802	m	800	m	δ(C=O) γ(N-D)
750	w	792	m	
713	m	760	m	
		748	w	
		698	m,br	
621	s			ν(M-F)
599	s	600	sh	γ(C=O)
578	s			ν(M-F)
565	s	568	m	γ(C=O)
541	m	550	sh	γ(C=O)
510	w	495	m	γ(C=O)
465	w	448	w	skeletal
435	w	380	w	
375	sh	358	w	
360	sh	350	w	
334	s			δ(Ge-F) skeletal
323	s			

tions. Since only two bands can be assigned to ν(Ge-F), no conclusion can be made as to the structure of $GeF_4 \cdot 2AZA\text{-}OCT\text{-}D$.

IV.I. Infrared Spectra of δ-Valerolactam (VAL) Adducts

IV.I.1. $GeF_4 \cdot 2VAL$

Assignments for bands in the solid state infrared spectrum of $GeF_4 \cdot 2VAL$ given in table 19 are based on comparisons with those of VAL (both spectra are shown in figures 63 and 64, appendix C) and pyrrolidinone. In the region 650 to 550 cm^{-1} there are five bands one of which could be a ligand vibration. The other four bands are probably due to Ge-F stretching vibrations. On this basis the compound is assigned a cis structure.

IV.I.2. $GeF_4 \cdot 2VAL\text{-}D$

Assignments for bands in the solid state infrared spectra of $GeF_4 \cdot 2VAL\text{-}D$ are based on a comparison with VAL-D (see figures 65 and 66, appendix C and table 20). Since it is possible to assign only two bands to ν(M-F) any conclusion as to geometry is uncertain.

IV.J. Infrared Spectrum of $GeF_4 \cdot 2TMU$

The assignments for infrared bands in TMU and $GeF_4 \cdot 2TMU$ (see figures 67 to 70, appendix C) given in table 21 are based on: (1) assignments for other tetramethylurea

Table 19. Infrared Spectra of VAL and $GeF_4 \cdot 2VAL$

$GeF_4 \cdot 2VAL$		VAL		Assignment
ν, cm^{-1}	Int.	ν, cm^{-1}	Int.	
3280	m	3290	m	ν(N-H)
3215	m	3190	m	
Nujol		Nujol		
1684	sh	1678	s,br	ν(C=O)
1675	sh			
1653	sh			
1628	s			
1499		1499		CH_2 sciss. or δ(N-H)
Nujol		Nujol		
1412	m	1410	w	CH_2 sciss. or δ(N-H)
1394	sh			
Nujol		Nujol		
1355	w	1353	m	δ(N-H) + ν(CN)
1330	m	1325	m	
1313	m	1320	sh	ν(CN)
1272	m	1305	w	
1184	w	1277	w	
1170	w	1180	sh	CH_2 wagging
1117	w	1173	m	$\nu(CH_2\text{-}N)$ + δ(N-H)
1102	w	1116	m	
981	m	1095	sh	CH_2 rocking
941	m	1054	m	
920	w	1045	sh	
880	m	985	w	
		937	w	
		920	sh	
844	s	850	m,br	γ(N-H)
820	m	769	m	CH_2 rocking
790	w			

(cont'd.)

Table 19 (cont'd.)

Infrared Spectra of VAL and $GeF_4 \cdot 2VAL$

$GeF_4 \cdot 2VAL$		VAL		Assignment
ν, cm^{-1}	Int.	ν, cm^{-1}	Int.	
730	sh	720	m	γ(N-H)
720	m	656	s	δ(C=O)
685	sh			
668	sh			
658	s			
605	sh			ν(M-F) + γ(C=O)
598	s			
570	s			
564	sh			
539	m			
		570	w	γ(C=O)
		504	s	γ(C=O)
490	w			γ(C=O)
473	m			
460	sh	450	sh	skeletal
452	m	435	s	
432	sh			
418	sh			
350	sh			skeletal
340	s			δ(M-F)
329	sh			
313	s			
300	sh			

Table 20. Infrared Spectra of VAL-D and $GeF_4 \cdot 2VAL\text{-}D$

$GeF_4 \cdot 2VAL\text{-}D$		VAL-D		Assignment
ν, cm^{-1}	Int.	ν, cm^{-1}	Int.	
3290	w	3200	w	ν(N-H)
Nujol		Nujol		
2435	s	2660	w	
2410	s	2525	w	
2390	m	2470	sh	
2360	sh	2440	m	
		2355	m,br	ν(N-D)
		2230	m	
		2190	sh	
		2125	w	
		2080	w	
1615	s,br	1658	s,br	ν(C=O)
1480	s	1489	m	CH_2 sciss.
Nujol		Nujol		
1412	m	1414	m	
1405	m	1408	sh	
Nujol		Nujol		
1359	s	1355	m	
1333	m	1339	m	
1315	m	1315	m	δ(N-D) + ν(CN)
1275	m	1270		ν(CN)
1258	w	1255	w	δ(N-D)
1180	sh	1211	s	CH_2 wagging
1165	m	1278		
		1265	s	$\nu(CH_2\text{-}N)$ + δ(N-D)
		1112	w	
1093	w	1095	w	
1075	w	1072	w	
1006	w	1010	m	
980	m	1006	sh	$\nu(CH_2\text{-}N)$ + δ(N-D)
915	sh	982	s	
		940	w	CH_2 rocking
		926	w	δ(N-D)
905	m	906	s	δ(N-D) + ν(CN)
845		840	w	
820	w	829	m	

(cont'd.)

Table 20 (cont'd.)

Infrared Spectra of VAL-D and $GeF_4 \cdot 2VAL-D$

$GeF_4 \cdot 2VAL-D$		VAL-D		Assignment
ν, cm^{-1}	Int.	ν, cm^{-1}	Int.	
785	m	765	m	δ(C=O)
Nujol		Nujol		
670	s	660	s,br	γ(C=O)
655	sh	625	sh	γ(N-D)
599	s			ν(M-F)
578	s			
525	w	530	sh	γ(C=O)
		504	s	
472	m	453	m	skeletal
450	m	433	s	
		425	sh	
345	sh			δ(M-F) skeletal
327	sh			
321	sh			
314	s			
300	sh			
290	sh			

Table 21. Infrared Spectra of TMU and $GeF_4 \cdot 2TMU$

$GeF_4 \cdot 2TMU$		TMU		Assignment
ν, cm^{-1}	Int.	ν, cm^{-1}	Int.	
		2990	sh	ν(C-H)
Nujol		Nujol		
		1640	s	ν(C=O)
1620	m			ν_a(NCN)
1595	sh			ν(CO)
1578	s			
1560	sh			
1545	s			
		1560	w	
		1505	sh	
		1490	s	ν_a(NCN)
1485	sh	1455	m	
1475	sh	1425	w	
Nujol		1403	w	δ_a(C-H)
1432	m	1368	s	
1420	m	1308	w	δ_s(C-H)
1403	m			
Nujol				
1327	s			
1245	m	1245	sh	unassigned ligand vib.
1235	m	1230	m	
1165	s	1134	s	ν_a(CN) + ν_s(CN) + $r_s(NCH_3)$
1113	w			
1072	m			ν_a(CN) + ν_s(CN) + $\delta_a(NCH_3)$
1055	w	1046	m	
		1015	m	unassigned ligand vib.
908	m	910	m	

(cont'd.)

Table 21 (cont'd.)

Infrared Spectra of TMU and $GeF_4 \cdot 2TMU$

$GeF_4 \cdot 2TMU$		TMU		Assignment
ν, cm^{-1}	Int.	ν, cm^{-1}	Int.	
744	s	778	m	δ(C=O)
755	s	732		
Nujol				
632	s			ν(M-F)
585	m	590	sh	unassigned ligand vib.
568	m	576	m	
		550	m	
430	m			
		408	m	$\delta_a(NCH_3) + r_a(NCH_3)$
380	m	350	sh	unassigned ligand vib.
		341	m	
307	s			δ(M-F)
281	m			
270	m			

complexes (66), and (2) a vibrational analysis and infrared spectrum of tetramethylthiourea (80). Because of the complexity of the spectra some of the bands remain unidentified, awaiting a normal co-ordinate analysis of tetramethylurea. Attempts to synthesize $SiF_4 \cdot 2TMU$ and $SnF_4 \cdot 2TMU$ were unsuccessful.

The band at 1640 cm^{-1} in the spectrum of TMU is assigned to $\nu(C=O)$, and the N-C-N antisymmetric stretch occurs at 1490 cm^{-1}. In $GeF_4 \cdot 2TMU$ these bands cannot be identified since there are six bands in the region 1620 to 1510 cm^{-1}. A similar observation in other TMU complexes (66) was observed and attributed to a merging of the absorptions associated with the C=O and N-C-N vibrations. The former shifts to a lower frequency and the latter to a higher frequency on co-ordination through oxygen (66).

A comparison of the solid state spectrum of $GeF_4 \cdot 2TMU$ with that of TMU (neat liquid) indicates that the single strong band at 632 cm^{-1} is undoubtedly a Ge-F stretching vibration. Two other bands at 585 and 568 cm^{-1} are most likely ligand vibrations. Thus the compound is assigned a <u>trans</u> structure in the solid state. However, the IR spectrum of $GeF_4 \cdot 2TMU$ in $ClCH_2CN$ solution (see figure 70, appendix C) shows bands at 637, 598, 583, 570 and 537 cm^{-1}. The IR spectrum of TMU in $ClCH_2CN$ contains two bands at 576 and 555 cm^{-1}. It appears that three bands in the spectrum of $GeF_4 \cdot 2TMU$ can be assigned to Ge-F stretching modes and

therefore a cis structure is present in solution. These well defined bands are replaced by a broad band centred at 600 cm^{-1} (see figure 71, appendix C) when the complex is exposed to moist air. This broad band is undoubtedly due to GeF_6^{2-} formed by hydrolysis of the complex.

IV.K. Infrared Spectrum of GeF_4·TMEN

The infrared spectra of TMEN complexes of SiF_4, GeF_4 and SnF_4 have been studied in detail by several workers (11,26,81) and in each case the complex was assigned a cis-C_{2v} structure in the solid state.

GeF_4·TMEN was the only complex found to be sufficiently soluble in chloroacetonitrile. A comparison of its solid state and solution spectra (see figures 73 and 74, appendix C) shows that the four bands at 620, 607, 595 and 540 cm^{-1} assigned to ν(M-F) are only slightly shifted in solution where they appear at 626, 605, 591 and 541 cm^{-1}; therefore, the complex seems to have the same cis-C_{2v} structure in solution.

IV.L. Infrared Spectrum of SnF_4·2Isoquinoline (ISOQ)

Assignments for bands in the solid state infrared spectrum of SnF_4·2ISOQ (see figure 76, appendix C) in the region 700 to 475 cm^{-1} are based on comparisons with assignments made by Hickie (11) for SiF_4·2ISOQ, GeF_4·ISOQ and ISOQ (spectrum shown in figure 75, appendix C) as summarized in

the following table:

$SnF_4 \cdot 2ISOQ$	ISOQ	
	655 w	
633 m	636 s	ligand
	620 m	vib.
	612 w	
	568 w	
558 s,br		(M-F)
	532 sh	ligand
	522 m	vib.
	503 s	
490 s		
480 s		

A lone Sn-F stretching mode appears at 558 cm^{-1}. This is probably coincident with a ligand vibration since such a vibration occurs at 554 and 560 cm^{-1} in $GeF_4 \cdot 2ISOQ$ and $SiF_4 \cdot 2ISOQ$ respectively

On this basis the compound is tentatively assigned a trans structure in agreement with Hickie (11) who also ascribed a trans geometry to both $SiF_4 \cdot 2ISOQ$ and $GeF_4 \cdot 2ISOQ$.

IV.M. Infrared Spectrum of $GeF_4 \cdot CAP$

Band assignments for the solid state infrared spectrum of $GeF_4 \cdot CAP$ (see figure 77, appendix C) given in

table 22 were made by comparisons with $GeF_4 \cdot 2CAP$, $SiF_4 \cdot 2CAP$ and CAP. The C=O stretching frequency, which appears at 1660 cm^{-1} in CAP, is split into two bands in $GeF_4 \cdot CAP$, one of which occurs at 1627 (s,br), the other as a shoulder of medium intensity at 1685 cm^{-1}. On this basis co-ordination is assumed to be through the carbonyl oxygen.

Spectra of $GeF_4 \cdot CAP$ and $GeF_4 \cdot 2CAP$ are similar from 1600 to 750 cm^{-1}. However, only the former has a strong broad band at 739 cm^{-1} (possibly the composite of more than one mode). This could be assigned to either a Ge-F stretching mode for a five co-ordinate species or to a ligand vibration. Of the five bands in the region 690 to 640 cm^{-1}, none can definitely be assigned to ν(M-F) because of ligand vibrations which are active in this region. Possible structures for this 1:1 complex are:

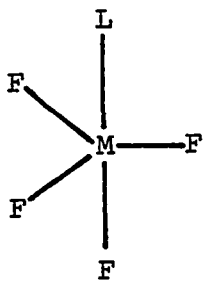

(C_{3v})

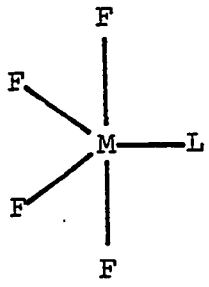

(C_{2v})

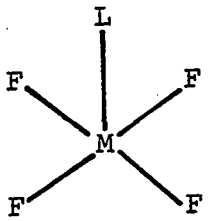

(C_{4v})

The C_{3v} structure is slightly preferred over the C_{2v} geometry on the basis of fewer F-F repulsion interactions at 90°. Examples of five co-ordinate molecules exhibiting a

Table 22. Infrared Spectra of CAP and GeF_4·CAP

GeF_4·CAP		CAP		Assignment
ν, cm^{-1}	Int.	ν, cm^{-1}	Int.	
3310	s	3285	m	ν(N-H)
3260	sh	3200	s	
		3055	s,br	
Nujol		Nujol		
1686	sh	1655	s,br	ν(C=O)
1625	s,br			
1505	sh	1481	s	CH_2 sciss.
1500	s			
Nujol		Nujol		
1405	sh	1421	s	CH_2 sciss. or δ(N-H)
Nujol		Nujol		
1374	m	1349	m	δ(N-H) + ν(CN)
1353	m	1330	m	
1335	m	1312	m	
1326	w			
1315	w			
1288	m	1287	m	ν(CH_2-N) + δ(N-H)
1281	m	1253	m	
1262	m	1234	m	
1258	m	1195	s	ν(CN)
1238	w	1162	w	CH_2 wagging
1195	s	1120	s	
1105	w			
1085	m	1082	m	CH_2 rocking
1020	m	1070	sh	
979	m	1015	w	
965	m	995	w	
892	m	979	s	
869	m	960	m	
		878	m	
		862	m	

(cont'd.)

Table 22 (cont'd.)

Infrared Spectra of CAP and GeF_4·CAP

GeF_4·CAP		CAP		Assignment
ν, cm^{-1}	Int.	ν, cm^{-1}	Int.	
830	s	843	sh	
790	s,br	835	sh	CH_2 rocking
		818	s	γ(N-H)
		800	s	
739	s,br			ν(M-F) or ligand vib.
720	sh	736	w	CH_2 rocking
		715	sh	γ(N-H)
		685	m	δ(C=O)
		665	sh	
690	m			
683	sh			ν(M-F)
666	sh			δ(C=O)
657	s			γ(C=O)
642	s			
611	m			
588	s	582	s	
		502	s	γ(C=O)
498	m	495	sh	
424	m	395	m	
		325	sh	skeletal
		318	m	
341	s			skeletal
300	s			δ(M-F)

C_{4v} geometry are rare.

IV.N. Infrared Spectrum of $GeF_4 \cdot S_4N_4$

Assignments for bands in the infrared spectrum of $GeF_4 \cdot S_4N_4$ were made by comparisons with S_4N_4 (both spectra are shown in figures 78 and 79, appendix C) and other S_4N_4 adducts (69), in table 23. Since an accurate normal coordinate analysis has not been performed for S_4N_4, only a few bands can be assigned.

Bands at 1050 cm^{-1} and 813 cm^{-1} in the complex are reported to be characteristic of S_4N_4 acting as a monodentate ligand (69), therefore $GeF_4 \cdot S_4N_4$ is probably not polymeric.

At least three and possibly four M-F stretches can be assigned. The structural possibilities for this complex are the same as those proposed for $GeF_4 \cdot CAP$.

IV.O. Infrared Spectra of $[(CH_3CH_2CH_2)_2NH_2]_2MF_6$ (M=Ge and Sn)

Assignments for bands in the solid state infrared spectra of $[(CH_3CH_2CH_2)_2NH_2]_2MF_6$ (where M = Ge and Sn) from 700 to 300 cm^{-1} (see figures 80 and 81, appendix C and table 24) are based upon comparisons with previously reported spectra of other hexafluorogermanates and hexafluorostannates (72,82,83). The spectra of $(NH_4)_2GeF_6$ and $BaGeF_6$ have been analyzed in terms of site symmetry O_h and D_{3d}, respectively

Table 23. Infrared Spectra of S_4N_4 and $GeF_4 \cdot S_4N_4$

$GeF_4 \cdot S_4N_4$*		S_4N_4		Assignment
ν, cm^{-1}	Int.	ν, cm^{-1}	Int.	
Nujol		Nujol		
1050	s			ν(S-N) co-ordinated N
1020	m			
968	s			ν(S-N) non-co-ordinated N
		925	s	ν(S-N)
927	sh			unassigned
871	s			unassigned
813	m			ν(S-N) co-ordinated N
735	sh			unassigned
720	m	722	m	
		697	s	
688	s			ν(M-F)
665	sh			ligand vib.
635	m			ν(M-F)
625	m			ν(M-F) or ligand vib.
590	m			ν(M-F)
570	sh			ligand vib.
557	sh			ligand vib.

(cont'd.)

*Spectrum measured until 400 cm^{-1}.

Table 23 (cont'd.)

Infrared Spectra of S_4N_4 and $GeF_4 \cdot S_4N_4$

$GeF_4 \cdot S_4N_4$*		S_4N_4		Assignment
ν, cm^{-1}	Int.	ν, cm^{-1}	Int.	
		545	s	ligand vib.
517	s			
475	sh			
448	sh			
428	s			
418	sh			
		337	s	

*Spectrum measured until 400 cm^{-1}.

Table 24

Infrared Spectra of $[(CH_3CH_2CH_2)_2NH_2]_2MF_6$, M = Ge and Sn

$[(CH_3CH_2CH_2)_2NH_2]_2SnF_6$		$[(CH_3CH_2CH_2)_2NH_2]_2GeF_6$		
ν, cm^{-1}	Int.	ν, cm^{-1}	Int.	
685	m	680	m	cation vib.
630	w,sh			
		642	m	ν(M-F)
595	m	598	s,br	
		565	s	cation vib.
575	m			ν(M-F) or
550	s			cation vib.
531	s			ν(M-F)
505	sh	500	w	cation vib.
		476	m	ν(M-F)
455	m			ν(M-F)
		375	sh	δ(Ge-F),
		355	s	cation
		345	s	vib.
		324	sh	
360	w			
338	w			cation vib.
330	w	290	w	
308	m			δ(Sn-F)?
292	m			

(83) and most MF_6^{2-} (M = Si, Ge or Sn) species seem to fall into one of these two categories (72,83). Calculations show (83) that O_h should have two IR active bands while D_{3d} will have five.

IV.O.1. Infrared Spectrum of $[(CH_3CH_2CH_2)_2NH_2]_2GeF_6$

Table 24 shows that while some Ge-F modes can be easily assigned others remain uncertain because of ligand vibrations. There are at least five Ge-F modes in the infrared spectrum of $[(CH_3CH_2CH_2)_2NH_2]_2GeF_6$ so that the site symmetry of this molecule is undoubtedly closer to D_{3d} than O_h.

The solution spectrum of $[(CH_3CH_2CH_2)_2NH_2]_2GeF_6$ (see figure 82, appendix C) contains a single strong band at 602 cm^{-1} with a shoulder at 640 cm^{-1}. A comparison with $[(CH_3CH_2CH_2)_2NH_2]_2SnF_6$ (see figure 83, appendix C) indicates that the 640 cm^{-1} band might be a ligand vibration so that the band at 602 cm^{-1} is assigned to the t_{1u} stretching vibration expected for O_h symmetry.

IV.O.2. Infrared Spectrum of $[(CH_3CH_2CH_2)_2NH_2]_2SnF_6$

Examination of table 24 shows that the Sn-F stretching and bending vibrations in the solid state infrared spectrum of $[(CH_3CH_2CH_2)_2NH_2]_2SnF_6$ cannot be assigned with certainty.

It is clear that the site symmetry is definitely

not O_h, but this compound will have to await an X-ray structure determination to establish its true site symmetry. The solution infrared spectrum shows a single strong band at 555 cm^{-1} which is the t_{1u} stretching mode for O_h symmetry with a weak band 605 cm^{-1} which is probably a ligand vibration.

IV.P. ^{19}F NMR Spectra of SiF_4 Adducts

The ^{19}F NMR spectrum of SiF_4·Dipy at 32° (see figure 96, appendix E) showed two triplets of equal intensity at δ = 122.5, J = 12.9 ± 0.9 Hz and at δ = 144.9, J = 12.5 ± 0.7 Hz. This is the expected spectrum for a cis complex which contains two sets of non-equivalent fluorine atoms with two equivalent fluorines in each set, i.e. an A_2X_2 case.

The results obtained for SiF_4·2DMP and SiF_4·2PYROL are summarized below:

Compound	δ(ppm) at 32°	Width at Half Peak Height (Hz)	δ(T°)	Width at Half Peak Height (Hz)
SiF_4·2DMP	136.0	19.6 ± 1.7	126.8 (-79 to -81)	81.8 ± 6.0
SiF_4·2PRYOL	132.7	34.8 ± 2.6	127.0 (-82 to -83)	75.0 ± 3.2

At 32° both complexes gave only a single resonance which shifted downfield and broadened on cooling. The solutions did not freeze but became viscous. No spin coupling between silicon and fluorine nuclei (^{29}Si - ^{19}F) was observed.

The fact that these two complexes showed only a single resonance over this range cannot be interpreted conclusively. Several explanations are offered for the lone peak.

(A) A trans-$SiF_4 \cdot 2L$ structure.

(B) Fast exchange between a cis and trans structure i.e. a rapid internal rearrangement.

(C) Fast ligand exchange of the type:

$$SiF_4 \cdot 2L \rightleftharpoons SiF_4 \cdot L + L$$

(D) A SiF_6^{2-} species

(E) An ionic exchange mechanism.

Muetterties (32) studied the ^{19}F NMR spectra of $SiF_4 \cdot 2L$ complexes (with various oxygen and nitrogen monodentate donors and the single bidentate donor 8-hydroxyquinoline) over a wide temperature range and found only a single resonance. This observation was attributed to either ligand exchange or to the trans isomer of the octahedral complexes. He also claimed that SiF_4 did not form stable complexes with ketones, ethers or nitriles.

In contrast to this, our complexes are stable and in one case ($SiF_4 \cdot$Dipy) the ^{19}F NMR spectrum showed that ligand exchange did not occur at 32°. However, we cannot exclude the possibility of ligand exchange in the case of $SiF_4 \cdot$2DMP or $SiF_4 \cdot$2PYROL. Evidence for such exchange has been found in the case of $TiF_4 \cdot$2DEF (60). Ionic exchange seems unlikely since examples of this have not been found in $MF_4 \cdot 2L$ (M = Ti, Sn) adducts (32,34,35,36,38,39,60).

The chemical shift of SiF_6^{2-} in H_2O has been reported (72) to occur at +51.0 ppm relative to trifluoroacetic acid as an external reference. This corresponds to a

chemical shift of approximately 127.6 ppm with reference to $CFCl_3$. Although this is close to the chemical shift of the single resonance in the spectra of $SiF_4 \cdot 2DMP$ and $SiF_4 \cdot 2PYROL$, the broadness of the resonance indicates that it is more likely the result of exchange between two (or more) non-equivalent F sites. The broadness of the resonance at lower temperature also rules out a trans-$SiF_4 \cdot 2L$ geometry since this species should give a narrow peak. The absence of ^{29}Si-^{19}F coupling supports the idea of fluorine or ligand exchange.

IV.Q. ^{19}F NMR Spectra of GeF_4 Adducts

The ^{19}F NMR spectra of ten octahedral complexes of GeF_4 are shown in appendix E, figures 97 to 106 inclusive. The ligands were dipyridyl and tetramethylethylenediamine, both bidentate nitrogen donors and the following monodentate oxygen donors: pyrrolidinone δ-valerolactam, caprolactam, azacyclo-octanone, azacyclononanone, 2,6 dimethyl-γ-pyrone, hexamethylphosphoramide and tetramethylurea. Chemical shifts are summarized in table 25 and in figure 1.

Germanium tetrafluoride appears to form an unstable complex with the solvent chloroacetonitrile. The ^{19}F NMR spectrum of a solution of GeF_4 in this solvent showed only a singlet (δ = 128.3 ppm, T = 32°) which shifted downfield on cooling (δ = 117.7 ppm, T = -24 to -32°).

The ^{19}F NMR spectra of $GeF_4 \cdot Dipy$ and $GeF_4 \cdot TMEN$ at 32° both consisted of two triplets of equal intensity corres-

Table 25

^{19}F NMR Measurements of $GeF_4 \cdot LL$ and $GeF_4 \cdot 2L$ Complexes in Chloroacetonitrile

Compound	Temperature	Chemical Shifts in ppm Relative to External CCl_3F. Coupling Constants J in Hz				
$GeF_4 \cdot$Dipy	32°	113.1, t J_{FF} 59.0 ± 5.2				146.0, t J_{FF} 57.9 ± 4.2
$GeF_4 \cdot$TMEN	32°	130.1, t J_{FF} 55.9 ± 2.6				145.2, t J_{FF} 55.9 ± 1.8
$GeF_4 \cdot$2PRYOL	32°	115.5	116.7			127.9
	-52 to -67°	115.2, t J_{FF} 57.3 ± 3.0	117.0[a]	118.3[b]	119.2[b]	127.2, t J_{FF} 63.5 ± 3.7
$GeF_4 \cdot$2VAL	32°		112.4			120.1
	-47 to -51°	109.2, t J_{FF} 57.8 ± 4.3	111.6[a]	115.6		121.8, t J_{FF} 57.9 ± 4.1
$GeF_4 \cdot$2CAP	32°	110.9	112.9		119.8	124.3
	-59°	110.7, t J_{FF} 58.0 ± 3.1	113.5[a]	116.7[b]	117.4[b]	124.5, t J_{FF} 60.5 ± 1.1
$GeF_4 \cdot$2AZA-OCT	32°	110.7	112.5			121.4
	-47 to -55°	110.8, t J_{FF} 60.3 ± 2.8	112.8[a]	115.9[b]	116.7[b]	122.3, t J_{FF} 59.1 ± 4.5
$GeF_4 \cdot$2AZA-NON	32°			117.5		
	-52 to -54°	111.6, t[d] J_{FF} 66.2 ± 3.2	111.7[a]			120.8, t J_{FF} 59.3 ± 4.2
$GeF_4 \cdot$2DMP	32°	114.1				121.2
	-43°	113.0, t J_{FF} 58.1 + 4.0	114.3[a]			125.2, t J_{FF} 59.8 ± 3.9

Table 25 (cont'd.)

Compound	Temperature	Chemical Shifts in ppm Relative to External CCl_3F. Coupling Constants J in Hz				
$GeF_4 \cdot 2HMPA$	32°		111.2			119.9
	-42°	109.7[c], t J_{FF} 56.6 ± 4.6	111.2[d]	116.3[b]	117.1[b]	120.4, t 58.7 ± 2.2
$GeF_4 \cdot 2TMU$	32°			118.2		
	-42 to -47°	107.3, t J_{FF} 60.3 ± 2.5	113.4[a]			126.9, t J_{FF} 60.9 ± 2.1

[a] Assigned to the trans isomer.

[b] A resonance probably due to a hydrolysis impurity $[GeF_5L]^{1-}$ or $2-$ ($L = H_2O$ or CH^-).

[c] Only the first two parts of the low field triplet were observed with the third part believed to be hidden under the more intense singlet at 114.3 ppm.

[d] The middle part of the triplet was not observed because of its close proximity to the more intense singlet at 111.7 ppm.

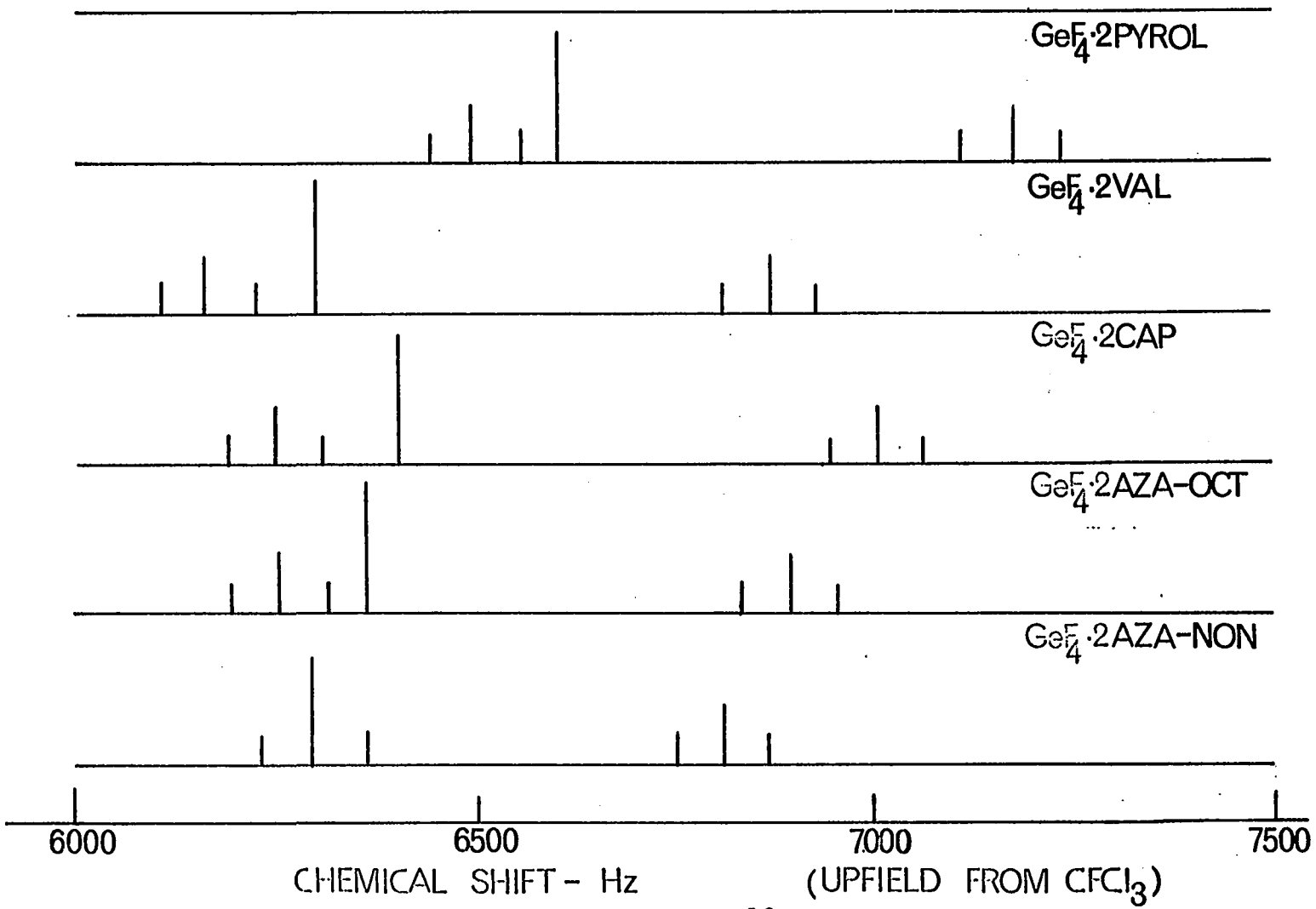

Figure 1. Diagrammatic Representation of the ^{19}F NMR Signals for $GeF_4 \cdot LL$ and $GeF_4 \cdot 2L$ Adducts in Chloroacetonitrile at Low Temperature.

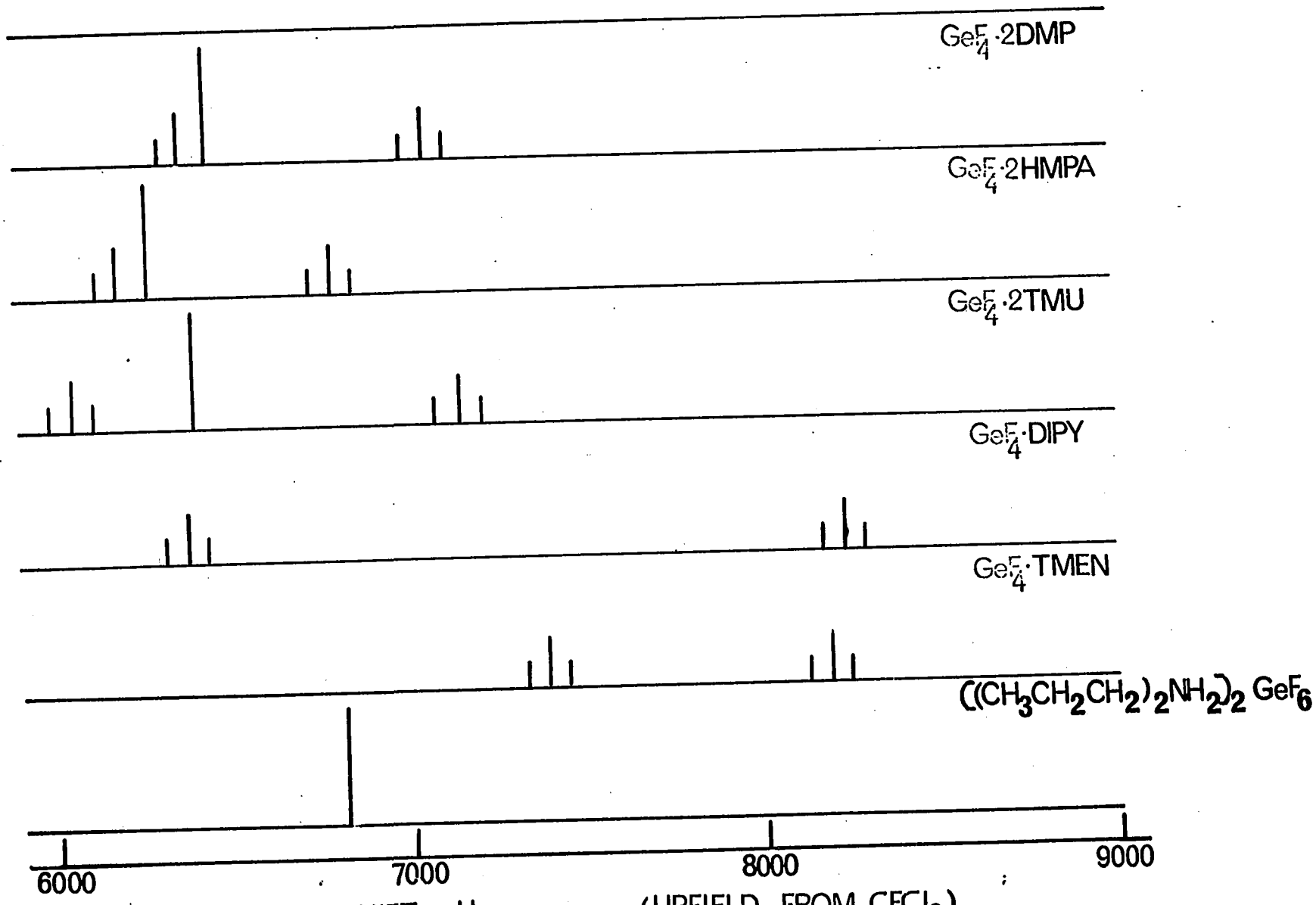

Fig. 1 (cont'd.) Diagrammatic Representation of the ^{19}F NMR Signals for $GeF_4 \cdot LL$ and $GeF_4 \cdot 2L$ Adducts in Chloroacetonitrile at Low Temperature.

ponding to the A_2X_2 pattern expected for a cis structure with a bidentate donor.

$GeF_4 \cdot 2TMU$ and $GeF_4 \cdot 2AZA\text{-}NON$ showed only a single resonance at 32°. At the same temperature $GeF_4 \cdot 2DMP$ gave two broad resonances of unequal intensity, while $GeF_4 \cdot 2VAL$ and $GeF_4 \cdot 2HMPA$ showed a single peak and a broad resonance; $GeF_4 \cdot 2PYROL$ and $GeF_4 \cdot 2AZA\text{-}OCT$ both had two broad resonances with a width at half peak height of approximately 200 Hz in addition to a single peak. In addition to the latter, $GeF_4 \cdot 2CAP$ had a second broad resonance.

On cooling each solution, two triplets of an A_2X_2 spectrum appeared, indicating that the cis isomer was present at lower temperatures and that axial-equatorial exchange was occurring in this isomer at 32° for $GeF_4 \cdot 2DMP$, $GeF_4 \cdot 2VAL$, $GeF_4 \cdot 2HMPA$, $GeF_4 \cdot 2AZA\text{-}OCT$, $GeF_4 \cdot 2PYROL$. In the case of $GeF_4 \cdot 2VAL$ and $GeF_4 \cdot 2HMPA$ one of the "missing" broad resonances is probably coincidental with the single peak at 32°.

All spectra at low temperatures also showed a single resonance which is assigned to the trans isomer for the following reasons:

(1) Since the two triplets in the spectra of all the complexes at low temperature were completely resolved, a fast exchange involving the cis isomer is eliminated.

(2) For $GeF_4 \cdot 2PYROL$, $GeF_4 \cdot 2AZA\text{-}OCT$, $GeF_4 \cdot 2CAP$, $GeF_4 \cdot 2VAL$ and $GeF_4 \cdot 2HMPA$ the chemical shift of the single peak and its intensity were unchanged over the temperature range studied.

(3) In every case the single peak appeared at a slightly higher field than the low field triplet, and its chemical shift varied according to the ligand from 111.2 to 117.0 ppm.

(4) The resonance due to hexafluorogermanate occurs at 121.8 ppm at 32°C and at 122.1 ppm at -17°C. Addition of GeF_6^{2-} to a solution of $GeF_4 \cdot 2VAL$ caused no significant change in shift or intensity of the "trans" peak. This will be discussed in detail later.

It is not clear whether the cis isomer is present at 32° for $GeF_4 \cdot 2TMU$ and $GeF_4 \cdot 2AZA\text{-}NON$. The single resonance could be the result of:

(1) Rapid exchange of axial and equatorial fluorines in the cis isomer.

(2) Pure trans isomer.

(3) Rapid ligand exchange between cis and trans isomers.

(4) Fast ligand exchange of the type: $GeF_4 \cdot 2L \rightleftharpoons GeF_4 \cdot L + L$.

Proton NMR data will be described later which appear to eliminate the last possibility. The compound is probably not solely the trans isomer at 32°, since unlike $GeF_4 \cdot 2PYROL$, $GeF_4 \cdot 2AZA\text{-}OCT$, $GeF_4 \cdot 2CAP$, $GeF_4 \cdot 2VAL$ and $GeF_4 \cdot 2HMPA$, the single peak shifts at least 5 ppm on cooling.

In the trans isomer the fluorines are all cis to the two donor molecules. For the cis-complex the F_α fluorines, which have only a cis relationship to these molecules, are assigned to the low field triplet since the peak assigned to

the trans isomer always occurs close to the low field triplet.

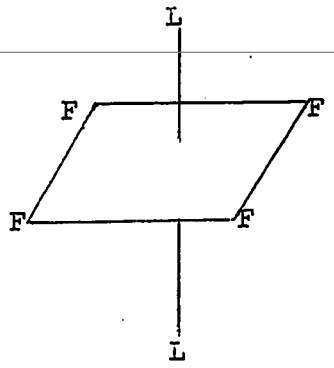

TRANS ISOMER

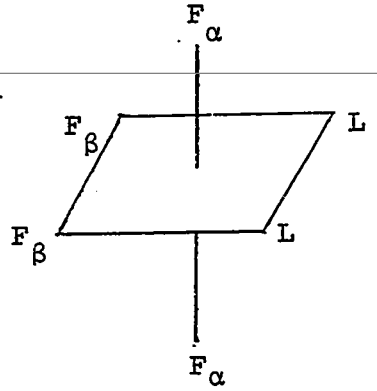

CIS ISOMER

In the case of the low temperature spectra of $GeF_4 \cdot 2L$ complexes (where L = pyrrolidinone, valerolactam, caprolactam, azacyclo-octananone), a doublet or a broad resonance appears between the singlet (due to the trans species) and the high field triplet. This is probably due to a species of the type $[GeF_5L]^{-1 \text{ or } -2}$ (where L = H_2O or OH^-) for reasons to be discussed.

Addition of GeF_6^{2-} to $GeF_4 \cdot 2VAL$ (see figure 107, appendix E) caused no significant change in the low temperature spectrum except for an increase in the intensity of the doublet plus the appearance of a new peak, possibly a quintet as shown below

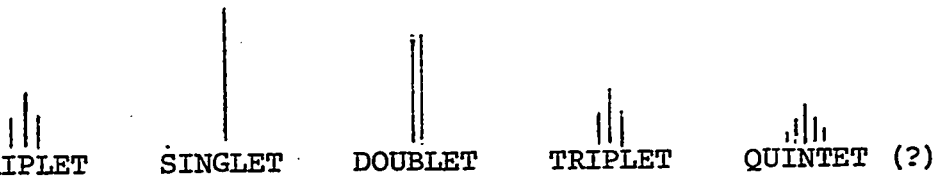

TRIPLET	SINGLET	DOUBLET	TRIPLET	QUINTET (?)
δ = 110.0	112.4	116.4	122.6	128.7

The value of J for the doublet was 31.2 $\pm$ 2.6 Hz

and because of poor resolution a value could not be established for the quintet. Species of the type $[GeF_5L]^{1-}$ or $^{2-}$ (where $L = H_2O$ or OH^-) might cause the doublet and quintet resonances. The predicted first order spectrum for this type of structure would consist of a quintet for the axial fluorine and a doublet for the equatorial fluorines. The quintet to doublet

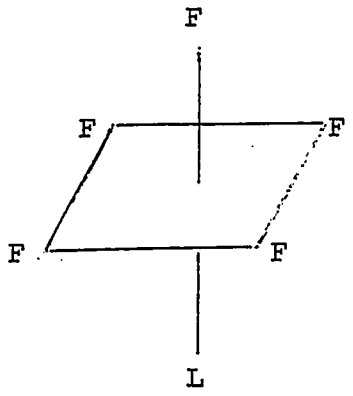

ratio would be 1 to 4. Octahedral group IVA and IVB $[MF_5X]^{1-}$ species of this type are well known (36,84).

If GeF_6^{2-} had reacted with $GeF_4 \cdot 2VAL$ to form $[GeF_5 \cdot VAL]^{1-}$,

$$GeF_6^{2-} + GeF_4 \cdot 2VAL \rightleftharpoons [GeF_5 \cdot VAL]^{1-}$$

one would have expected a decrease in intensity of the resonances of <u>cis</u>- and <u>trans</u>-$GeF_4 \cdot 2VAL$, but this was not apparent. An impurity of the type $[GeF_5(OH)]^{2-}$ or $[GeF_5(H_2O)]^{1-}$ seems more likely; these might be formed by the reaction of $GeF_4 \cdot 2L$ with a small amount of water present as an impurity.

The doublet downfield from the quintet is due to fluorines which are all cis to X in the species $[GeF_5 \cdot X]^{2-}$.

This supports the earlier hypothesis that the downfield triplet in the spectrum of all GeF_4 complexes is due to fluorines which are only cis to the ligand.

In order to explore the origin of the doublet and quintet peaks, $GeF_4 \cdot 2CAP$ was dissolved in water. Its 32° and -11° ^{19}F NMR spectra are shown in figure 108, appendix E. The following line diagram summarizes the results obtained at low temperature:

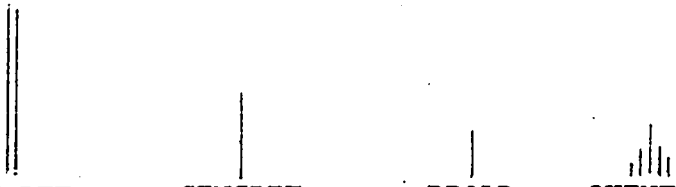

	BROAD DOUBLET	SINGLET	BROAD RESONANCE	QUINTET (?)
RESONANCE	119.2	123.4 ppm	127.2	129.5

A resonance which appears as though it may be a quintet is partially coincidental with a weak broad resonance. The coupling constant for the doublet and quintet are respectively 45.5 ± 5.0 Hz and 43.4 ± 4.6 Hz. These results support the idea of the presence of hydrolysis products in the solutions containing cis- and trans-$GeF_4 \cdot 2L$ but they are not conclusive. The single peak appearing at 123.4 ppm is presumably GeF_6^{2-} for the following reason. Dean and Evans (72) have reported the chemical shift for the latter to be 46.4 ppm to high field of external CF_3CO_2H reference. This

corresponds to a chemical shift of 123.0 ppm relative to $CFCl_3$ (the reference used in this study). The additional resonance which appears at 127.1 ppm might be due to F^- whose chemical shift varies considerably with solvent and concentration (85). The origin of the broad resonance on the low field doublet will be discussed later.

An examination of the infrared spectra indicated the $GeF_4 \cdot 2(\underbrace{CH_2)_n \overset{C=O}{\underset{N-H}{|}}}$ complexes (n = 3,4,5,6,7) could be dissolved and recovered from water unchanged. This is unusual since $MX_4 \cdot 2L$ (M = Si, Ge and Sn) complexes have been thought to undergo irreversible hydrolysis (1). The ratio of the calculated to experimental molecular weight* for $GeF_4 \cdot 2CAP$ in water was found to be 4.21 indicating that hydrolysis had occurred. Lactam complexes dissolved in water proved to be acid when tested with litmus. Since $GeF_4 \cdot 2DMP$ behaved similarly, but did not undergo exchange in D_2O, it is concluded that the acidity was not due to the N-H proton of the lactams. Since the ^1H NMR spectrum of $GeF_4 \cdot 2CAP$ in D_2O was the same as that of caprolactam itself, it seems

---

* Molecular weight measurements were performed by Beller Microanalytical Laboratories, Gottingen, Germany. The following ratios (calculated to experimental molecular weight) were also found: $GeF_4 \cdot 2DMP$, 4.13; $GeF_4 \cdot 2PYROL$, 4.09; $GeF_4 \cdot 2VAL$, 4.13; $GeF_4 \cdot 2AZA\text{-}OCT$, 4.43; $GeF_4 \cdot 2AZA\text{-}NON$, 4.23.

likely that the ligand is no longer co-ordinated in water. Perhaps an equilibrium of the following kind was established:

$$(4 + x)H_2O + 2GeF_4 \cdot 2L \rightleftharpoons [GeF_5(OH)]^{2-} + 4L + xF^- + (4 + x)H^+ + [GeF_{(3-x)}OH_{3+x}]$$

The broad resonance appearing just to low field of the doublet could be due to $[GeF_{3-x}OH_{3+x}]^{2-}$ species. Small amounts of GeF_6^{2-} are probably formed by the reaction of $[GeF_5(OH)]^{2-}$ with H^+ and F^-

$$[GeF_5(OH)]^{2-} + H^+ + F^- \longrightarrow GeF_6^{=} + H_2O$$

On the basis of solvent extraction, solubility and potentiometric studies Benoit and Place (86) were not able to demonstrate conclusively the presence of GeF_6^{2-} in acid solutions. Their results were interpreted in terms of a series of mononuclear fluorohydroxygermanium (IV) species in which the number of fluorines bound per germanium tends to a maximum of five. Our results indicate the presence of a small concentration of GeF_6^{2-} in an aqueous solution of $GeF_4 \cdot 2CAP$ and a large concentration of $[GeF_5(OH)]^{2-}$.

Muetterties (32) observed only a single resonance in the ^{19}F NMR spectra of a series of $GeF_4 \cdot 2L$ complexes (L = DMSO, DMF, py, $(CH_3)_2NC_6H_5$, and $(CH_3)_2C{=}NOH$) over a wide

temperature range. As in the case of $SiF_4 \cdot 2L$ complexes, the absence of fine structure was explained in terms of two possibilities, (1) a trans formulation or (2) fast ligand exchange of the type

$$GeF_4 \cdot 2L \rightleftharpoons GeF_4 \cdot L + L$$

At 32° our spectra clearly show the presence of only the cis isomer for GeF_4 complexes with bidentate donors. For all complexes with monodentate oxygen donors both the cis and trans isomers exist at lower temperatures, and for all except two of the eight studied there is clear evidence that both isomers are present at 32°.

At 32° the ^{19}F NMR spectrum of the 1:1 complex $GeF_4 \cdot CAP$ consisted of a single resonance (δ = 119.7 ppm). On cooling (-58 to -68°) the spectrum showed (see figure 109, appendix E) a single strong broad resonance (δ = 105.4 ppm) and two broad peaks (δ = 111.9 ppm, medium intensity and δ = 119.2 ppm, weak intensity). Possible structures for $GeF_4 \cdot CAP$ were discussed previously (see IV.M.). The ^{19}F NMR spectrum seems to eliminate the possibility of C_{2v} and C_{4v} symmetries since the former would yield two triplets of equal intensity while the latter would give a single resonance. If one assumes that the weak resonance (δ = 119.2 ppm) is an impurity and the resonances at δ = 105.4 and 111.9 ppm are an unresolved doublet and quartet, respectively, then the

spectrum may be interpreted in terms of an AX_3 pattern expected for the C_{3v} structure.

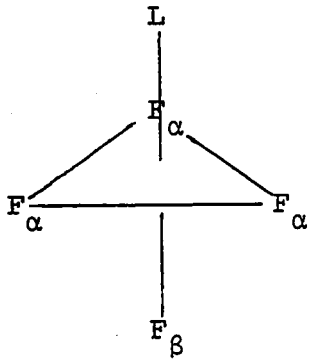

The ratio of the areas under the two main peaks is 2.5 which is consistent with the above proposal. The ratio is only approximate since the resonances are broad and overlap.

IV.R. ^{19}F NMR Spectra of SnF_4 Adducts

The ^{19}F NMR spectra of SnF_4 complexes with pyrollidinone, caprolactam, azacyclononane, 2,6-dimethyl-γ-pyrone and hexamethylphosphoramide are shown in appendix E, figures 110 to 114 inclusive. Chemical shifts are summarized in table 26 and in figure 2.

The ^{19}F NMR spectrum of a solution of SnF_4 in chloroacetonitrile showed a broad peak (δ = 156.3, T = 32°) which did not shift appreciably on cooling (δ = 156.0, T = -46 to -50°).

Complexes of SnF_4 with dipyridyl and tetramethyl-

Table 26

^{19}F NMR Measurements of $SnF_4 \cdot 2L$ Complexes in Chloroacetonitrile

Compound	Temperature °C	Chemical Shifts in ppm Relative to External CCl_3F. Coupling Constant J in Hz				
$SnF_4 \cdot 2PYROL$	32°	148.6 51.3 ± 4.3	150.2[a]	-	-	159.0 J_{FF} 48.0 ± 2.9
$SnF_4 \cdot 2CAP$	32°	143.9 J_{FF} 52.5 ± 1.8	146.7[a]	150.3[b]	151.1[b]	156.1 J_{FF} 52.0 ± 2.2
$SnF_4 \cdot 2AZA\text{-}NON$	32°	142.8 J_{FF} 49.8 ± 1.3	145.9[a]	149.8[b]	150.5[b]	155.0 J_{FF} 50.6 ± 2.4
$SnF_4 \cdot 2DMP$	32°	147.6[c] J_{FF} 53.2 ± 1.2	148.7[a]	151.4[b]	152.2[b]	157.0 J_{FF} 51.5 ± 1.7
$SnF_4 \cdot 2HMPA$	32°	149.2[c] J_{FF} 50.2 ± 1.2	150.2[a]	152.0[b]	152.8[b]	155.6 J_{FF} 49.8 ± 2.7

[a] Assigned to the trans isomer.

[b] A resonance probably due to hydrolysis impurity $[SnF_5L]^{1-}$ or $^{2-}$ ($L = H_2O$ or OH^-).

[c] Only the first two parts of the low field triplet were observed with the third part hidden under the more intense singlet.

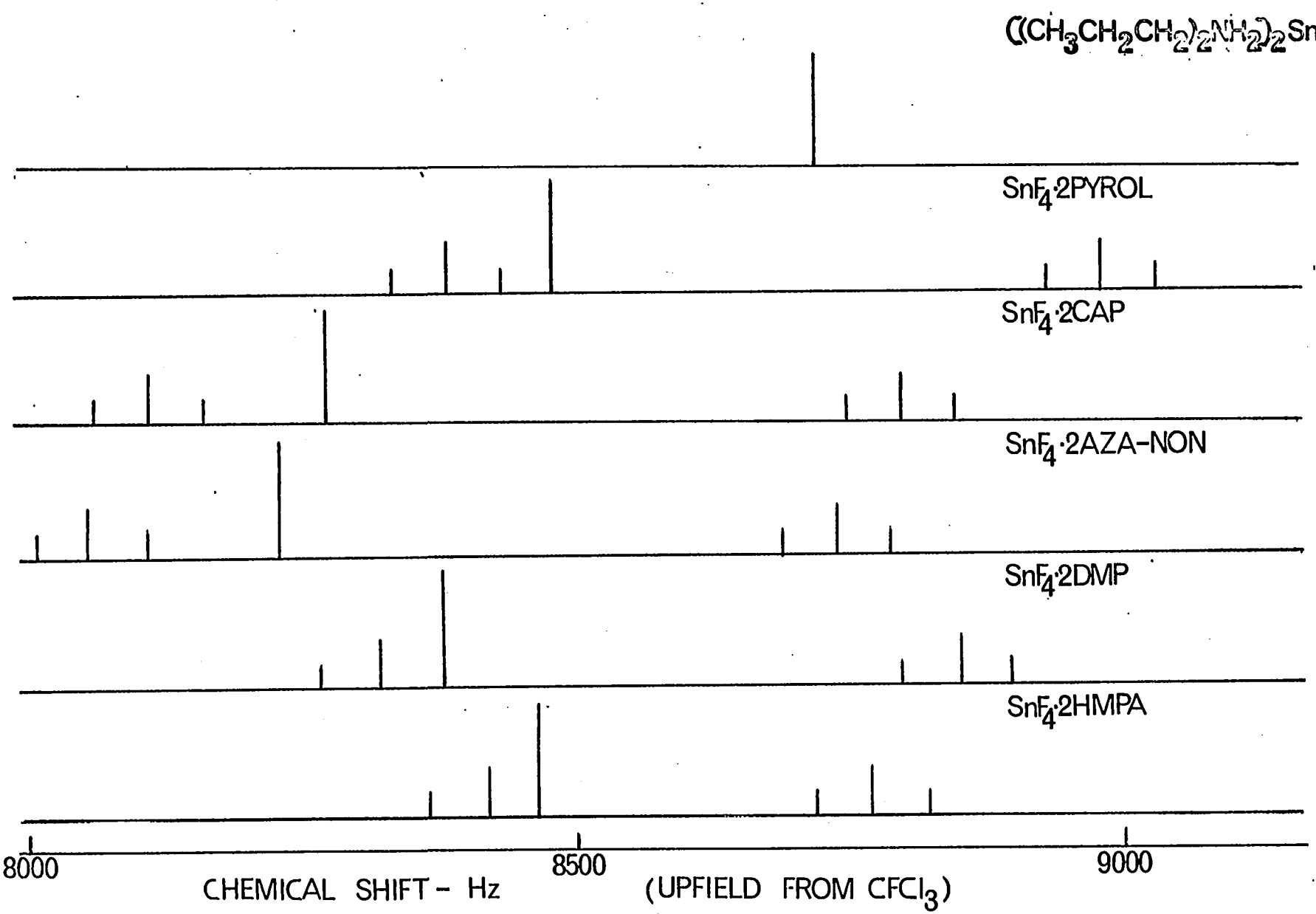

Figure 1. Diagrammatic Representation of the ^{19}F NMR Signals for $SnF_4 \cdot 2L$ Adducts in Chloroacetonitrile at 32°. (cont'd.)

ethylenediamine were insufficiently soluble in chloroacetonitrile to permit ^{19}F NMR measurements.

At 32° all spectra contained two triplets of equal intensity indicating an A_2X_2 spectrum characteristic of a cis isomer. A single narrow peak was also present in each spectrum. It is assigned to the trans isomer for the following reasons:

(1) This resonance always occurred slightly to high field of the low field triplet and its chemical shift varied according to the particular complex from 145.9 to 150.2 ppm.

(2) The chemical shift for SnF_6^{2-} was 154.9 ppm, well out of the above range. Ragsdale and Stewart (33) reported a shift for SnF_6^{2-} in EtOH of 158 ppm which is only 4 ppm removed from trans-$SnF_4 \cdot 2EtOH$ (δ = 162 ppm) and 9.5 ppm from the A_2B_2 multiplet (δ = 167.5 ppm).

The low field triplet in the spectra of the $SnF_4 \cdot 2L$ series is assigned to the fluorines which are cis to the ligand for reasons stated in the discussion of the ^{19}F NMR spectra of $GeF_4 \cdot 2L$ complexes.

Four of the five complexes studied had a doublet in their spectrum. The addition of SnF_6^{2-} to $SnF_4 \cdot 2AZA\text{-}NON$ gave a spectrum at 32° shown in figure 115, appendix E and summarized as follows:

	TRIPLET	SINGLET	DOUBLET	TRIPLET	QUINTET
δ =	141.6	144.6	148.9	153.5	161.2

The triplet and singlet portions of the spectrum did not change significantly in intensity or shift from that of $SnF_4 \cdot 2AZA\text{-}NON$. However, the doublet ($\delta$ = 148.9 ppm, $J = 44.0 \pm 0.9$ Hz) was more intense, and what was apparently a quintet (δ = 161.2 ppm, $J = 43.2 \pm 5.7$ Hz) appeared. These resonances of an AX_4 system are presumably due to a species of the type $[SnF_5L]^{1-\text{ or }2-}$ (L = H_2O or OH^-). The relative positions of the doublet and quintet corroborate the assignment of the low field triplet in $SnF_4 \cdot 2L$ complexes to fluorines which are only cis to L. The high field triplet in the solution spectrum of SnF_6^{2-} + $SnF_4 \cdot 2AZA\text{-}NON$ may have an additional resonance coincidental with the centre. This peak (δ = 153.5 ppm) is probably due to SnF_6^{2-}.

$SnF_4 \cdot 2PYROL$ and $SnF_4 \cdot 2CAP$ were insufficiently soluble in water to give a ^{19}F NMR spectrum. The spectrum of $SnF_4 \cdot 2HMPA$ (see figure 116, appendix E) consisted of a large number of resonances none of which could be identified.

Chemical shifts obtained by Dean and Evans (34) for $[SnF_5(OH)]^{2-}$ and $SnF_5(H_2O)]^{1-}$ in water are compared with our results for $[SnF_5L]^{1-\text{ or }2-}$ (L = H_2O or OH^-) in chloroacetonitrile in the table below. The former workers gave chemical shifts with respect to internal SnF_6^{2-}; these were changed to

conform to the reference used in this study, $CFCl_3$, by adding 155.9 ppm*.

COMPOUND	CHEMICAL SHIFTS (PPM) DOUBLET	QUINTET	J (Hz)
$[SnF_5(OH)]^{2-}$	146.9	146.6	29 ± 1
$[SnF_5(H_2O)]^{1-}$	153.8	160.4	No fine structure observed at 22°
$[SnF_5L]^{1-\text{ or }2-}$	148.9	161.2	44.0 ± 2.9, 43.2 ± 5.7

The chemical shift of $[SnF_5 \cdot L]^{1-\text{ or }2-}$ is closer to the value for L = H_2O, but since values for the coupling constant cannot be compared, this species cannot be positively identified.

Only the $SnF_4 \cdot 2HMPA$ complex was sufficiently soluble in $ClCH_2CN$ to show satellite peaks due to ^{119}Sn-^{19}F and ^{117}Sn-^{19}F spin-spin splitting. The ^{119}Sn-^{19}F coupling constant for this adduct together with values obtained for some other octahedral tin-fluorine complexes are summarized in the following table:

*This value obtained using the following data: SnF_6^{2-} is 79.3 ppm to high field of external CF_3CO_2H (34) and $CFCl_3$ is 76.6 ppm to low field of CF_3CO_2H (84). The sum of these values is 155.9 ppm.

COMPLEX	SOLVENT	$J(^{119}Sn-^{19}F)$	REFERENCE
TRANS-$SnF_4 \cdot 2EtOH$	EtOH	1800	33
TRANS-$[SnF_4(NCO)_2]^=$	H_2O	1648 ± 3	34
TRANS-$SnF_4 \cdot 2HMPA$	$ClCH_2CN$	1655 ± 7	This work
SnF_6^{2-}	$ClCH_2CN$	1597 ± 4	This work
SnF_6^{2-}	VARIED	1557-1603	34

Dean and Evans (34) studied a hundred different anions of the type $[SnF_{6-n}X_n]^{2-}$ and were unable to observe any simple relationship in the $J(^{119}Sn-^{19}F)$ values.

The ^{19}F NMR spectrum of $SnF_4 \cdot 2ISOQ$ (figure 117, appendix E) summarized below was more complex than those of

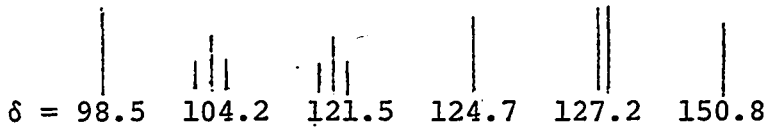

the other SnF_4 complexes. In addition to a pair of triplets (δ = 104.2 ppm, J = 50.3 ± 3.8 Hz; δ = 121.5 ppm, J = 48.8 ± 2.9 Hz) due to cis-$SnF_4 \cdot 2ISOQ$, a singlet (δ = 98.5 ppm), due to trans-$SnF_4 \cdot 2ISOQ$ and a doublet (δ = 127.2 ppm, J = 38.5 ± 5.0 Hz) which might be part of an AX_3 spectrum due to

$SnF_4 \cdot ISOQ$, there were single resonances at δ = 124.7 and 150.8 ppm which could not be assigned. Perhaps these two additional resonances are due to decomposition products of the complex in the $ClCH_2CN$ solution. The marked downfield shift of the pair of triplets by comparison with other cis-$SnF_4 \cdot 2L$ complexes is not too surprising since the ligand used is a nitrogen donor, whereas all the others were oxygen donors.

In the case of $SnF_4 \cdot 2L$ complexes with various monodentate oxygen and nitrogen donors, Muetterties (32) found evidence for only the cis isomer in the room temperature ^{19}F NMR spectra. Dean and Evans (34) found evidence for only cis-$SnF_4 \cdot 2DMSO$ supporting Muetterties's work (32). In contrast to this, Ragsdale and Stewart (33) concluded from the ^{19}F NMR spectrum of $SnF_4 \cdot 2EtOH$ that the cis structure predominated over the trans structure at room temperature while at -50° the isomers were of approximately the same concentration. Our measurements made only at 32° show clear evidence for both cis- and trans-$SnF_4 \cdot 2L$ complexes at this temperature.

IV.S. Fluorine-Fluorine Coupling Constants

The factors influencing the magnitude of indirect F-F coupling constants have been the subject of numerous studies recently (87-91). The complete Hamiltonian for electron-nuclear interactions consists of three parts (92):

(1) Electron-Orbital Term. This represents the interaction of the nuclear magnetic moment with electron orbital motion.

(2) Electron-Dipole Term. This represents the interaction of the nuclear magnetic moment with the electron spin density at a distance from the nucleus.

(3) Fermi Contact Term. This represents the interaction of the nuclear magnetic moment with the electron density at the nucleus.

The Fermi contact term is considered to make the largest contribution to proton-proton coupling, the other terms being neglected and the coupling proceeds almost entirely through the bonding electrons.

Ng and Sederholm (89) measured the magnitude of the vicinal fluorine coupling constants and suggested that two effects operate, one "through space" and the other "through bonds". The former mechanism contributes to the coupling when two fluorine atoms are close to each other. The "through bond" mechanism ceases to give a contribution when the sum of the electron-withdrawing powers of all atoms attached to the carbon-carbon skeleton becomes sufficiently large. An exact expression for "through space" coupling has

not been derived although this interaction becomes significant when the internuclear distance is less than 2.73Å (the sum of the van der Waals radii of the two interacting F atoms). Later work has both supported (90) and criticized (88,91) this proposal.

Dyer and Ragsdale (93) have discussed the factors which influence F-F coupling constants in octahedral fluorotitanate complexes. For the para-substituted pyridine-N-oxides, $Z\text{-}C_5H_4NO$, changes in Z (from an electron donating to an electron withdrawing group) which were known to have considerable influence on the σ and π bonding ability of the N → O oxygen had no effect on the $^{19}F\text{-}^{19}F$ coupling constants in the complexes $TiF_4 \cdot DMA \cdot 4ZC_5H_4NO$ and $TiF_4 \cdot TMU \cdot 4ZC_5H_4NO$. This insensitivity was thought to be caused by F-F interaction "through space" rather than "through bonds". J_{FF} for these complexes varied from 34 to 49 Hz, small when compared to geminal coupling constants for other inorganic fluorides (88). If the signs of the couplings contributed by the two different effects were opposite, the resultant cancellation would cause the small value. The authors thought a more likely explanation was that the ionic character of the Ti-F bond does not permit "through bond" interaction. Both high ionic character in the σ bonds and π donations by fluorines can be described in terms of resonating valence bond structures such as:

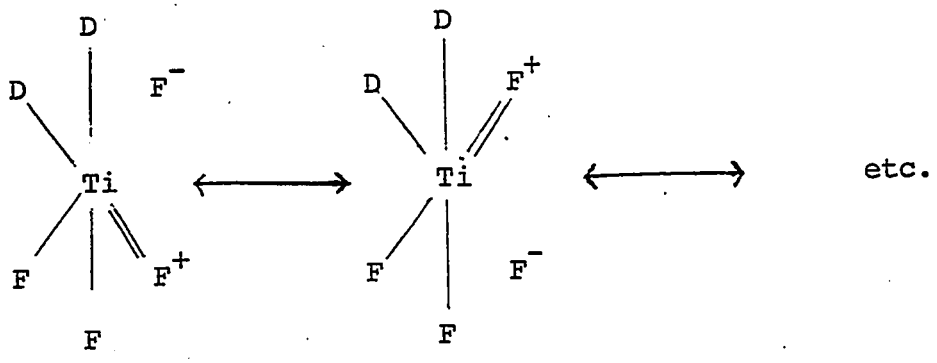

The only SiF_4 complex showing ^{19}F-^{19}F coupling was SiF_4·Dipy (J_{FF} = 12.5, 12.9 Hz). The only value in the literature is an estimate of <5Hz for the compound $(C_6H_5)_2SiF_3^-$ (94) based on the broad resonance observed at -100°. In our study of approximately ten GeF_4 adducts, values for J_{FF} ranged from 55.9 to 63.5 Hz, and in the case of six SnF_4 complexes the range was from 46.8 to 53.2 Hz. On the basis of this limited information the order is: $J_{FF}(Ge) > J_{FF}(Sn) > J_{FF}(Si)$.

Recent X-ray data (74) on the series MF_4·Dipy shows that the distance between the axial and equatorial fluorines increases as M is changed from Si to Ge to Sn. An explanation that uses solely a "through space" concept in rationalizing coupling constants does not seem justified since such reasoning should give the order: $J_{FF}(Si) > J_{FF}(Ge) > J_{FF}(Sn)$.

There are a number of variables, not necessarily independent, which could affect J_{FF} in the series MF_4·2L (M = Si, Ge, Sn). These include:

(1) The hybridization of bonds to fluorine will vary with

changes in the metal and ligand. In turn this will lead to differences in the magnitude of "through bond" coupling.

(2) Differences in ionic character of the M-F bond as the electronegativity of the metal changes. Nuclear spin coupling proceeds less effectively through ionic bonds.

(3) Variations in M-F π-bonding and the contribution to J from this effect. McConnell (95) concluded in his study of indirect F-F coupling that where p-orbitals are used in bonding significant contributions are made to the "through bond" effect by both the dipole and orbital terms of the Hamiltonian.

(4) Influence of steric factors such as F-F repulsions or ligand-fluorine interactions which might cause distortions from normal octahedral geometry.

In conclusion the observed sequence for J_{FF} cannot be explained in terms of a single phenomenon but may be the composite of many effects.

IV.T. ^{19}F Chemical Shifts

Saika and Slichter (96) suggested that changes in the ^{19}F chemical shifts were primarily dependent on changes in the local paramagnetic contribution (σ_p) to screening of the nucleus. Gross correlation of the ^{19}F chemical shift of simple binary fluorides with ionic character of the bond to fluorine has been observed by Gutowsky and Hoffman (97).

In an early study involving comparison of ^{19}F resonances in group IVa and IVb hexafluometallates, Dean and Evans (72) observed that the former were at considerably lower applied fields than the latter. These results could not be explained in terms of electronegativity differences since it is thought that the electronegativity of group IVa elements is lower than that of group IVb. The larger ionic character of an M-F bond for group IVa would imply a smaller value of σ_p thereby increasing the shielding of the fluorines and also the value H_o required for resonance. Exactly the opposite is observed. A possible explanation for the reversal is enhanced π-bonding (F → M) for metals involving group IVa (the only ones with empty d-orbitals) which would deshield the fluorines. A paramagnetic effect arising from the mixing of fluorine p-orbitals with vacant d-orbitals of group IVa under the influence of the applied magnetic field was invoked as an alternate reason (72).

Dyer and Ragsdale (37) supported the π-bonding theory on the basis of chemical shifts of cis-$TiF_4 \cdot 2EtOH$ and cis-$SnF_4 \cdot 2EtOH$. The fluorine resonances in the former are separated by 60 ppm, whereas in the latter the separation is approximately 1 ppm. Reduced $p\pi$-$d\pi$ interaction is anticipated for $Sn(4d^{10})$ compared with $Ti(3d^0)$, causing the difference in shift. The same workers interpreted chemical shifts of a series of cis-$TiF_4 \cdot DD'$ complexes on the basis of differences in π-bonding (39). Competition between a

fluorine and a ligand trans to it for available dπ-orbitals might determine the amount of (F → M) π-bonding and hence the ^{19}F chemical shifts of the complexes.

Dean and Evans (34) observed that replacement of a F in SnF_6^{2-} by a less electronegative substituent usually resulted in shifts to lower applied fields instead of the opposite expected if a local paramagnetic effect operated. They concluded that other factors were influencing the chemical shift. On the basis of some previous studies (98, 99) they suggested that van der Waals interactions might be significant; these originate from polar groups in the molecule which create permanent intramolecular electric fields. Deshielding of fluorines close to bulky groups was first suggested by Tiers (98). Boden et al. (99) studied chlorofluorobenzenes and explained the large deshielding observed for F with ortho-chlorine neighbours by comparison with those having para-chlorine neighbours as primarily the result of intramolecular van der Waals interactions between a fluorine and an ortho substituent.

In $[SnF_nX_{6-n}]^{2-}$ complexes Dean and Evans (34) observed an additivity of cis- and trans-effects on the chemical shifts and proposed that van der Waals interactions played a large part in determining shifts produced by cis substituents.

Since chemical shifts were measured for both SiF_4·Dipy and GeF_4·Dipy, it was of interest to try to explain

the differences on the basis of theoretical ideas just discussed. The former shows two triplets at δ = 122.5 and 144.9 ppm while in the latter they appear at 113.1 and 146.0 ppm. The differences in chemical shifts between F_α and F_β for Si and Ge complexes are 22.4 and 32.9 ppm respectively. If π bonding (F → M) were the reason for this difference, the resonances due to F_β should occur to low field of those due to F_α since such bonding would deshield the former relative to the latter. This is observed for various $TiF_4 \cdot 2L$ complexes. For $GeF_4 \cdot 2L$ and

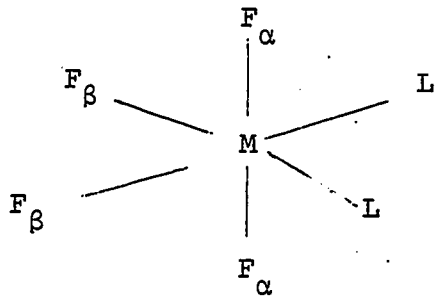

$SnF_4 \cdot 2L$ complexes (L = various oxygen donors) we have shown that the reverse is true i.e. F_α is to low field of F_β. The relative positions of F_α and F_β in group IVa and IVb might be explained in the following way. The outer d-orbitals of Si, Ge and Sn are less available for π-bonding than the inner d-orbitals of Ti so that F → M π-bonding may be considerably reduced in the former case. An inductive effect may predominate. F_β is more electronegative than a nitrogen trans to it and this may result in an electron

density shift toward this fluorine thereby shielding it relative to F_α.

A comparison of the chemical shifts of the two sets of triplets for SiF_4·Dipy (122.5, 144.9 ppm) and GeF_4·Dipy (113.1, 146.0 ppm) indicates that the high field triplets due to F_β are approximately the same while the F_α giving the low field triplets are deshielded to a greater extent for Ge. These results might be explained using Allred and Rochow's electronegativity scale (100) for group IVb elements (Si = 1.90, Ge = 2.09, Sn = 1.93). Although this scale is commonly cited, its use in explaining chemical differences between these elements has been controversial (1). Examination of the scale indicates that Ge is better able to compete with N for the electrons between them than is Si. On the other hand F is better able to withdraw electrons from Si-F than from Ge-F bonds. These two effects might counterbalance one another to the extent that the chemical shift of F_β is the same in GeF_4·Dipy and SiF_4·Dipy. In the case of F_α the electronegativity order Ge > Si explains why F_α is deshielded to a greater extent for Ge. The use of orbital electronegativities (101) does not change these proposals since the relative order of electronegativities is the same (Si = 2.25, Ge = 2.50, Sn = 2.44). Both the electronegativity scales (Allred and Rochow, orbital electronegativity) are calculated for tetrahedral geometries and the extrapolation to octahedral systems may not be valid.

For $GeF_4 \cdot$Dipy and $SiF_4 \cdot$Dipy there is no way of verifying the hypothesis that F_α resonances lie to low field of F_β without additional experimental evidence. This assignment was made by comparison with $GeF_4 \cdot 2L$ and $SnF_4 \cdot 2L$ complexes where L was an oxygen donor. Since Dipy has empty π-orbitals it is possible that (M → L) and (F → M) π bonding may be occurring. This would deshield F_β relative to F_α and the latter would appear to low field of the former in agreement with the order found for $TiF_4 \cdot 2L$ complexes. However one would still not be able to explain why the chemical shift difference between the triplets for $GeF_4 \cdot$Dipy was greater than for $SiF_4 \cdot$Dipy.

If van der Waals forces were important, the paramagnetic effect would also deshield the F_α's more in the case of Si (simply on the basis of the closer proximity of F_α to the ligand) which would cause the internal triplet difference to be greater in $SiF_4 \cdot$Dipy than in $GeF_4 \cdot$Dipy.

The shift separations of the two triplets in cis-$GeF_4 \cdot 2L$ and cis-$SnF_4 \cdot 2L$, where L is the same for both cases, is shown in the following table:

Chemical Shift Separations (ppm) for A_2X_2 Triplets

L	$GeF_4 \cdot 2L$*	$SnF_4 \cdot 2L$ (T=32°)
PYROL	12.0	10.4
CAP	13.8	12.2
AZA-NON	9.2	12.2

(continued)

*measured at temperatures varying from -42 to -67°.

Chemical Shift Separations (ppm) for A_2X_2 Triplets (cont'd.)

DMP	12.2	9.4
HMPA	10.7	6.4

Except for the case of azacyclononane where steric factors may be involved, the shift separation is always larger in the case of Ge complexes. This may be the result of one or a combination of factors:

(1) An inductive effect may occur. Assuming the electronegativity order Ge > Sn is valid, the shift separation should be greater for the former. This argument may also explain why the fluorines in Ge complexes are always more deshielded than those of Sn complexes.

(2) van der Waals forces should deshield F_α's to a greater extent in Ge complexes because of their proximity to the ligand (L).

The assumption made in comparing the internal triplet shifts is that exchange between fluorines does not occur. This may not necessarily be true and could only be tested by studying the internal triplet shift as a function of temperature.

IV.U. Proton Chemical Shifts

IV.U.1. Proton Chemical Shifts of DMP Complexes

The proton chemical shifts of 2,6 dimethyl-γ-pyrone (DMP) and its complexes $SiF_4 \cdot 2DMP$, $GeF_4 \cdot 2DMP$ and $SnF_4 \cdot 2DMP$ are shown in figures 118 to 122 of appendix E and summarized in table 27. The ligand has the following resonance forms:

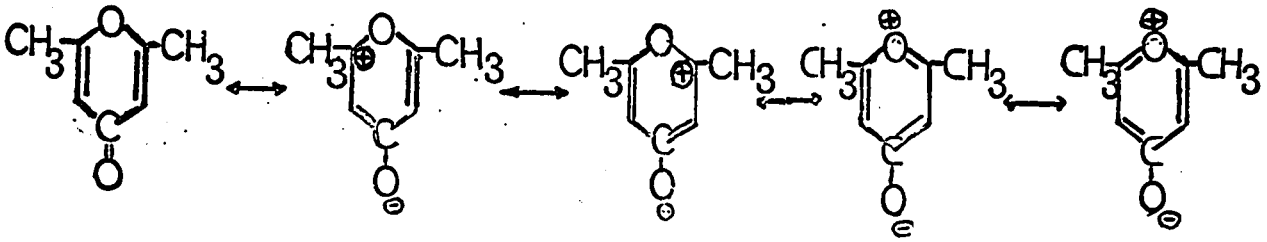

Protons H_α which are closest to the carbonyl-oxygen (site of co-ordination) are expected to show a greater change in chemical shift on complexing than the β-methyl protons which are further removed. This was observed for all the complexes.

The resonance due to H_α in the spectrum of $SnF_4 \cdot 2DMP$ at 38° is split into two lines of unequal intensity at $\delta = 7.12$,

Table 27

^1H Chemical Shift* Data for DMP and $MF_4 \cdot 2DMP$ Complexes

Compound	T	α-H	β-CH_3
2,6-dimethyl-γ-pyrone (DMP)	38°	6.0	2.2
$SiF_4 \cdot 2DMP$	38°	6.6	2.5
	-34°	6.8	2.6
	-46°	6.9	2.6
	-60°	6.9	2.6
$GeF_4 \cdot 2DMP$	38°	7.1	2.5
	-28°	7.16, 7.09, 6.91	2.6
	-60°	7.24, 7.18	2.6
$SnF_4 \cdot 2DMP$	38°	7.1, 7.0	2.5
	-34°	7.12, 7.06	2.6
$GeF_4 \cdot 2DMP$ + Excess DMP	38°	6.4	2.3
	-34°	7.2, 6.2	2.6, 2.4
$SnF_4 \cdot 2DMP$ + Excess DMP	38°	7.0, 6.0	2.5, 2.2

*in ppm relative to internal TMS.

7.05 ppm downfield from δ = 6.0 ppm for DMP itself. Cooling the solution to -34° produced no significant change. The ratio of the integrated areas of the two peaks for the β-methyl protons was the expected 1 to 3. The origin of this splitting cannot be unequivocally assigned. It is probably not the result of long range coupling of ^{1}H with either ^{119}Sn or ^{19}F since such coupling should give two resonances of the same intensity. Tanaka et al. (17), observed long range ^{119}Sn-^{1}H coupling in the case of bis(kojato)-dichloro tin (IV) complex. Since the effect was observed only for H_3 (see below*) and not for H_6, the suggestion was made that

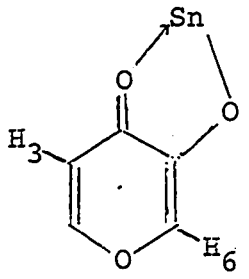

coupling occurred more strongly through the π electron system of the carbon oxygen double bond than through the electron system of the C-O single bond. Only a single peak occurred for the β-methyl protons in DMP on co-ordination and it shifted downfield approximately 0.3 ppm compared to DMP.

Since the ^{19}F NMR spectrum showed the presence of both cis- and trans-$SnF_4 \cdot 2DMP$ at 38°, it is conceivable that the α proton environment is sufficiently different in these

---

* The formula diagram shown is incomplete

isomers to give separate resonances. Proton NMR studies (46) of dichloro (β-diketonato)germanium (IV) have been interpreted in terms of the presence of both cis and trans isomers. Similarly, interpretation of ^1H NMR spectrum of bis(acetylacetonato)diacetasilicon (IV) led to the conclusion that both isomers were present. For $SnF_4 \cdot 2DMP$, either slow exchange occurred between the cis and trans isomers or the two isomers were present independently of one another. Only a study of the temperature dependence of the cis to trans isomer ratio would establish which was the case.

The ^1H NMR spectrum of $GeF_4 \cdot 2DMP$ at 38° contained a single resonance at $\delta = 7.1$ ppm which is assigned to the α protons. The addition of DMP to $GeF_4 \cdot 2DMP$ resulted in a resonance at $\delta = 6.4$ ppm. Since the latter is intermediate between co-ordinated DMP in $GeF_4 \cdot 2DMP$ and DMP alone, ligand exchange probably occurred. The ^{19}F NMR spectrum of $GeF_4 \cdot 2DMP$ indicated fluorine exchange. These results can be explained in terms of the following equilibria:

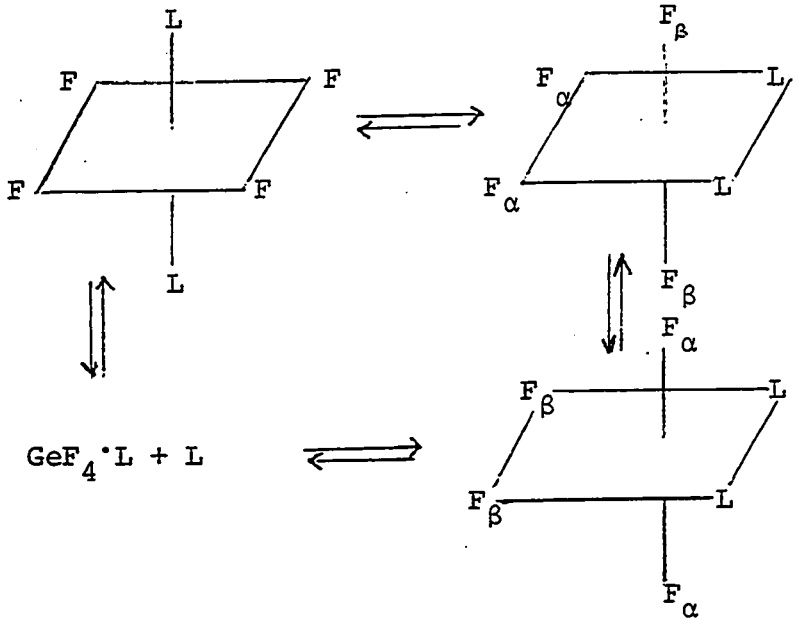

There was no evidence for fast exchange at lower temperatures. The proton spectrum of $GeF_4 \cdot 2DMP$ at -28° consisted of two resonances at δ = 7.16, 7.09 ppm which are assigned to the cis and trans isomers. There is a third peak of relatively weak intensity at δ = 6.91 ppm which we are unable to assign. At -60° there was no significant change in the spectrum except for a broadening of the weak resonance making it difficult to assign its chemical shift exactly.

At 38° the α proton resonance of DMP in $SiF_4 \cdot 2DMP$ occurred at δ = 6.6 ppm and this shifted downfield to 6.9 ppm at -60°. It was not possible to identify the species present in solution on the basis of the measured ^{19}F and ^{1}H NMR spectra.

At low temperature the order of chemical shifts for H_α in the three complexes $MF_4 \cdot 2DMP$ (M = Si, Ge and Sn) was Sn ≃ Ge > Si. The difference between Ge and Si was only 0.2 ppm. Co-ordination of DMP to the metal tetrafluoride should decrease the electron density around H_α. The contribution to the shielding of protons from the local diamagnetic effect (σ_{LD}) has been related to the electron density in the hydrogen 1s atomic orbital. If this were the only effect which influenced proton chemical shifts one might be able to deduce an order of Lewis acid strengths from the data obtained with DMP. However, we cannot exclude differences in remote shielding effects which may result from changing the central metal ion, or differences in ring current

effects for the conjugated ligand DMP which may vary with the acid as well as variation in deshielding effects caused by the proximity of the carbonyl bond. Since the relative magnitudes of the different effects are not known, no conclusion can be drawn about the relative Lewis acid strengths of the tetrafluorides.

IV.U.2. Proton Chemical Shifts of CAP Complexes

The proton chemical shifts of caprolactam (CAP) and its complexes $SiF_4 \cdot 2CAP$, $GeF_4 \cdot 2CAP$, $GeF_4 \cdot CAP$ and $SnF_4 \cdot 2CAP$ are shown in figures 123 to 128 of appendix E and summarized in table 28. At 38° the resonance due to the hydrogen on the nitrogen for CAP was broad and flat presumably the result of nuclear quadrupole relaxation effects present for nitrogen. The broad apparent triplet at δ = 3.2 ppm has been assigned (61) to the ω-CH_2 group on the N atom, and the resonance at δ = 2.4 ppm to the α-CH_2 group on the C=O bond. The remaining six protons (β, γ and δ-CH_2) are assigned to the peak centred at δ = 1.7 ppm. For caprolactam deshielding of the proton on nitrogen varies directly with concentration and inversely with temperature. Variation of the N-H chemical shift in amines has been interpreted in terms of a monomer-dimer equilibrium (102) and such an equilibrium probably occurred with CAP. The lower the temperature and the more concentrated the solution the greater the possibility of intermolecular association. On cooling the solution the resonance due to the N-H protons

Table 28

^1H Chemical Shift* Data for CAP, $MF_4 \cdot 2CAP$ and $GeF_4 \cdot CAP$

Compound	Temp.	N-H	ω-CH_2	β,γ,δ-CH_2	α-CH_2
CAPROLACTAM					
1.0M	38°	6.4	3.2	1.7	2.4
	-46°	7.4	3.2	1.7	2.4
2.0M	38°	6.5	3.2	1.7	2.4
	-46°	7.7	3.2	1.7	2.4
3.6M	38°	6.9	3.2	1.7	2.4
	-46°	7.8	3.2	1.8	2.4
$SiF_4 \cdot 2CAP$	38°	8.0	3.4	1.7	2.6
	-33.5°	8.4	3.5	1.8	2.6
$GeF_4 \cdot 2CAP$	38°	8.8	3.5	1.8	2.7
	-47°	8.9	3.6	1.9	2.8
$SnF_4 \cdot 2CAP$	38°	8.8	3.5	1.8	2.7
	-46°	9.2	3.6	1.8	2.8
$GeF_4 \cdot CAP$	38°	8.8	3.5	1.8	2.7
	0°	8.8	3.5	1.8	2.7
	-33.5°	8.8	3.5	1.8	2.7
$GeF_4 \cdot 2CAP$ + Excess CAP	38°	7.5	3.2	1.7	2.4
	-53°	9.2,8.2	3.2	1.7	2.4
$SnF_4 \cdot 2CAP$ + Excess CAP	38°	7.4	3.2	1.7	2.4
	-53°	9.5,8.0	3.2	1.7	2.4
$GeF_4 \cdot CAP$ + Excess CAP	38°	8.8,7.6	3.3	1.7	2.5
	-33.5°	9.0,7.8	3.4	1.7	2.6

*in ppm relative to internal TMS.

split into an apparent triplet. At lower temperature quadrupole relaxation effects are not as significant and may be the result of coupling with the ω-CH_2 group. The downfield shift of the N-H proton after co-ordination may be interpreted in terms of a greater contribution of resonance

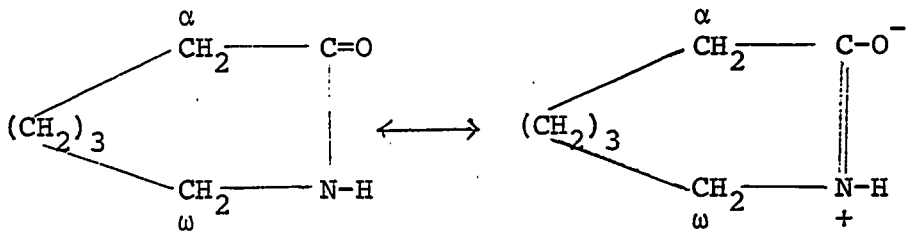

I II

structure II. At low temperature the difference in chemical shift for this proton between free and co-ordinated CAP shows an order Sn > Ge > Si which is the same as the Lewis acid strength of the metal tetrafluorides towards pyridine (103, 104). Smaller shifts were observed for the α-CH_2 and ω-CH_2 protons because these protons are less affected by co-ordination. Rapid ligand exchange occurred at 38° for $GeF_4 \cdot 2CAP$ and $SnF_4 \cdot 2CAP$, but cooling the solutions slowed this exchange. There was no evidence for ligand exchange at 38° or -33.5° for $GeF_4 \cdot 2CAP$. The ^{19}F NMR of $GeF_4 \cdot 2CAP$ at 32° did not indicate the presence of any $GeF_4 \cdot CAP$ suggesting that the equilibrium constant for the dissociation may be small.

V. Discussion and Conclusions

In the preceding section of this thesis the vibrational and ^{19}F NMR spectra of $MF_4 \cdot 2L$ complexes were discussed independently of one another. It is now necessary to compare the conclusions about geometry that were reached from each of these techniques in order to reveal the existence of any patterns. An attempt will also be made to discuss the factors which are believed to be significant in influencing stereochemistry.

V.A. General Properties of MF_4 Complexes

The most frequently occurring acceptor to donor ratio for the adducts with monodentate donors was 1:2 and with bidentate donors the expected 1:1 ratio was found. Only two adducts with a 1:1 ratio of acceptor to monodentate donor were isolated, $GeF_4 \cdot CAP$ and $GeF_4 \cdot S_4N_4$. These results are in agreement with our literature survey and Beattie's (1) which indicated the 1:2 stoichiometry is more prevalent with such donors than the 1:1 stoichiometry. It is only recently that structural assignments have been proposed for 1:1 adducts (106,107) and our results will be compared with these later on.

A comparison of tables 2, 3, and 4 indicates that SiF_4 complexes as a group were generally more unstable with respect to decomposition and sensitivity to moisture than the corresponding GeF_4 or SnF_4 complexes. An exception to

this was the Dipy series where all three complexes were stable and insensitive to atmospheric moisture.

Although exhaustive solubility tests were not made, chloroacetonitrile was the only solvent found which dissolved all of the GeF_4 and SnF_4 complexes with lactams sufficiently to permit ^{19}F NMR studies. This solvent was also used because it had no strong bands in the infrared region where Ge-F and Sn-F stretching modes occur, permitting the deduction of structures in solution.

While the ^{19}F NMR spectrum of $GeF_4 \cdot 2CAP$ in aqueous solution and the molecular weights of several $GeF_4 \cdot 2Lactam$ complexes in water were interpreted in terms of a reversible hydrolysis, these results were not conclusive and a more detailed study of the behaviour of $MF_4 \cdot 2L$ complexes in aqueous solution is necessary.

V.B. Stereochemistry of $SiF_4 \cdot 2L$ and $SiF_4 \cdot LL$ Complexes

In table 29 the geometries of $SiF_4 \cdot 2L$ and $SiF_4 \cdot LL$ complexes, as deduced from solid state vibrational spectra and ^{19}F NMR measurements, are compared. Only in the case of $SiF_4 \cdot$Dipy were conclusive results obtained. The cis isomer, which is expected in the case of a bidentate donor such as Dipy, was present in both solid and solution phases. X-ray studies on single crystals of this compound confirmed its cis molecular structure (74).

The solid state vibrational spectra of $SiF_4 \cdot 2py$

Table 29

Evidence for Stereochemistry of $SiF_4 \cdot 2L$ and $SiF_4 \cdot LL$ Adducts

Compound	Solid State Vibrational Spectra	Solution ^{19}F NMR
$SiF_4 \cdot 2py$	trans-D_{2h} (IR,R)	Not done
$SiF_4 \cdot Dipy$	cis (IR,R)	cis
$SiF_4 \cdot 2HMPA$	Inconclusive	Not done
$SiF_4 \cdot 2DMP$	cis (IR)*	Inconclusive
$SiF_4 \cdot 2PYROL$	cis (IR)*	Inconclusive
$SiF_4 \cdot 2CAP$	cis (IR)*	Not done
$SiF_4 \cdot 2AZA\text{-}NON$	cis (IR)*	Not done

*The possibility that the structure is trans-C_1 cannot be excluded (see Appendix B).

were interpreted in terms of a trans-D_{2h} structure rather than trans-D_{4h} as was previously proposed (11,105). The trans-D_{2h} symmetry agrees with X-ray results for this compound (7). It is clear that X-ray data are necessary before firm conclusions can be made about molecular symmetry. Any conclusions made on the basis of IR and Raman measurements on microcrystalline samples can only be tentative. Although solid state measurements on the SiF_4 complexes of DMP, PYROL, CAP and AZA-NON were interpreted in terms of a cis-C_{2v} structure, the possibility of the complexes being trans-C_1 cannot be excluded. It was previously assumed (11) that ligands behaved as point masses and that the number of metal-fluorine stretching modes could be used in deciding between trans-D_{4h} and cis-C_{2v} symmetries, but is now recognized that such assumptions led to incorrect conclusions. Infrared and Raman spectra of microcrystalline compounds must be interpreted with considerable caution. Correlation of the number of metal-halogen vibrational modes with possible symmetries is questionable because splitting of degenerate modes can occur with variation in site symmetry. Moreover, a band which is thought to be a lone M-X stretching mode may in fact be the composite of several bands.

Single crystal and solution Raman studies on these compounds might be helpful in establishing symmetry. Cis-$MF_4 \cdot 2L$ complexes would have two polarized vibrations in the region of ν(M-F) while trans-$MF_4 \cdot 2L$ would have only one.

Because of the low solubility of these complexes and the difficulty in growing single crystals, this technique may not be widely applicable. In addition, polarization measurements on orientated single crystals are possible at the present time only if the crystals have symmetry no lower than orthorhombic. Recently Beattie and Ozin (107) used both solution and oriented single crystal Raman measurements to support a C_{3v} structure for $GeCl_4 \cdot Me_3N$.

^{29}Si NMR measurements have been made on a series of tetrahedral Si compounds by Hunter and Reeves (50) and the results were discussed previously (see Introduction). No measurements on any octahedral Si complexes have been reported and it is suggested that these be done in the hope of revealing differences between cis and trans isomers. The difference in the displacement of ligands in cis- and trans-$SiX_4 \cdot 2L$ isomers might cause a difference in the electronic environment around Si which in turn would be reflected in the ^{29}Si chemical shift. It has been proposed that π-bonding is more effective when the ligands are cis to one another than when they are trans (114). If (L → Si) π-bonding were present for the cis isomer a ^{29}Si resonance to high field of a resonance due to a trans complex would be expected.

V.C. Stereochemistry of $GeF_4 \cdot 2L$ and $GeF_4 \cdot LL$ Complexes

The symmetries of $GeF_4 \cdot 2L$ and $GeF_4 \cdot LL$ complexes

Table 30

Evidence for Stereochemistry of $GeF_4 \cdot 2L$ and $GeF_4 \cdot LL$ Adducts

Compound	Solid State Vibrational Spectra	Solution	
		IR	^{19}F NMR
$GeF_4 \cdot 2py$	trans (IR,R)	Insufficiently soluble in $ClCH_2CN$	
$GeF_4 \cdot Dipy$	cis (IR,R)[A]	cis	cis
$GeF_4 \cdot TMEN$	cis (IR,R)[A]	cis	cis
$GeF_4 \cdot 2PYROL$	cis (IR,R)[A]	cis	cis+trans
$GeF_4 \cdot 2VAL$	cis (IR)[A]	not done	cis+trans
$GeF_4 \cdot 2CAP$	cis (IR,R)[A]	Inconclusive	cis+trans
$GeF_4 \cdot 2AZA\text{-}OCT$	cis (IR,R)[A]	not done	cis+trans
$GeF_4 \cdot 2AZA\text{-}NON$	Inconclusive (IR)	Inconclusive	cis+trans
$GeF_4 \cdot 2DMP$	Inconclusive (IR)	cis	cis+trans
$GeF_4 \cdot 2TMU$	trans (IR)[B]	cis	cis+trans
$GeF_4 \cdot 2HMPA$	trans (IR,R)[B]	cis	cis+trans

[A] The possibility that the structure is trans-C_1 cannot be excluded (see Appendix B).

[B] The possibility that the structure is cis-C_{2v} cannot be excluded.

suggested by solid state and solution vibrational spectra as well as ^{19}F NMR measurements are compared in table 30.

Vibrational and ^{19}F NMR measurements gave identical results only in the case of $GeF_4 \cdot LL$ (LL = Dipy and TMEN) where the expected cis structure was verified. Contrasting solid state and solution IR results were obtained for $GeF_4 \cdot 2HMPA$ and $GeF_4 \cdot 2TMU$. Solution IR measurements indicate that the complexes with monodentate oxygen donors were cis, whereas ^{19}F NMR measurements revealed the presence of both isomers at low temperatures. At 32° all spectra except those with TMU and AZA-NON indicated the presence of both isomers. For these two exceptions it was proposed that rapid exchange involving both isomers produced the observed single resonance. Supporting this explanation is the solution infrared spectrum of $GeF_4 \cdot 2TMU$ which indicates the presence of a cis isomer and does not exclude the possibility of a trans isomer. Since a lone M-F stretching mode due to trans-$GeF_4 \cdot 2L$ could be superimposed on bands due to the cis isomer, solution infrared results do not permit confirmation of the trans isomer. Only ^{19}F NMR measurements allow the detection of cis and trans isomers in a solution provided that rapid fluorine exchange does not occur.

Although 1:1 adducts with monodentate donors have been known for some time (106), no X-ray data are available. On the basis of vibrational spectra, adducts of the type $MCl_4 \cdot NMe_3$ (M = Si, Ge, Sn or Ti) have been assigned a C_{3v}

structure (107). Our ^{19}F NMR results for $GeF_4 \cdot CAP$ while not conclusive also suggest a C_{3v} model.

V.D. Stereochemistry of $SnF_4 \cdot 2L$ and $SnF_4 \cdot LL$ Complexes

Geometries from solid state and solution vibrational spectra and ^{19}F NMR measurements for $SnF_4 \cdot 2L$ and $SnF_4 \cdot LL$ adducts are summarized in table 31.

Solution IR and ^{19}F NMR measurements provide the most noticeable difference for $SnF_4 \cdot 2CAP$; according to the former this compound was believed to be trans while the latter indicates that cis and trans are present. Probably not just one, as was originally proposed, but three bands at 593, 580 and 560 cm^{-1} are Sn-F stretching modes. For all complexes studied by both techniques, it is clear that ^{19}F NMR measurements are more valuable than solution infrared spectra in establishing geometries. Conclusions made from the latter are unreliable and lack the preciseness of the former which are able to indicate the presence of both isomers.

A systematic Sn-119 Mössbauer spectroscopy study (see Introduction for a detailed discussion) might be of value in establishing symmetry differences in the solid state. Yeats et al. (54), have recently reviewed the literature on the application of this technique to $SnX_4 \cdot 2L$ adducts and have also made measurements on complexes with oxygen donors. In contrast to similar complexes formed by nitrogen donors (51),

Table 31

Evidence for Stereochemistry of $SnF_4 \cdot 2L$ and $SnF_4 \cdot LL$ Adducts

Compound	Solid State Vibrational Spectra	Solution	
		IR	^{19}F NMR
$SnF_4 \cdot 2py$	trans (IR)	Insufficiently soluble in $ClCH_2CN$	
$SnF_4 \cdot Dipy$	cis (IR,R)[A]	Insufficiently soluble in $ClCH_2CN$	
$SnF_4 \cdot 2PYROL$	cis (IR,R)[A]	cis	cis+trans
$SnF_4 \cdot 2CAP$	cis (IR,R)[A]	trans	cis+trans
$SnF_4 \cdot 2AZA\text{-}NON$	cis (IR,R)[A]	cis	cis+trans
$SnF_4 \cdot 2DMP$	Inconclusive	cis	cis+trans
$SnF_4 \cdot 2HMPA$	trans (IR,R)[B]	Inconclusive	cis+trans
$SnF_4 \cdot 2ISOQ$	trans (IR)[B]	Not done	cis+trans

[A] The possibility that the structure is trans-C_1 cannot be excluded (see Appendix B).

[B] The possibility that the structure is cis-C_{2v} cannot be excluded.

all oxygen donor adducts showed quadrupole splittings. Single crystal X-ray and infrared data were used to support the proposal that the splitting was the result of an imbalance of electrons in tin orbitals caused by a weak Lewis acid-Lewis base interaction for some adducts and molecular distortion due to steric hindrance by bulky groups in others. Yeats et al. (54) tentatively assigned a trans structure to $SnCl_4 \cdot 2[Cl_2(C_6H_5)PO]$ and $SnCl_4 \cdot C_4H_8O_2$ on the basis of large quadrupole splittings and suggested that other physical measurements are necessary to confirm these assignments. Further Mössbauer measurements are necessary before the value of this technique in assigning stereochemistry for $SnX_4 \cdot 2L$ complexes is established.

^{119}Sn NMR measurements have been made on a series of tetrahedral Sn compounds by Hunter and Reeves (50) and the results were discussed previously (see Introduction). Although no measurements on any octahedral Sn complexes have been reported, this technique might reveal electronic differences around the tin nucleus produced by cis and trans configurations.

Evidently, for the series $MF_4 \cdot 2L$ (M = Si, Ge and Sn) solid state and/or solution vibrational spectra do not provide a sufficiently reliable basis to distinguish between cis and trans geometries. Valuable results from infrared spectra might be obtained by comparisons with isotopically enriched (e.g. Sn^{119} in $SnX_4 \cdot 2L$) molecules in order to detect

minor shifts in metal-halogen stretching modes. On the other hand ^{19}F NMR measurements for the series $GeF_4 \cdot 2L$ and $SnF_4 \cdot 2L$ gave results which could be interpreted in a conclusive fashion.

The following table summarizes ^{19}F NMR results obtained on $MF_4 \cdot 2L$ complexes in this and Muetterties' study (32):

Table 32

Evidence for Isomers Present

Compound	This Study	Muetterties' Study
cis-$SiF_4 \cdot LL$	Yes	No
cis-$SiF_4 \cdot 2L$	No	No
trans-$SiF_4 \cdot 2L$	No	No
cis-$GeF_4 \cdot LL$	Yes	-
cis-$GeF_4 \cdot 2L$	Yes	No
trans-$GeF_4 \cdot 2L$	Yes	No
cis-$SnF_4 \cdot LL$	-	-
cis-$SnF_4 \cdot 2L$	Yes	Yes
trans-$SnF_4 \cdot 2L$	Yes	No

V.E. Factors Affecting Stereochemistry of $MF_4 \cdot 2L$ and $MF_4 \cdot LL$ Complexes

The factors influencing stereochemistry of six coordinate addition compounds of group IVa and IVb metal tetra-

halides have been the subject of numerous studies (1,32,34, 37). Since our ^{19}F NMR results for the series $MF_4 \cdot LL$ and $MF_4 \cdot 2L$ (M = Si, Ge and Sn) are significantly different from a previous study (see Table 32) it is of interest to re-investigate the factors which may affect isomerism in $MX_4 \cdot 2L$ adducts. These factors are:

1. Symmetry effects.
2. Solvation effects.
3. Steric factors.
4. Pi Bonding.

V.E.1. Symmetry Effects

Ragsdale and Dyer (37) pointed out that the cis isomer has a lower symmetry than the trans isomer and as a result the former has a higher entropy. Consequently, for the reaction:

$$\text{trans-}MF_4 \cdot 2L \rightleftharpoons \text{cis-}MF_4 \cdot 2L$$

ΔS is positive assuming that steric factors and π-bonding are not involved. A comparison of cis- and trans-$MX_4 \cdot 2L$ reveals that there are twelve equivalent geometrical structures for the former but only three for the latter. Therefore, on a statistical basis and in the absence of any other effects the cis isomer is four more times probable than the trans isomer. This corresponds to a small difference

in entropy of 2.8 e.u. between the isomers, indicating that symmetry differences have an almost negligible effect on the entropy change.

V.E.2. Solvation Effects

Because the cis to trans isomer ratio remained constant for $SnF_4Cl_2^{2-}$ in $CHCl_3$, CH_3OH and $HCONH_2$, Dean and Evans (34) concluded that solvent effects were not important. On the other hand, a study of bis(acetylacetonato)diacetatosilicon (IV) revealed that while the complex was trans in the solid state, on standing in solution, the trans isomer slowly isomerized to the cis form until equilibrium was established (49). The authors proposed that the isomerism took place because the cis isomer has the higher dipole moment and therefore is more stabilized in the polar solvent. Since the cis to trans ratio for this complex was not compared in solvents of varying dielectric constant, such a conclusion would appear to be premature.

Chloroacetonitrile has been used as a solvent in several ^{19}F NMR studies of $TiF_4 \cdot 2L$ and $TiF_4 \cdot LL'$ complexes (37,39,93). There was no evidence to suggest that these complexes dissociated in this solvent. Proton and fluorine NMR results obtained in this study of $MF_4 \cdot 2L$ (M = Si, Ge and Sn) complexes did not indicate any reaction with the solvent, $ClCH_2CN$.

The high dipole moments of amides and ureas (71) may account for the solubility of their MF_4 complexes in the polar solvent chloroacetonitrile. The question of whether the solvent preferentially stabilizes an isomer can only be answered by measuring the cis/trans ratio in a number of solvents of varying dielectric constant.

V.E.3. Steric Factors

A comparison of the cis and trans isomers indicates that there are four "nearest neighbour" fluorine-ligand (F-L) repulsions for the former and eight for the latter. Since Muetterties (32) found evidence only for the cis isomer in $SnF_4 \cdot 2L$ complexes, he proposed that L-F repulsions were structure determining. However, no significant differences between the cis and trans structures from the standpoint of (L-F) or ligand-ligand (L-L) repulsions were evident from the molecular models that he made.

Beattie (1) concluded on the basis of (L-L) repulsions that cis adducts are favoured by small ligands and trans adducts by large sterically-hindered ligands.

Dean and Evans (34) studied the cis-trans ratio in the series $SnF_4X_2^{2-}$ (X = Cl, Br and I) and found that it increased with increasing size of the halogen, supporting Muetterties' proposal that L-F repulsions were structure determining.

Dyer and Ragsdale (37) discussed the influence of

fluorine-fluorine (F-F) repulsions on stereochemistry. If present, the trans configuration would be favoured because there are five (F-F) repulsions (at 90°) in a cis complex and four in a trans complex. The authors proposed that because of the relatively small size of the fluorine such repulsion might not be significant for the case where M was Ti or Sn but would be as the size of M decreases. Using Fisher-Hirschfelder-Taylor models, Dyer and Ragsdale found no evidence for (L-L) repulsions in $TiF_4 \cdot 2[2,6(CH_3)_2C_5H_3NO]$ even though one might expect interaction between the methyl groups. They obtained ^{19}F NMR evidence for only the trans isomer of $TiF_4 \cdot 2[2,6(CH_3)_2\ C_5H_3NO]$, and for isomers of $TiF_4 \cdot 2[3,5(CH_3)_2C_5H_3NO]$ with the cis isomer predominating. Their models indicated that there was considerable steric interaction between the methyl groups and fluorine only in the former case. This in turn caused steric interaction between the fluorines (donor induced F-F repulsion) which could only be relieved by isomerization to the trans structure.

A recent X-ray study (74) on the series $MF_4 \cdot$Dipy (M = Si, Ge and Sn) does not completely support Dyer's and Ragsdale's proposal (37) that F-F repulsions should increase with decreasing size of the metal. The structures are all slightly distorted (see p.175) from the ideal cis-C_{2v} structure. The M-F bond distances decrease in the order Sn > Ge > Si. Although the F_1MF_2 angle is distorted the most for Si and least for Sn, the F_3MF_4 angle is the order Si < Ge < Sn.

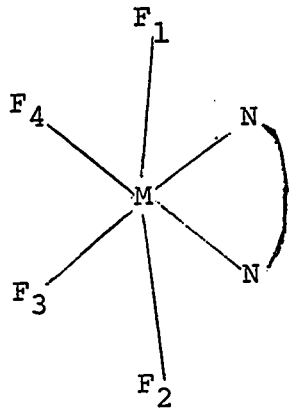

Molecular models ("Framework Molecular Models") were used to examine ligand-ligand and ligand-fluorine interactions in cis- and trans-$MF_4 \cdot 2L$ (where M = Si, Ge and Sn; L = HMPA, AZA-NON, CAP and TMU). The covalent radius of fluorine was assumed to be 0.64Å. Using X-ray data on the series $MF_4 \cdot$Dipy (M = Si, Ge and Sn) the covalent radii of the central atoms, M, were calculated to be 1.01, 1.11, and 1.30Å respectively. The van der Waals radius of fluorine used was 1.35Å.

Although the models for cis-$MF_4 \cdot 2$HMPA indicated that free rotation of the ligands was not possible because of strong L-L interactions and weak L-F interactions, stable conformers were possible. Models for the trans isomer gave similar results, although L-L interactions did not seem to be as significant as for the cis isomer.

Models for cis and trans-$MF_4 \cdot 2$AZA-NON indicated hindered rotation of the donors primarily because of strong

L-F interactions. Similar observations were made for both isomers of $MF_4 \cdot 2CAP$, although L-F interactions did not appear to be as strong as for AZA-NON complexes.

Models for cis- and trans-$MF_4 \cdot 2TMU$ indicated no L-L interactions and only weak L-F interactions.

In conclusion, our models for a few complexes indicate that where L-L and/or L-F interactions occur in $MF_4 \cdot 2L$ complexes they are not appreciably different in magnitude for the cis and trans isomer.

Many authors have implicitly assumed that the geometry in the solid state and solution are the same. The assumption that a single isomer exists in the solid state has been verified experimentally many times and intuitively it makes sense. However, our results for $MF_4 \cdot 2L$ (M = Ge and Sn) complexes indicate that cis and trans isomers are present in solution. Therefore, one may conclude that the factors which determine stereochemistry in the solid state and solution are not necessarily the same. Intermolecular forces in the solid state may influence both the molecular stereochemistry and the crystal structure. A molecule may adopt a particular stereochemistry because of crystal lattice effects. It is impossible to verify this theory without much more experimental data.

Ideally one would like to have vibrational data for $MX_4 \cdot 2L$ molecules in the gas phase where intermolecular forces and solvent effects are absent. Solution measurements (NMR

and infrared) in a non-interacting solvent represent a reasonably reliable alternative basis on which to discuss stereochemistry.

V.E.4. Pi Bonding

Comprehensive surveys of (p → d)π bonding in tetracovalent compounds (108,109) indicate considerable conflict in the literature as to existence of such bonding. A similar controversy exists for octahedral species (to be discussed later) where such bonding has been used to explain differences in stereochemistry.

In a recent discussion on P=O and S=O bond lengths Bartell et al. (110) have reviewed the literature and indicated there is considerable controversy (in experimental evidence and theoretical calculations) on outer d-orbital participation in bonding for such elements as phosphorus and sulphur. Such orbitals were often considered to be too high in energy and too diffuse to permit sufficient overlap with ligand orbitals. Calculations (111) have indicated that when the surrounding atoms are highly electronegative the effective nuclear charge of the central atom is increased thereby lowering the d-orbital energy and decreasing its size sufficiently to permit bonding. There is controversy in the literature on the question of how far 3d-orbitals extend in space and the suggestion has been made that effective overlap may occur independently of any orbital contraction

(112). An extended Huckel M.O. study by Bartell et al. (110) indicated that variation in P=O and S=O bond lengths could be accounted for even when d-orbitals are totally neglected in the M.O. calculation. However the addition of a small amount of d character to the wave function improves the correlation between overlap population and bond lengths. For $MF_4 \cdot 2L$ (M = Si, Ge and Sn) complexes, sp^3d^2 hybridization has been assumed in simple bonding discussions. Theoretical calculations are not presently sufficiently sophisticated to indicate which factors determine effective π-bonding in these complexes.

In a recent study of the relative acceptor properties of SiF_4 and $SiCl_4$ in octahedral complexes, Beattie and Ozin (113) proposed a bonding scheme in which d-orbital participation could be disregarded. It was represented pictorially by a hybrid sp orbital perpendicular to a p orbital and this combination is used to form the planar SiX_4. Perpendicular to both the sp and p orbitals is another p orbital which forms three centre molecular orbitals with the two ligand orbitals (L-M-L) as shown below

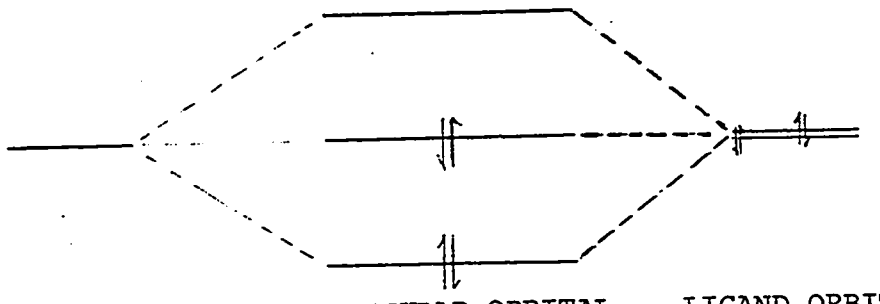

The four ligand electrons are used to fill a bonding and non-bonding molecular orbital. This explanation, while perhaps pictorially attractive, has not been verified experimentally or theoretically.

On the basis of proposals made by Jaffé (114) it is believed that for octahedral molecules $MX_4 \cdot 2L$, overlap of the halogen p-orbitals with the metal d_{xy}, d_{xz} and d_{yz} orbitals may be more effective in the cis structure where π-donation can occur into different d-orbitals than in the trans structure where there would be competition for the same d-orbital. Similarly, ligand to metal π-bonding will also stabilize the cis isomer.

Single crystal X-ray data obtained for $SiF_4 \cdot 2py$ and $SiF_4 \cdot$Dipy are summarized below:

Intramolecular Bond Lengths (Å)

		cis-$SiF_4 \cdot$Dipy	trans-$SiF_4 \cdot 2py$
Si-F	axial (average)	1.658 ± 0.004	1.64 ± 0.015
	equatorial (average)	1.631 ± 0.004	
M-N		1.977 ± 0.005	1.93 ± 0.015

For $SiF_4 \cdot$Dipy the difference between the axial and equatorial Si-F bond lengths is less than 2%. Thus while (F → Si) π-bonding may be present, the evidence indicates that it may not be significant. Similarly, a comparison of the M-N bond distance in the two complexes does not suggest

any M to N π-bonding. Such bonding would make this distance shorter for $SiF_4 \cdot$Dipy than for $SiF_4 \cdot$2py. In fact the opposite is observed.

In contrast to these results, bond distances obtained from single crystal X-ray measurements for the octahedral d^{10} complexes $GaCl_3 \cdot$Terpyridyl and cis-$GaCl_2 \cdot (Dipy)_2^+$ (115) have been interpreted in terms of a trans-effect. The Ga-Cl bond distance trans to a Ga-N was shorter by approximately 5% than a Ga-Cl trans to a Ga-Cl.

Beattie (1) concluded that π-bonding appeared to be of major importance for tin tetrafluoride since Muetterties (32) had found evidence for only the cis isomer in a ^{19}F NMR study of $SnF_4 \cdot 2L$ complexes. In our ^{19}F NMR spectra both cis and trans isomers of $SnF_4 \cdot 2L$ were clearly evident, indicating that Beattie's conclusion was based on erroneous data.

On the basis of ^{19}F NMR measurements on $TiF_4 \cdot LL'$ complexes (where L = DMA and L' = various parasubstituted pyridine-N-oxides) Ragsdale and Dyer (39) concluded that competition between fluorine and L' for the available dπ orbitals determined the amount of F → M π-bonding and the ^{19}F chemical shift. They also proposed that trans-$TiF_4 \cdot 2D$ complexes are formed only when steric interactions become large enough to overcome symmetry effects and pπ-dπ bonding which tend to stabilize the cis isomer.

The chemical shift difference for the two triplets due to cis-$TiF_4 \cdot 2EtOH$ (which we shall represent by $\delta_{F_\alpha F_\beta}$) was

approximately 60 ppm as compared to 1 ppm for cis-$SnF_4 \cdot 2EtOH$. Ragsdale and Dyer (37) interpreted this difference in terms of reduced $p\pi \rightarrow d\pi$ interaction for tin which has a d^{10} configuration. For $SnF_4 \cdot 2L$ complexes (where L = various oxygen donors) in this study $\delta_{F_\alpha F_\beta}$ was approximately 10 ppm. When this is compared to $TiF_4 \cdot 2L$ complexes (where L are oxygen donors, e.g. various substituted pyridine-N-oxides) for which $\delta_{F_\alpha F_\beta}$ varies from 20 to 25 ppm the difference is not as significant. $TiF_4 \cdot 2L$ complexes show larger $\delta_{F_\alpha F_\beta}$ values than corresponding $SnF_4 \cdot 2L$ complexes. Whether such differences in $\delta_{F_\alpha F_\beta}$ should be interpreted in terms of π-bonding is questionable in the light of the following:

(1) The internal chemical shift for the two triplets is larger in $GeF_4 \cdot$Dipy than in $SiF_4 \cdot$Dipy, even though π-bonding is generally assumed to be greater in the latter.

(2) Remote shielding may influence the fluorine chemical shifts in cis-$[SnF_{6-n}X_n]^{2-}$ (34).

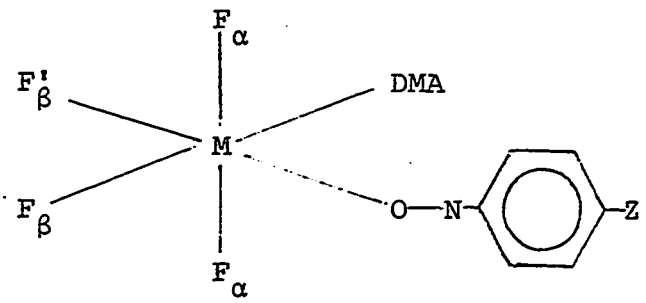

The relative π-bond ability of Si, Ge and Sn might

be determined using ^{19}F measurements on the complex shown above (where M = Si, Ge and Sn; Z = CH_3O, CH_3, H, Cl, Br, $CH_3\overset{\overset{O}{\|}}{C}O$, NO_2) continuing Ragsdale and Dyer's (31) study in which M = Ti. For each metal the variation of the chemical shift of F'_β as Z was changed would be measured. To show that the change at F'_β was the result of a π effect transmitted from Z (which is para to the NO) similar measurements would be made where Z was changed to the meta position.

The following examples in the literature illustrate the current controversy which exists about π-bonding and its influence in determining the stereochemistry of octahedral complexes. On the basis of a study of the vibrational spectra of the mixed halo species $MX_4Y_2^{2-}$ (M = Ti or Sn; X = Cl, Br or I) Clark et al. (29) concluded that most and probably all of the species possessed the cis configuration in the solid state. It was proposed that π-bonding between metal and the halogens was the major factor favouring the cis configurations over the more sterically favoured trans. In contrast to this evidence, cis and trans isomers were found for $[SnCl_2F_4]^{2-}$ and $[SnBr_2F_4]^{2-}$ using ^{19}F NMR measurements and evidence was presented which suggested that L-F repulsions (see previous discussion) were structure determining (34).

From ^1H NMR and dipole moment measurements on SnX_2L_2 complexes (where X = Cl, Br or I; L = acetylacetonate or dibenzoylmethanate), Nelson (15) concluded that these com-

plexes were cis and that tin-halogen π-bonding was the predominating factor in determining structure. In contrast to this, a recent ^1H NMR study of $Ge(acac)_2Cl_2$ (46) established the existence of cis and trans isomers and it was suggested that the difference between the ability of Cl and O to π bond might not be significant in influencing stereochemistry.

It is clear that there are numerous factors which are probably simultaneously affecting stereochemistry in group IVb metal tetrafluoride adducts. From our results it is reasonable to conclude that the factors which influence stereochemistry in the solid state may not necessarily be the same as those which predominate in solution. There seems to be no evidence that either symmetry effects, steric factors or π-bonding are singularly effective in determining geometry for $GeF_4 \cdot 2L$ or $SnF_4 \cdot 2L$ complexes in solution. It is apparent that further theoretical calculations and physical measurements are necessary in order to elucidate the factors influencing stereochemistry for group IVa and IVb octahedral complexes.

VI. Summary and Contributions to Knowledge

1. Vibrational spectra (infrared and for some cases Raman) of the following MF_4 adducts with bidentate donors were interpreted in terms of the expected cis-C_{2v} structure: SiF_4·Dipy (I), GeF_4·Dipy (II), GeF_4·TMEN (III), SnF_4·Dipy (IV). This was confirmed by ^{19}F NMR measurements on I, II and III in chloroacetonitrile solution.

2. Vibrational spectra (infrared and for some cases Raman) were used to deduce the molecular symmetries of the following MF_4·2L complexes in the solid state:

Complex	Symmetry
SiF_4·2py (V)	trans-D_{2h}
SiF_4·2DMP (VI), SiF_4·2PYROL (VII), SiF_4·2CAP (VIII) and SiF_4·2AZA-NON (IX)	cis
GeF_4·2py (X), GeF_4·2TMU (XI), and GeF_4·2HMPA (XII)	trans
GeF_4·2PYROL (XIII), GeF_4·2VAL (XIV), GeF_4·2CAP (XV) and GeF_4·2AZA-OCT (XVI)	cis
SnF_4·2py (XVII), SnF_4·2HMPA (XVIII) and SnF_4·2ISOQ (XIX)	trans
SnF_4·2PYROL (XX), SnF_4·2CAP (XXI) and SnF_4·2AZA-NON (XXII)	cis

The symmetries of SiF_4·2HMPA (XXIII), GeF_4·2AZA-NON (XXIV), GeF_4·2DMP (XXV) and SnF_4·2DMP (XXVI) could not be assigned on the basis of their vibrational spectra.

3. ^{19}F NMR measurements in chloroacetonitrile indicated

the presence of cis- and trans-$MF_4 \cdot 2L$ complexes for XI, XII, XIII, XIV, XV, XVI, XVIII, XIX, XX, XXI, XXII, XXIV, XXV and XXVI.

4. Solid state infrared and ^{19}F NMR spectra of $GeF_4 \cdot CAP$ were both compatible with a C_{3v} molecular structure.

5. The chemical shift separation between the A_2X_2 triplets in the ^{19}F NMR spectra were generally larger for cis-$GeF_4 \cdot 2L$ complexes (XII, XV, XXV, XII) than for the corresponding cis-$SnF_4 \cdot 2L$ complexes (XX, XXI, XXVI and XVIII). This was explained in terms of inductive effects and/or van der Waals forces.

6. The chemical shift separation between the A_2X_2 triplets in the ^{19}F NMR spectrum was greater for II than for I. This was attributed to differences in the electronegativities of Si and Ge.

7. Proton NMR studies on solutions of $MF_4 \cdot 2L$ complexes (M = Ge, L = DMP and CAP; M = Sn, L = CAP) indicated that fast ligand exchange occurs at 38° but not below about -30°.

8. At temperatures in the range -33 to -46° the difference between the N-H proton chemical shift of free and co-ordinated CAP (XIII, XV, XXI) showed the order Sn > Ge > Si, which is the same as the Lewis acid strength of the metal tetrafluorides to py. The change in the P=O stretching frequency in the

infrared on co-ordination in the HMPA complexes (XXIII, XII and XVIII) also followed the order Sn > Ge > Si.

9. At temperatures in the range -28 to -34° the difference in chemical shift for α-H in free and co-ordinated DMP (VI, XXV and XXVI) showed the order Sn ≃ Ge > Si. Splitting of H_α in ^1H NMR spectrum of XXV and XXVI, was attributed to environmental differences for H_α in the cis and trans isomers.

10. Infrared spectra confirmed that $GeF_4 \cdot 2$Lactam complexes could be dissolved and recovered from water unchanged. An equilibrium reaction involving a $GeF_5(OH)^{2-}$ species was proposed.

11. Molecular models of a few $MF_4 \cdot 2L$ complexes (M = Si, Ge and Sn; L = HMPA, AZA-NON, CAP AND TMU) indicated that where L-L and/or L-F interactions occur, they are not appreciably different in magnitude for the cis and trans isomer.

12. A comparison of solid state infrared spectra and ^{19}F NMR spectra in chloroacetonitrile solution indicates that the factors which determine stereochemistry in the solid state and solution may not necessarily be the same.

13. Infrared, Raman and ^{19}F NMR spectra of $MF_4 \cdot 2L$ complexes were interpreted on the basis that symmetry effects,

steric factors, and π-bonding are not singularly effective in determining geometry.

VIII. Bibliography

1. I.R. Beattie, Quart. Rev. 17, 382 (1963).
2. C.I. Branden, Acta Chem. Scand. 17, 759 (1963).
3. Y. Hermodsson, Acta Cryst. 13, 656 (1960).
4. M. Webster and H.E. Blayden, J. Chem. Soc. (A), 2443 (1969).
5. I. Lindqvist, "Inorganic Adducts of Oxo Compounds", Springer, Berlin (1963).
6. D.M. Barnhart, C.N. Caughlan and M. Ul-Haque, Inorg. Chem. 7, 1135 (1968).
7. V.A. Bain, R.C.G. Killean and M. Webster, Acta Cryst. B25, 156 (1969).
8. R. Hulme, G.T. Leigh and I.R. Beattie, J. Chem. Soc. 366 (1960).
9. I.R. Beattie, M. Milne, M. Webster, R.C.G. Killean, J.L. Lawrence and, (in part) H.E. Blayden and P.J. Jones, J. Chem. Soc. (A), 482 (1969).
10. I.R. Beattie, T. Gilson, M. Webster and G.P. McQuillan, J. Chem. Soc. 238 (1964).
11. H. Hickie, M.Sc. Thesis, McGill University (1965).
12. T.L. Brown and M. Kubota, J. Amer. Chem. Soc. 83, 332 (1961).
13. M.A. Mullins and C. Curran, Inorg. Chem. 11, 2017 (1967).
14. R.J.H. Clark and C.J. Wilkins, Spectrochim. Acta 21, 1861 (1965).
15. W.H. Nelson, Inorg. Chem. 6, 1509 (1967).
16. E. Schlemper, Inorg. Chem. 6, 2012 (1967).
17. J. Otera, Y. Kawasaki and T. Tanaka, Inorg. Chim. Acta 1, 294 (1967).
18 I.R. Beattie and L. Rule, J. Chem. Soc. 3267 (1964).

19. I.R. Beattie and L. Rule, J. Chem. Soc. 2995 (1965).

20. I.R. Beattie, G.P. McQuillan, L. Rule and M. Webster, J. Chem. Soc. 1514 (1963).

21. I.R. Beattie, M. Webster and G.W. Chantry, J. Chem. Soc. 6172 (1964).

22. J.P. Clark and C.J. Wilkins, J. Chem. Soc. (A), 871 (1966).

23. G.W.A. Fowles, D.A. Rice and R.A. Walton, Spectrochim. Acta 25A, 1035 (1969).

24. T. Tanaka, Inorg. Chim. Acta 1, 217 (1967).

25. P.V. Gogorishvilli, E.A. Kvezerelli and V.G. Lebedev, Zh. Neorgan. Khim. 11, 1755 (1966).

26. C.J. Wilkins and H.M. Haendler, J. Chem. Soc. 3174 (1965).

27. S.C. Jain and R. Rivest, J. Inorg. Nucl. Chem. 29, 2787 (1967).

28. R. Rivest, S. Singh and C. Abraham, Can. J. Chem. 45, 3137 (1967).

29. R.J.H. Clark, L. Maresca and R.J. Puddephatt, Inorg. Chem. 7, 1603 (1968).

30. I. Douek, M.J. Frazer, Z. Goffer, M. Goldstein, B. Rummer and H.A. Willis, Spectrochim. 23A, 343 (1967).

31. G.A.S. Ozin, D.Phil.Thesis, Oxford (1967).

32. E.L. Muetterties, J. Amer. Chem. Soc. 82, 1082 (1960).

33. R.O. Ragsdale and B.B. Stewart, Proc. Chem. Soc. 194 (1964).

34. P.A.W. Dean and D.F. Evans, J. Chem. Soc. (A), 1164 (1968).

35. J.W. Downing and R.O. Ragsdale, Inorg. Chem. 7, 1675 (1968).

36. R.O. Ragsdale and B.B. Stewart, Inorg. Chem. 2, 1002 (1963).

37. D.S. Dyer and R.O. Ragsdale, Inorg. Chem. 8, 1116 (1969).

38. D.S. Dyer and R.O. Ragsdale, Chem. Comm. 601 (1966).

39. D.S. Dyer and R.O. Ragsdale, Inorg. Chem. 6, 8 (1967).

40. D.C. Bradley and C.E. Holloway, Chem. Comm. 381 (1965).

41. D.C. Bradley and C.E. Holloway, J. Chem. Soc. (A), 282 (1969).

42. J.A. Smith and E.J. Wilkins, Chem. Comm. 381 (1965).

43. J.A.S. Smith and E.J. Wilkins, J. Chem. Soc. (A), 1749 (1966).

44. R.C. Fay and R.N. Lowry, Inorg. Chem. 6, 1512 (1967).

45. N. Serpone and R.C. Fay, Inorg. Chem. 6, 1835 (1967).

46. T.J. Pinnavaia, L.J. Matienzo and Y.A. Peters, Inorg. Chem. 9, 993 (1970).

47. M.M. McGrady and R.S. Tobias, J. Amer. Chem. Soc. 87, 1909 (1965).

48. Y. Kawasaki, T. Tanaka and R. Okawara, Bull. Soc. Chem. Japan 37, 903 (1966).

49. C.E. Holloway, R.L. Luonogo and R.M. Pike, J. Amer. Chem. Soc. 88, 2060 (1966).

50. B.K. Hunter and L.W. Reeves, Can. J. Chem. 46, 1399 (1968).

51. N.N. Greenwood and J.N. Ruddick, J. Chem. Soc. (A), 1679 (1967).

52. J.C. Hill, R.S. Drago and R.H. Herber, J. Amer. Chem. Soc. 91, 1944 (1969).

53. R.V. Parish and R.H. Platt, J. Chem. Soc. (A), 2145 (1969).

54. P.A. Yeats, J.R. Sams and F. Aubke, Inorg. Chem. 9, 740 (1970).

55. M.A. Mullins and C. Curran, Inorg. Chem. 7, 2584 (1968).

56. B.W. Fitzsimmons, N.J. Seeley and A.W. Smith, J. Chem. Soc. (A), 143 (1969).

57. R.R. Berrett and B.W. Fitzsimmons, J. Chem. Soc. (A) 1679 (1967).

58. J.J. Zuckerman, J. Inorg. Nucl. Chem. 29, 2191 (1967).

59. C.A. Clausen III and M.L. Good, Inorg. Chem. 9, 817 (1970).

60. D.S. Dyer and R.O. Ragsdale, J. Amer. Chem. Soc. 89, 1528 (1967).

61. R.M. Silverstein and G. Clayton Bassler "Spectrometric Identification of Organic Compounds". 2nd ed. Wiley, N.Y. (1967).

62. D. Cook, Can. J. Chem. 39, 1184 (1961).

63. J.H.S. Green, W. Kynaston and H.M. Paisley, Spectrochim. Acta 19, 549 (1963).

64. F. Herail and J. Lecomte, Compt. Rend. 262, 22 (1966).

65. O. Bohunovsky, S.C. Jain and R. Rivest, Can. J. Chem. 47, 1689 (1969).

66. Sr. Michael Schaefer and C. Curran, Inorg. Chem. 5, 265 (1966).

67. P. Cheuychit, R.A. Jones and W.F. Sasse, J. Chem. Soc. 4557 (1964).

68. S.P. Sinha, Spectrochim. Acta 20, 879 (1964).

69. P.J. Ashley and E.G. Tomble, Can. J. Chem. 47, 2587 (1969).

70. Jacques Guertin, Ph.D. Thesis, McGill University (1964).

71. "Handbook of Chemistry and Physics", 47 ed., The Chemical Rubber Co., Cleveland, Ohio (1966-67).

72. P.A.W. Dean and D.F. Evans, J. Chem. (A), 698 (1967).

73. G.C. Kulasingham, W.R. McWhinnie and R.R. Thomas, Spectrochim. Acta 22, 1365 (1966).

74. Personal communication with Dr. P. Bird, Sir George Williams University.

75. J.T. Donoghue, E. Fernandez, J.A. McMillan and D.A. Peters, J. Inorg. Nucl. Chem. 31, 1431 (1969).

76. J.T. Donoghue and R.S. Drago, Inorg. Chem. 2, 572 (1963).

77. J.T. Donoghue and R.S. Drago, Inorg. Chem. 1, 866 (1962).

78. J.T. Donoghue and R.S. Drago, Inorg. Chem. 2, 1158 (1963).

79. D. Brown, J.F. Easey and J.G.H. du Preez, J. Chem. Soc. (A), 258 (1966).

80. R.K. Gosavi, U. Agarwala and C.N. Rao, J. Amer. Chem. Soc. 89, 235 (1967).

81. G.G. Strathdee. Ph.D. Thesis, McGill University (1967).

82. G.M. Begun and A.C. Rutenberg, Inorg. Chem. 6, 2212 (1967).

83. J.E. Griffiths and D.E. Irish, Inorg. Chem. 3, 1134 (1964).

84. R.O. Ragsdale and B.B. Stewart, Inorg. Chem. 4, 740 (1965).

85. A. Carrington, F. Dravicks and M.C.R. Symons, Mol. Phys. 3, 174 (1960).

86. R.L. Benoit and J. Place, Can. J. Chem. 41, 1170 (1963).

87. L. Petrakis and C.H. Sederholm, J. Chem. Phys. 35, 1243 (1961).

88. N. Boden, J. Feeney and L.H. Sutcliffe, J. Chem. Soc. 3482 (1965).

89. S. Ng and C.H. Sederholm, J. Chem. Phys. 40, 2090 (1964).

90. K.L. Servis and Kai-Nan Fang, J. Amer. Chem. Socl 90, 6712 (1968).

91. M. Barfield and M. Karplus, J. Amer. Chem. Soc. 91, 1 (1969).

92. J.A. Pople, W.G. Schneider and H.J. Bernstein, "High Resolution Nuclear Magnetic Resonance", McGraw-Hill Book Company Inc., New York (1959).

93. D.S. Dyer and R.O. Ragsdale, J. Phys. Chem. 71, 2309 (1967).

94. F. Klanberg and E.L. Muetterties, Inorg. Chem. 7, 155 (1968).

95. H.M. McConnell, J. Chem. Phys. 24, 460 (1956).

96. A. Saika and C.P. Slichter, J. Chem. Phys. 22, 26 (1954).

97. H.S. Gutowsky and C.J. Hoffman, J. Chem. Phys. 19, 1259 (1951).

98. G. Van D. Tiers, J. Amer. Chem. Soc. 78, 2914 (1956).

99. W. Boden, J.W. Emsley, J. Feeney and L.H. Sutcliffe, Mol. Phys. 8, 133 (1964).

100. A.L. Allred and E.G. Rochow, J. Inorg. Nucl. Chem. 20, 167 (1961).

101. R. Rich "Periodic Correlations", Benjamin, N.Y. (1965).

102. J.L. Mateos, R. Centina and O. Chao, Chem. Comm. 519 (1965).

103. G. Vandrish and M. Onyszchuk, J. Chem. Soc. (A), 1970. In Press.

104. J.M. Miller and M. Onyszchuk, J. Chem. Soc. (A), 1132 (1967).

105. I.R. Beattie and M. Webster, J. Chem. Soc. 3672 (1965).

106. I.R. Beattie and T. Gilson, J. Chem. Soc. 6595 (1965).

107. I.R. Beattie and G.A. Ozin, J. Chem. Soc. (A), 370 (1970).

108. F. Glockling "The Chemistry of Germanium", Academic Press, 1969.

109. E.A.V. Ebsworth "Volatile Silicon Compounds", Pergamon Press, 1963.

110. L.S. Bartell, L.S. Su and Hsiukang Yow, Inorg. Chem. 9, 1903 (1970).

111. D.P. Carig and E.A. Magnusson, Discussions Faraday Soc., No. 26, 116 (1958).

112. D.W. Cruickshank, B.C. Webster and D.F. Mayers, J. Chem. Phys. 40, 3733 (1964).

113. I.R. Beattie and G.A. Ozin, J. Chem. Soc. (A), 2267 (1969).

114. H.H. Jaffé, J. Phys. Chem. 58, 185 (1954).

115. G. Beran, A.J. Carty, H.A. Patel and G.J. Palenik, Chem. Comm. 222 (1970).

116. R.J.H. Clark and W. Errington, J. Chem. Soc. (A), 258 (1967).

117. Yu. A. Buslaev, D.S. Dyer and R.O. Ragsdale, Inorg. Chem. 6, 2208 (1967).

118. G.W.A. Fowles and R.A. Walton, J. Chem. Soc. 4330 (1964).

119. H.J. Campbell and E.A.V. Ebsworth, J. Chem. Soc. (A), 705 (1967).

120. J.P. Guertin and M. Onyszchuk, Can. J. Chem. 47, 1275 (1969).

121. P. Clerc, Bull. Soc. Chim. France 8, 2455 (1966).

122. M.F. Farona and J.G. Grasselli, Inorg. Chem. 6, 1675 (1967).

123. R.C. Poller and D.L.B. Toley, J. Chem. Soc. (A), 1578 (1967).

124. R.C. Poller, J.N.R. Ruddick, M. Thevarasa and W.R. McWhinnie, J. Chem. Soc. (A), 2327 (1969).

125. N.W. Isaacs, C.H.L. Kennard and W. Kitching, Chem. Comm. 820 (1968).

126. T. Tanaka and K. Kamitani, Inorg. Chim. Acta 2, 175 (1968).

127. F.W.B. Einstein and B.R. Penfold, Chem. Comm. 780 (1966).

128. R.C. Poller and J.N.R. Ruddick, J. Chem. Soc. (A), 2145 (1969).

129. M. Komura, T. Tanaka and R. Okawara, Inorg. Chim. Acta 2, 321 (1968).

130. Y. Maeda and R. Okawara, J. Organometal Chem. 10, 247 (1967).

131. K. Nakamoto, "Infrared Spectra of Inorganic and Co-ordination Compounds", Wiley, N.Y. (1963).

132. R.B. Badachape, G. Hunter, L.D. McCory and J.L. Margave, Inorg. Chem. 5, 929 (1966).

133. I. Wharf and D.F. Shriver, Inorg. Chem. 8, 914 (1969).

APPENDIX A

Octahedral Compounds of Titanium, Silicon, Germanium and Tin

Abbreviations

DMSO	dimethylsulphoxide
DMSe	dimethylselenoxide
py	pyridine
Dipy	dipyridyl
TMEN	tetramethylethylenediamine
ISOQ	isoquinoline
DMA	dimethylacetamide
DMF	dimethylformamide
DEF	diethylformamide
o-phen	o-phenanthroline
DTH	dithiahexane
EtCN	ethylnitrile
MeCN	acetonitrile
Me_3N	trimethylamine
Et_2O	diethylether
Et_2S	diethylsulphide
PNO	pyridine 1-oxide
acac	acetylacetonate
bzac	dibenzoylmethanate
HOX	8-hydroxyquinoline
OX	8-hydroxyquinolate
TMU	tetramethylurea

TPP	triphenylphosphine
TPAs	triphenylarsine
TPPO	triphenylphosphine oxide
Me_2CO	acetone
DME	dimethoxyethane
Me_3P	trimethylphosphine
Me_3PO	trimethylphosphine oxide
N.C.	no conclusion

Octahedral Compounds of Titanium

Compound	Proposed Geometry	Technique	Reference
$TiF_4 \cdot 2$ ethanol	cis	^{19}F NMR	32,36
$TiF_4 \cdot 2$[2-chloropyridine]	cis	" "	35
$TiF_4 \cdot 2$[2-bromopyridine]	cis	" "	35
$TiF_4 \cdot$[DMA][4-ZC_5H_4NO] (where Z = CH_3O, CH_3, H, Cl, Br, $CH_3\overset{O}{C}O$, NO_2	cis	" "	39
$TiF_4 \cdot 2$[3,5-$(CH_3)_2C_5H_3NO$]	cis	" "	37
$TiF_4 \cdot 2$[4-$CH_3C_5H_4NO$]	cis	" "	37
$TiF_4 \cdot 2$PNO	cis	" "	38
$TiF_4 \cdot 2$(2-$C_2H_5C_5H_4NO$)	cis + trans	" "	37
$TiF_4 \cdot 2$(2-$CH_3C_5H_4NO$)	cis + trans	" "	38
$TiF_4 \cdot$[2,4-$(CH_3)_2C_5H_3NO$]	cis + trans	" "	37
$TiF_4 \cdot 2$[2,6-$(CH_3)_2C_5H_3NO$]	trans	" "	38
$TiF_4 \cdot 2$TMU + 4-$CH_3C_5H_4NO$ formed: cis+trans-$TiF_4 \cdot 2$TMU; cis-$TiF_4 \cdot 2$[4$CH_3C_5H_4NO$]; cis+trans-TiF_4[TMU][4$CH_3C_5H_4NO$]		" "	37
$TiF_4 \cdot 2$TMU	cis	" "	32
$TiF_4 \cdot 2$DMA + 2,6-$(CH_3)_2C_5H_3NO$ formed: cis-$TiF_4 \cdot 2$DMA; cis+trans-TiF_4[DMA][2,6$(CH_3)_2C_5H_3NO$]; trans-$TiF_4 \cdot 2$[2,6$(CH_3)_2C_5H_3NO$]		" "	37

Octahedral Compounds of Titanium (cont'd.)

Compound	Proposed Geometry	Technique	Reference
$TiF_4 \cdot 2TMU + 4\text{-}NO_2C_5H_4NO$ formed: cis+trans-$TiF_4 \cdot 2TMU$ cis-$TiF_4[TMU][4NO_2C_5H_4NO]$		^{19}F NMR	37
*$TiF_4 \cdot 2DMA$	cis	" "	32
$TiF_4 \cdot 2DMSO$	cis	IR	116
*$TiF_4 \cdot 2DMSO$	cis	^{19}F NMR	32
*$TiF_4 \cdot 2DMA$	cis	" "	32
*$TiF_4 \cdot 2(CH_3)_2C{=}NOH$	cis	" "	32
*$TiF_4 \cdot 2C_3H_7OH$	cis	" "	32
*$TiF_4 \cdot TMEN$	cis	" "	32
$TiF_4 \cdot 2(CH_2)_4O$	cis	" "	32
*$TiF_4 \cdot 2CH_3COOH$	cis	" "	32
*$TiF_4 \cdot 2DME$	cis	" "	32
$TiF_4 \cdot 2DME$	cis(?)	IR	116
*$TiF_4 \cdot HOX$	cis	^{19}F NMR	32
$TiF_4 \cdot HOX$	N.C.	IR	30
*$TiF_4 \cdot 2Me_2CO$	cis	^{19}F NMR	32
$TiF_4 \cdot 2DEF$	cis	" "	60
$TiF_4 \cdot 2H_2O$	cis	" "	117
$TiF_4 \cdot$o-phen	cis(?)	IR	116
$TiF_4 \cdot$Dipy	cis(?)	"	116
$TiF_4 \cdot 2py$	trans	"	116

*It is assumed that the compound was measured by this technique since details of its synthesis were given. It is not clear whether it was specifically measured since results are presented for a group of compounds.

Octahedral Compounds of Titanium (cont'd.)

Compound	Proposed Geometry	Technique	Reference
$TiCl_4 \cdot S_4N_4$	polymeric	IR	69
$TiCl_4 \cdot 2TPP$	cis	"	118
$TiCl_4 \cdot 2C_4H_8OS$	cis	"	118
$TiCl_4 \cdot Dipy$	cis	IR,Raman	23
$TiCl_4 \cdot 2HOX$	N.C.	IR	30
$TiCl_4 \cdot HOX$	five co-ordinate	"	30
$[TiCl_4 \cdot Br_2]^{2-}$	cis	IR,Raman	29
$[TiCl_4I_2]^{2-}$	cis	" "	29
$TiCl_4 \cdot$ succinimide	N.C.	IR	27
$2TiCl_4 \cdot$ phthalimide	N.C.	"	27
$TiCl_4 \cdot$ 1,2-cyclohexaphthalimide	N.C.	"	27
$TiCl_4 \cdot$ phthalamide	cis	"	30
$TiCl_2(OX)_2$	N.C.	"	30
$TiBr_4 \cdot S_4N_4$	polymeric	IR	69
$[TiBr_4Cl_2]^{2-}$	cis	IR,Raman	29
$TiBr_4 \cdot Dipy$	cis	" "	23
$TiBr_4 \cdot 2$ phthalimide	cis	IR	27
$TiBr_4 \cdot$ phthalamide	N.C.	"	27
$TiBr_4 \cdot$ succinimide	N.C.	"	27
$TiBr_4 \cdot$ 1,2-cyclohexaphthalimide	N.C.	"	27
$TiBr_2OX_2$	trans	"	30

Octahedral Compounds of Titanium (cont'd.)

Compound	Proposed Geometry	Technique	Reference
$Ti(acac)_2X_2$ (where X - CH_3O, C_2H_5O, CF_3CH_2O, Pr^iO, Bu^nO, Cl, $1/2[OCH_2C(CH_3)_2CH_2O]$)	cis	IR ^1H NMR	40,41 42,43
$Ti(acac)_2X_2$ (where X = F, Cl, Br)	cis	X-ray powder, ^1H NMR	44
$Ti(acac)_2Cl_2$	N.C.	IR	30
$Ti(acac)_2I_2$	cis + trans	^1H NMR	46
$Ti(bzac)_2X_2$ (where X = F, Cl, Br)	cis	^1H and ^{19}F NMR	45
$Ti(bzbz)X_2$ (where X = F, Cl, Br; bzbz = 1,3-diphenyl-1,3-propanedione)	cis	^1H and ^{19}F NMR	45

Octahedral Compounds of Silicon

Compound	Proposed Geometry	Technique	Reference
$SiF_4 \cdot Dipy$	cis	IR	11
$SiF_4 \cdot 2py$	N.C.	"	119
$SiF_4 \cdot 2py$	trans	"	11,105,120
$SiF_4 \cdot 2py$	trans	X-ray	7
$SiF_4 \cdot 2ISOQ$	trans	IR	11
$SiF_4 \cdot 2Me_3N$	trans	IR,Raman	107
$SiF_4 \cdot 2Me_3N$	N.C.	^{19}F NMR	32
$SiF_4 \cdot 2DMSO$	N.C.	" "	32
$SiF_4 \cdot 2DMF$	N.C.	" "	32
$SiF_4 \cdot 2(CH_3)_2NC_6H_5$	N.C.	" "	32
$SiF_4 \cdot 2HOX$	N.C.	" "	32
$SiF_4 \cdot 2TPPO$	trans	IR	105
$SiF_4 \cdot 2Me_3P$	trans	IR,Raman	107
$SiCl_4 \cdot 2py$	cis	IR	10,11
$SiCl_4 \cdot 2py$	N.C.	IR,Raman	107
$SiCl_4 \cdot 2py$	trans	X-ray	7
$SiCl_4 \cdot 2TPPO$	N.C.	IR	105
$SiCl_4 \cdot 2Me_3N$	trans	IR,Raman	107
$SiCl_2(Me_3PO)_4^{+2}$	cis	" "	105

Octahedral Compounds of Silicon (cont'd.)

Compound	Proposed Geometry	Technique	Reference
$SiBr_4 \cdot Dipy$	cis	IR	11
$SiBr_4 \cdot 2py$	cis	"	11
$SiBr_4 \cdot 2Me_3P$	trans	IR,Raman	107
$SiBr_4 \cdot 2ISOQ$	trans	IR	11
$SiBr_4 \cdot 2TPPO$	N.C.	"	10
$[SiI_2(py)_4]^{2+}$	cis	IR	10
$Si(acac)_2 \cdot (CH_3CO)_2O$	trans-solid state cis and trans solution	IR ^1H NMR	49

Octahedral Compounds of Germanium

Compound	Proposed Geometry	Technique	Reference
$GeF_4 \cdot 2py$	N.C.	^{19}F NMR	32
$GeF_4 \cdot 2py$	trans	IR	11
$GeF_4 \cdot (CH_3)_2C{=}NOH$	N.C.	^{19}F NMR	32
$GeF_4 \cdot 2DMSO$	N.C.	" "	32
$GeF_4 \cdot 2DMF$	N.C.	" "	32
$GeF_4 \cdot 2(CH_3)_2NC_6H_5$	N.C.	" "	32
$GeF_4 \cdot Dipy$	cis	IR	11
$GeF_4 \cdot TMEN$	cis	"	11
$GeF_4 \cdot 2ISOQ$	trans	"	11
$GeCl_4 \cdot 2py$	trans	IR	11
$GeCl_4 \cdot 2py$	trans	X-ray	8
$GeCl_4 \cdot Dipy$	cis	IR	20,11
$GeCl_4 \cdot o\text{-phen}$	cis	"	20
$GeCl_4 \cdot 2Me_3P$	trans	IR,Raman	107
$GeCl_4 \cdot TMEN$	cis	IR	11
$GeCl_4 \cdot 2ISOQ$	trans	"	11
$GeCl_4 \cdot 2DMF$	trans	"	11
$GeBr_4 \cdot 2py$	trans	IR	11
$GeBr_4 \cdot 2ISOQ$	trans	"	11
$GeBr_4 \cdot Dipy$	cis	"	11

Octahedral Compounds of Germanium (cont'd.)

Compound	Proposed Geometry	Technique	Reference
$Ge(acac)_2Cl_2$	cis	^1H NMR	43
$Ge(acac)_2Cl_2$	cis + trans	" "	46
$Ge(bzac)_2Cl_2$	cis	" "	43
$GeCl_2(OX)_2$	N.C.	IR	30
$[GeBr_2(NH_2NHC_6H_5)_4]Br_2$	trans	IR	25
$[GeBr_2(NH_2NHC_6H_4NO_2)_4]Br_2$	trans	"	25
$[GeI_2(NH_2NHC_6H_5)_4]I_2$	trans	IR	25
$[GeI_2(NH_2NHC_6H_4NO_2)_4]I_2$	trans	"	25
$GeI_2(OX)_2$	N.C.	"	30
$Ge(OH)_2(OX)_2$	trans-solid state cis-solution	Theoretical Calculation	121

Octahedral Compounds of Tin

Compound	Proposed Geometry	Technique	Reference
*$SnF_4 \cdot 2py$	cis	^{19}F NMR	32
$SnF_4 \cdot 2py$	trans	IR	26
$SnF_4 \cdot Dipy$	cis	"	26
$SnF_4 \cdot TMEN$	cis	"	26
$SnF_4 \cdot 2$ tetrahydrofuran	trans	"	26
$SnF_4 \cdot 2Me_3N$	trans	"	26
$SnF_4 \cdot DME$	cis	"	26
$SnF_4 \cdot 2TPPO$	cis	"	26
$SnF_4 \cdot 2PNO$	cis	"	26
*$SnF_4 \cdot 2DMSO$	cis	^{19}F NMR	32,34
*$SnF_4 \cdot 2DMF$	cis	" "	32
*$SnF_4 \cdot 2TMU$	cis	" "	32
*$SnF_4 \cdot 2(CH_3)_2C{=}NOH$	cis	" "	32
*$SnF_4 \cdot 2HOX$	cis	" "	32
$SnF_4 \cdot 2EtOH$	cis + trans	" "	38,84
$[SnF_{6-n}X_n]^{2-}$ where X = wide range of unidentate or half a bidentate ligand.	evidence generally exhibited for all possible isomers	" "	34

*It is assumed that the compound was measured by this technique since details of its synthesis were given. It is not clear whether it was specifically measured since results are presented for a group of compounds.

Octahedral Compounds of Tin (cont'd.)

Compound	Proposed Geometry	Technique	Reference
$SnCl_4 \cdot 2C_2H_5CN$	cis	IR,Raman	19
$SnCl_4 \cdot 2CH_2=CH-C\equiv N$	cis	IR	122
$SnCl_4$·o-phenylenebisdimethylamine	cis	"	116
$SnCl_4 \cdot [\{(C_6H_5)_2PO\}_2NH]$	cis-molecular or related polymer	Mössbauer	51
$SnCl_4$·1HOX	five co-ordinate	IR	30
$SnCl_4$·1HOX	cis-molecular, ligand bidentate	Mössbauer	51
$SnCl_4$·2HOX	N.C.	IR	30
$SnCl_4 \cdot N_2O_4$ formed: $[NO][SnCl_4 \cdot NO_3]$	with NO_3 acting as a bidentate ligand	IR, Mössbauer	51
$SnCl_4 \cdot 2(CH_2)_4O$	trans	IR,Raman	18,19
$SnCl_4 \cdot 2(CH_2)_4S$	trans	" "	18,19
$SnCl_4 \cdot 2Me_3N$	trans	" "	18,19
$SnCl_4 \cdot 2Et_2O$	trans	" "	18,19
$SnCl_4 \cdot 2Et_2S$	trans	IR	18
$SnCl_4$·TMEN	possibly trans bridged	"	18

Octahedral Compounds of Tin (cont'd.)

Compound	Proposed Geometry	Technique	Reference
$SnCl_4 \cdot 2TPPO$	cis	IR	26
$SnCl_4 \cdot 2TPPO$	cis	Mössbauer	54
$SnCl_4 \cdot 2py$	cis	IR	22
$SnCl_4 \cdot 2py$	trans	"	20
$SnCl_4 \cdot 2py$	trans	IR,Raman	23
$SnCl_4 \cdot 2py$	trans	X-ray	9
$SnCl_4 \cdot Dipy$	cis	IR	20,122
$SnCl_4 \cdot Dipy$	cis	IR,Raman	23
$SnCl_4 \cdot o\text{-phen}$	cis	IR	20
$SnCl_4 \cdot o\text{-phen}$	cis	IR,Raman	23
$SnCl_4 \cdot CN(CH_2)_3CN$	cis polymeric	X-ray	6
$SnCl_4 \cdot 2MeCN$	cis	IR	20,122
$SnCl_4 \cdot 2MeCN$	cis	X-ray	4
$SnCl_4 \cdot 2DMSO$	cis	X-ray	5
$SnCl_4 \cdot 2DMSO$	cis	IR	18,24
$SnCl_4 \cdot 2DMSO$	cis	Mössbauer	54
$SnCl_4 \cdot 2POCl_3$	cis	X-ray	2
$SnCl_4 \cdot 2SeOCl_2$	cis	X-ray	3
$SnCl_4 \cdot 2DMSeO$	cis	IR	24
$SnCl_4 \cdot DTH$	cis	IR,Raman	23
$SnCl_4 \cdot 2(Me_2CO)$	cis	" "	19
$SnCl_4 \cdot 2PNO$	cis	IR	26

Octahedral Compounds of Tin (cont'd.)

Compound	Proposed Geometry	Technique	Reference
$[SnCl_4I_2]^{2-}$	cis	IR,Raman	29
$[SnCl_4Br_2]^{2-}$	cis	" "	29
$SnCl_4 \cdot 2$(4,4-dipyridyl)	trans	IR	123
$SnCl_4 \cdot 2TPP$	trans	"	28
$SnCl_4 \cdot 2TPAs$	trans	"	28
$SnCl_4 \cdot 2$ salicaldehyde	N.C.	"	30
$SnCl_4 \cdot 2DMF$	cis	"	122
$SnCl_4 \cdot 2S_4N_4$	trans	"	69
$SnCl_4 \cdot 2L$	cis	Mössbauer	54
(where L = various sulphoxides, sulphones, phosphine oxides, ketones)			
$SnCl_4 \cdot 2$ phthalimide	N.C.	IR	27
$SnCl_4 \cdot$phthalamide	cis	"	27
$SnCl_4 \cdot$succinimide	N.C.	"	27
$SnCl_4 \cdot$1,2-cyclohexaphthalimide	N.C.	"	27
$SnCl_4 \cdot 2Me_3P$	trans	IR,Raman	107
$SnBr_4 \cdot 2py$	trans	X-ray	9
$SnBr_4 \cdot 2py$	cis	IR	22
$SnBr_4 \cdot$Dipy	cis	"	122
$SnBr_4 \cdot 2PNO$	cis	"	18,26
$SnBr_4 \cdot 2DMSO$	cis	"	24,18
$SnBr_4 \cdot 2HOX$	N.C.	"	30

Octahedral Compounds of Tin (cont'd.)

Compound	Proposed Geometry	Technique	Reference
$SnBr_4 \cdot 2TPPO$	cis	IR	26
$[SnBr_4I_2]^{2-}$	cis	IR,Raman	29
$[SnBr_4Cl_2]^{2-}$	cis	IR	29
$SnBr_4 \cdot 2TPAs$	trans	"	28
$SnBr_4 \cdot 2DMF$	cis	"	122
$SnBr_4 \cdot 2$ salicaldehyde	N.C.	"	30
$SnBr_4 \cdot 2MeCN$	N.C.	"	122
$SnI_4 \cdot Dipy$	cis	IR	122
$SnI_4 \cdot 2PNO$	cis	"	26
$SnI_4 \cdot 2TPPO$	cis	"	26
$[SnI_4Br_2]^{2-}$	cis	"	29
$[SnI_4Cl_2]^{2-}$	cis	IR,Raman	29
$SnI_4 \cdot 2DMSO$	cis	IR	24
$SnI_4 \cdot 2HOX$	N.C.	"	30

Compound	Proposed Geometry	Technique	Ref.
$(CH_3)_2SnCl_2 \cdot 2py$	trans methyl, cis py	IR	22, 14
$R_2SnCl_2 \cdot 2DMSO$ (where R = methyl, ethyl, phenyl)	trans R, cis DMSO	IR	10
$(CH_3)_2SnCl_2 \cdot 2DMSO$	trans methyl, cis DMSO	X-ray	125
$(CH_3)_2SnBr_2 \cdot 2DMSO$	trans methyl, trans DMSO	IR	24
$R_2SnCl_2 \cdot 2DMSeO$ (where R = methyl, ethyl, phenyl)	trans methyl, cis DmSeO	IR	126
$(CH_3)_2SnBr_2 \cdot 2DMSeO$	trans methyl, cis D,SeO	IR	126
$(CH_3)_2SnBr_2 \cdot 2DMSeO$	trans methyl, cis DMSeO	IR	126
$(CH_3)_2SnCl_2 \cdot 2TPPO$	trans methyl, cis TPPO	IR	22
$(CH_3)_2SnCl_2 \cdot 2PNO$	trans methyl, cis PNO	IR	22
$(C_4H_9)_2Sn(NCS)_2$ $(C_6H_5)_2Sn(NCS)_2$	bridged polymer butyl and phenyl groups are trans	IR Mössbauer	55
$(C_4H_9)_2Sn(NCS)(OX)$	dimer; butyl trans	Dipole Moment, Mössbauer	55
$(C_4H_9)_2Sn(NCS)_2 \cdot Dipy$	trans butyl	Dipole Moment, Mössbauer	55
$(C_6H_5)_2Sn(NCS)_2 \cdot Dipy$	cis phenyl	Dipole Moment, Mössbauer	55
$(C_4H_9)_2Sn(NCS)_2 \cdot o\text{-phen}$	trans butyl	Dipole Moment, Mössbauer	55
$(C_6H_5)_2Sn(NCS)_2 \cdot o\text{-phen}$	cis phenyl	Dipole Moment, Mössbauer	55
$[(CH_3)_2SnCl_2 \cdot terpyridyl]^+$	trans methyl distorted octahedral	X-ray	127

Compound	Inferred Arrangement of Hydrocarbon Groups	Technique	Ref.
$(C_4H_9)_2SnX_2 \cdot$o-phen (where X = Cl, Br, I)	trans	Dipole Moment	13
$(C_4H_9SnX_2 \cdot$Dipy (where X = Cl, Br, I)			
$R_2SnX_2 \cdot$Dipy			
$R_2SnX_2 \cdot$o-phen (where R = methyl, ethyl, butyl; X = Cl, Br, I)			
$(C_6H_5)_2SnCl_2 \cdot$Dipy	trans	Mössbauer	55
$(C_6H_5)_2SnCl_2 \cdot$o-phen			
$(CH_3)_2SnCl_2 \cdot$Dipy	trans	IR	22
$R_2SnX_2L_2$ (where R = Ph; X = Cl, Br, I; L = py, 1/2 Dipy etc.) (where R = Et; X = Cl, Br; L = py, 1/2 Dipy etc.)	trans	Mössbauer	124
$R_2SnCl_2 \cdot$4,4-dipyridyl (where R = butyl, phenyl, octyl)	N.C.	IR	123
$(C_4H_9)_2SnCl_2 \cdot$2[4-phenylpyridine]	N.C.	IR	123

Compound	Proposed Geometry	Technique	Ref.
$(C_6H_5)_2Sn(OX)_2$	cis	Dipole Moment, Mössbauer	55, 128
$(C_4H_9)_2Sn(OX)_2$	cis	Dipole Moment, Mössbauer	55 128
$(C_4H_9)_2Sn(OX)_2$	N.C.	IR	30
$(C_2H_5)_2Sn(OX)_2$	N.C.	IR	30
R_2SnL_2 (where R = methyl or phenyl; L = acac, bzac, OX, etc.)	trans R	IR, Raman ^1H NMR	47
$(CH_3)_2Sn$ bis(tropolonate)	trans methyl distorted octahedral	IR, ^1H NMR	129
$(CH_3)_2Sn$ bis(acetate)	trans methyl distorted octahedral	IR, ^1H NMR	130
$(CH_3)_2Sn$ bis(kojato)	trans methyl	IR, ^1H NMR	17
$Sn(acac)_2L_2$ (where L = Cl, Br, I)	cis	Dipole Moment, ^1H NMR	15, 42
$Sn(acac)_2L_2$ (where L =Cl, Br, I)	N.C.	IR	30
$Sn(bzac)_2L_2$	cis	Dipole Moment, ^1H NMR	15, 42
SnX_2L_2 (where X = Cl, Br; HL = salicaldehyde)	N.C.	IR	30

APPENDIX B

Point Groups and Fundamental Vibrational Frequencies of $MF_4 \cdot 2L$ Adducts

Previous studies of the solid state infrared spectra of complexes of the type $MF_4 \cdot 2L$ (M = Si, Ge or Sn; X = F, Cl, Br or I) have been based on the assumption that the ligands are point masses so that the symmetries can be represented ideally as either trans-D_{4h} or cis-C_{2v} (1,11). Only recently has this simplifying assumption been questioned and other molecular symmetries considered (9,81).

If the ligands occupy rigid positions in the solid, the following point groups are possible: trans-D_{4h}, trans-D_{2h}, trans-D_{2d}, trans-C_{2h}, trans-C_i, trans-C_2, trans-C_1, cis-C_{2v} and cis-C_1, depending upon the symmetries of the ligands and their orientations in the octahedral configuration, as shown in figures 1 to 7 inclusive. Rather than represent the ligands themselves in the diagrams, the plane and/or planes in which the ligands lie are shown together with the symmetry elements. Some of the geometries are valid only for the few cases where the ligand is both planar and symmetrical (e.g. pyridine); nevertheless, they are presented to illustrate how subtle differences in geometry can affect the number and spectral activity of bands.

Trans-C_1 and cis-C_1 would obviously occur only when the ligands are not planar and the molecule possesses only a

C_1 axis.

Table 33 shows how the six stretching modes for molecules of the type $MX_4 \cdot 2L$ in the various point groups are related to the fundamental stretching modes for MX_6^{2-} (O_h). The fundamental modes for the latter are well known (131) and the frequencies for the case X = F, M = Si, Ge or Sn are given in table 34. Table 35 shows which of the six modes belong to ν(M-F) and which to ν(M-L) for a particular symmetry. Also included in this table are the various deformation modes. The derivation of the various types and numbers of modes for the cases <u>cis</u>-C_{2v} and <u>trans</u>-D_{4h} have been discussed in detail previously (11); the same method has been used for other point groups in table 35.

These rigid structures in the solid state would persist in solution only if free rotation about the M-L bond were completely restricted. Molecular models indicate that there is little or no steric hindrance to free rotation for base complexes of the type $MF_4 \cdot 2L$ (32). In this case the $MX_4 \cdot 2L$ complex should be either <u>trans</u>-D_{4h} or <u>cis</u>-C_{2v}.

Examination of table 35 shows that <u>trans</u>-D_{4h} and <u>trans</u>-D_{2d} have a single IR active M-F stretching mode, <u>trans</u>-D_{2h}, <u>trans</u>-C_{2h}, and <u>trans</u>-C_i have two, while <u>trans</u>-C_2, <u>trans</u>-C_1, <u>cis</u>-C_{2v} and <u>cis</u>-C_1 have four.

Adducts with <u>trans</u>-D_{4h}, <u>trans</u>-D_{2h}, <u>trans</u>-C_{2h}, or <u>trans</u>-C_i symmetry possess a centre of symmetry. On the other

hand trans-D_{2d}, trans-C_2, trans-C_1, cis-C_{2v} and cis-C_1 do not. For molecules that possess a centre of symmetry there will be no fundamentals which are common in the infrared and Raman spectra. Thus, infrared and Raman spectra are useful in distinguishing between centrosymmetric and non-centrosymmetric structures.

It is not possible to determine the exact symmetry of an $MX_4 \cdot 2L$ complex from infrared and Raman measurements on microcrystalline samples. The observation of four infrared active ν(M-X) fundamentals in the solid state spectra previously attributed to cis-C_{2v} symmetry (1) might equally arise from trans-C_2, trans-C_1, or cis-C_1 configurations. However, for complexes in solution and provided there is free rotation about the M-L bonds, only one infrared active ν(M-X) band is expected for trans-D_{4h} symmetry and four for cis-C_{2v}. Only in this case is it possible to distinguish between cis and trans octahedral geometries.

TABLE 33

CORRELATION TABLE FOR O_h, D_{4h}, D_{2d}, D_{2h}, C_{2h}, C_{2v}, C_i AND C_2 SYMMETRIES WITH RESPECT TO THE STRETCHING MODES

O_h	trans-D_{4h}	trans-D_{2d}	trans-D_{2h}	trans-C_{2h}	trans-C_i	cis-C_{2v}	trans-C_2	cis- and trans-C_1
a_{1g}(R)	a_{1g}(R)	a_1(R)	a_g(R)	a_g(R)	a_g(R)	a_1(IR,R)	a(IR,R)	a(IR,R)
	a_{2u}(N.A.)	b_2(IR,R)	b_{1u}(IR)	a_u(IR)		a_1(R,IR)	2a(IR,R)	3a(IR,R)
t_{1u}(IR)	e_u(IR)	e(IR,R)	b_{2u}(IR)	$2b_u$(IR)	$3a_u$(IR)	b_1(R,IR)	b(IR,R)	
			b_{3u}(IR)			b_2(R,IR)		
e_g(R)	a_{1g}(R)	a_1(R)	a_g(R)	$2a_g$(R)	$2a_g$(R)	a_1(IR,R)	a(IR,R)	2a(IR,R)
	b_{1g}(R)	b_1(R)	b_{1g}(R)			b_1(IR,R)	b(IR,R)	

TABLE 34

FUNDAMENTAL VIBRATION FREQUENCIES OF MX_6^{2-} †

ANION	ν(M-F) A_{1g} ν_1	ν(M-F) E_g ν_2	δ(M-F) ν(M-F) T_{1u} ν_3	δ(M-F) T_{1u} ν_4	δ(M-F) T_{2g} ν_5	REF.
SiF_6^{2-}	656	474	744	487	400	132,72
	663	477	741	483	408	82
GeF_6^{2-}	624	471	603	359,339	335	82
	627	454	600	350	318	83
SnF_6^{2-}	584	470	556	301	241	133
	592	477	559	300	252	82

†The values included in this table are only representative. A more complete set of values are to be found in the references listed.

TABLE 35

Selection Rules for $MF_4 \cdot 2L$ Adducts

Symmetry	Γ_{total}	$\Gamma_{\nu(M-F)}$	$\Gamma_{\nu(M-L)}$	$\Gamma_{\delta(F-M-F)}$ (in plane)	$\Gamma_{\delta(F-M-F)}$ (out of plane)	$\Gamma_{\delta(L-M-L)}$
O_h	$a_{1g} + e_g + t_{2g} + 2t_{1u} + t_{2u}$	t_{1u} e_g a_{1g} (IR) (R) (R)	not applicable	t_{2g} t_{1u} t_{2u} (R) (IR) (inact.)		
trans-D_{4h}	$2a_{2u} + b_{1g} + b_{2g} + b_{2u} + e_g + 3e_u + 2a_{1g}$	e_u b_{1g} a_{1g} (IR) (R) (R)	a_{1g} a_{2u} (R) (IR)	e_u b_{2g} (IR) (R)	a_{2u} b_{2u} (IR) (inact.)	$e_g + e_u$ (R) (IR)
trans-D_{2h}	$3a_g + b_{1g} + 2b_{1u} + b_{2g} + 3b_{2u} + b_{3g} + 3b_{3u} + a_u$	a_g b_{1g} b_{2u} b_{3u} (R) (R) (IR) (IR)	a_g b_{1u} (R) (IR)	a_g b_{2u} b_{3u} (R) (IR) (IR)	b_{1u} a_u (IR) (inact.)	b_{2g} b_{3g} b_{2u} b_{3u} (R) (R) (IR) (IR)
trans-D_{2d}	$2a_1 + a_2 + b_1 + 3b_2 + 4e$	a_1 b_1 e (R) (R) (IR,R)	a_1 b_2 (R) (IR,R)	b_2 e (IR,R) (IR,R)	a_2 b_2 (NA) (IR,R)	2e (IR,R)
trans-C_{2h}	$4a_g + 3a_u + 3b_g + 6b_u$	$2a_g$ $2b_u$ (R) (IR)	a_g a_u (R) (IR)	a_g $2b_u$ (R) (IR)	$2a_u$ (IR)	$2b_g$ $2b_u$ (R) (IR)
trans-C_i	$6a_g + 9a_u$	$3a_g$ $3a_u$ (R) (IR)	a_g a_u (R) (IR)	a_g $2a_u$ (R) (IR)	$2a_u$ (IR)	$2a_g$ $2a_u$ (R) (IR)
cis-C_{2v}	$6a_1 + 2a_2 + 4b_1 + 3b_2$	$2a_1$ b_1 b_2 (IR,R) (IR,R) (IR,R)	a_1 b_1 (IR,R) (IR,R)	$2a_1$ a_2 b_1 b_2 (IR,R) (R) (IR,R) (IR,R)		a_1 a_2 b_1 b_2 (IR,R) (R) (IR,R) (IR,
trans-C_2	$7a + 8b$	$2a$ $2b$ (IR,R) (IR,R)	$2a$ (IR,R)	$a + 2b$ (IR,R) (IR,R)	$2b$ (IR,R)	$2a$ $2b$ (IR,R) (IR,R)
cis- and trans-C_1	$15a$	$4a$ (IR,R)	$2a$ (IR,R)	$3a$ (IR,R)	$2a$ (IR,R)	$4a$ (IR,R)

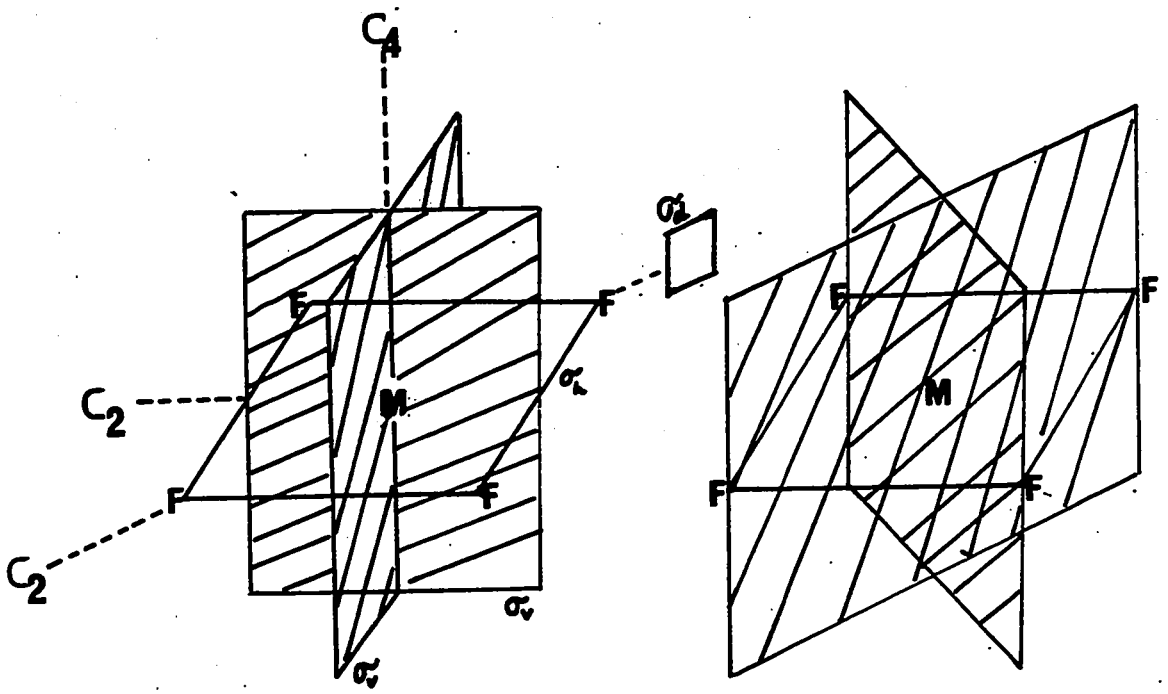

Figure 1. <u>trans</u>-D_{4h} (E, C_4, C_2, i, S_4, σ_h, σ_v, σ_d)

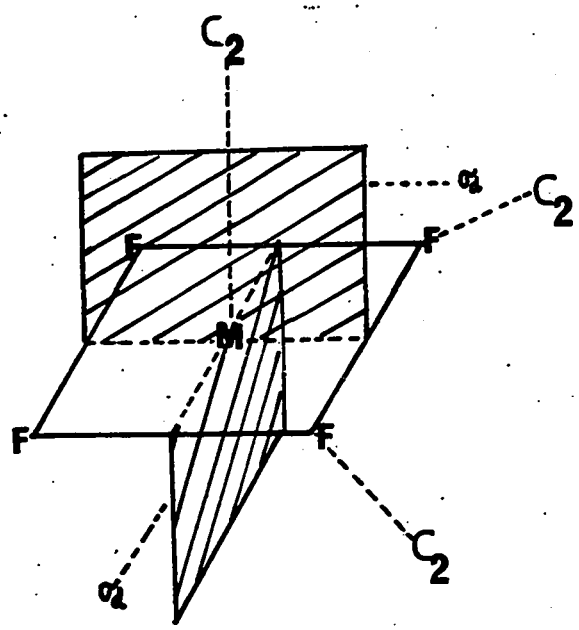

Figure 2. <u>trans</u>-D_{2d} (E, S_4, C_2, σ_d)

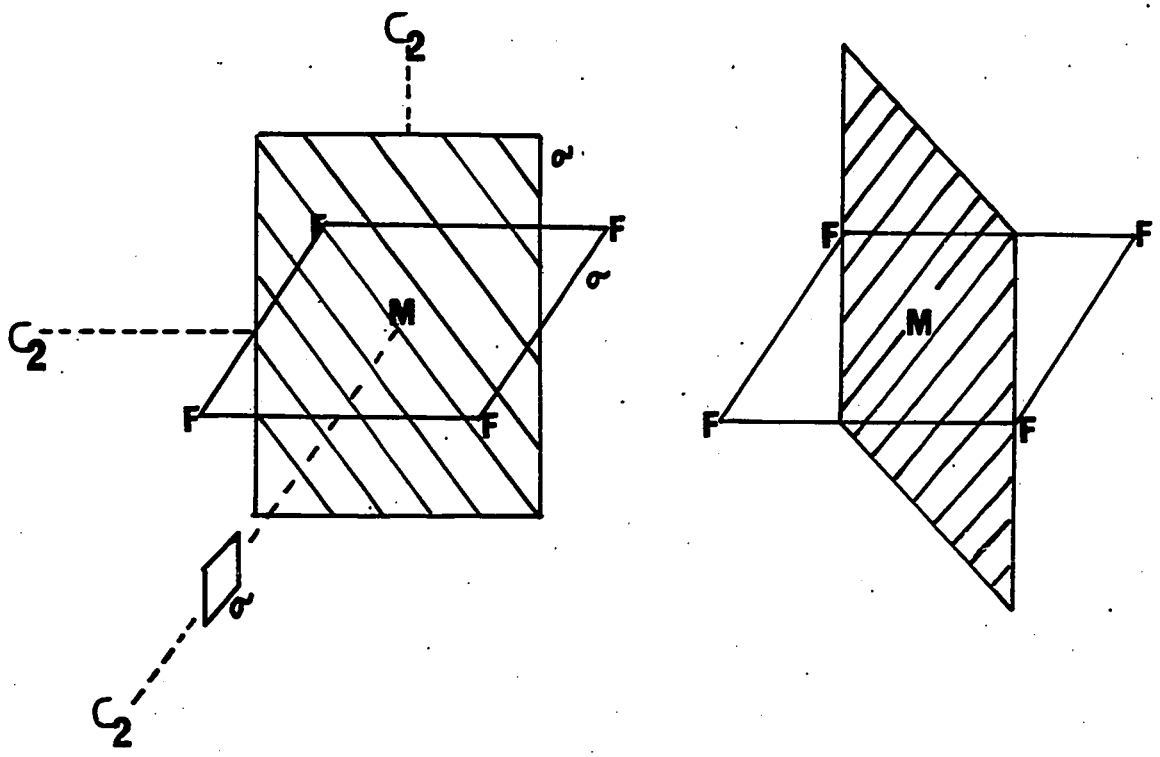

Figure 3. <u>trans</u>-D_{2h} (E, C_2, i, σ)

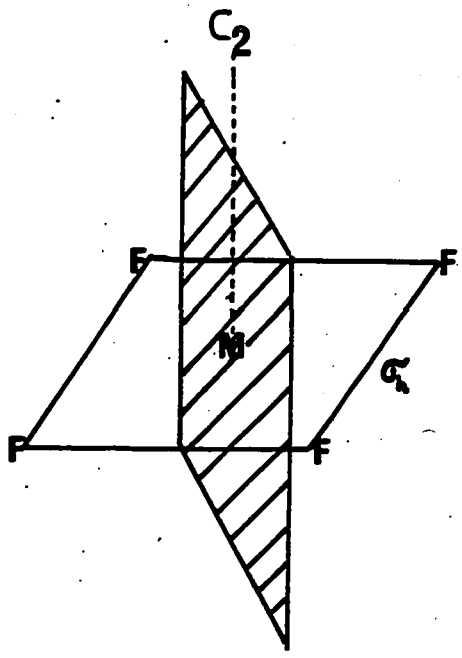

Figure 4. <u>trans</u>-C_{2h} (E, C_2, i, σ_h)

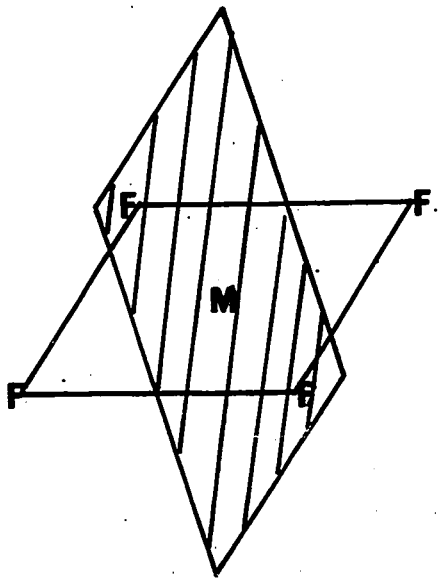

Figure 5. <u>trans</u>-C_i (E, i)

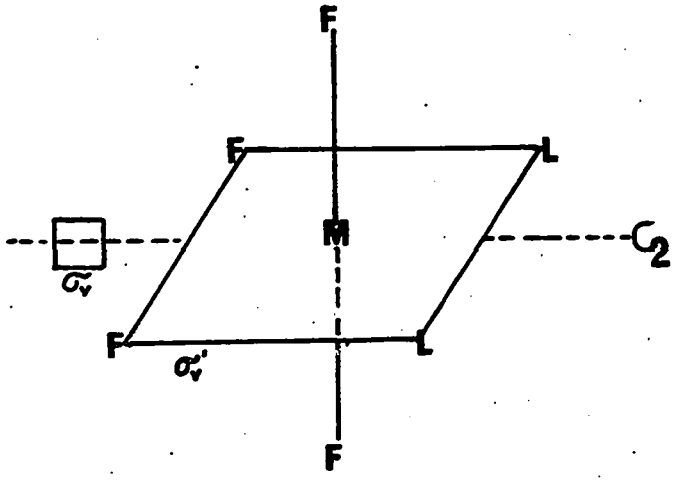

Figure 6. <u>cis</u>-C_{2v} (E, C_2, σ_v)

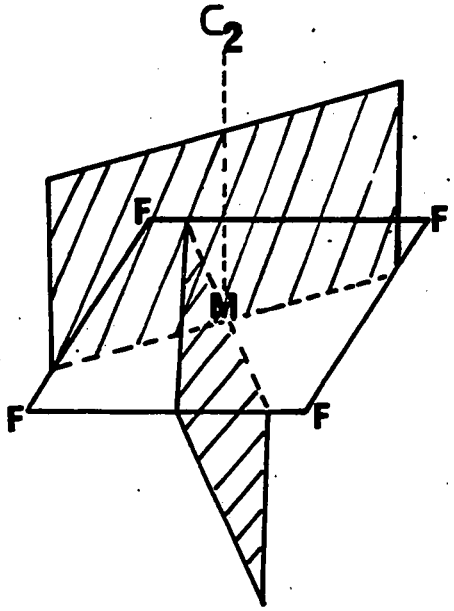

Figure 7. <u>trans</u>-C_2 (E, C_2)

APPENDIX C. Infrared Spectra (Solid State and Solution).

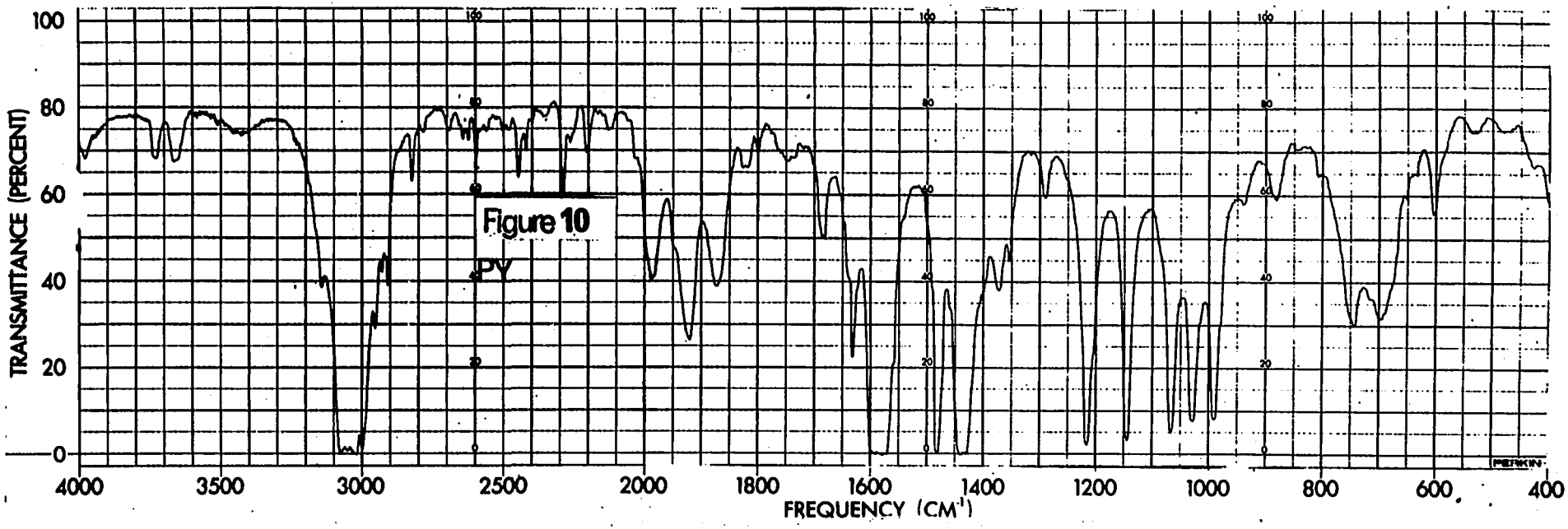

Figure 10

PY

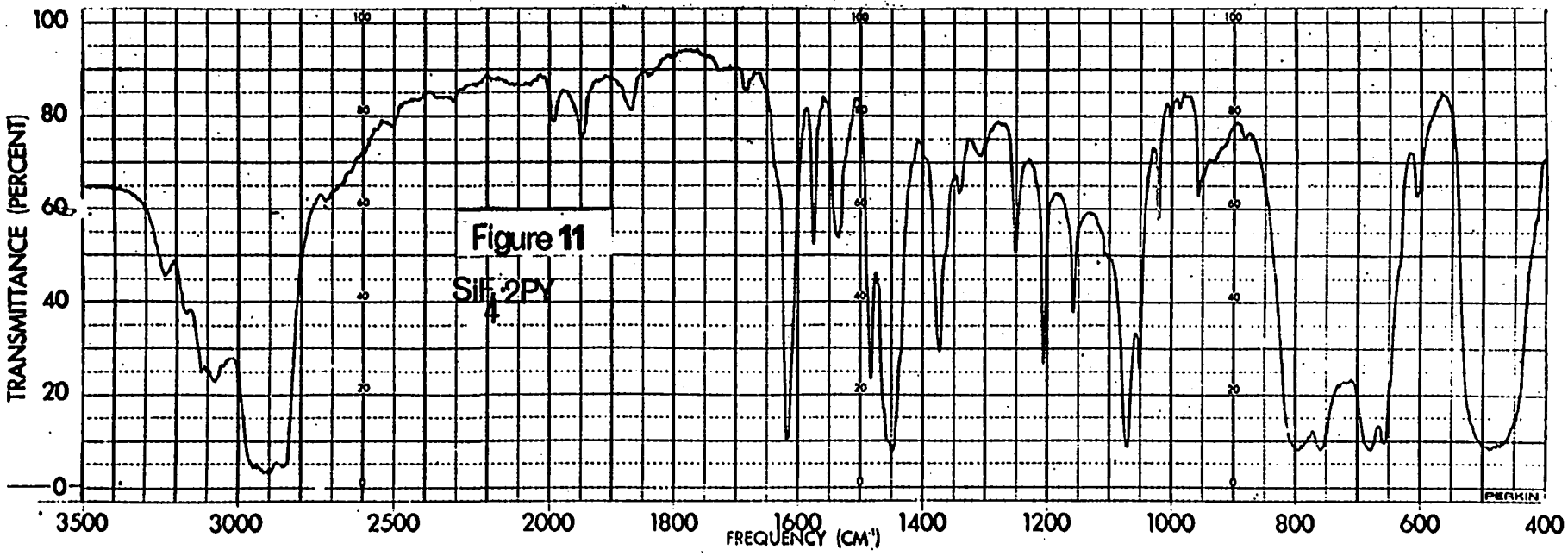

Figure 11

SiH_4-2PY

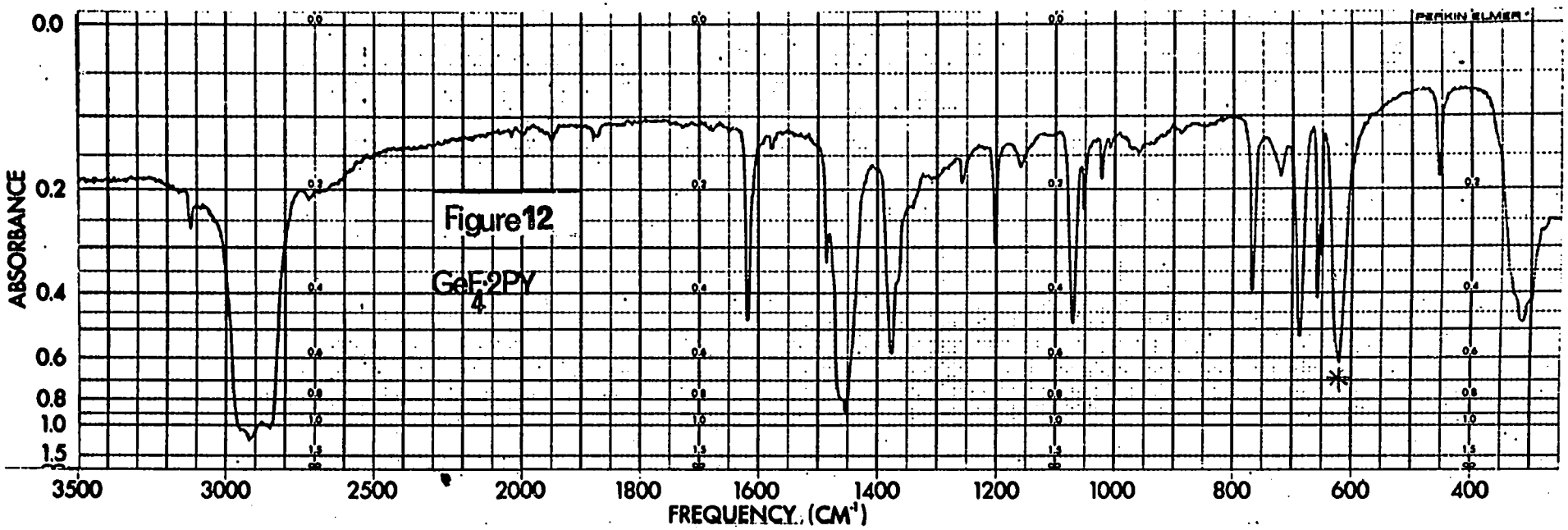

Figure 12

$GeF_4 \cdot 2PY$

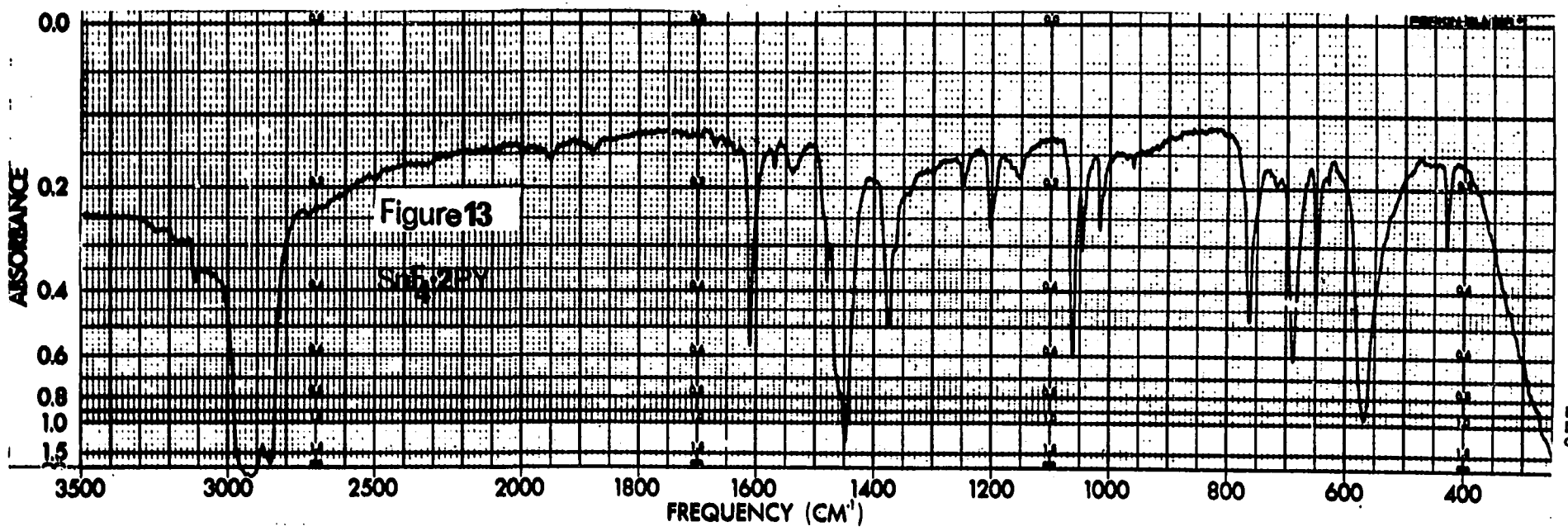

Figure 13

$SnF_4 \cdot 2PY$

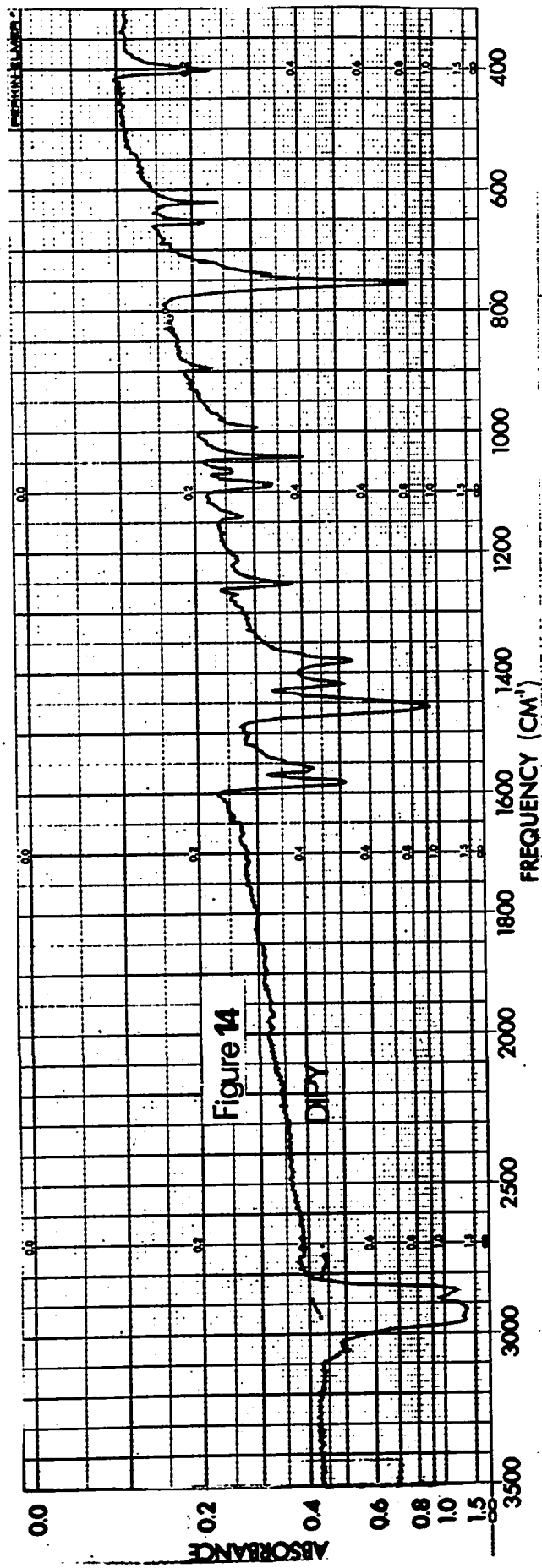

Figure 14

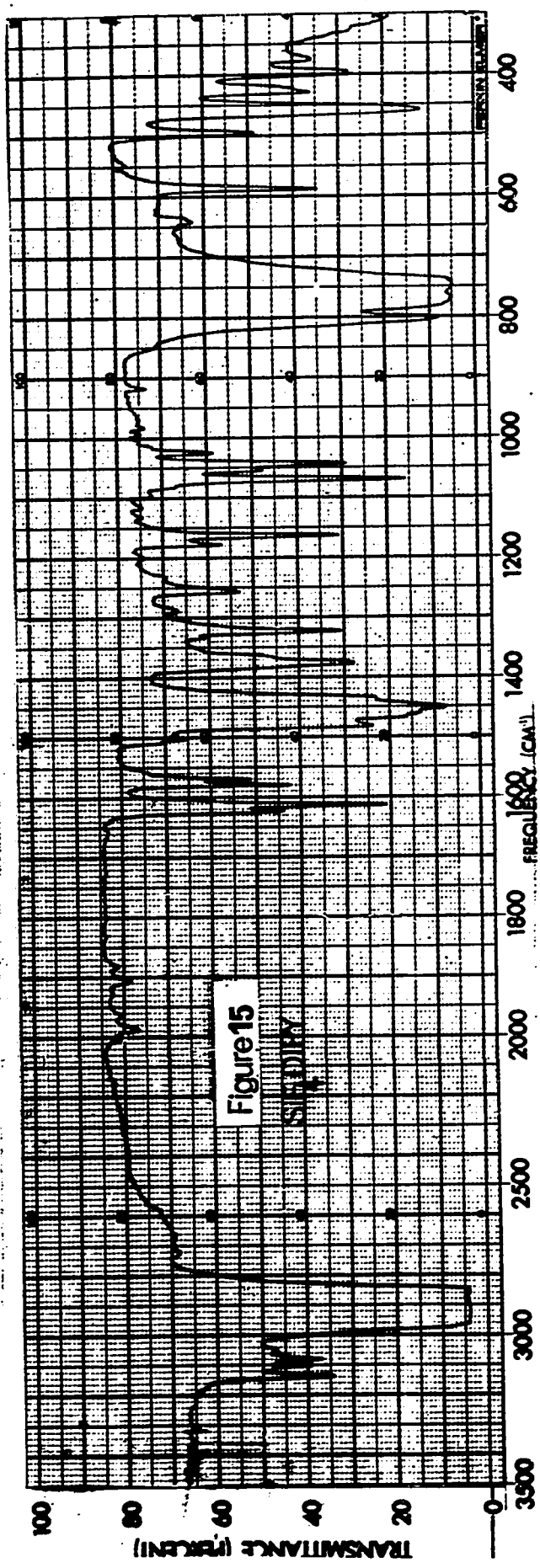

Figure 15

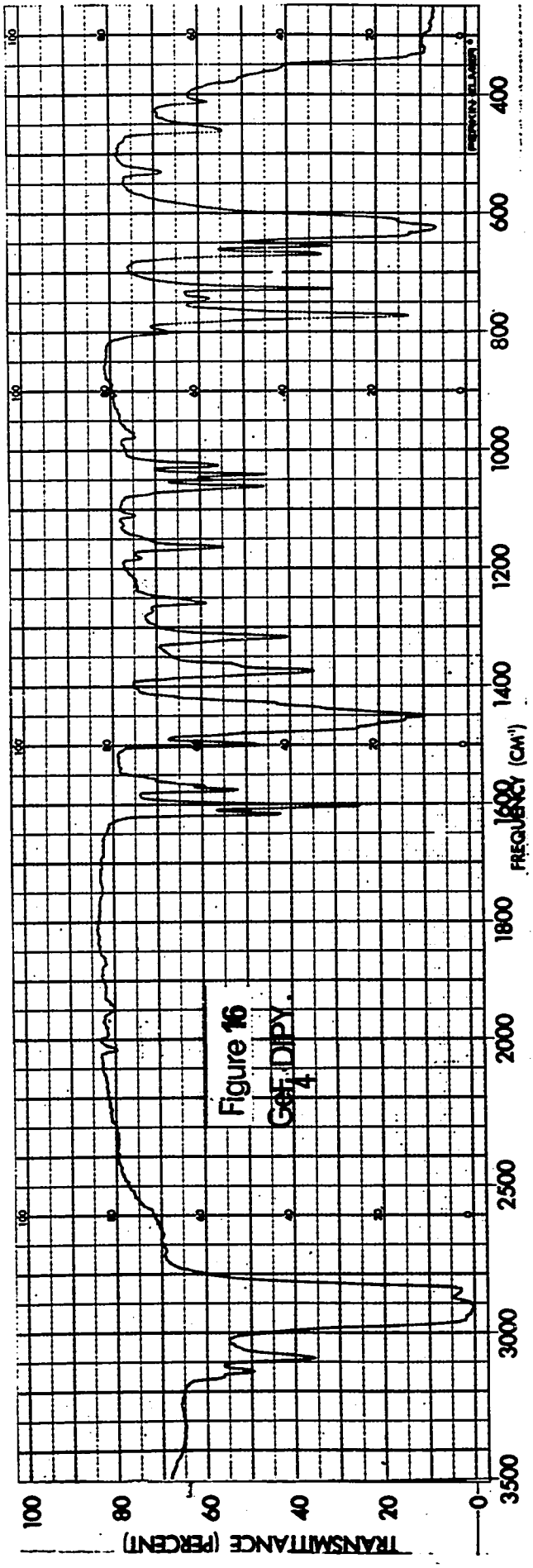

Figure 16
GeF_4.DIPY.

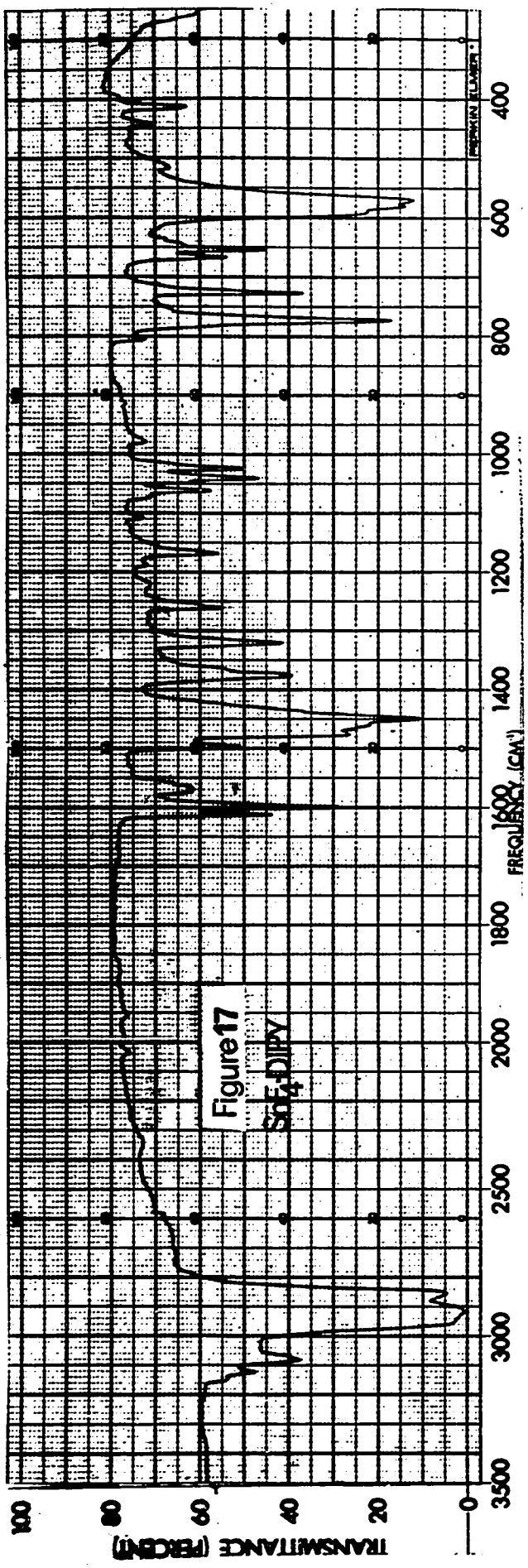

Figure 17
SnF_4.DIPY

SOLUTION INFRARED SPECTRA

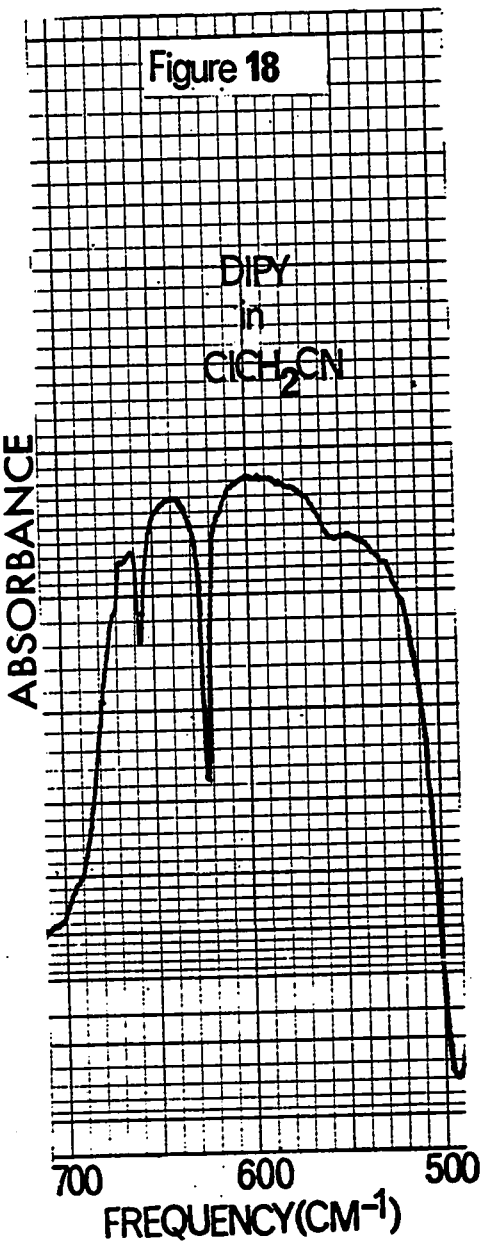

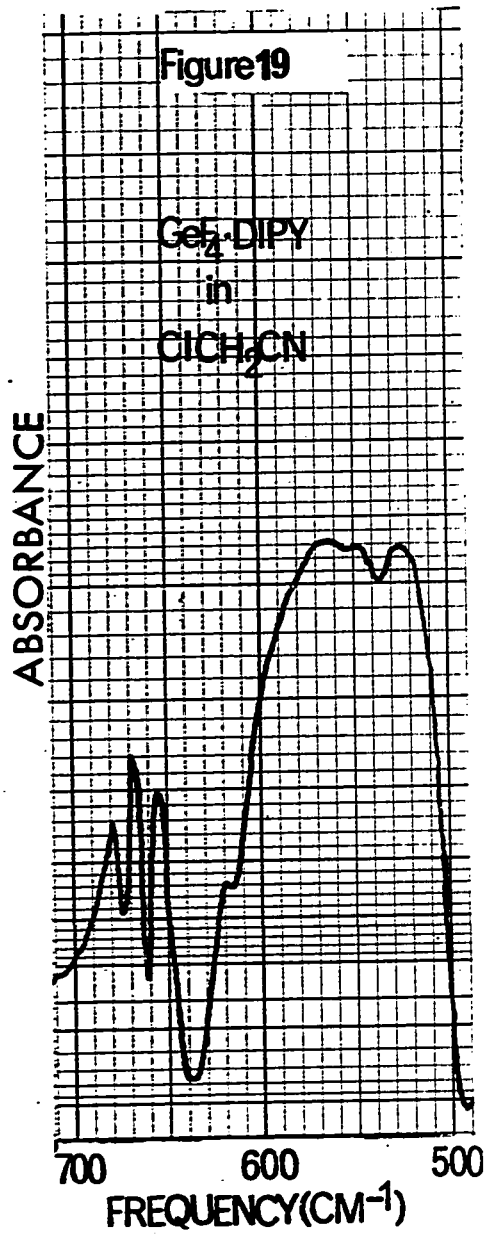

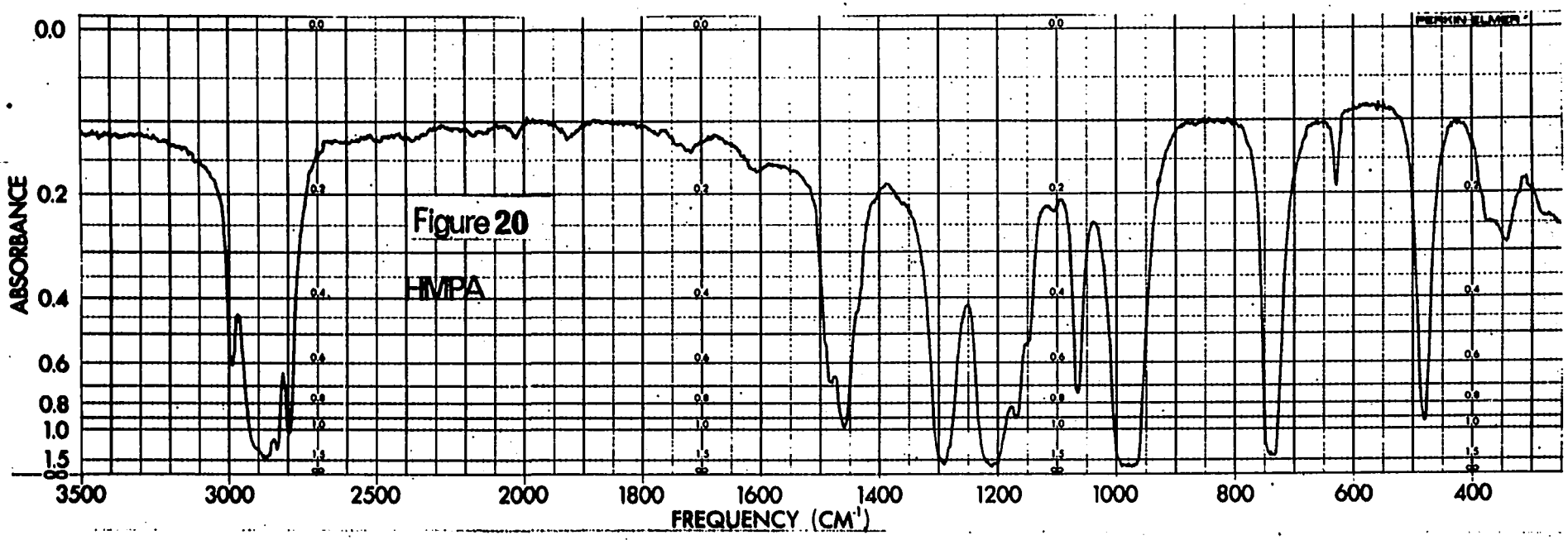

Figure 20

HMPA

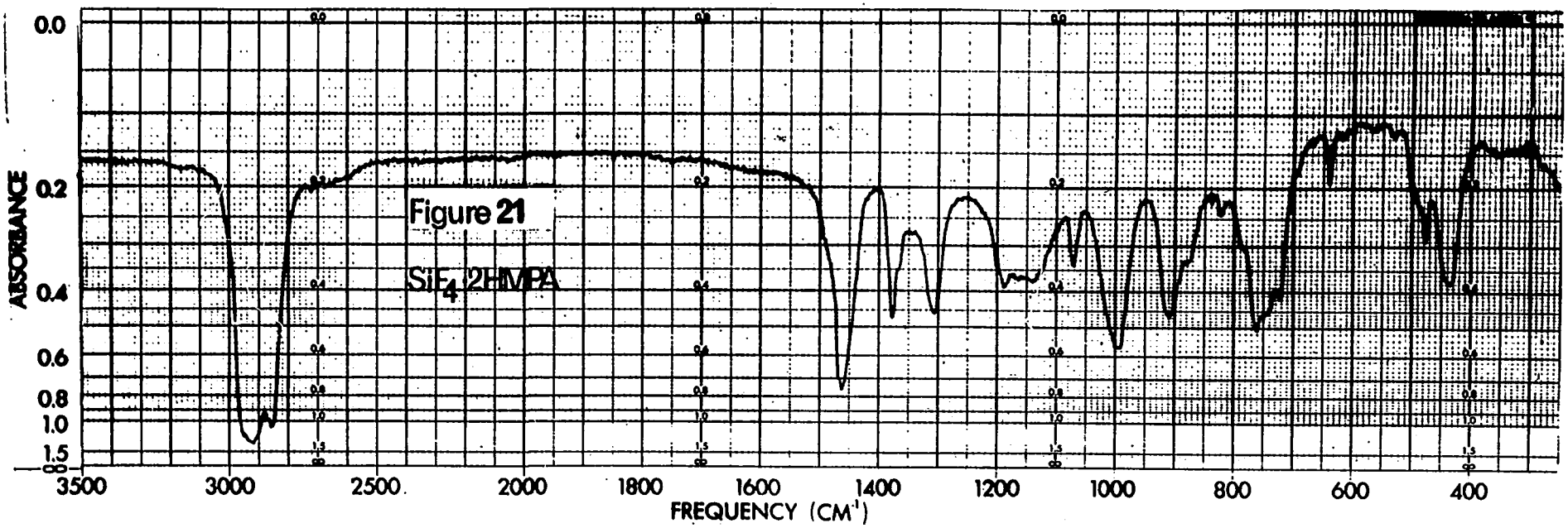

Figure 21

SiF_4 2HMPA

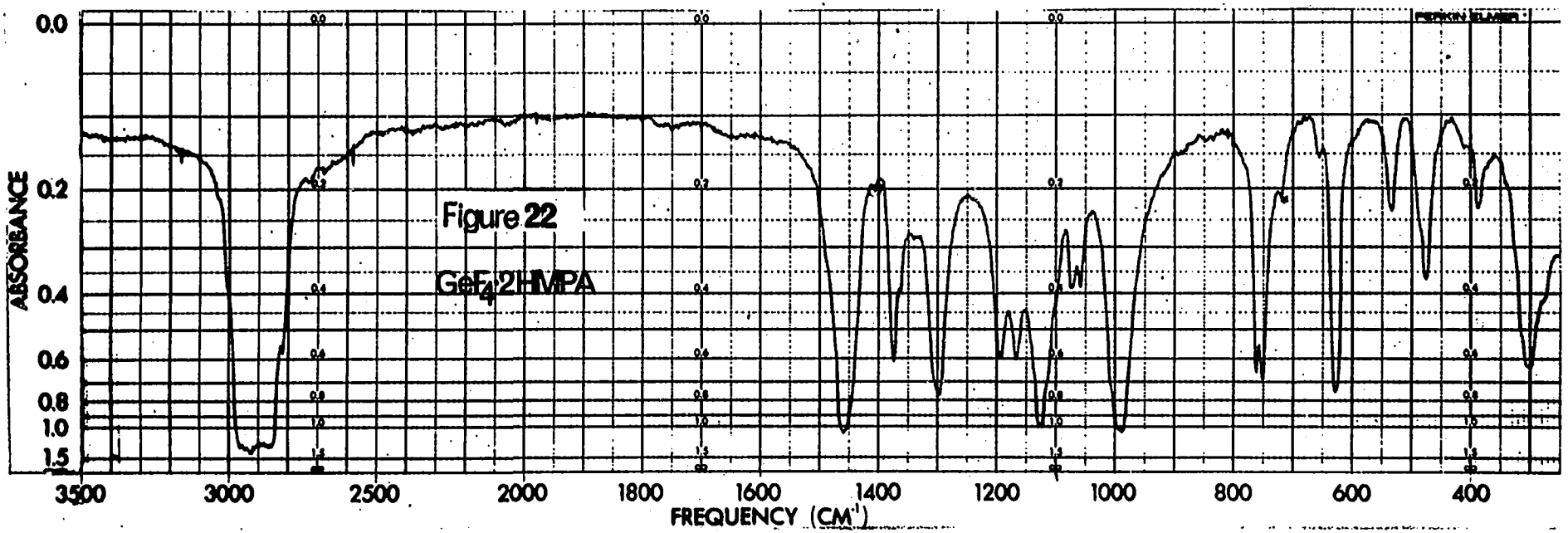

Figure 22

GeF_4·2HMPA

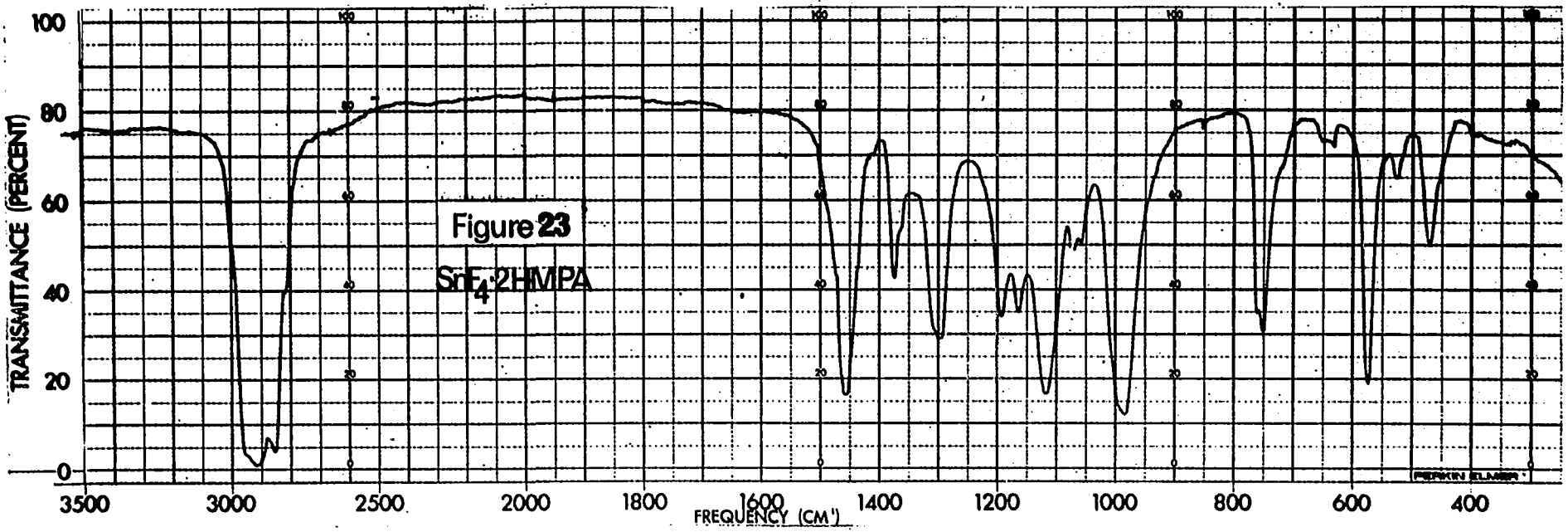

Figure 23

SnF_4·2HMPA

SOLUTION INFRARED SPECTRA

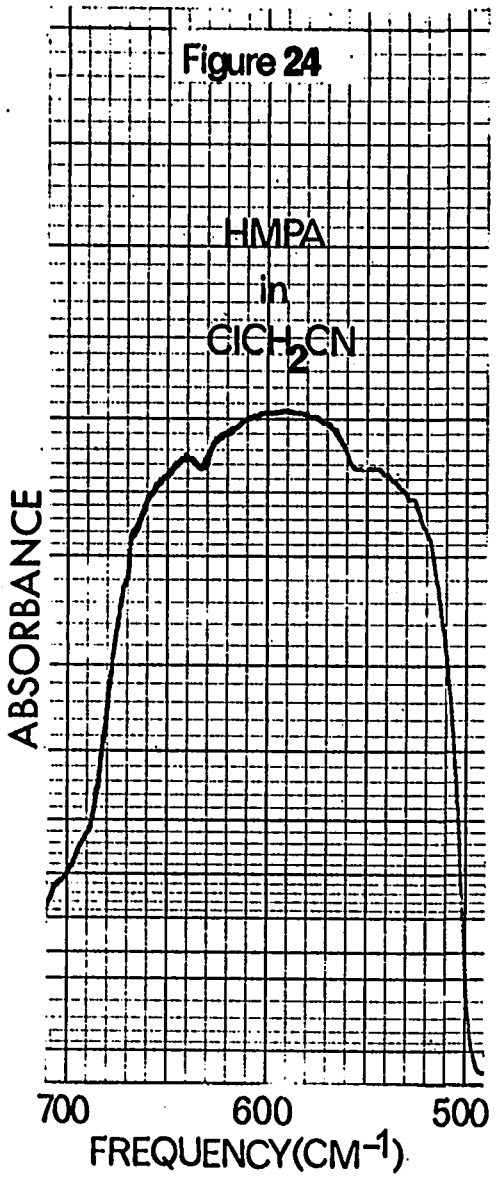

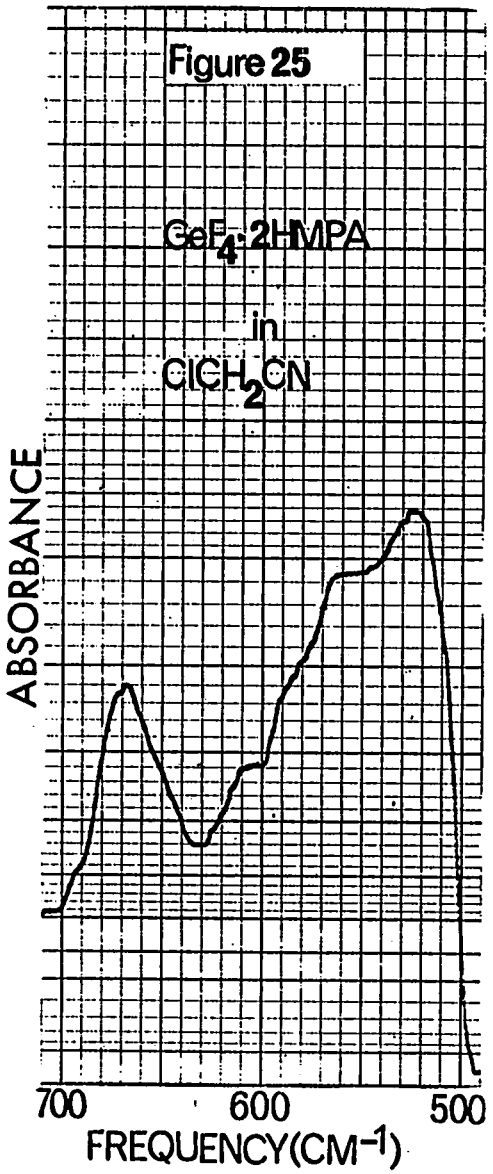

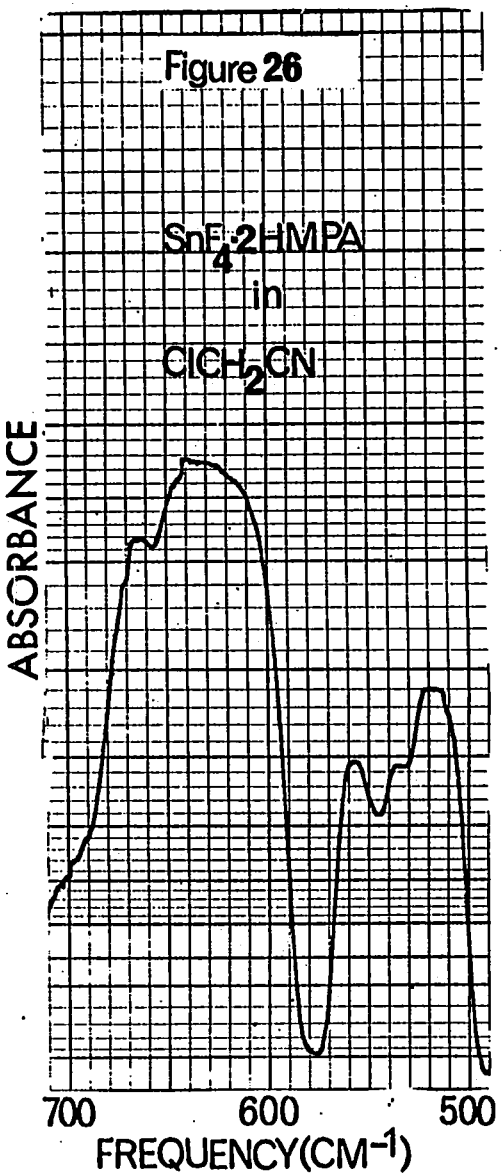

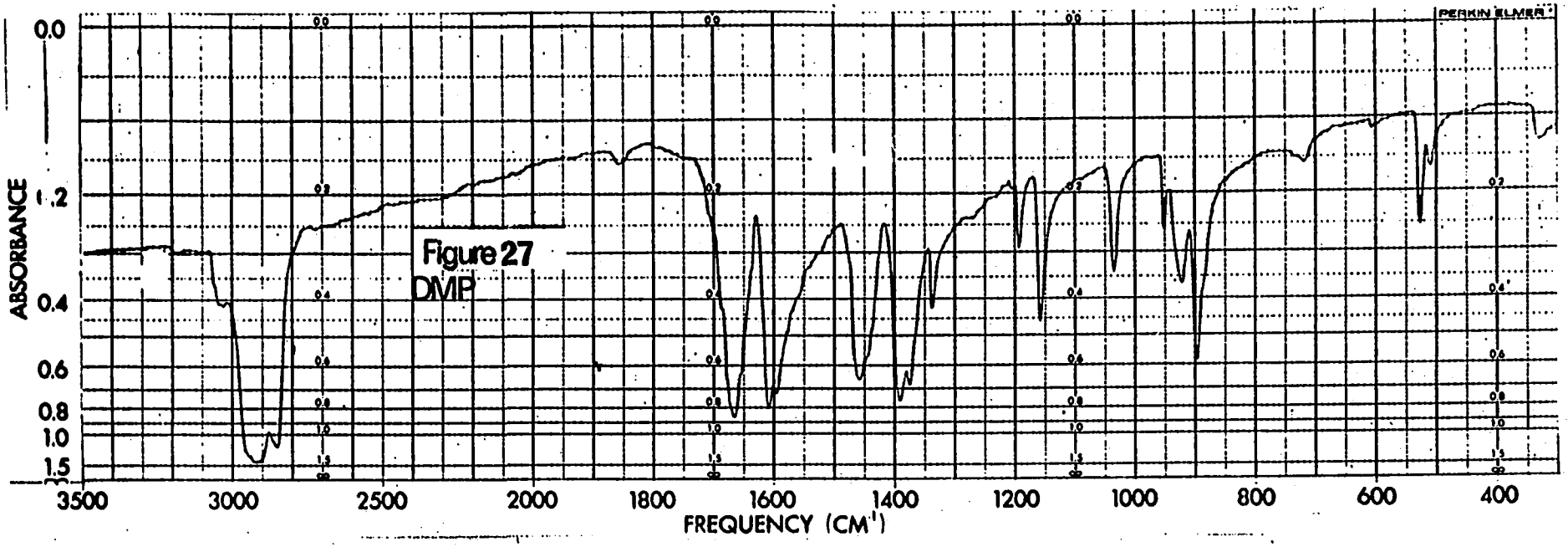

Figure 27
DMP

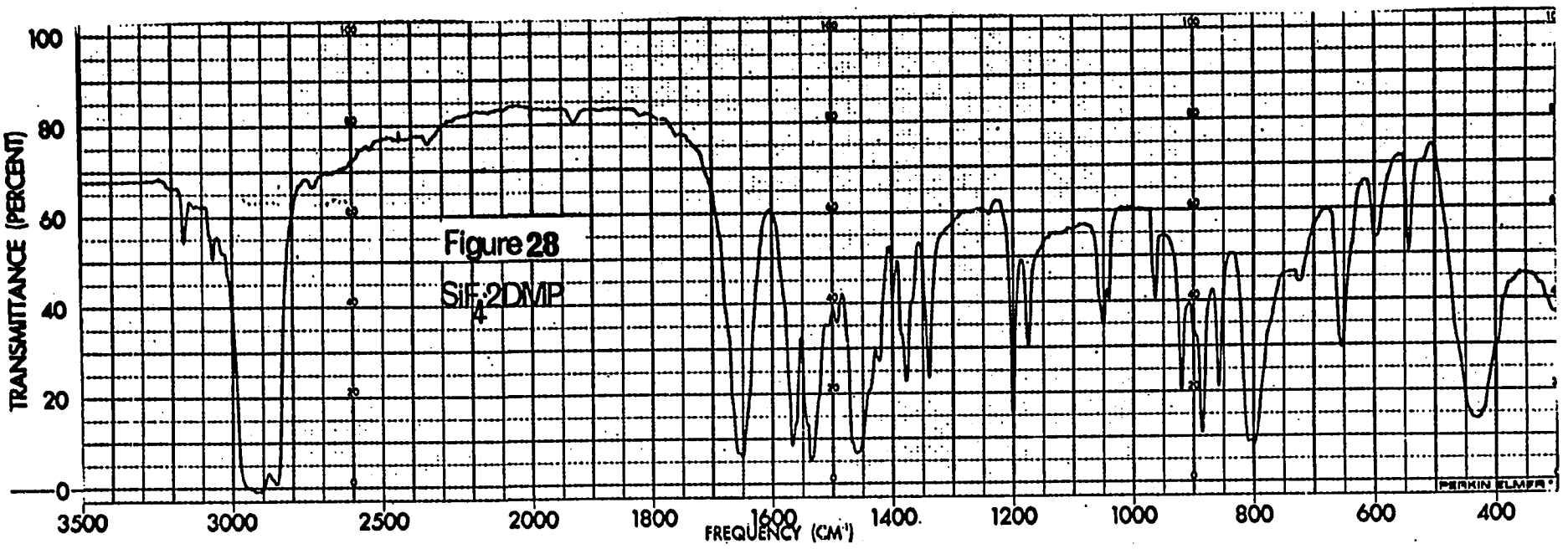

Figure 28
SiF_4:2DMP

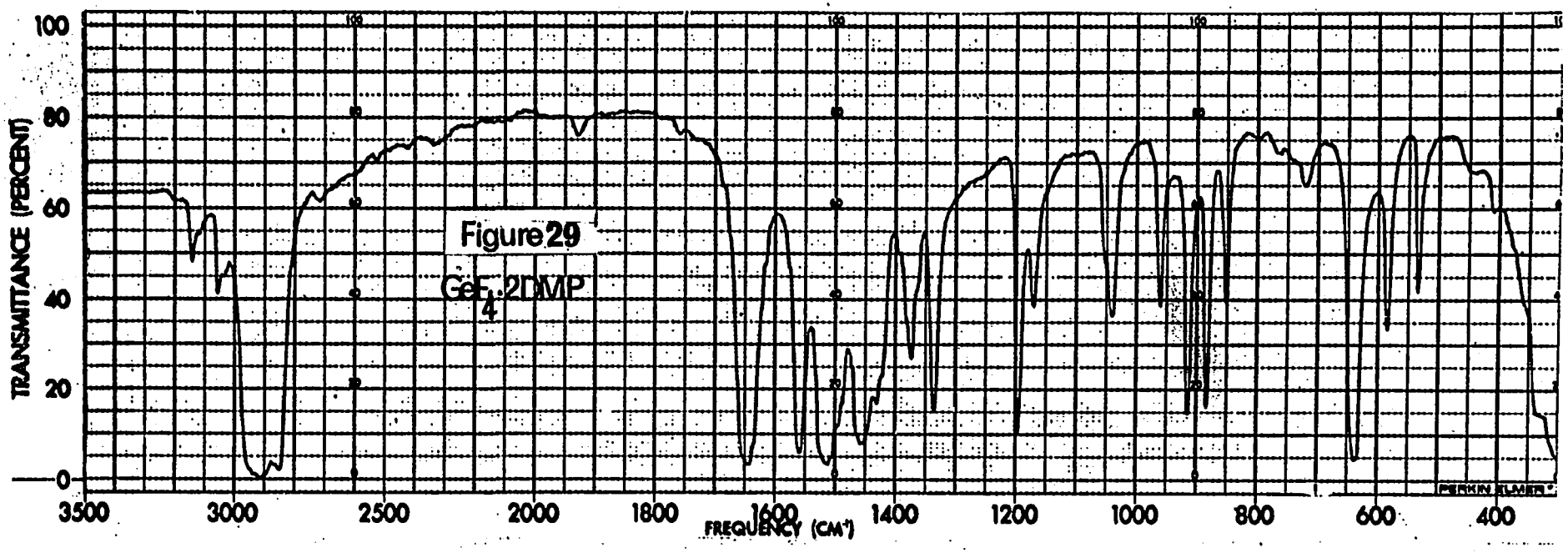

Figure 29

$GeF_4 \cdot 2DMP$

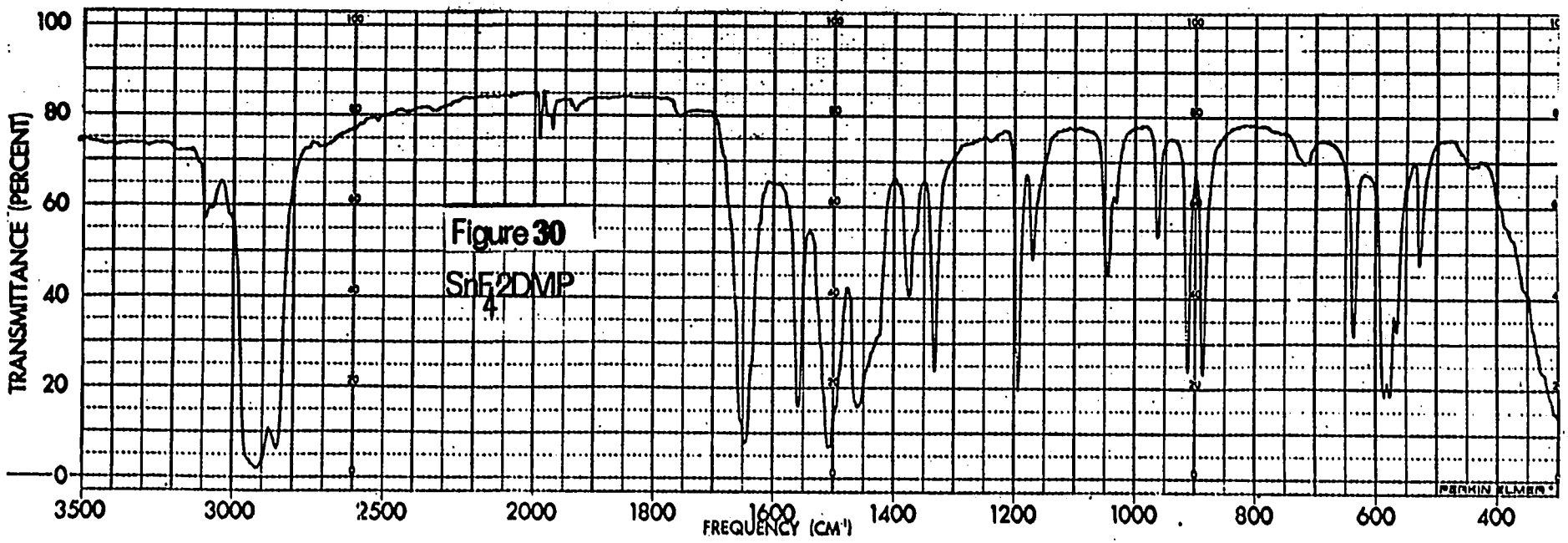

Figure 30

$SnF_4 \cdot 2DMP$

SOLUTION INFRARED SPECTRA

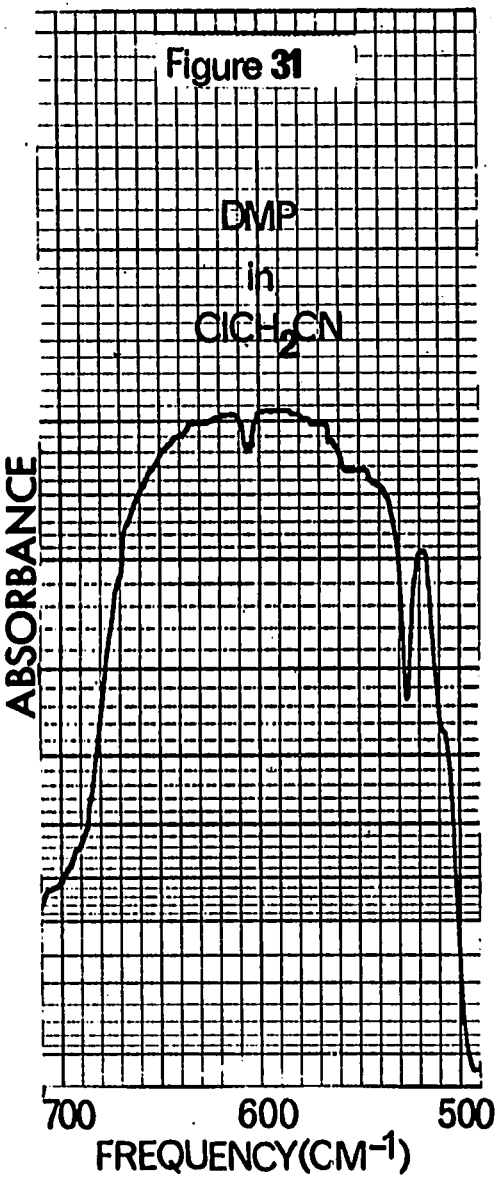

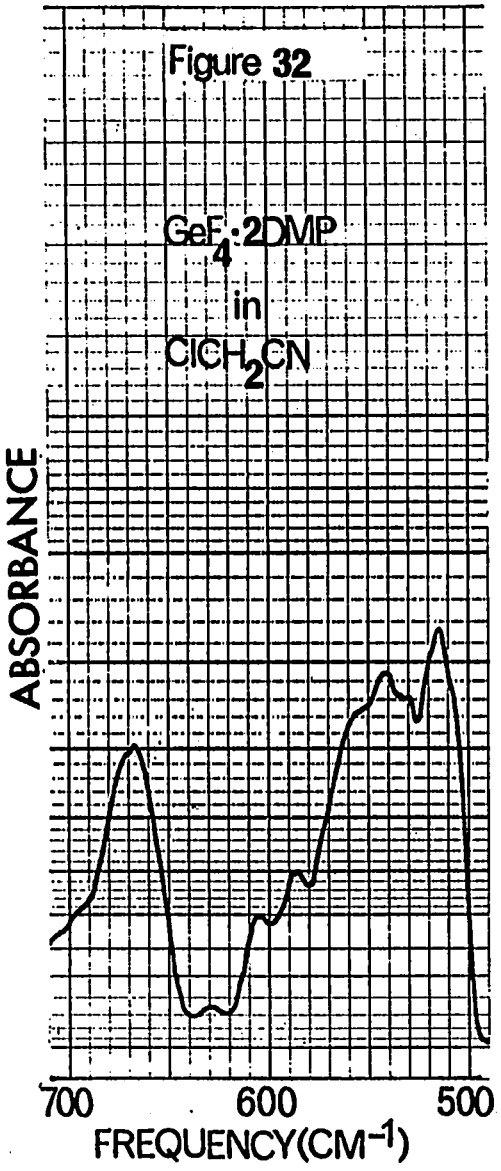

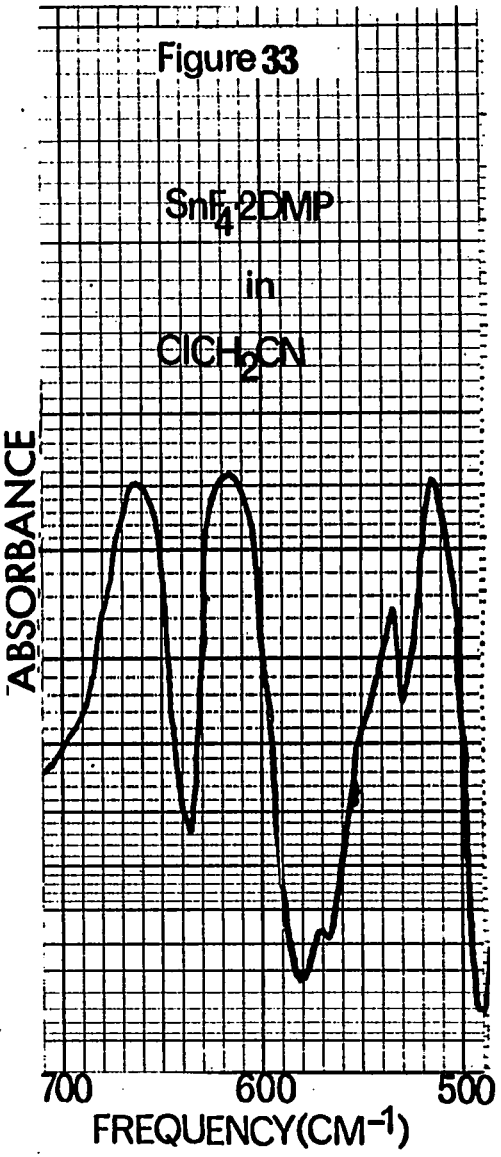

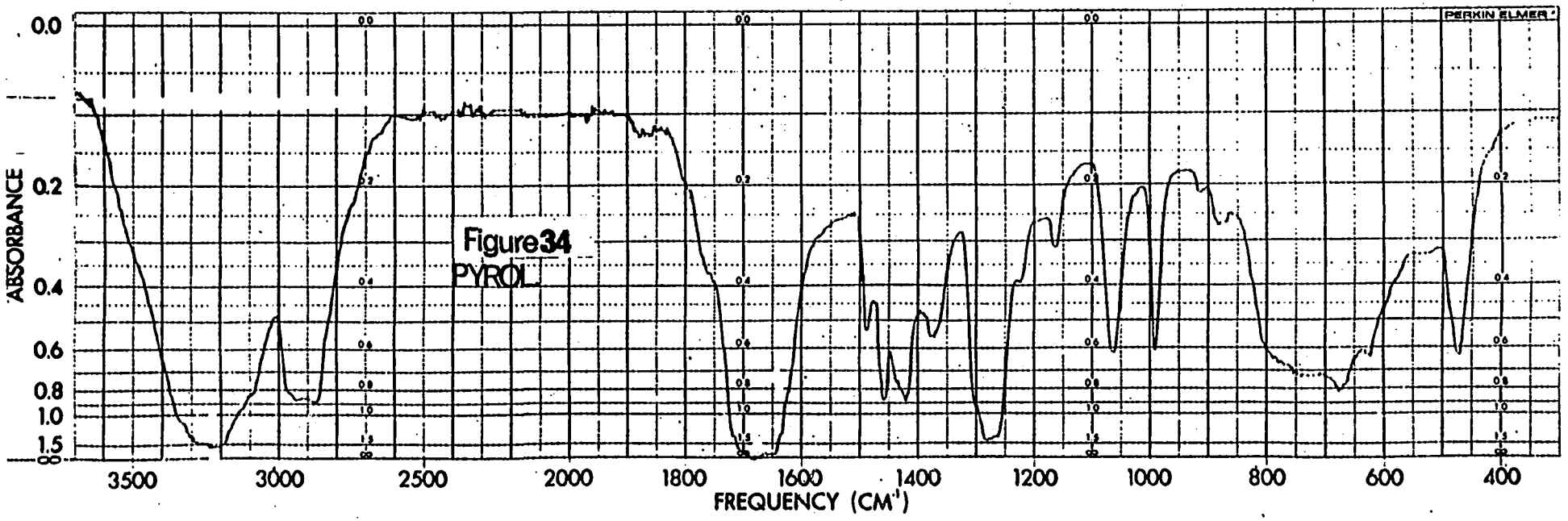

Figure 34
PYROL

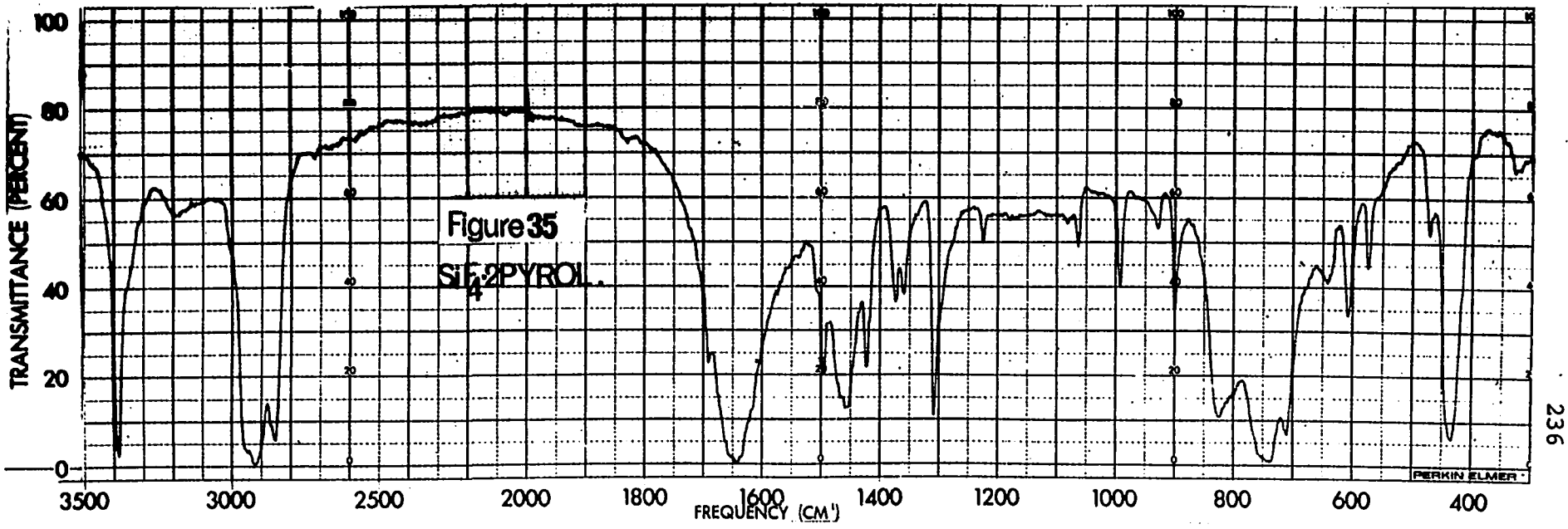

Figure 35
SiF_4-2PYROL

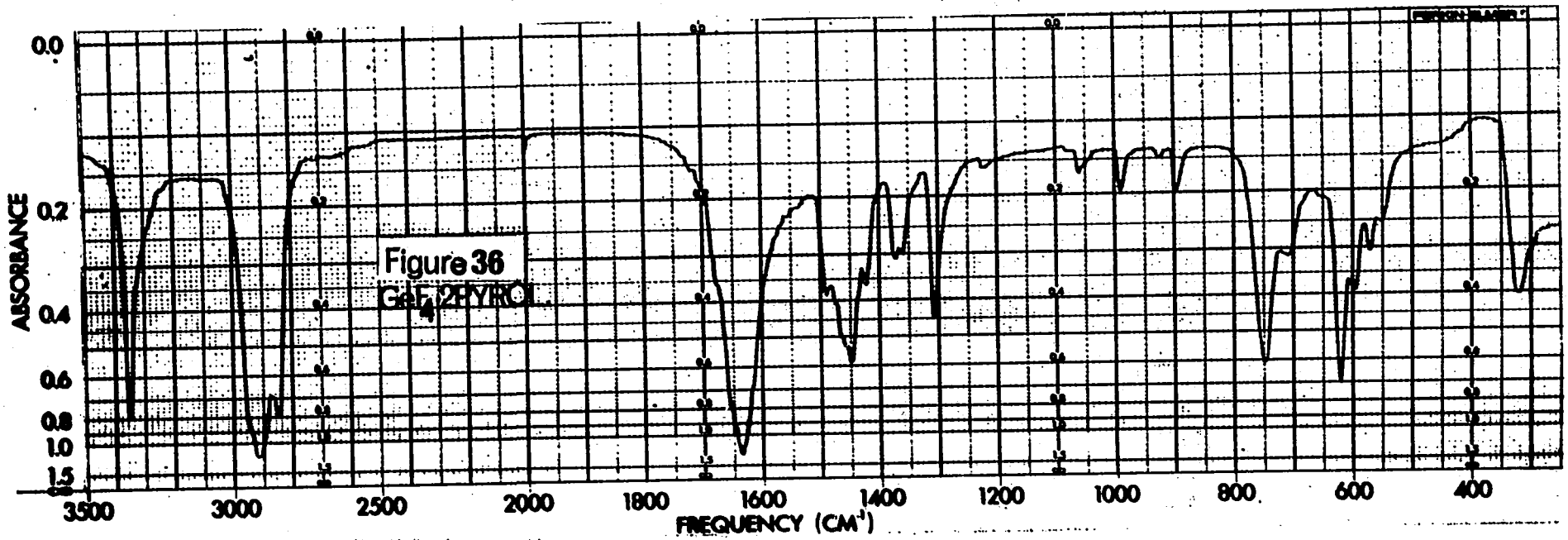

Figure 36
GeF_4:2PYROL.

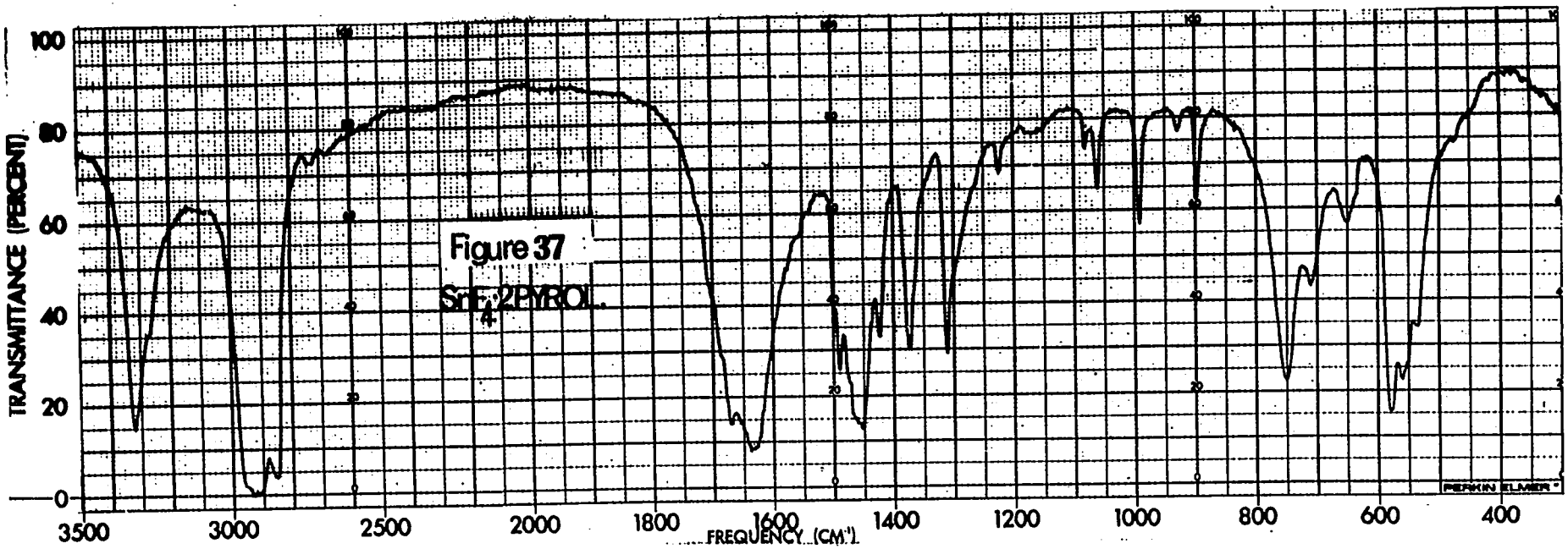

Figure 37
SnF_4:2PYROL.

SOLUTION INFRARED SPECTRA

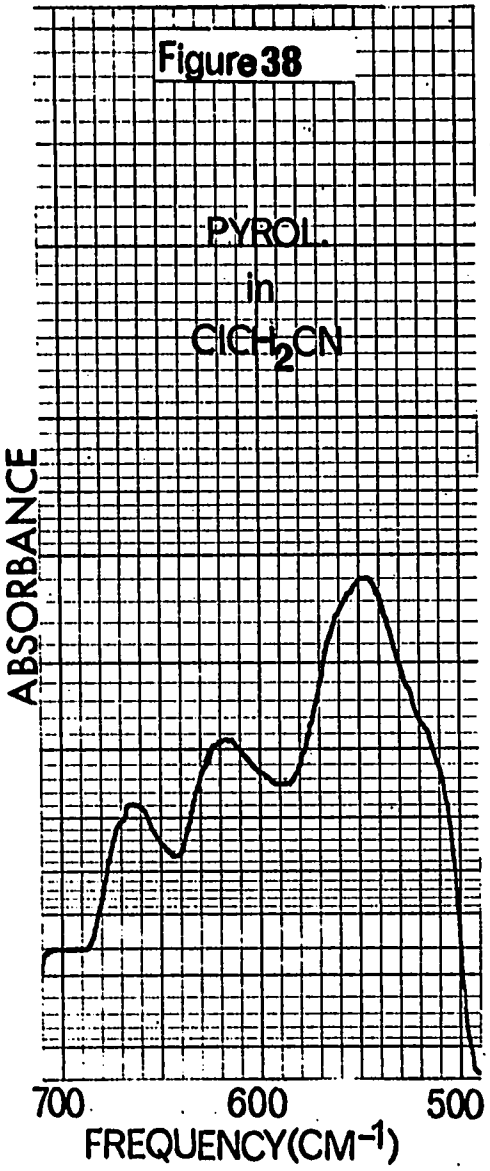

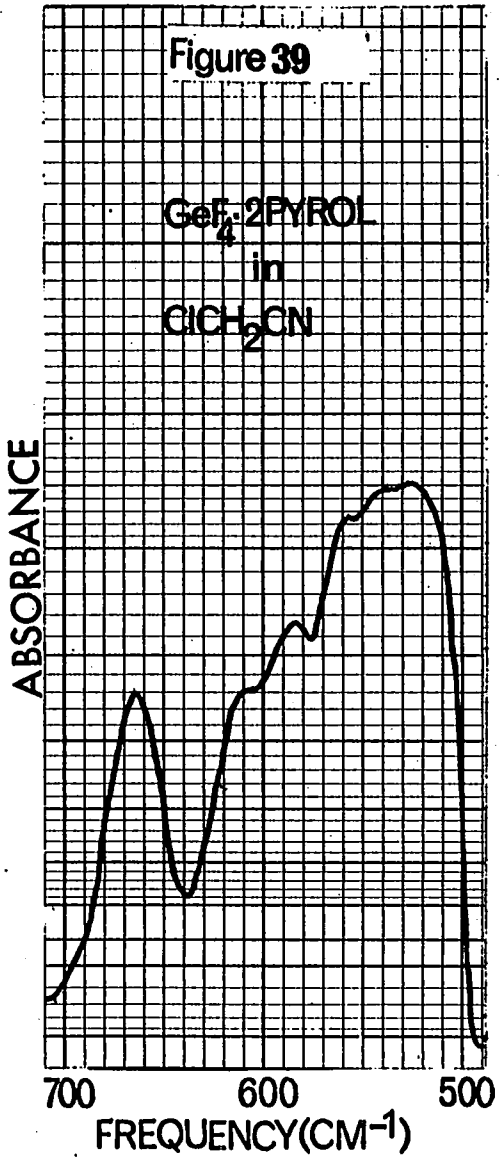

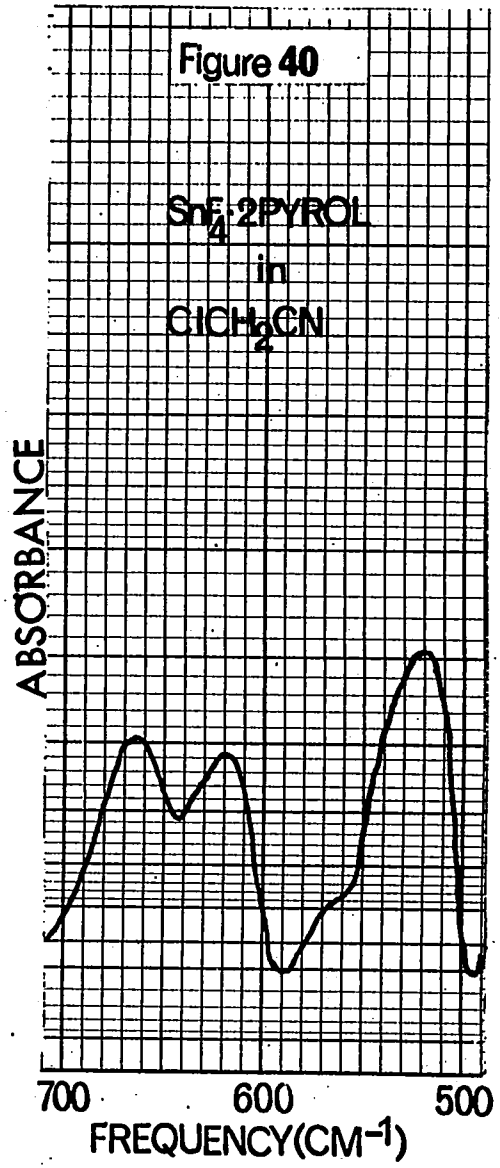

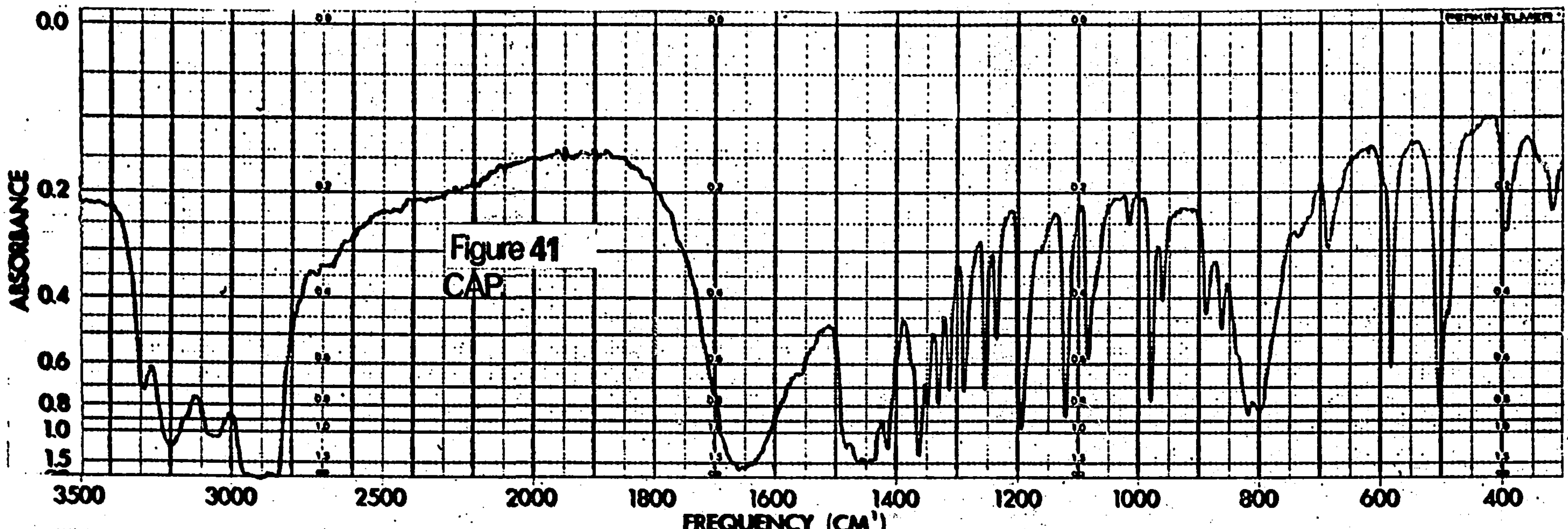

Figure 41
CAP

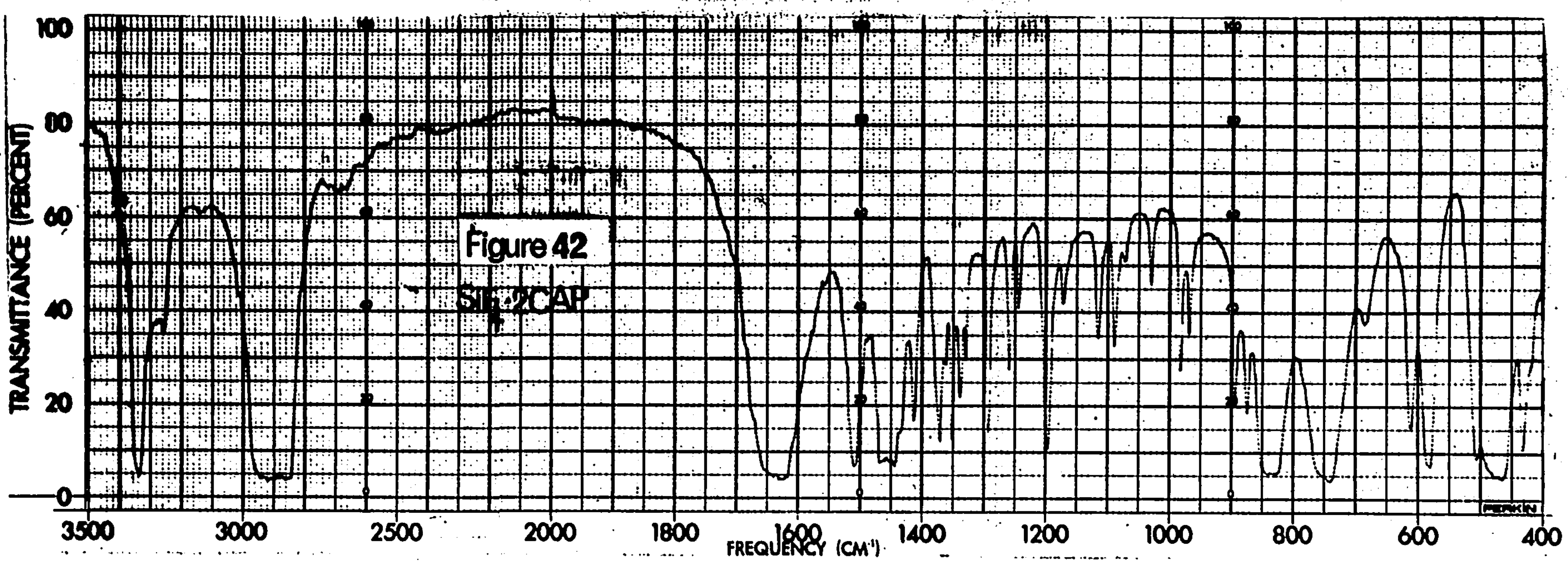

Figure 42
SiH_4 2CAP

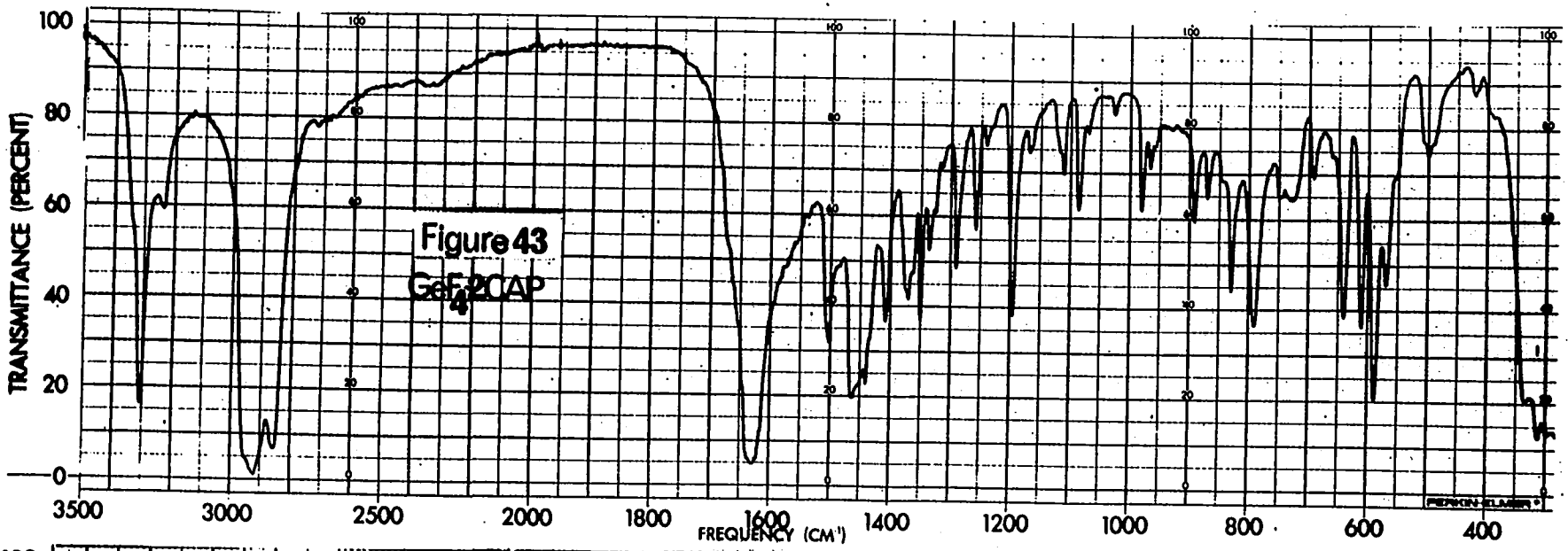

Figure 43
GeF_4-2CAP

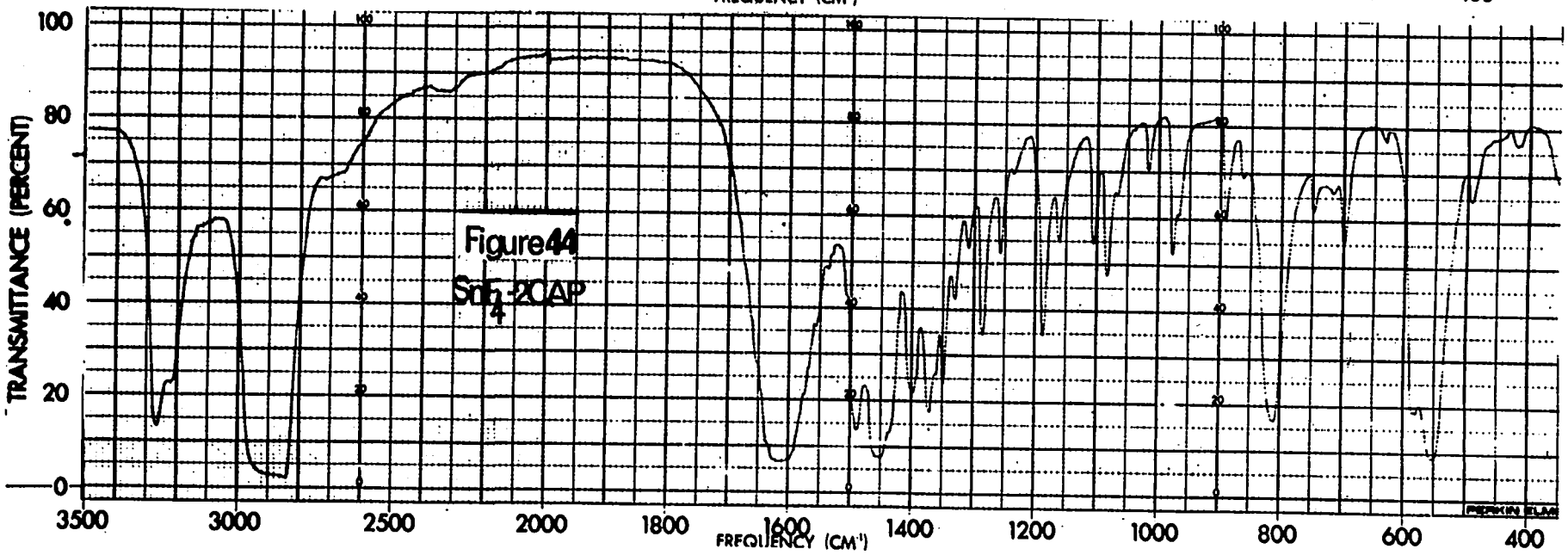

Figure 44
SnF_4-2CAP

SOLUTION INFRARED SPECTRA

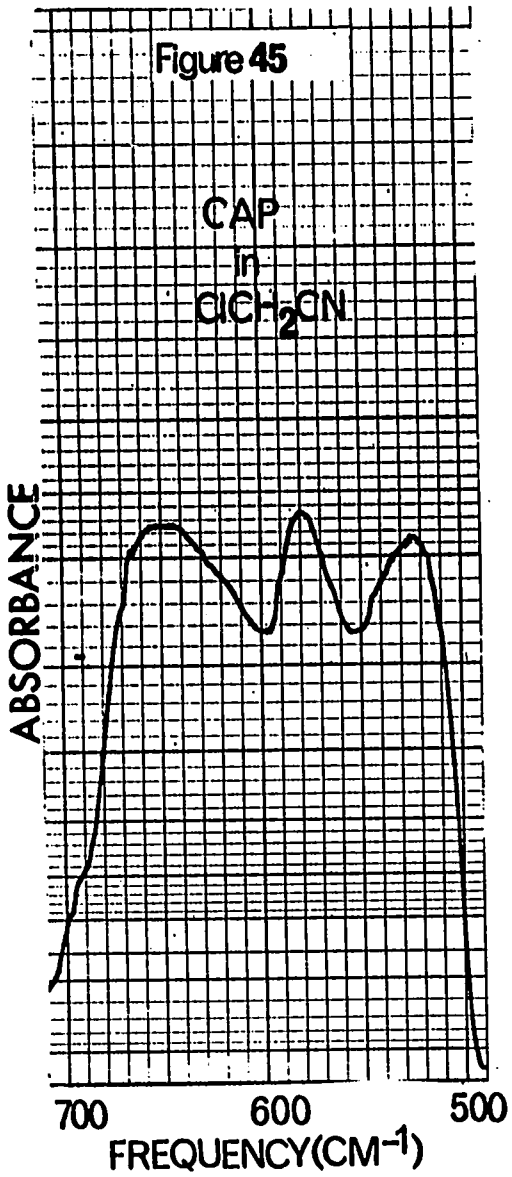

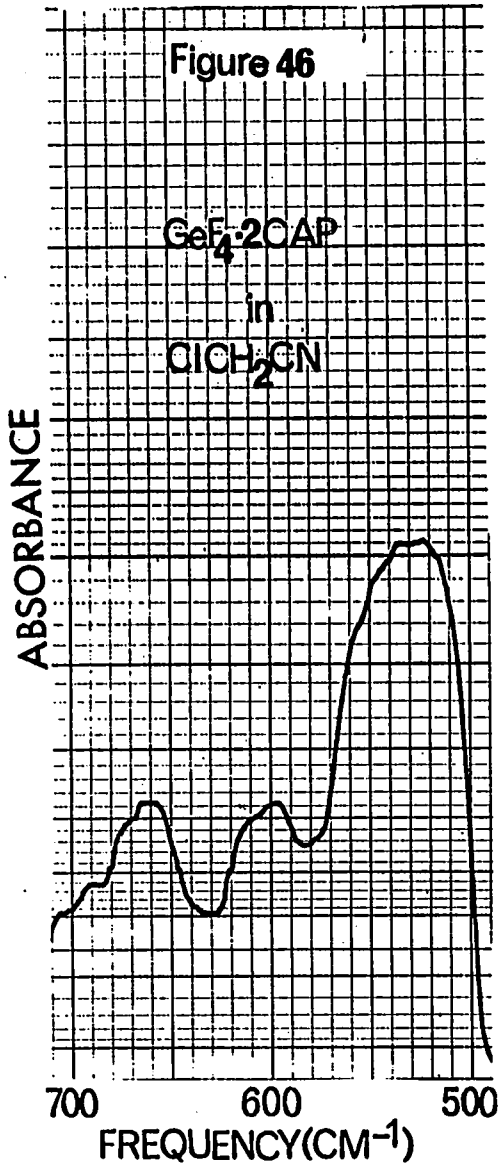

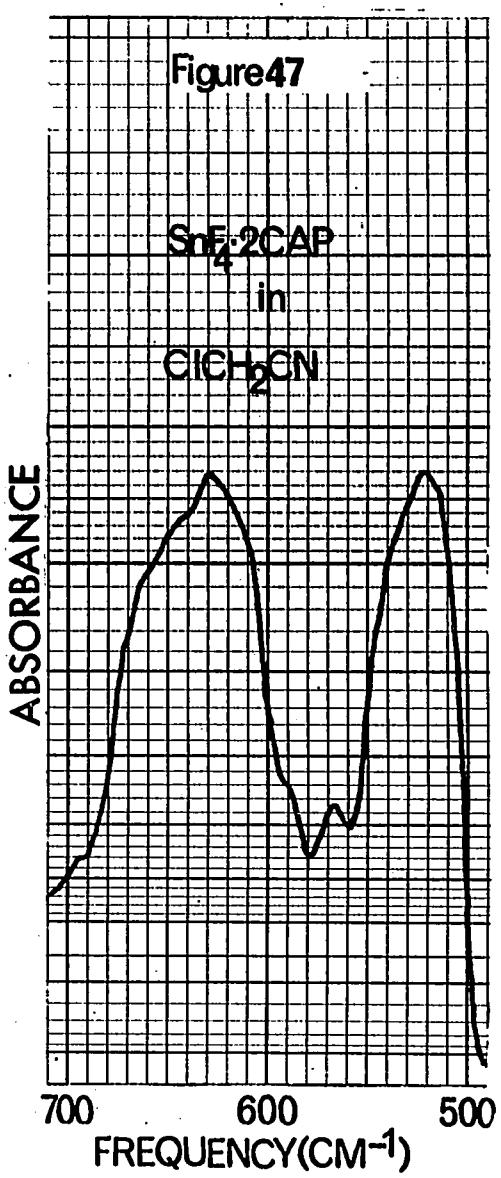

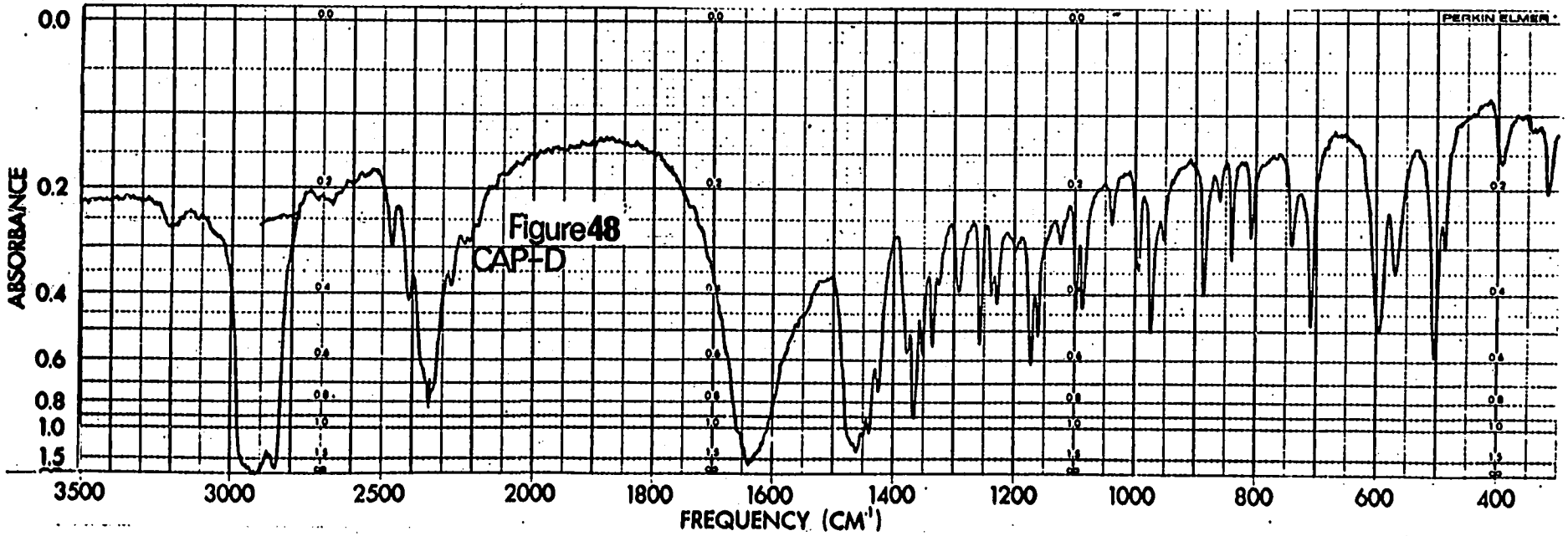

Figure 48
CAP-D

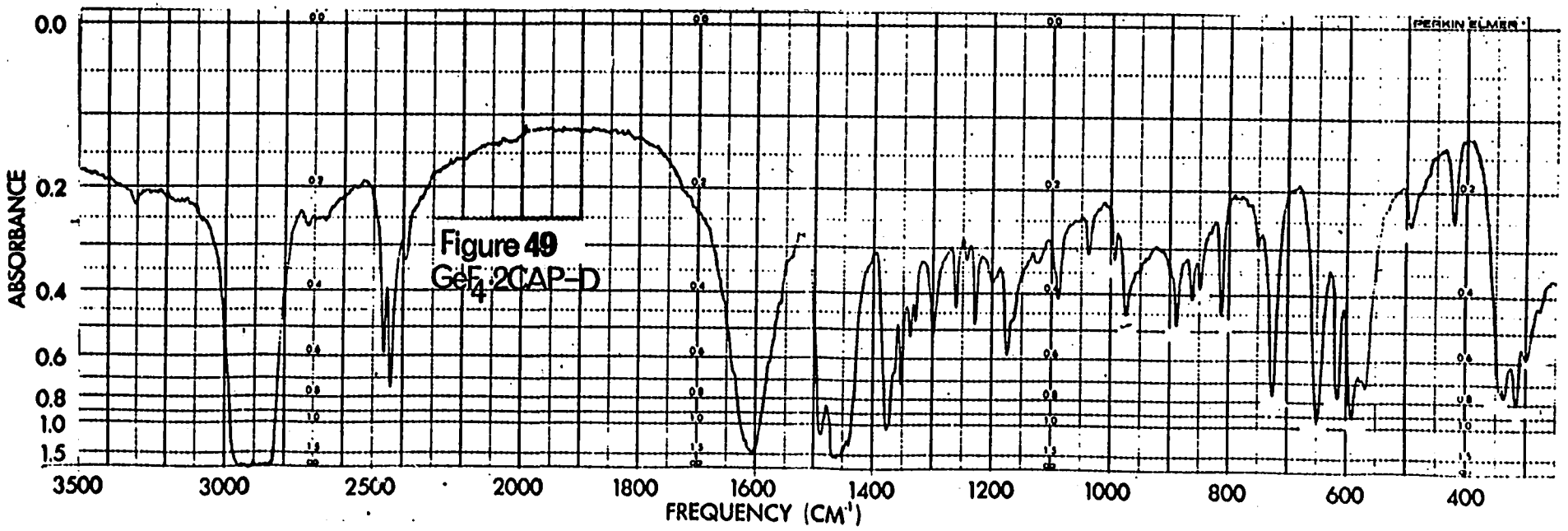

Figure 49
GeF_4·2CAP-D

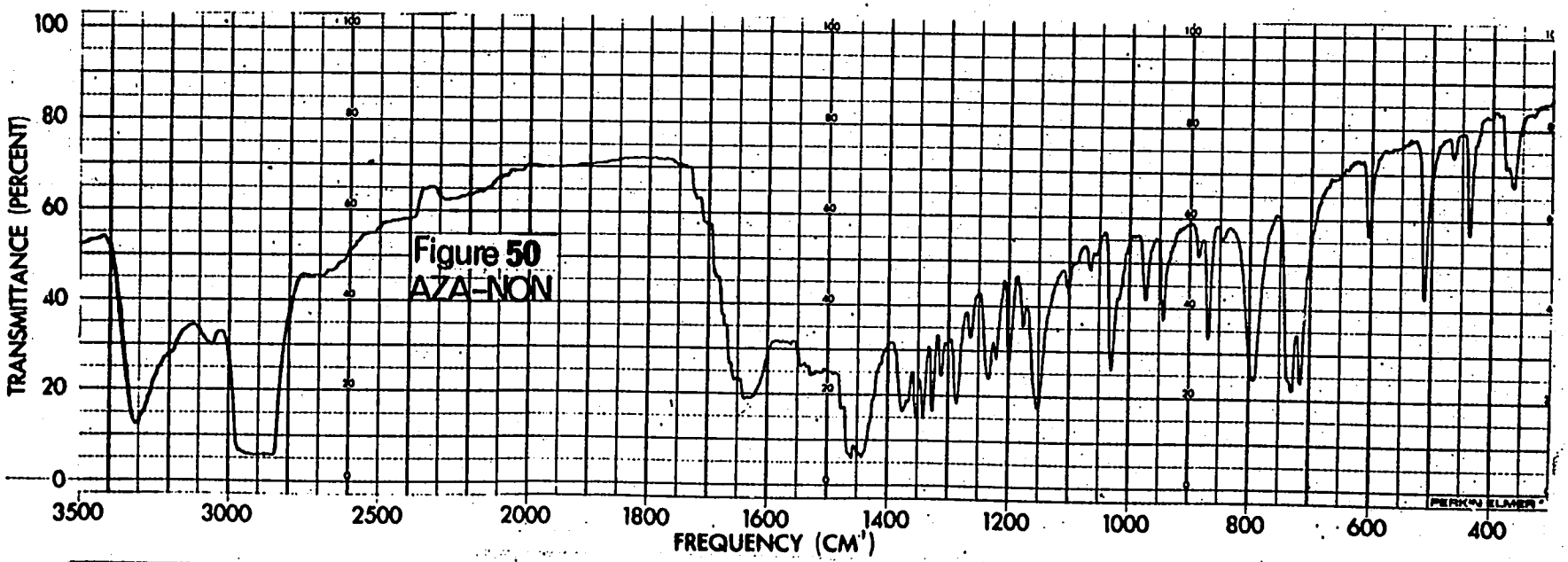

Figure 50
AZA-NON

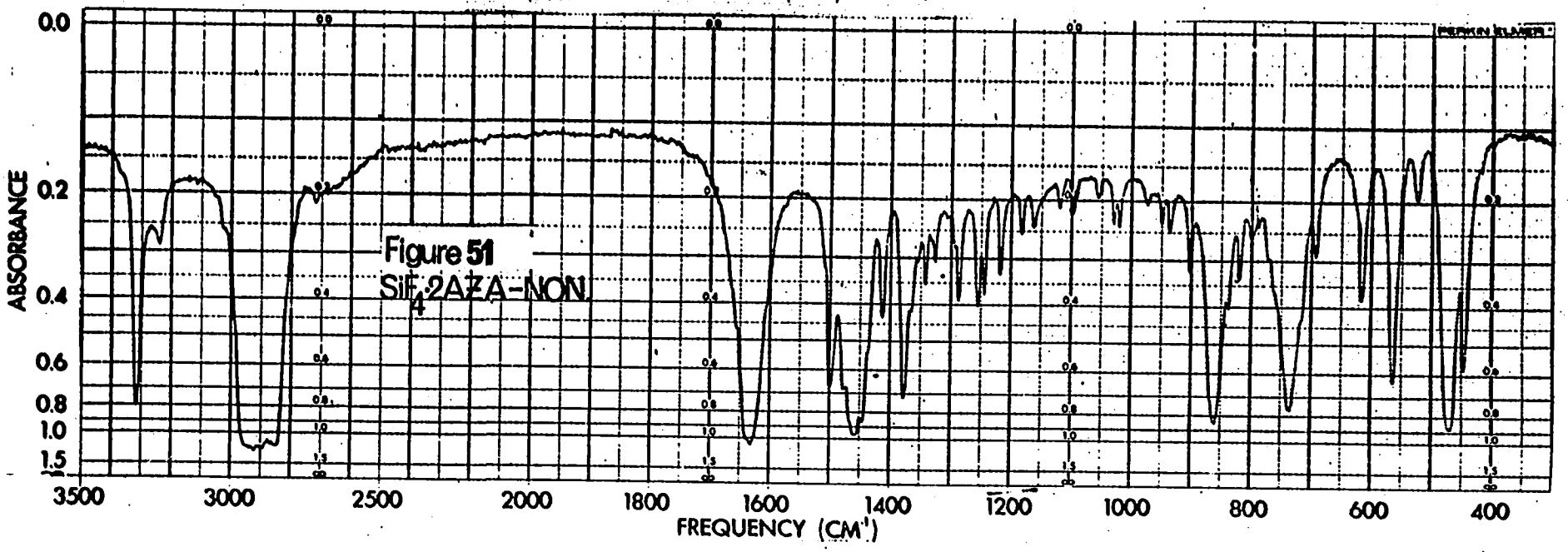

Figure 51
SiF_4-2AZA-NON

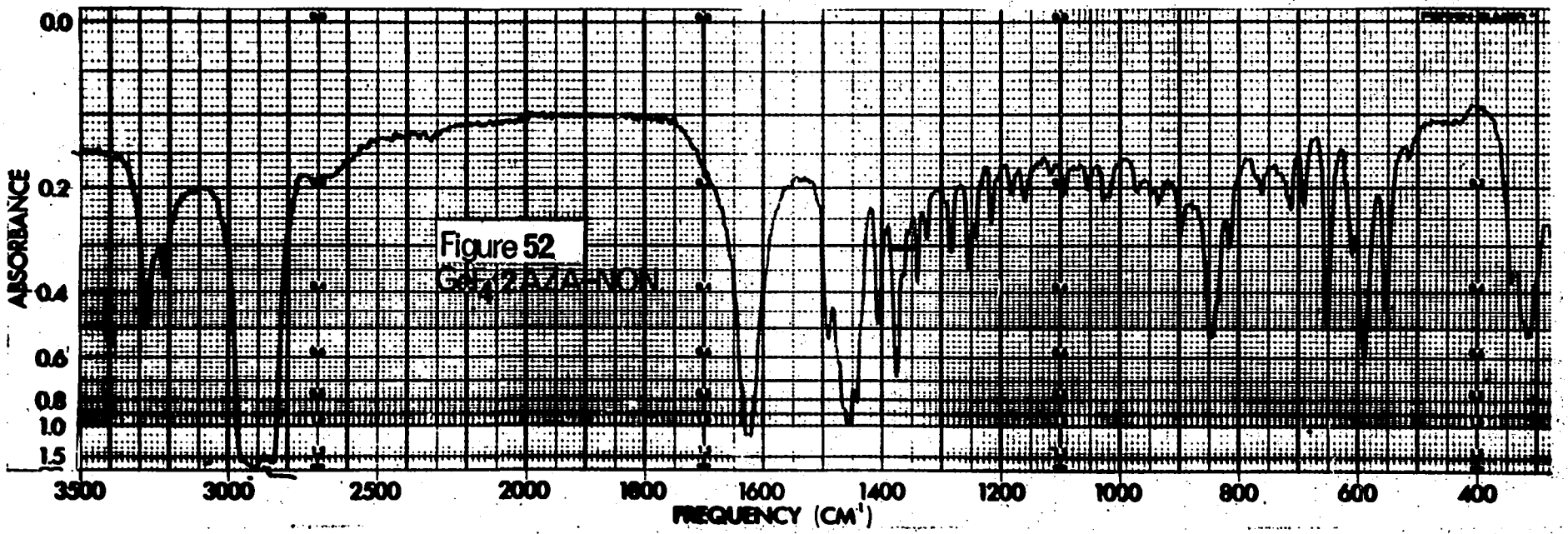

Figure 52
GeF_4:2AZA-NON.

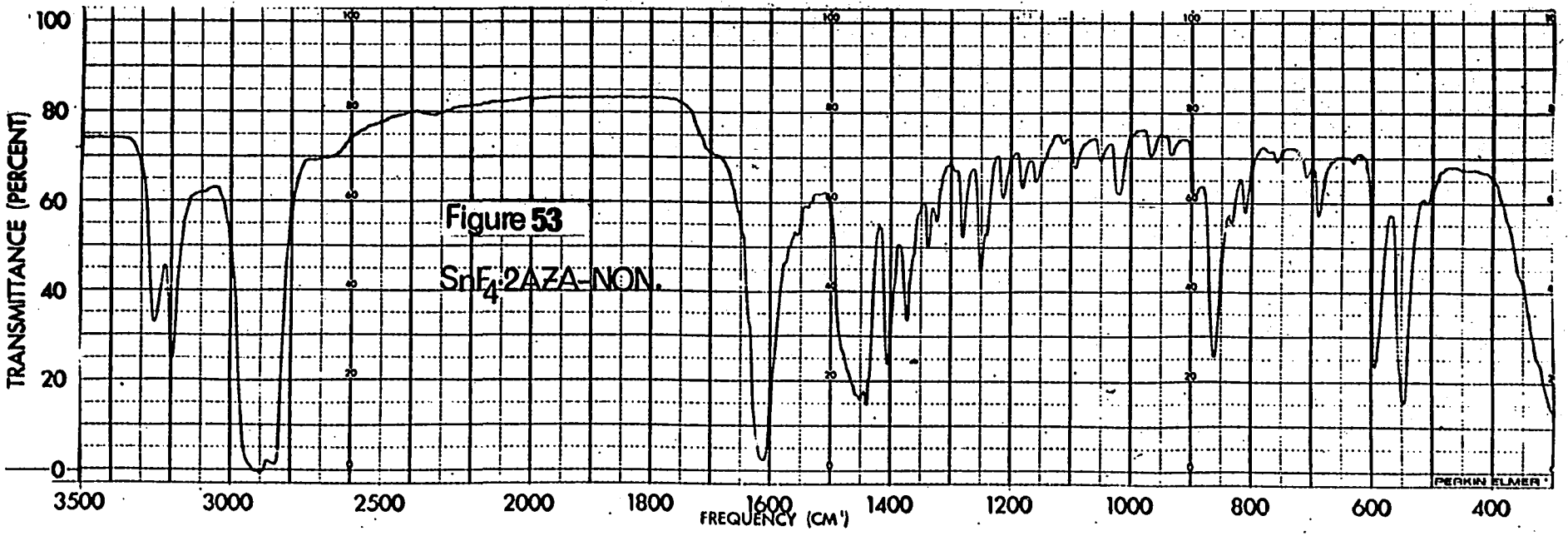

Figure 53
SnF_4:2AZA-NON.

SOLUTION INFRARED SPECTRA

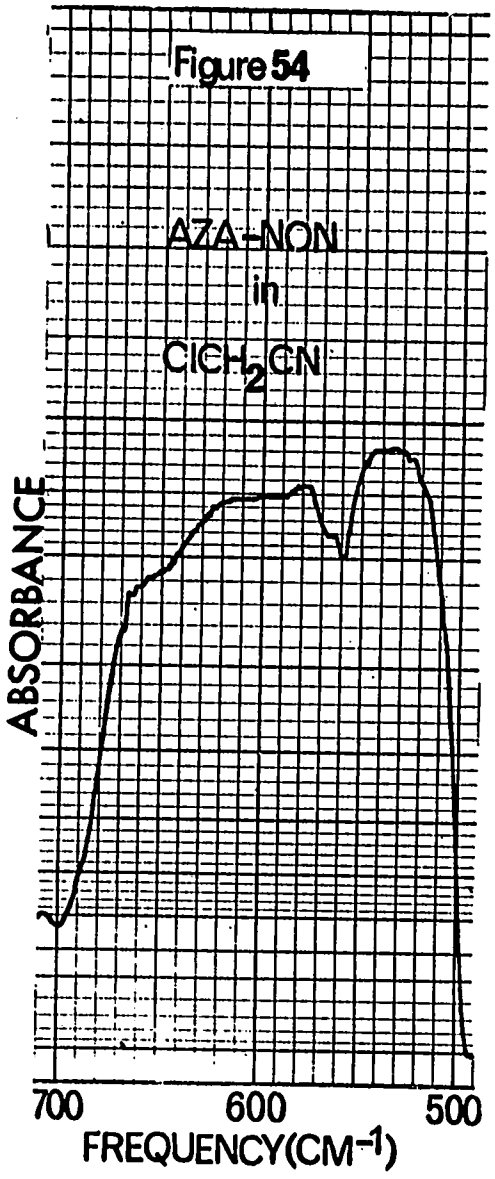

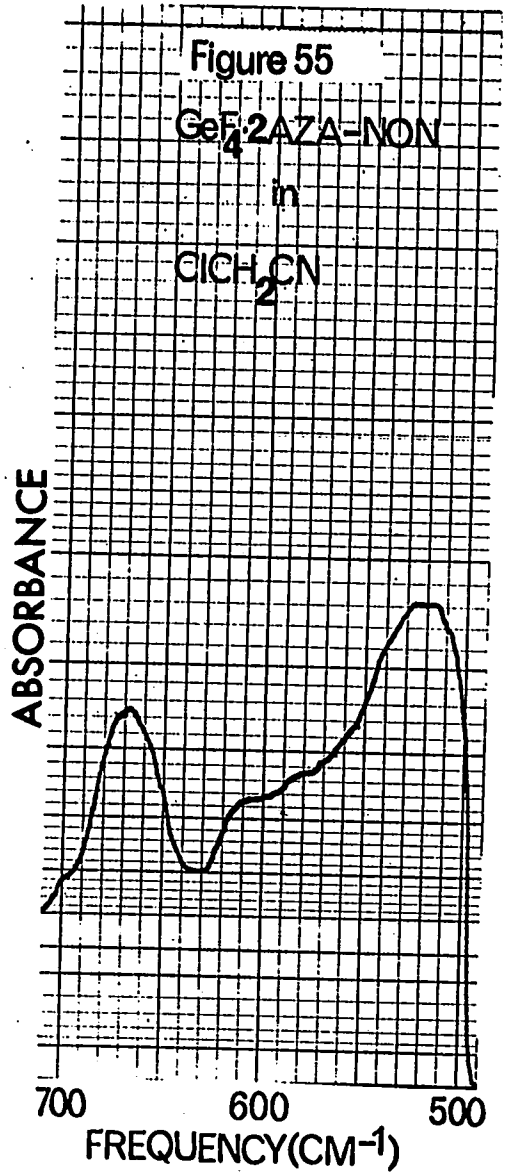

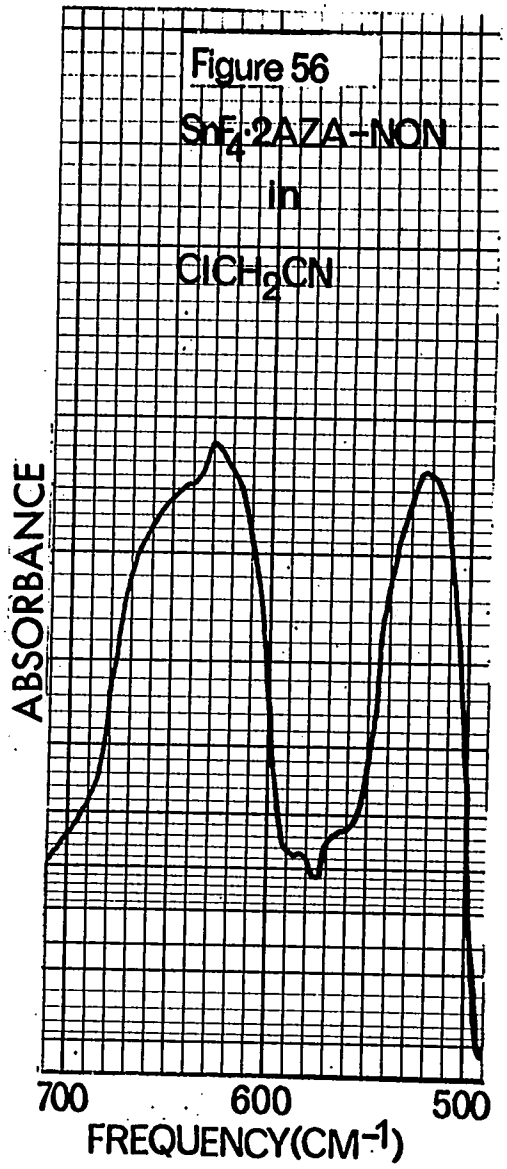

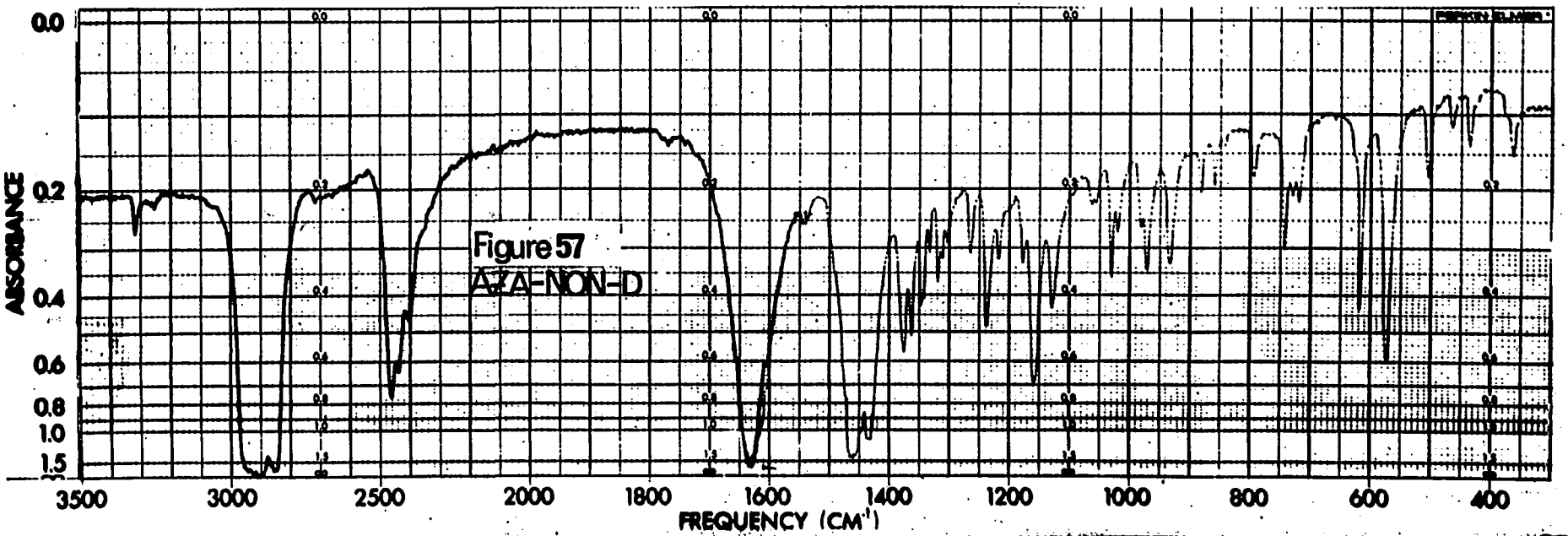

Figure 57
AZA-NON-D

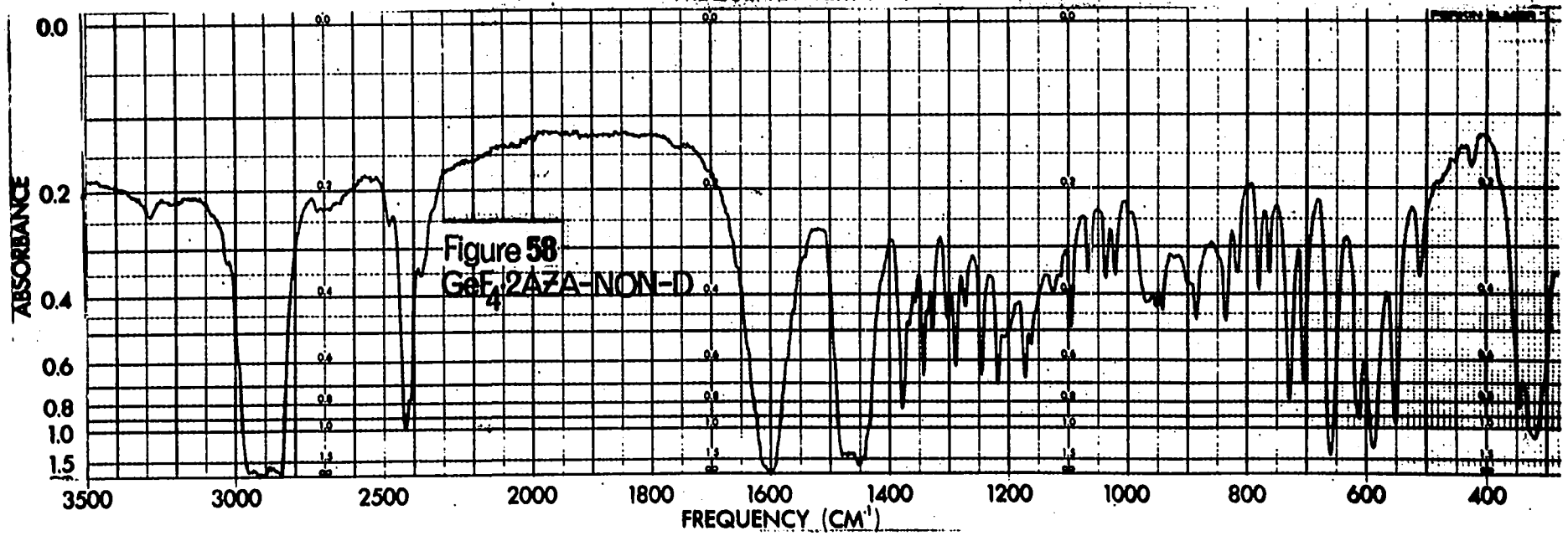

Figure 58
GeF_4 2AZA-NON-D

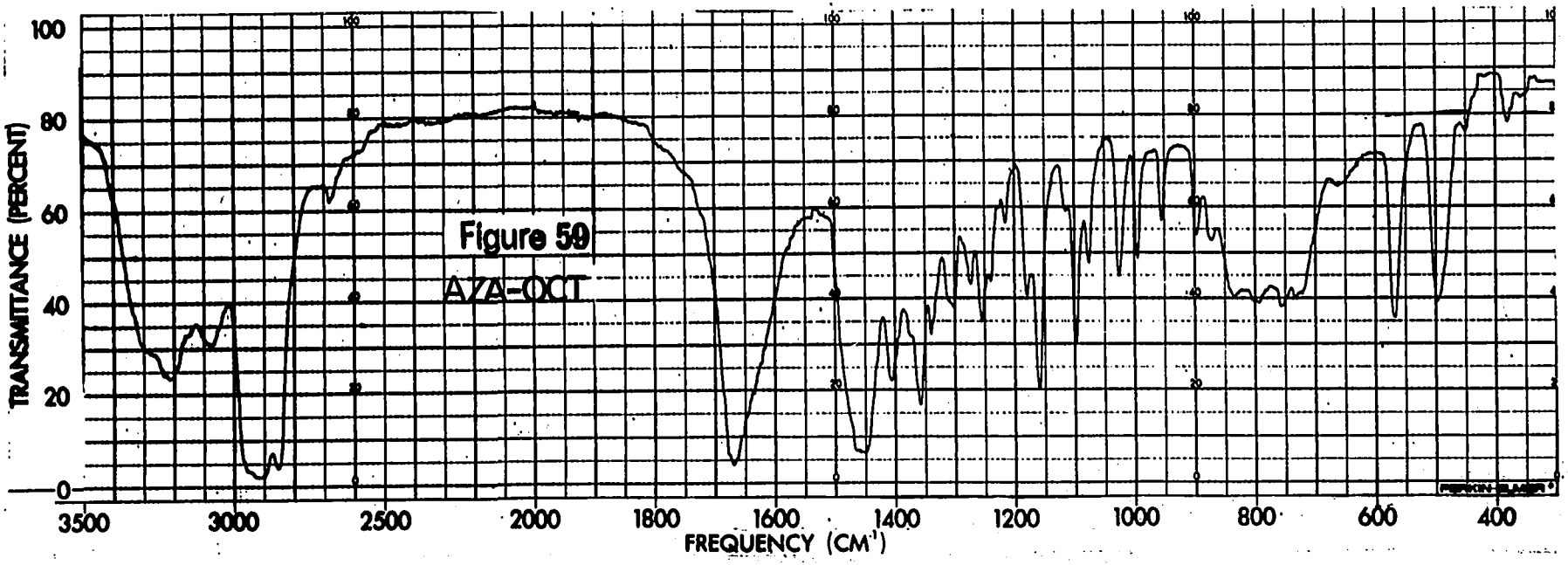

Figure 59
AZA-OCT

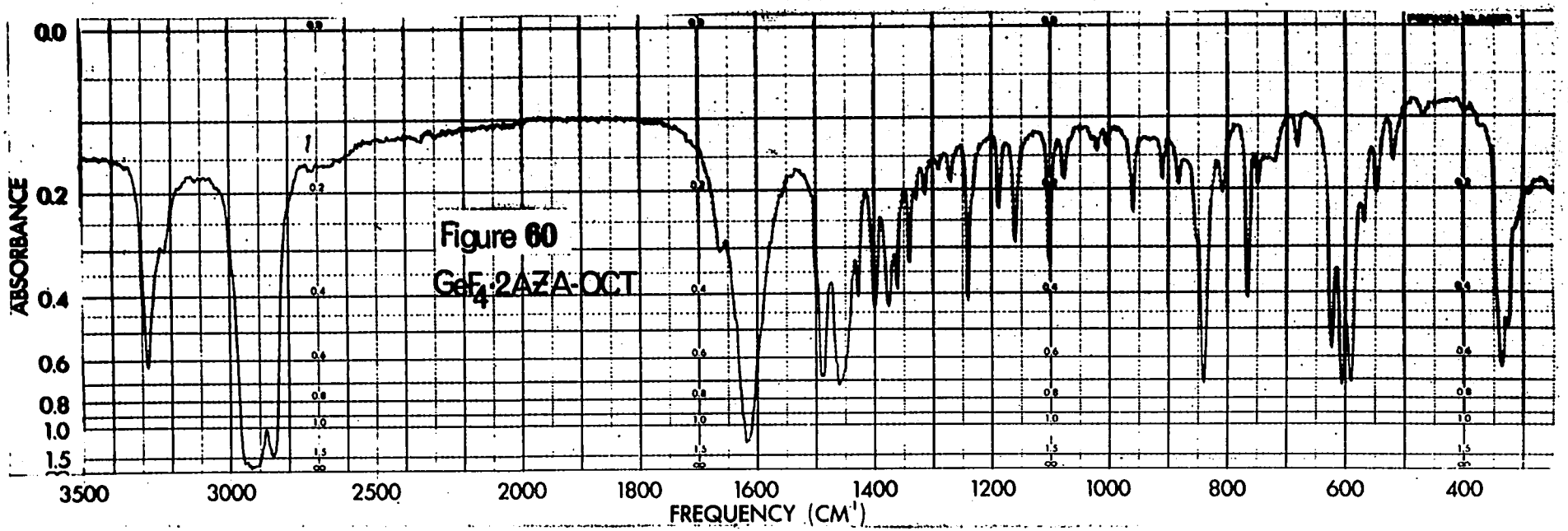

Figure 60
GeF_4·2AZA-OCT

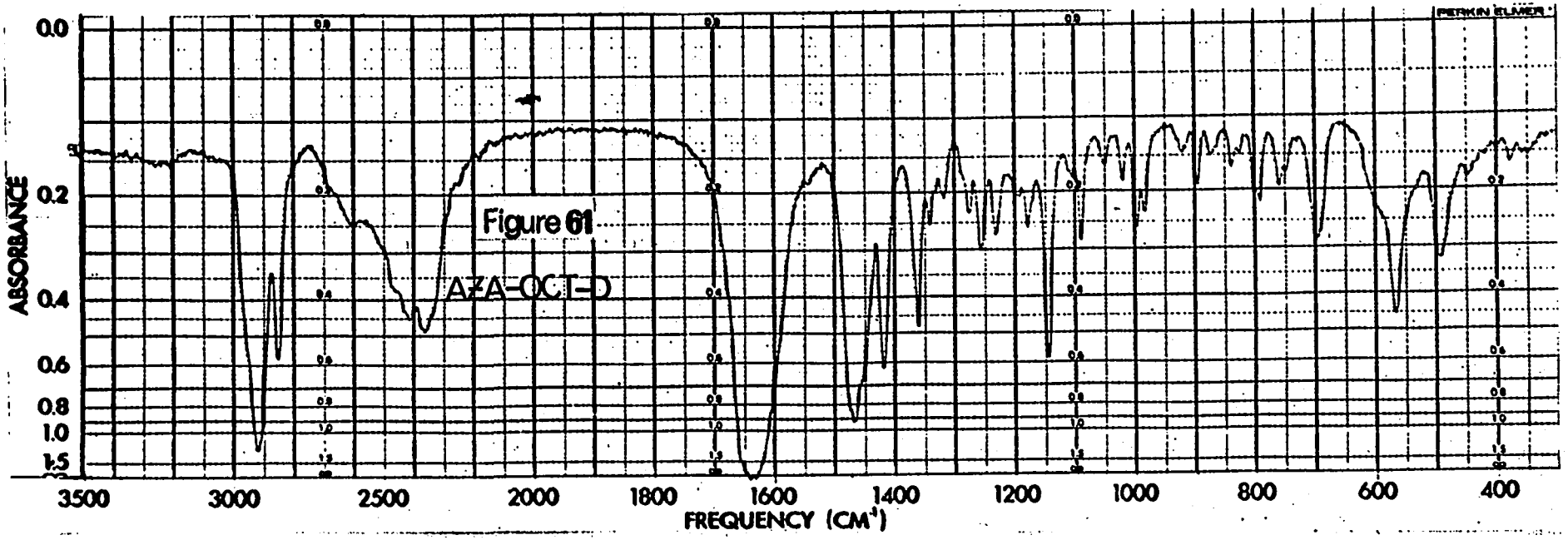

Figure 61

AZA-OCT-D

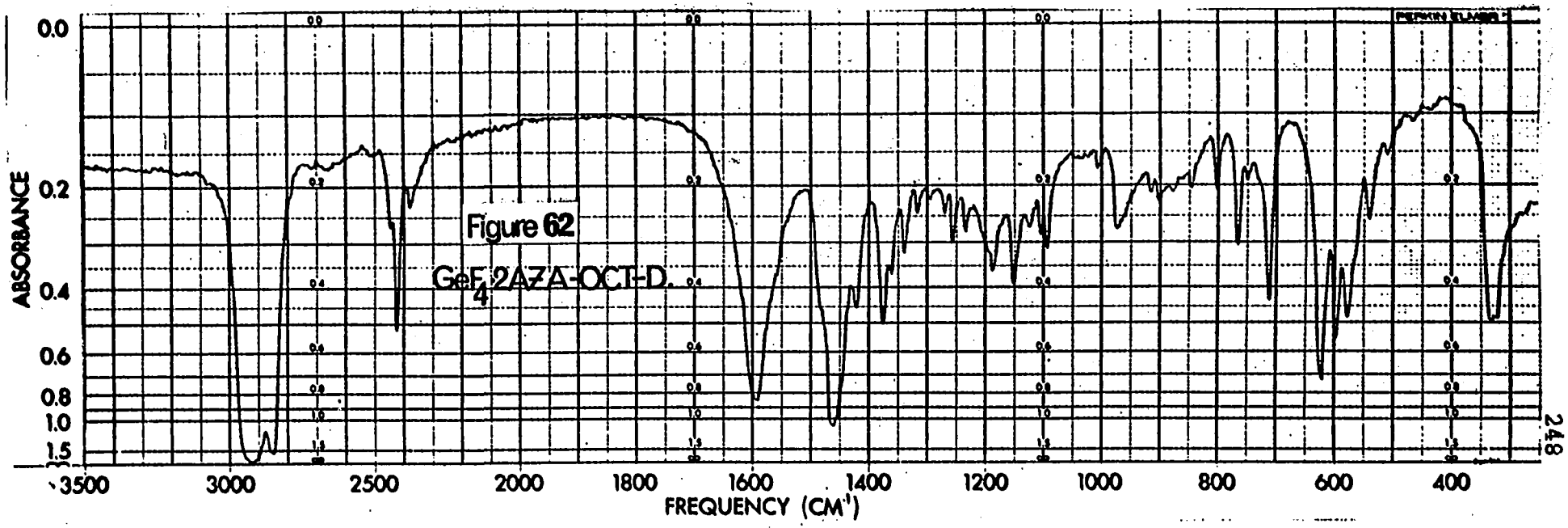

Figure 62

GeF_4:2AZA-OCT-D.

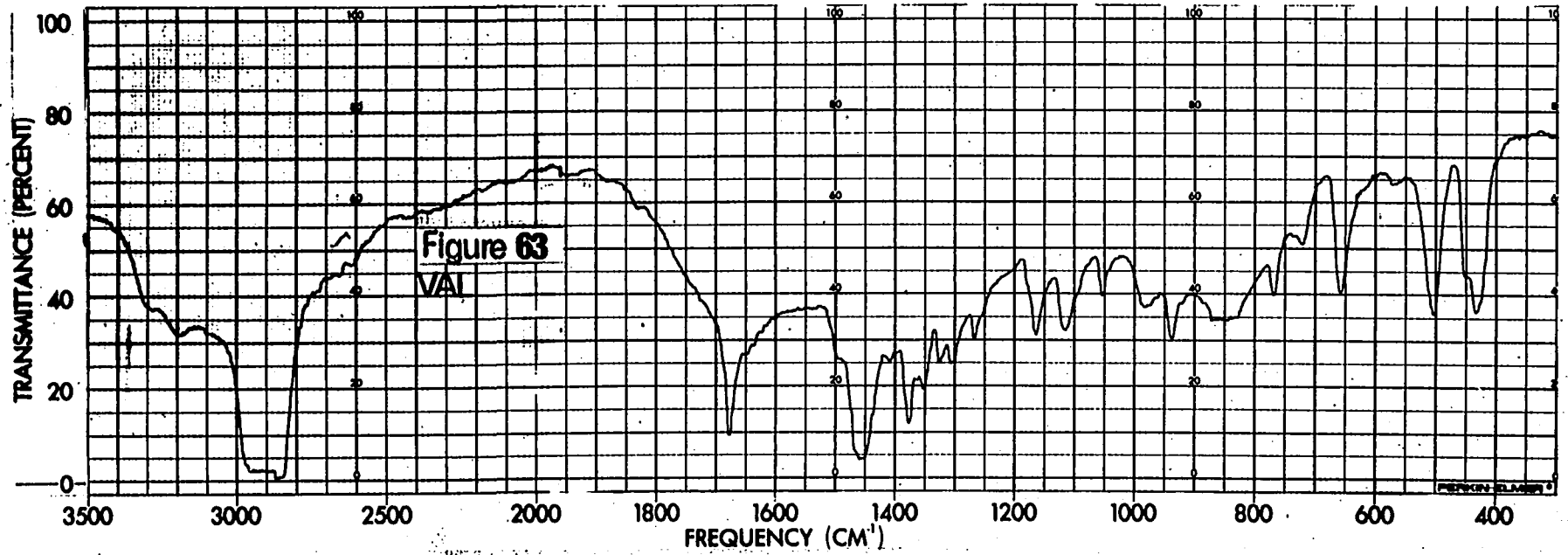

Figure 63
VAI

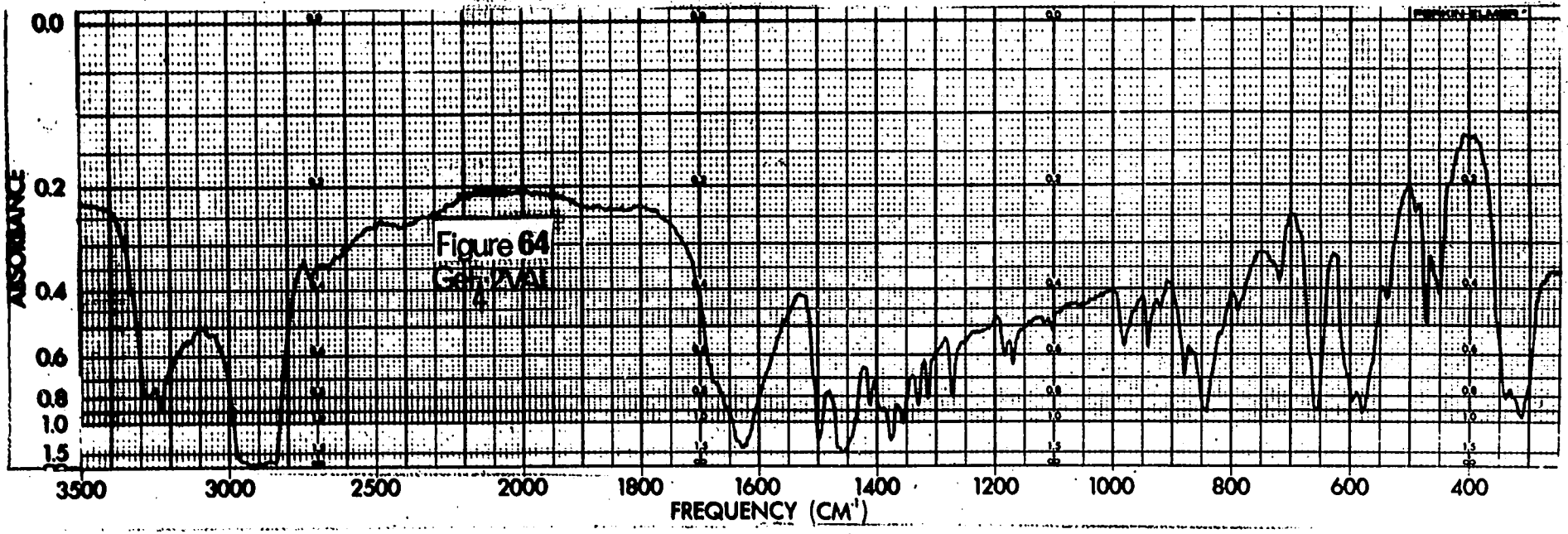

Figure 64
GeF₂/VAI

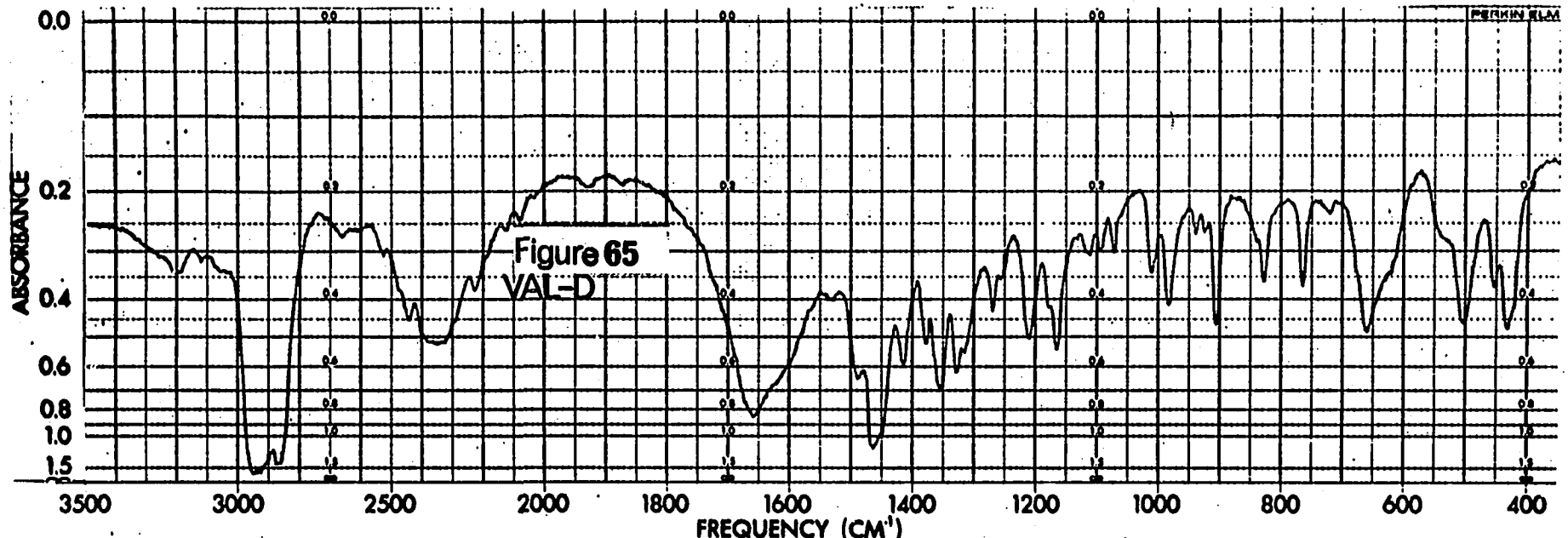

Figure 65
VAL-D

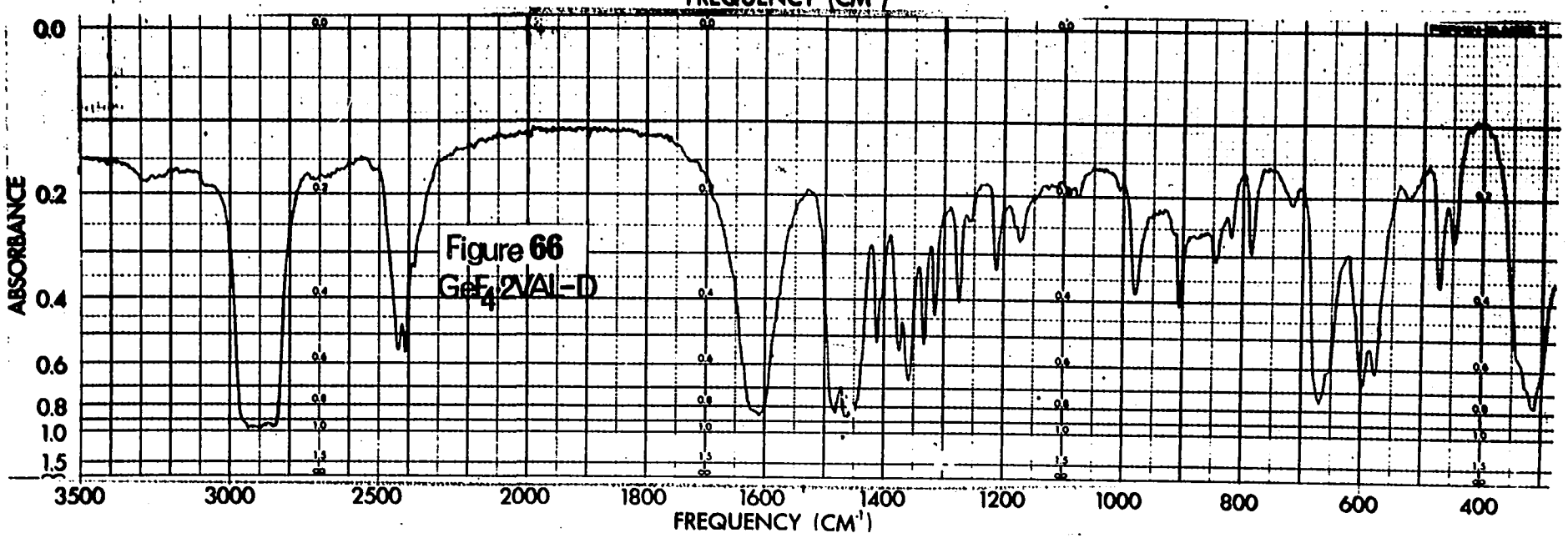

Figure 66
GeF_4 2VAL-D

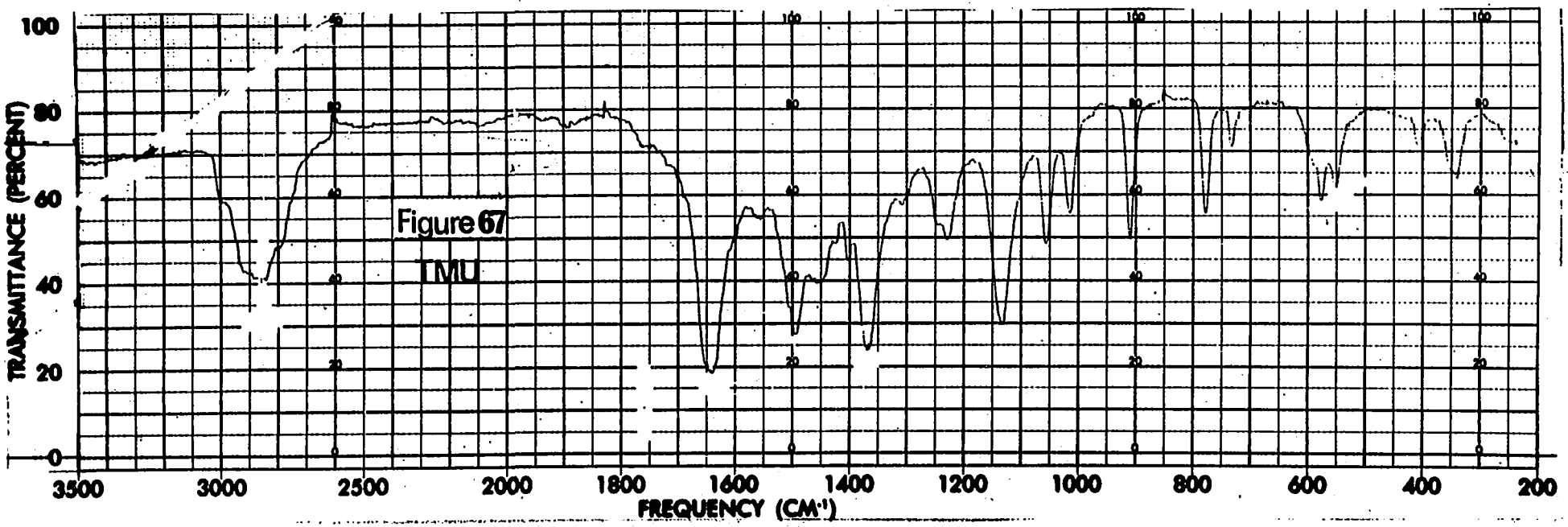

Figure 67

TMU

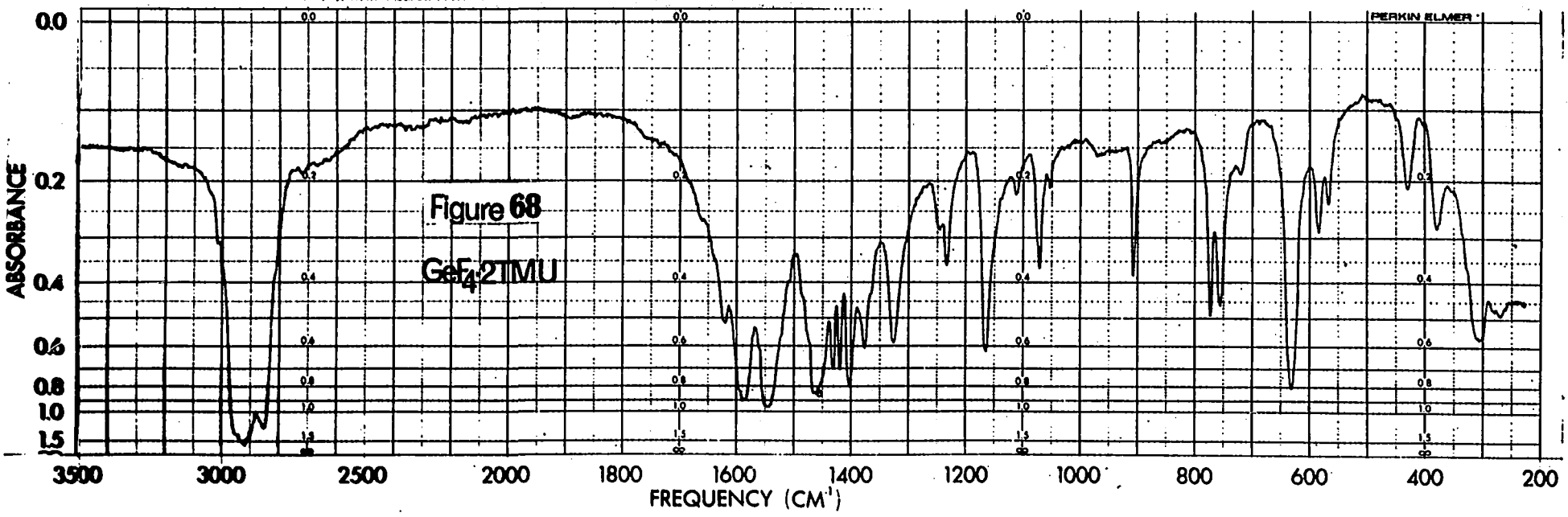

Figure 68

GeF_4·2TMU

SOLUTION INFRARED SPECTRA

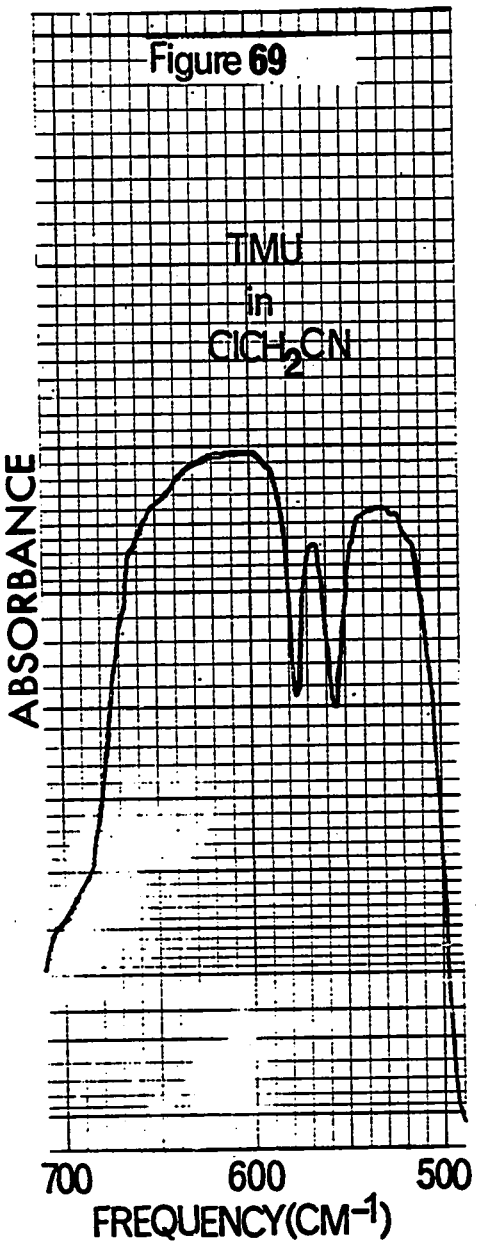

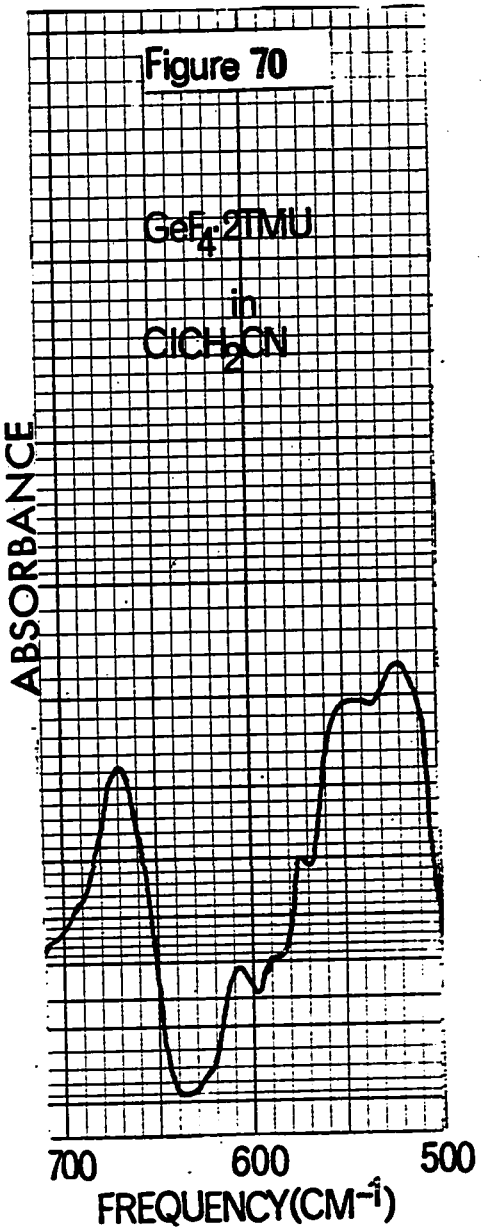

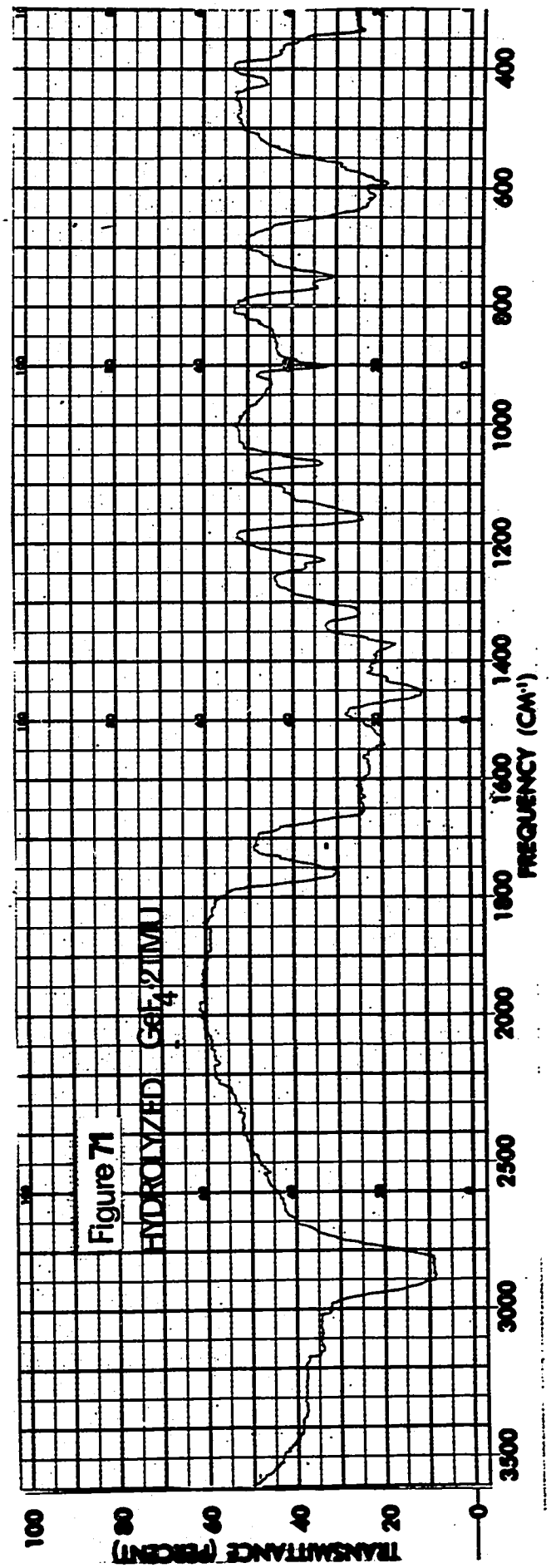

Figure 71

HYDROLYZED GeF_4-2-IIMU

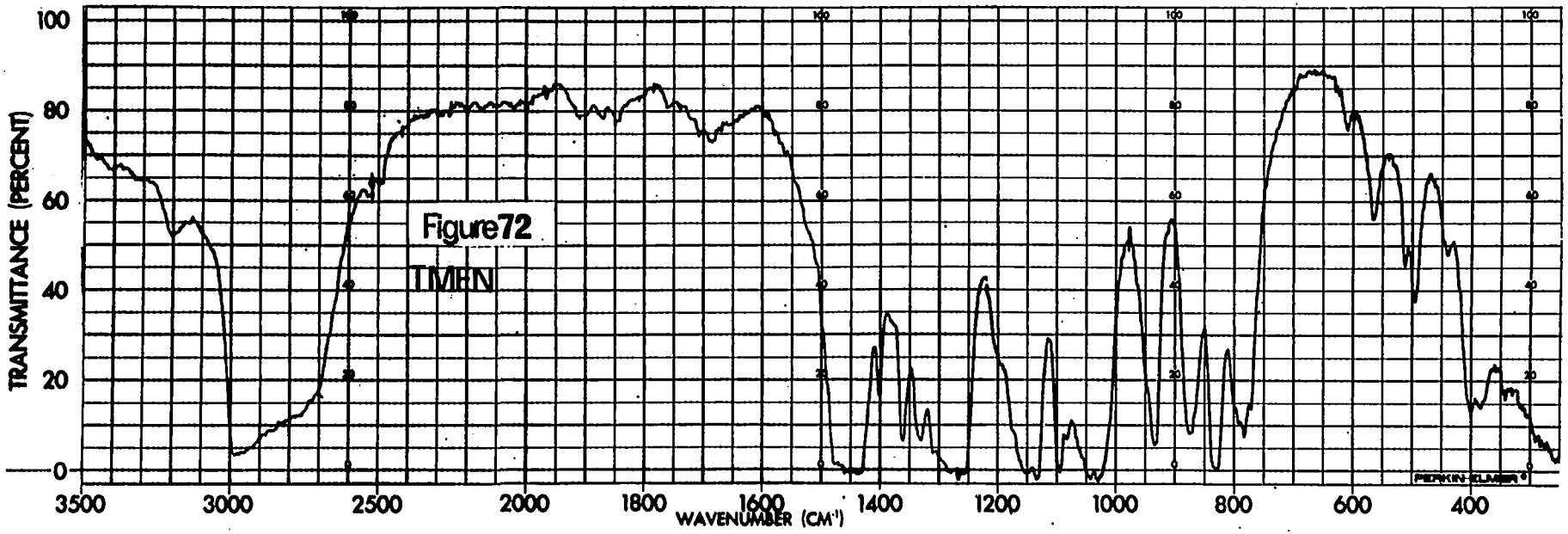

Figure72

TMEN

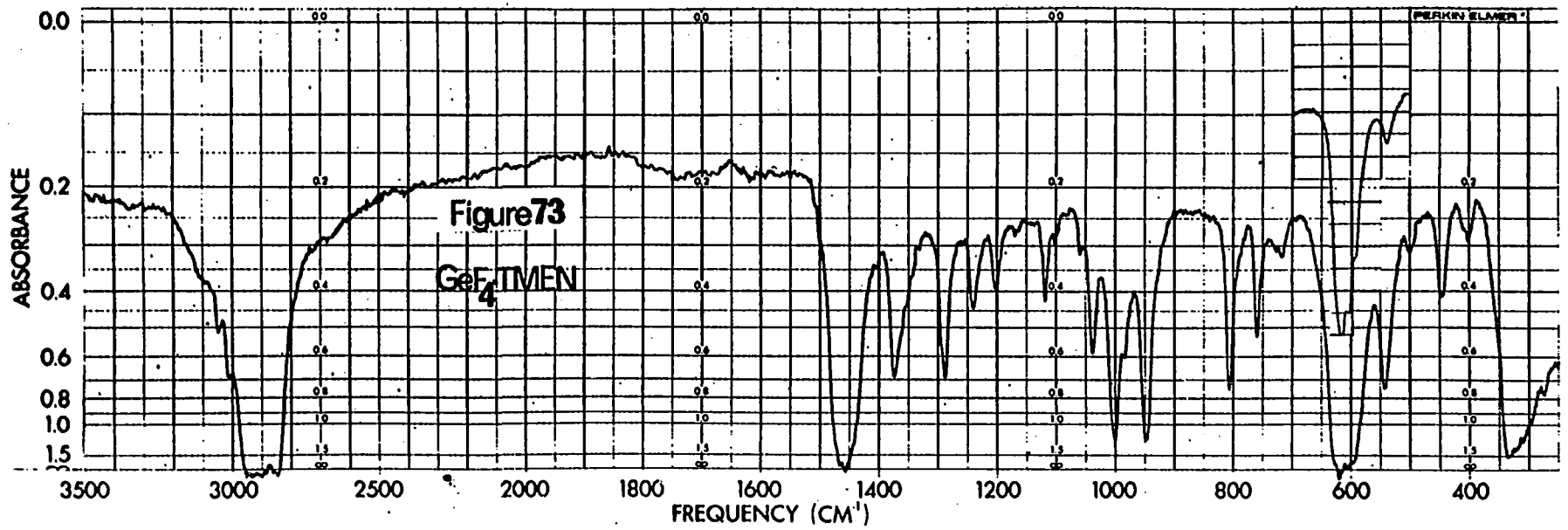

Figure73

GeF_4TMEN

SOLUTION INFRARED SPECTRUM

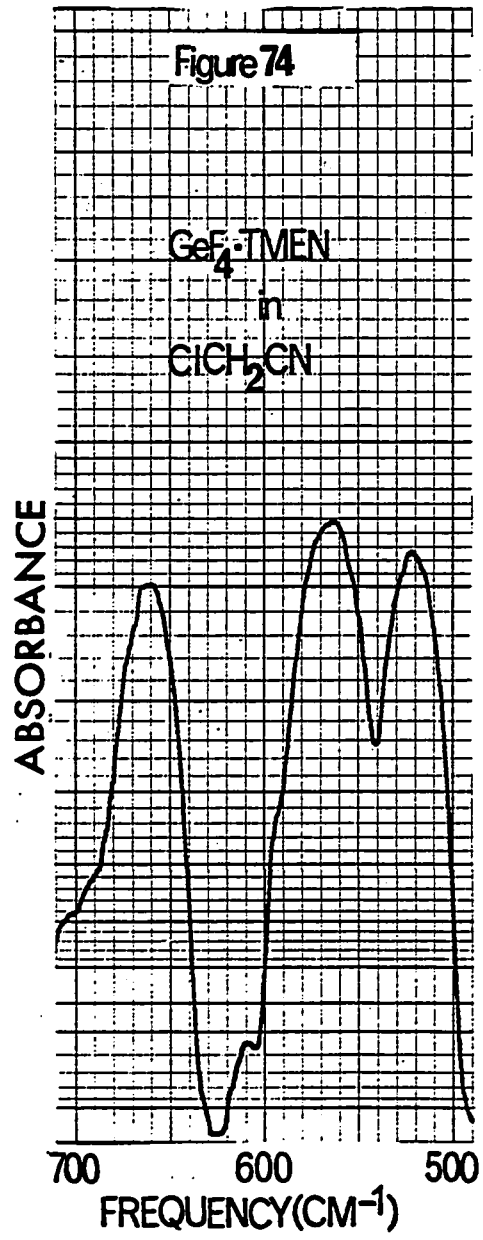

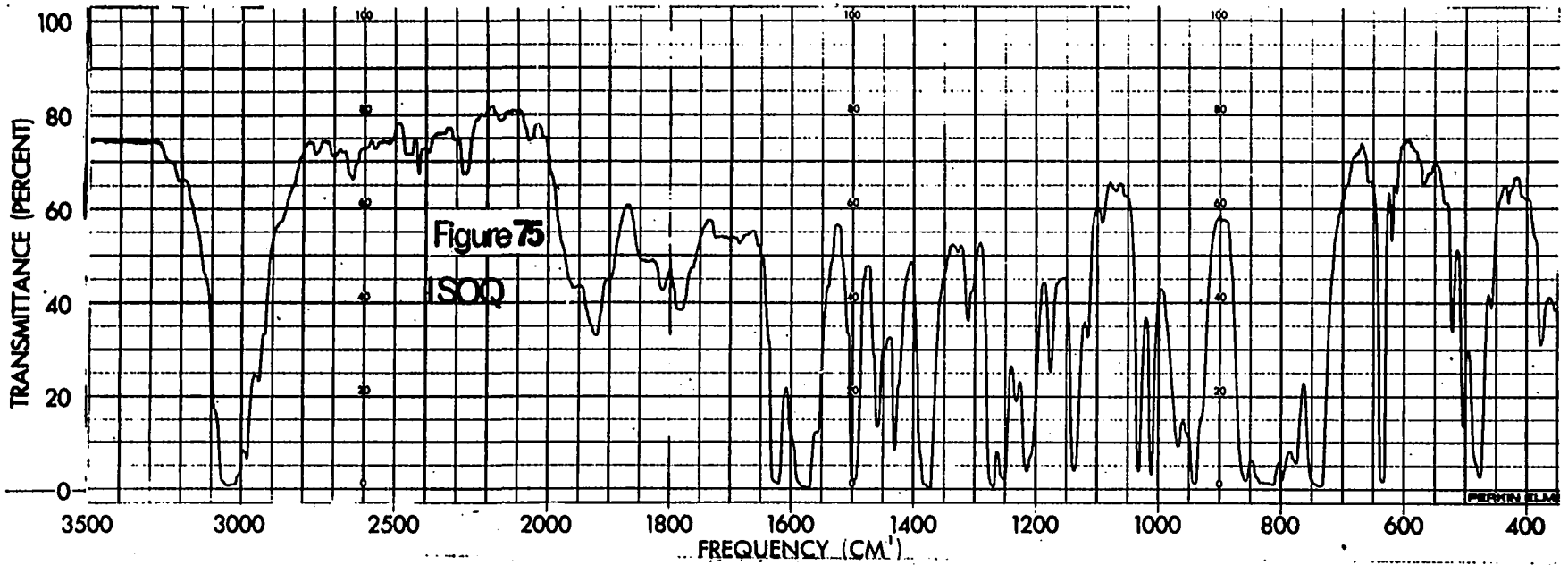

Figure 75
ISOQ

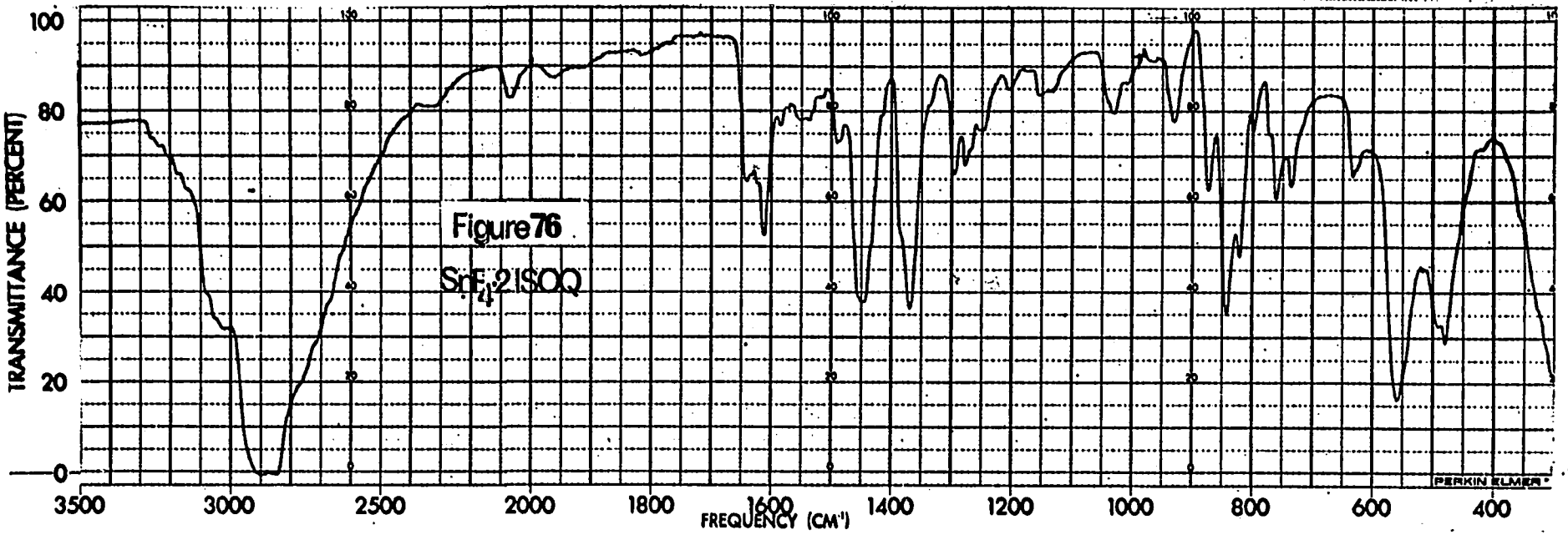

Figure 76
SnF_4·2ISOQ

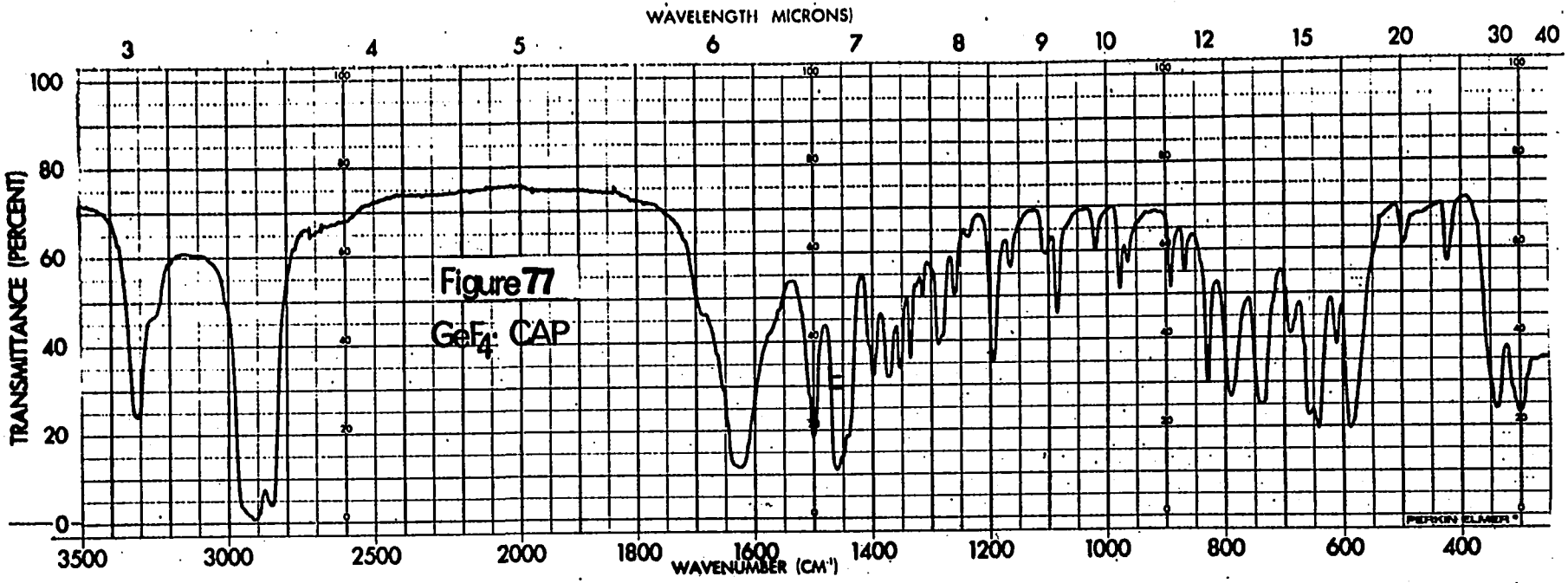

Figure 77

GeF_4: CAP

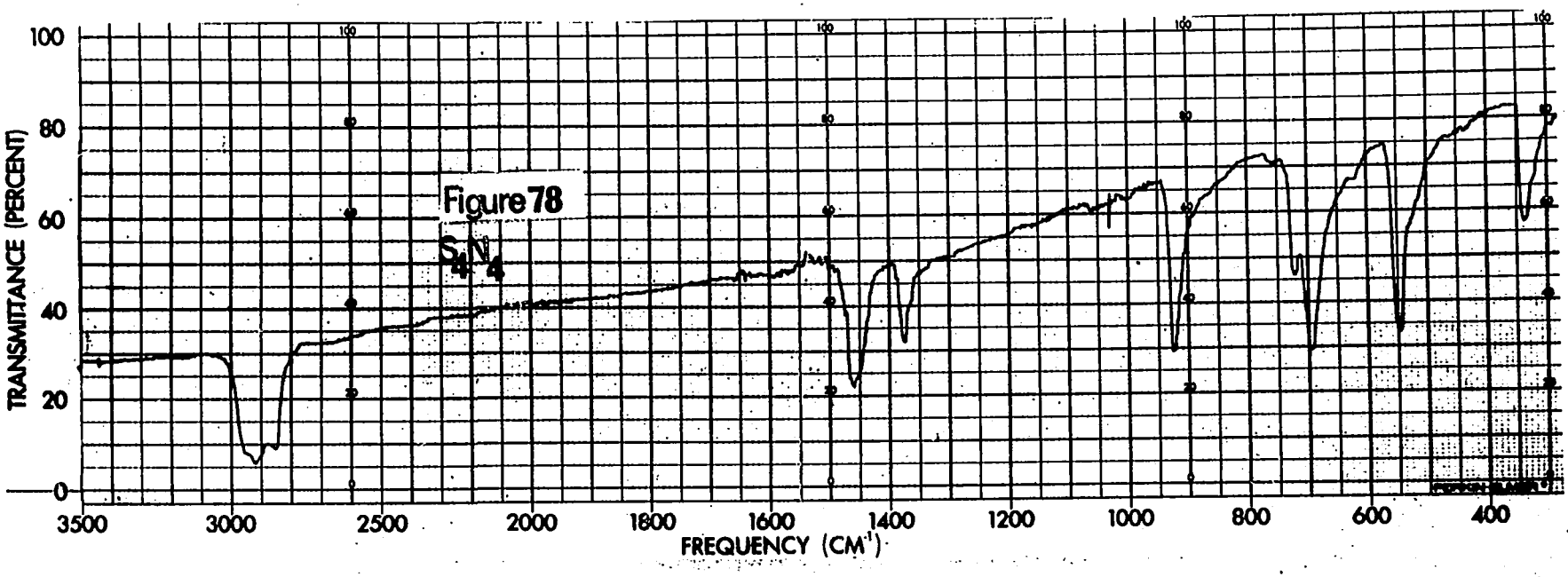

Figure 78
S_4N_4

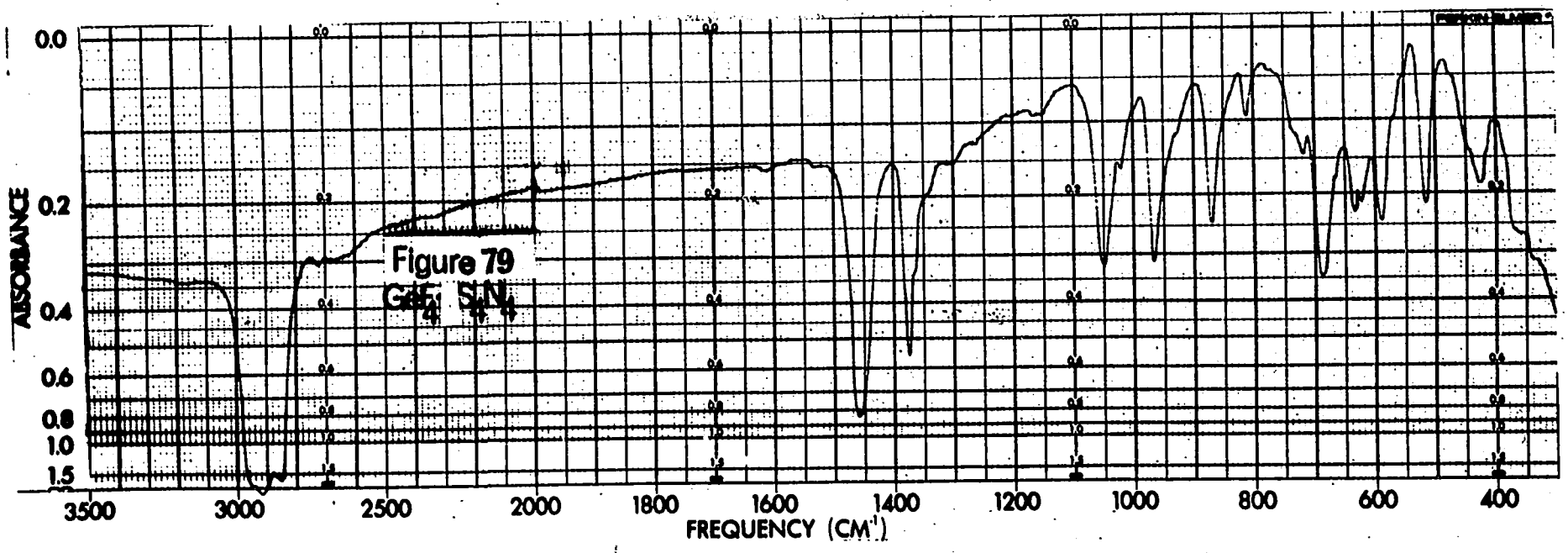

Figure 79
GeF_4 S_4N_4

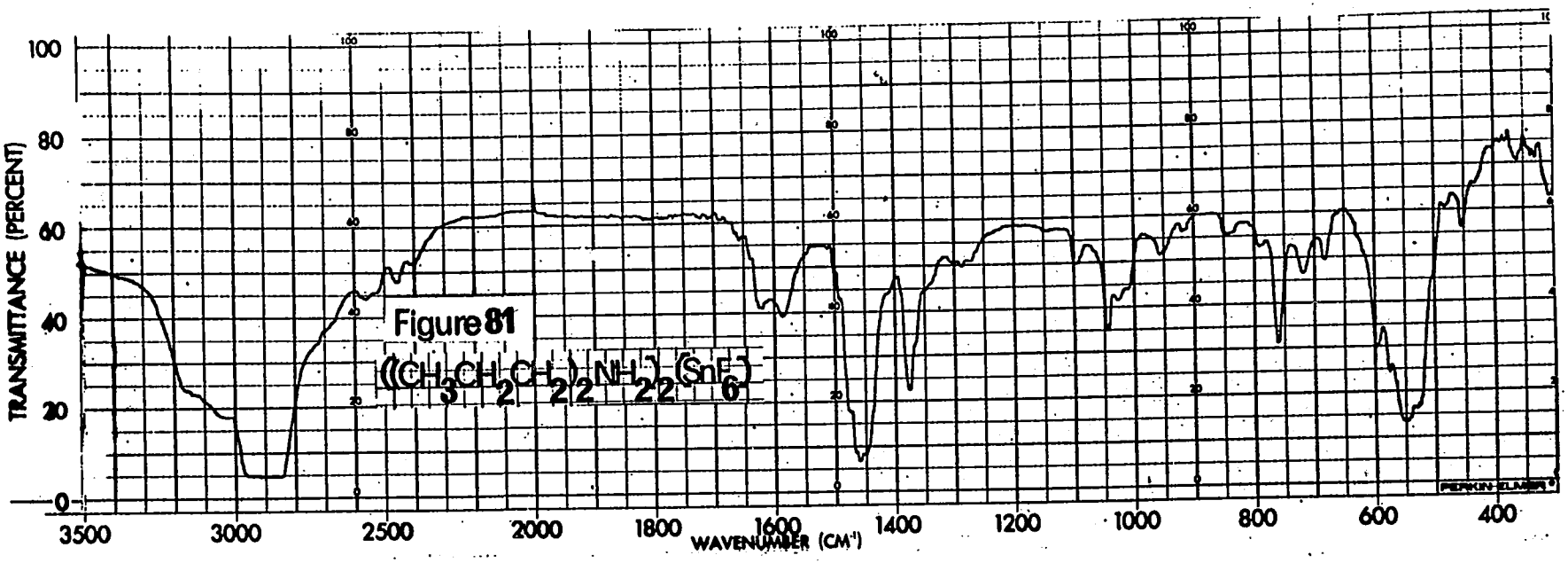

Figure 81
$((CH_3CH_2CH_2)_2NH_2)_2(SnF_6)$

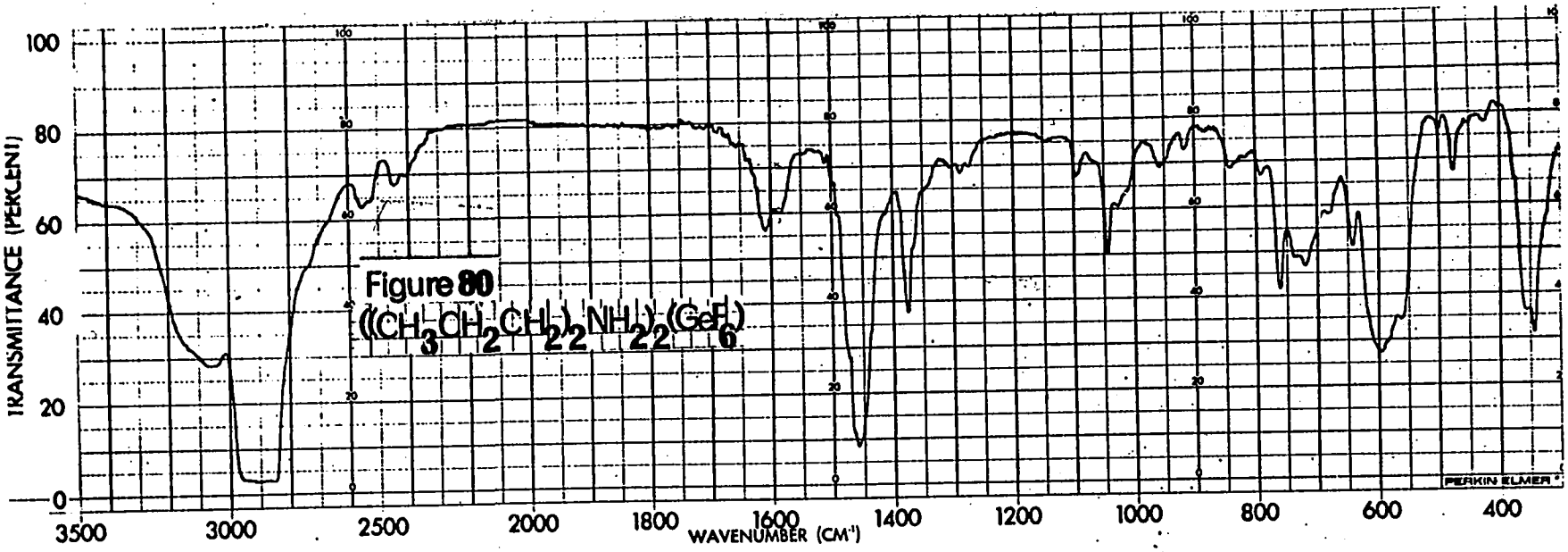

Figure 80
$((CH_3CH_2CH_2)_2NH_2)_2(GeF_6)$

SOLUTION INFRARED SPECTRA

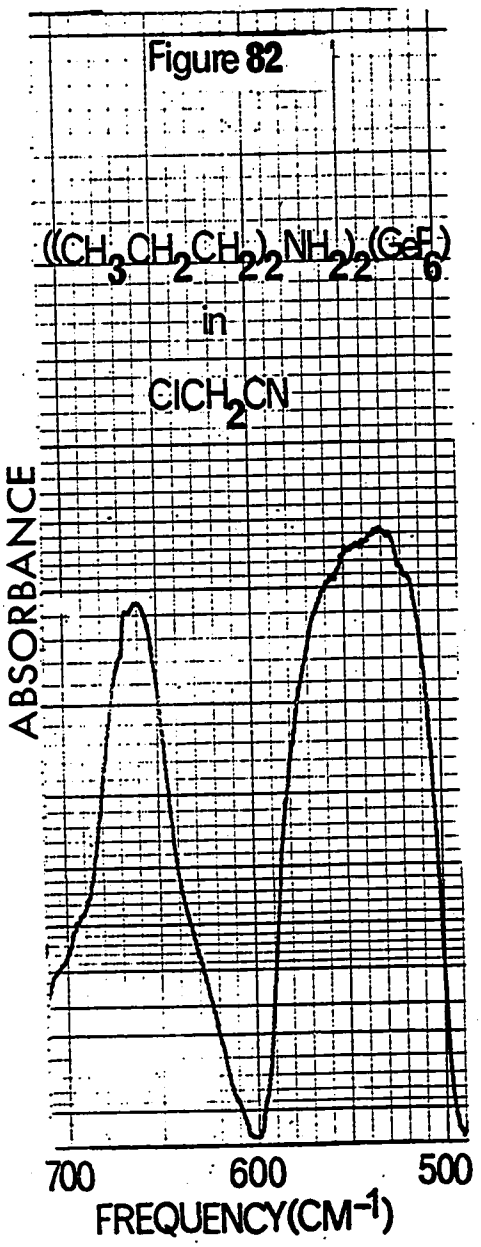

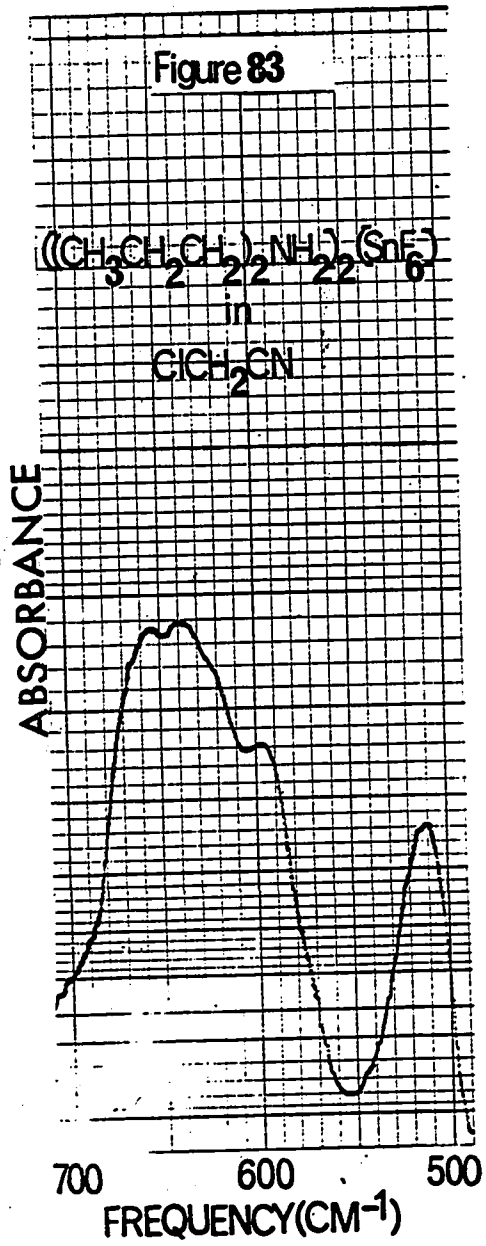

INFRARED SPECTRUM

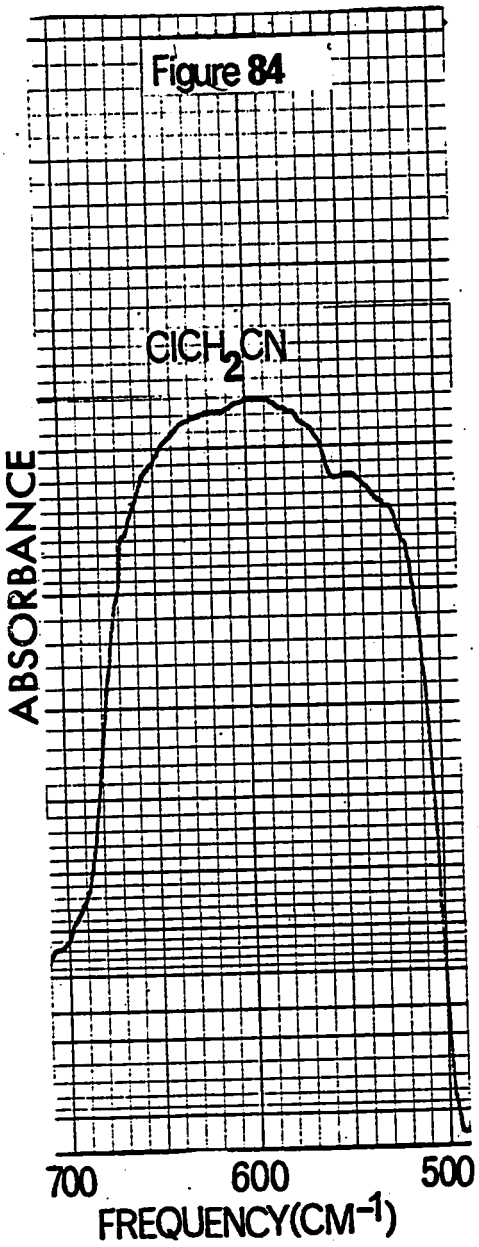

APPENDIX D. Raman Spectra (Solid State)

Figure 85
SOLID STATE
RAMAN SPECTRUM OF $GeF_4 \cdot 2PY$

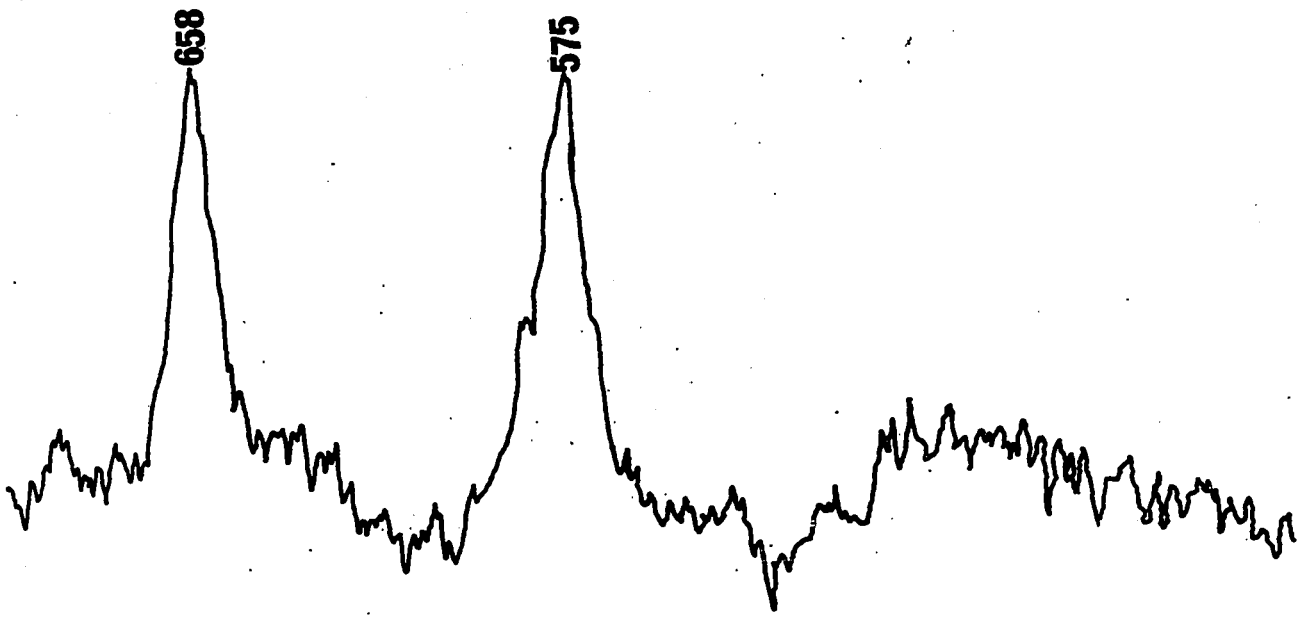

Figure 86
SOLID STATE
RAMAN SPECTRUM OF SiF_4·DIPY

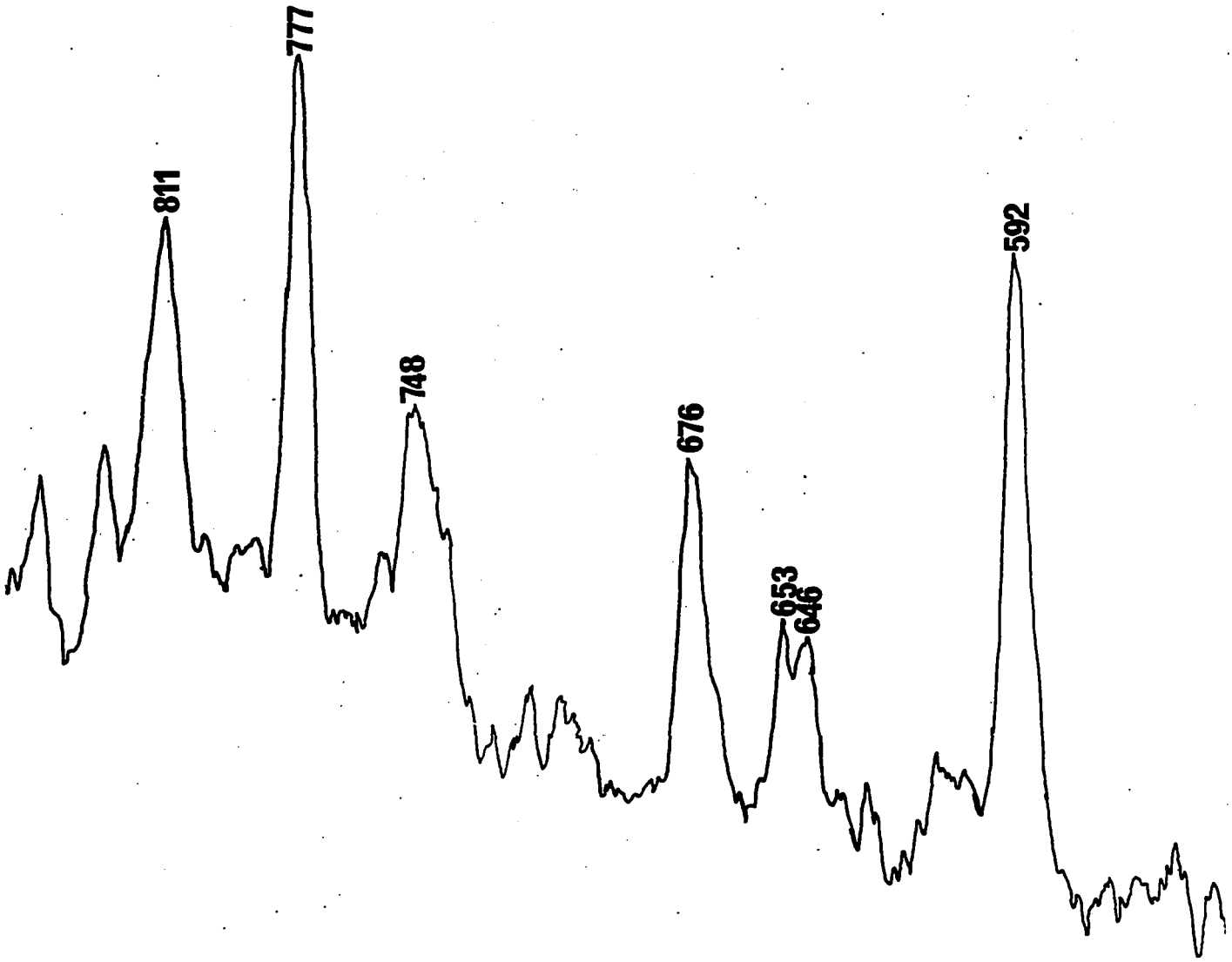

FIGURE 87
SOLID STATE
RAMAN SPECTRUM OF GeF_4·DIPY

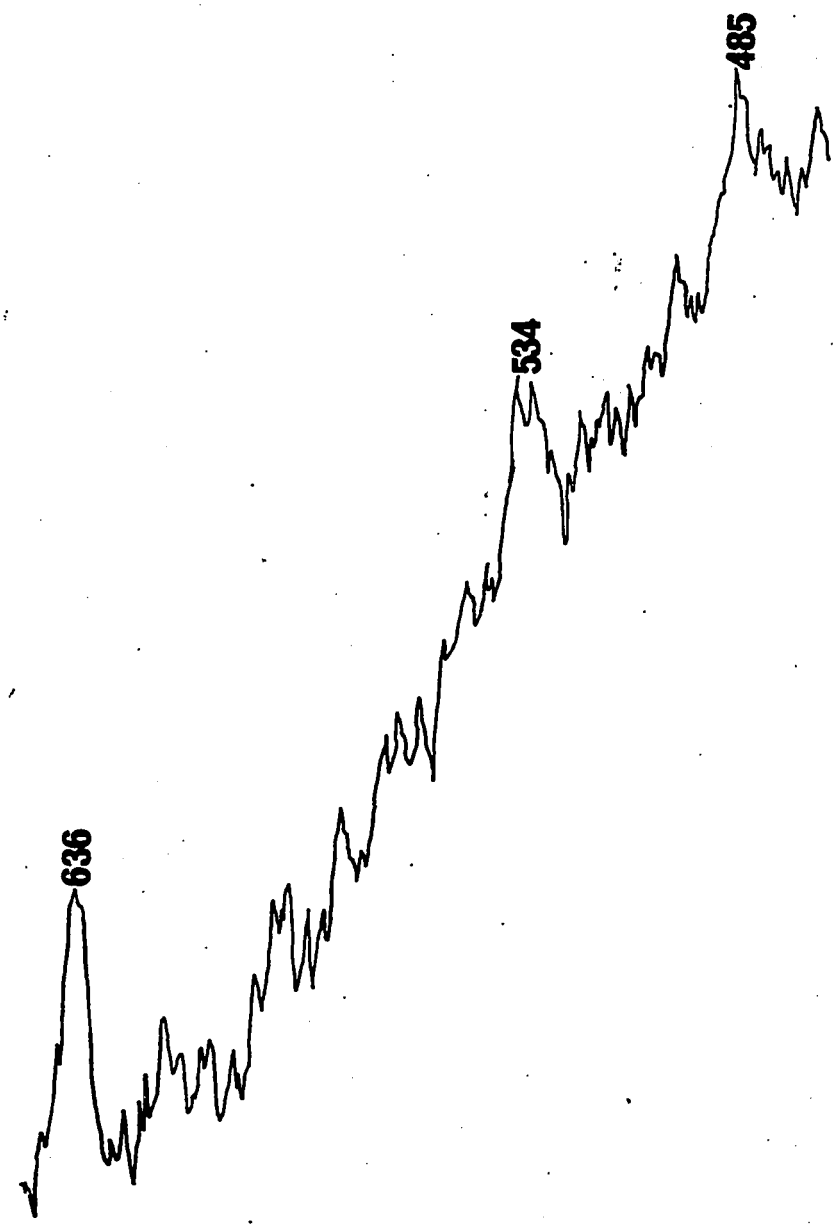

Figure 88.
SOLID STATE
RAMAN SPECTRUM OF SnF_4-DIPY

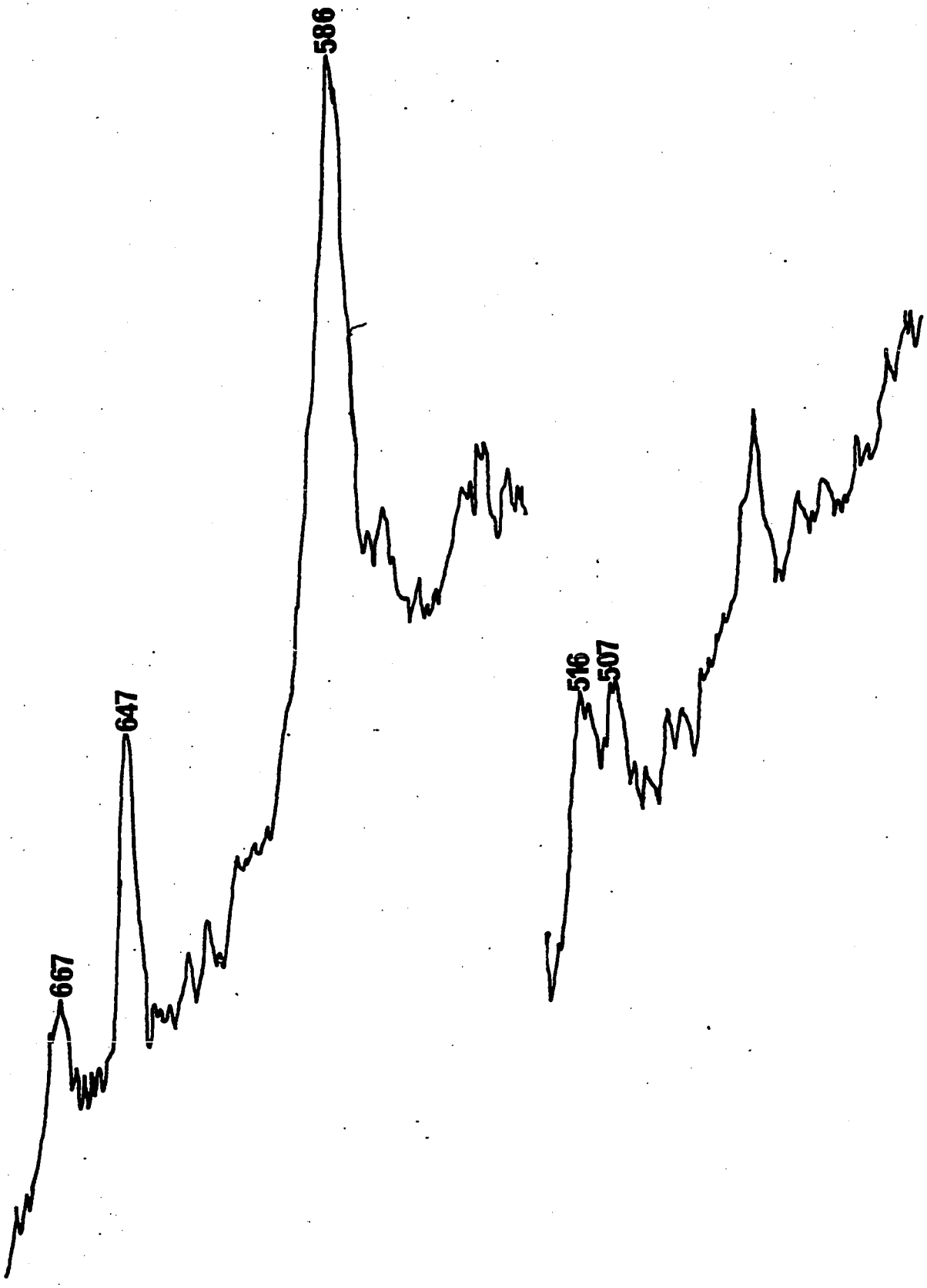

Figure 89

SOLID STATE
RAMAN SPECTRUM OF $GeF_4 \cdot 2HMPA$

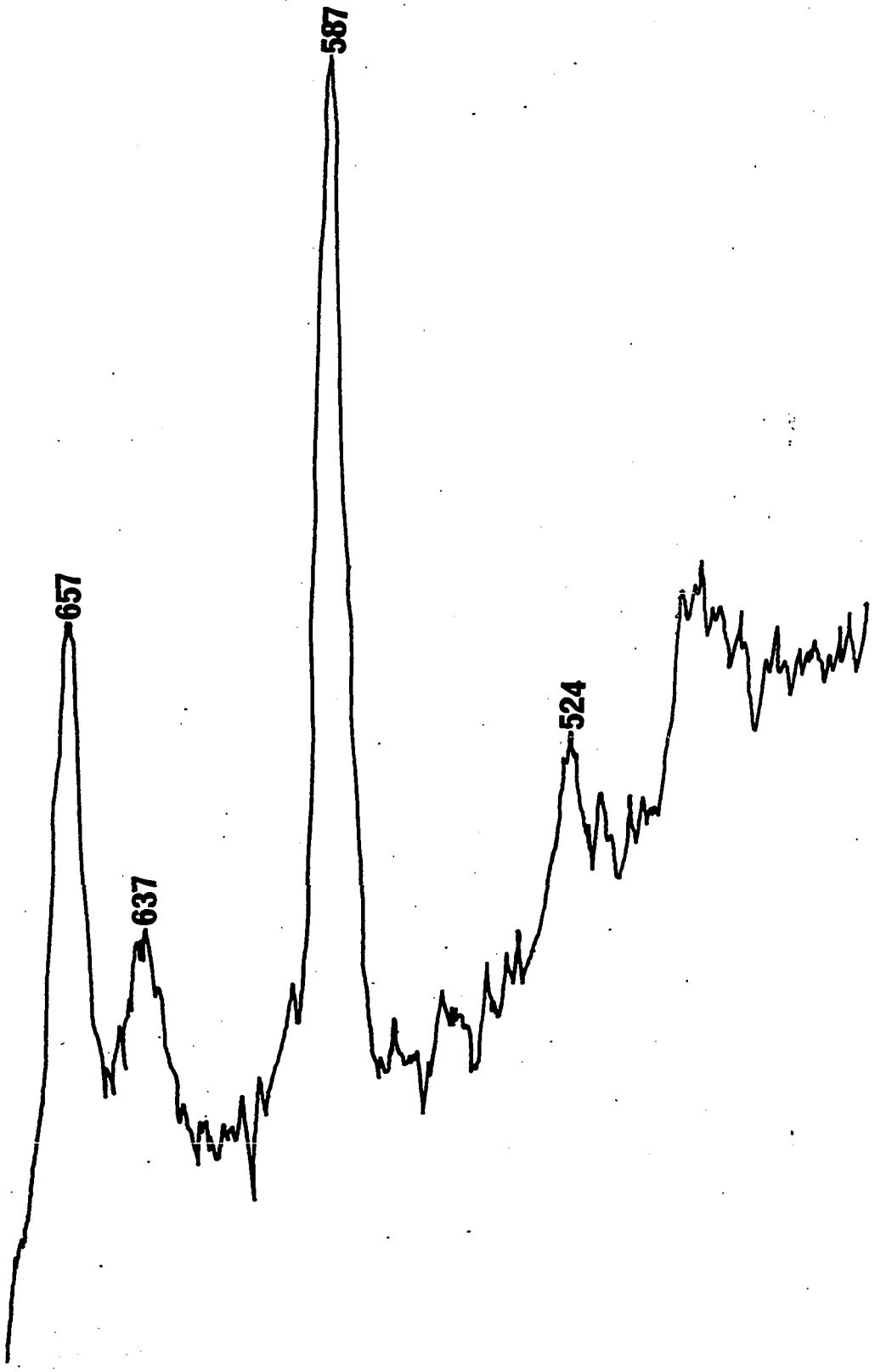

Figure 90

SOLID STATE
RAMAN SPECTRUM OF $GeF_4 \cdot 2PYROL$

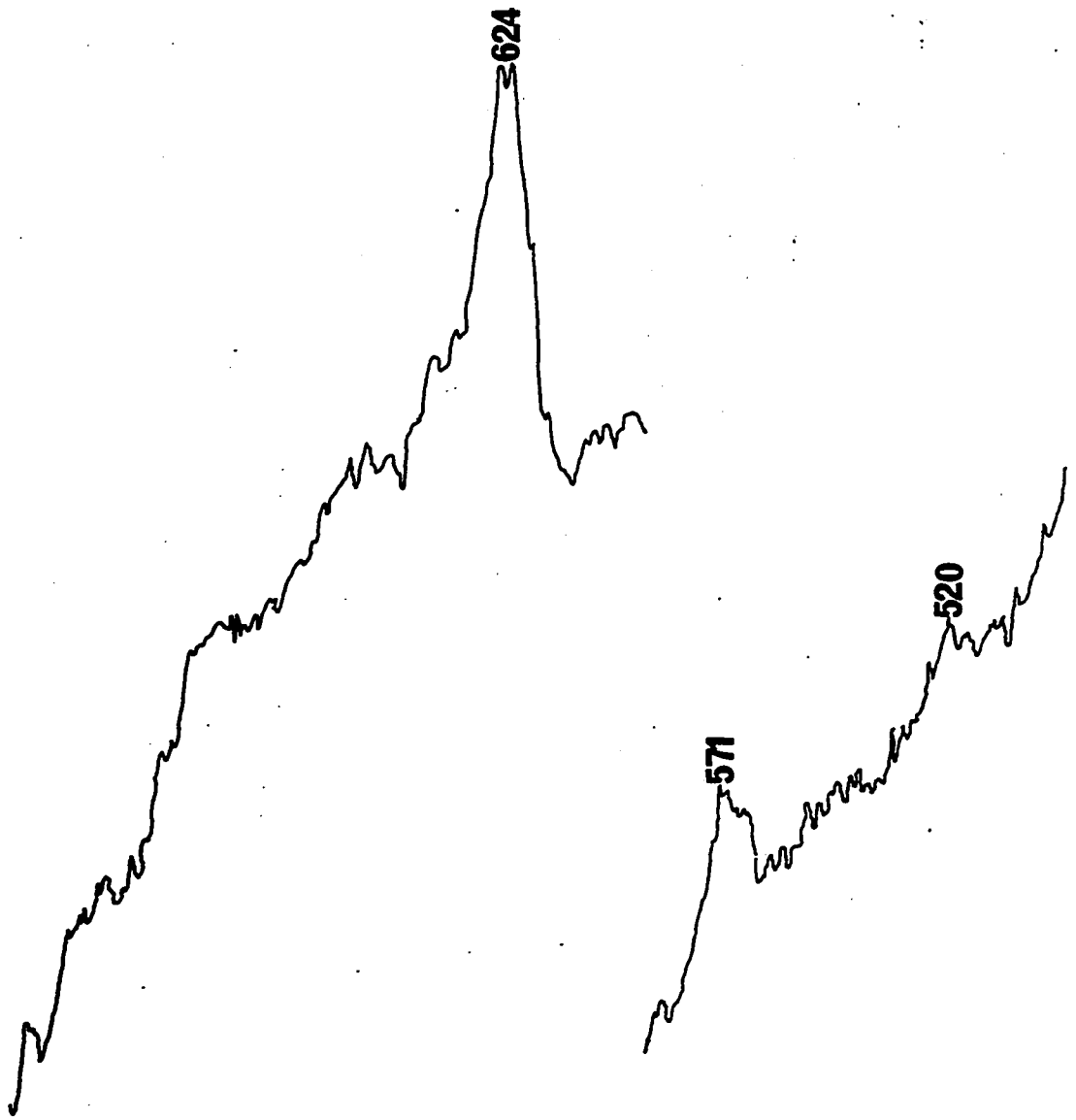

Figure 91. SOLID STATE RAMAN SPECTRUM OF $SnF_4 \cdot 2PYROL$

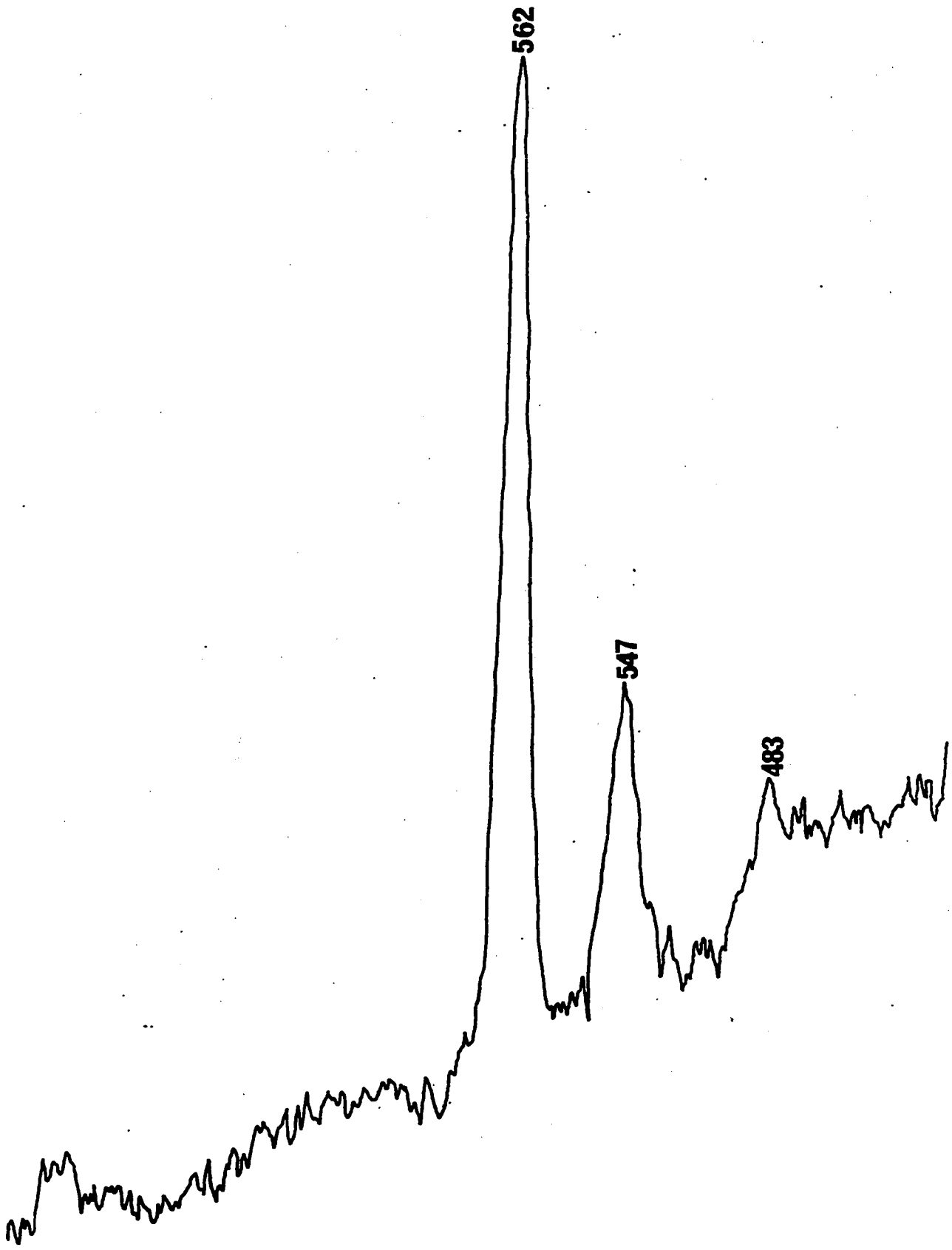

Figure 92

SOLID STATE
RAMAN SPECTRUM OF $GeF_4 \cdot 2CAP$

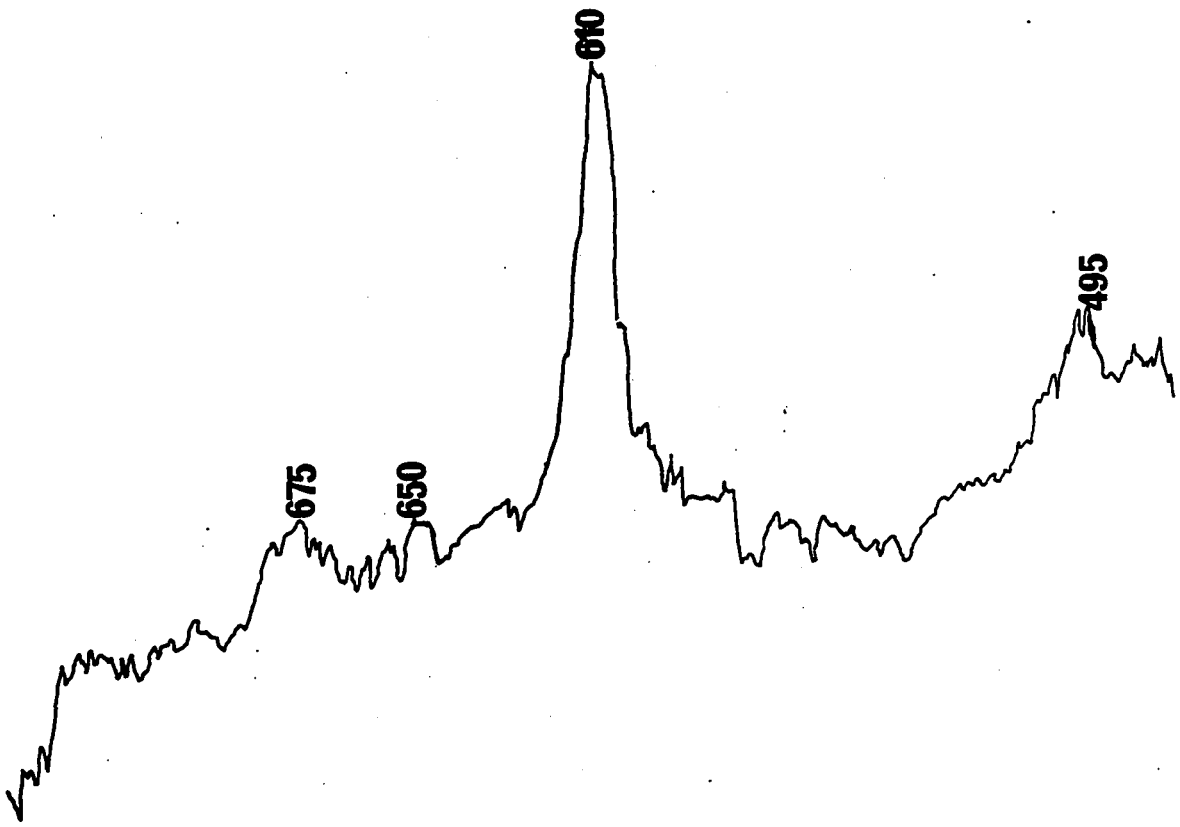

Figure 93

SOLID STATE
RAMAN SPECTRUM OF SnF_4·2CAP

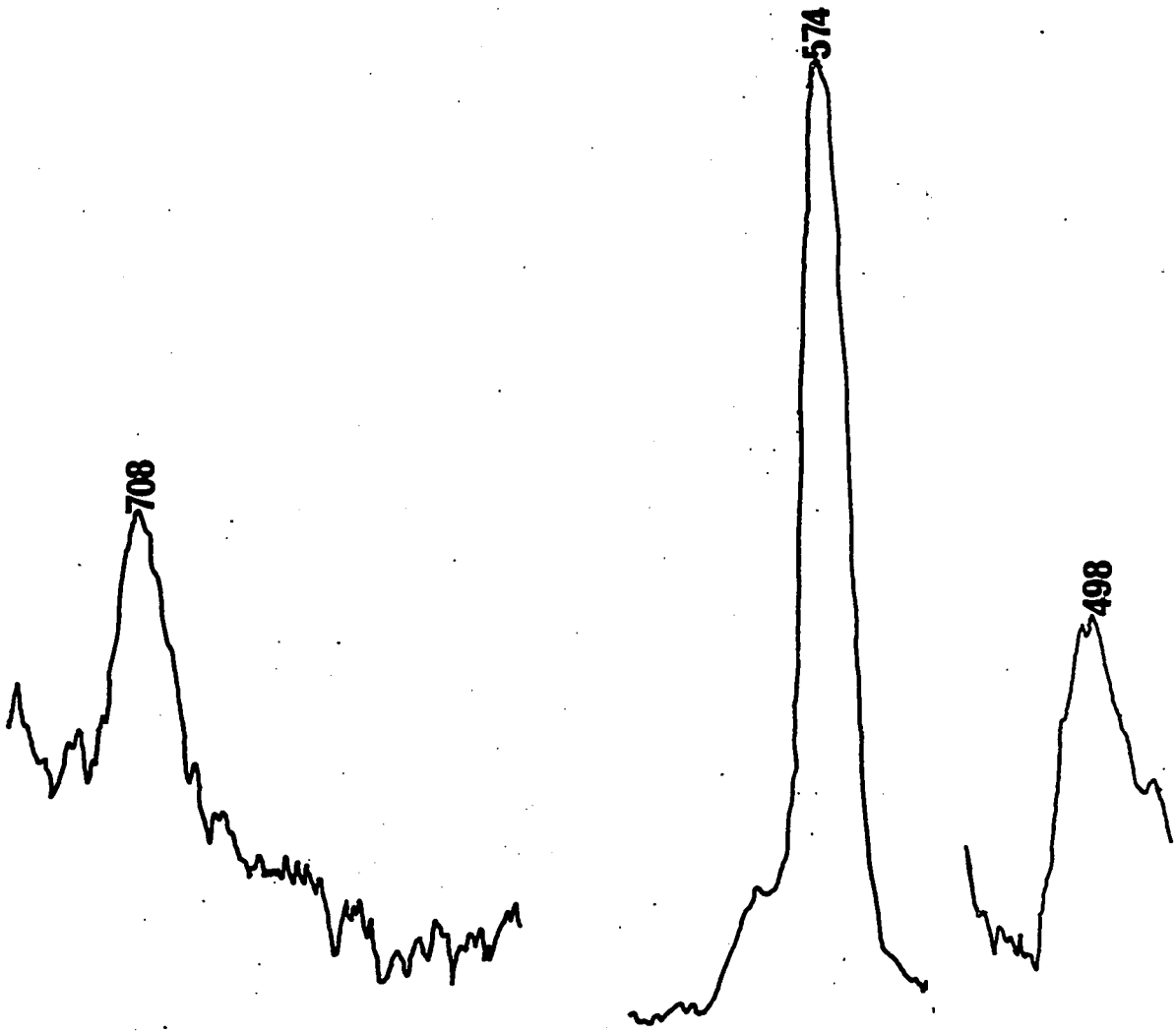

Figure 94

SOLID STATE
RAMAN SPECTRUM OF $SiF_4 \cdot 2AZA\text{-}NON$

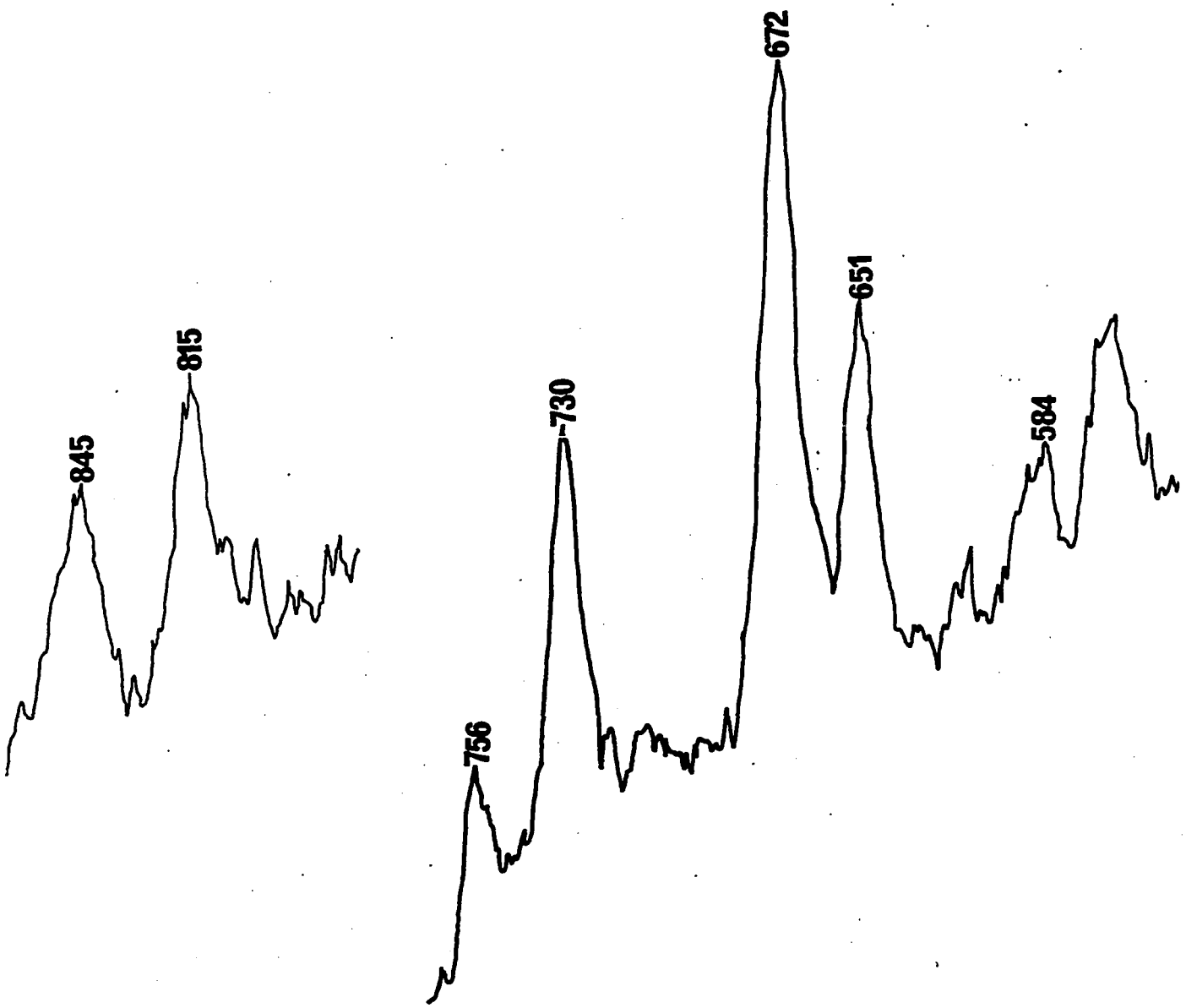

Figure 95

SOLID STATE
RAMAN SPECTRUM OF $SnF_4$2AZA-NON

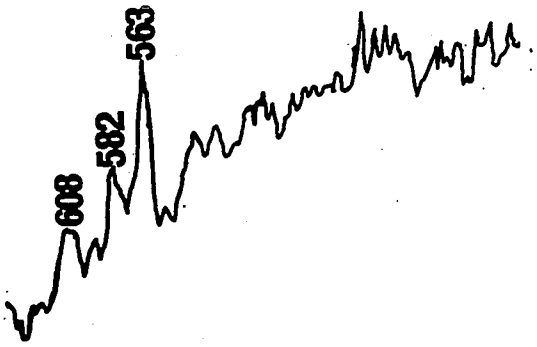

APPENDIX E. ^{19}F NMR and ^{1}H NMR Spectra.

Figure 96. ^{19}F NUCLEAR MAGNETIC RESONANCE SPECTRUM IN $ClCH_2CN$

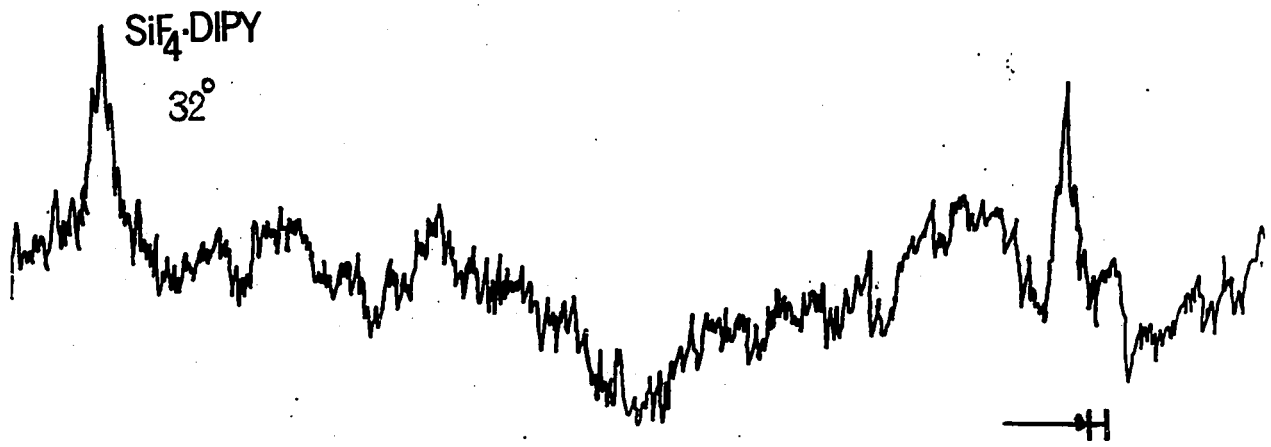

Figure 97. ^{19}F NUCLEAR MAGNETIC RESONANCE SPECTRUM IN $ClCH_2CN$

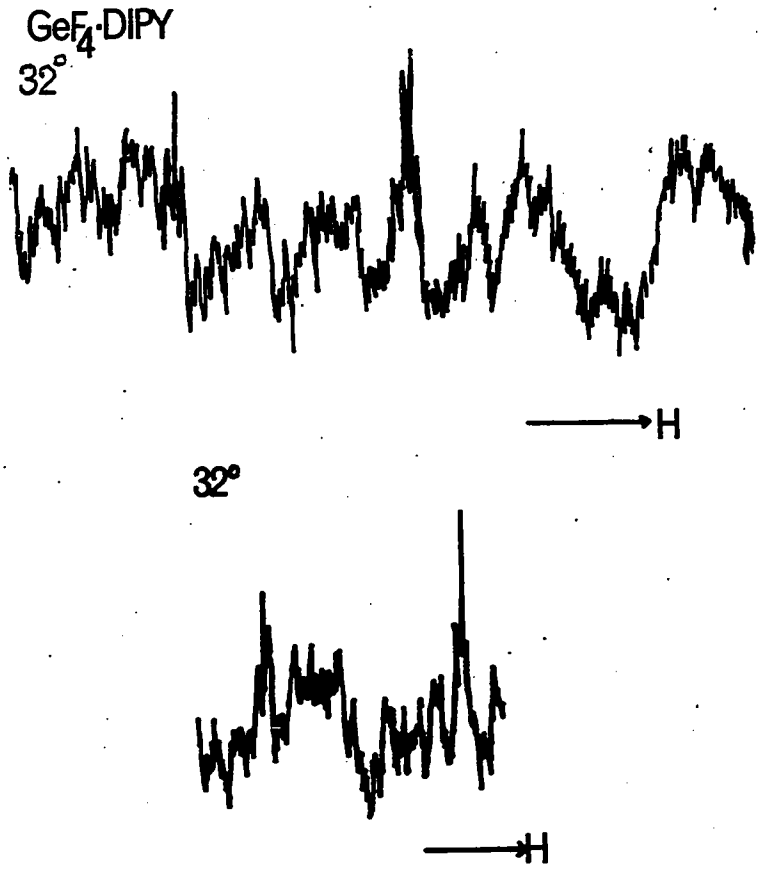

Figure 98. ^{19}F NUCLEAR MAGNETIC RESONANCE SPECTRUM IN $ClCH_2CN$

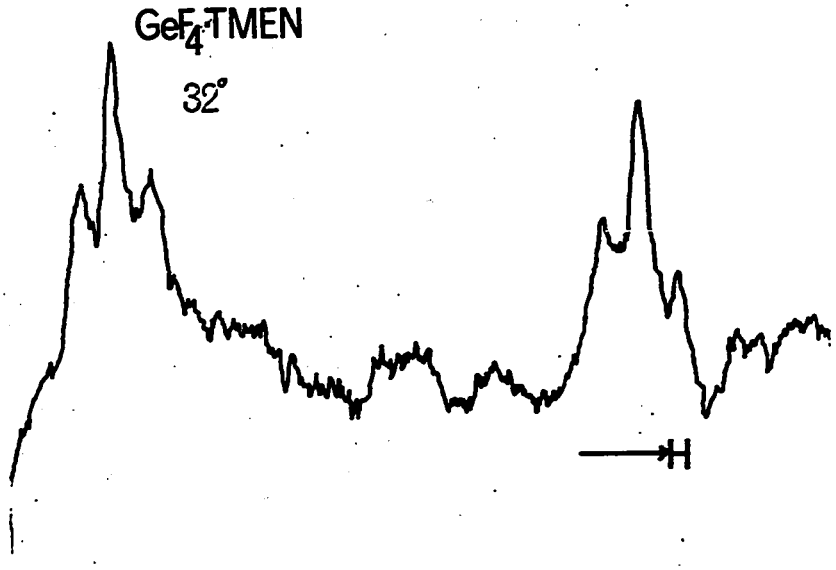

Figure 99. ^{19}F NUCLEAR MAGNETIC RESONANCE SPECTRUM IN $ClCH_2CN$

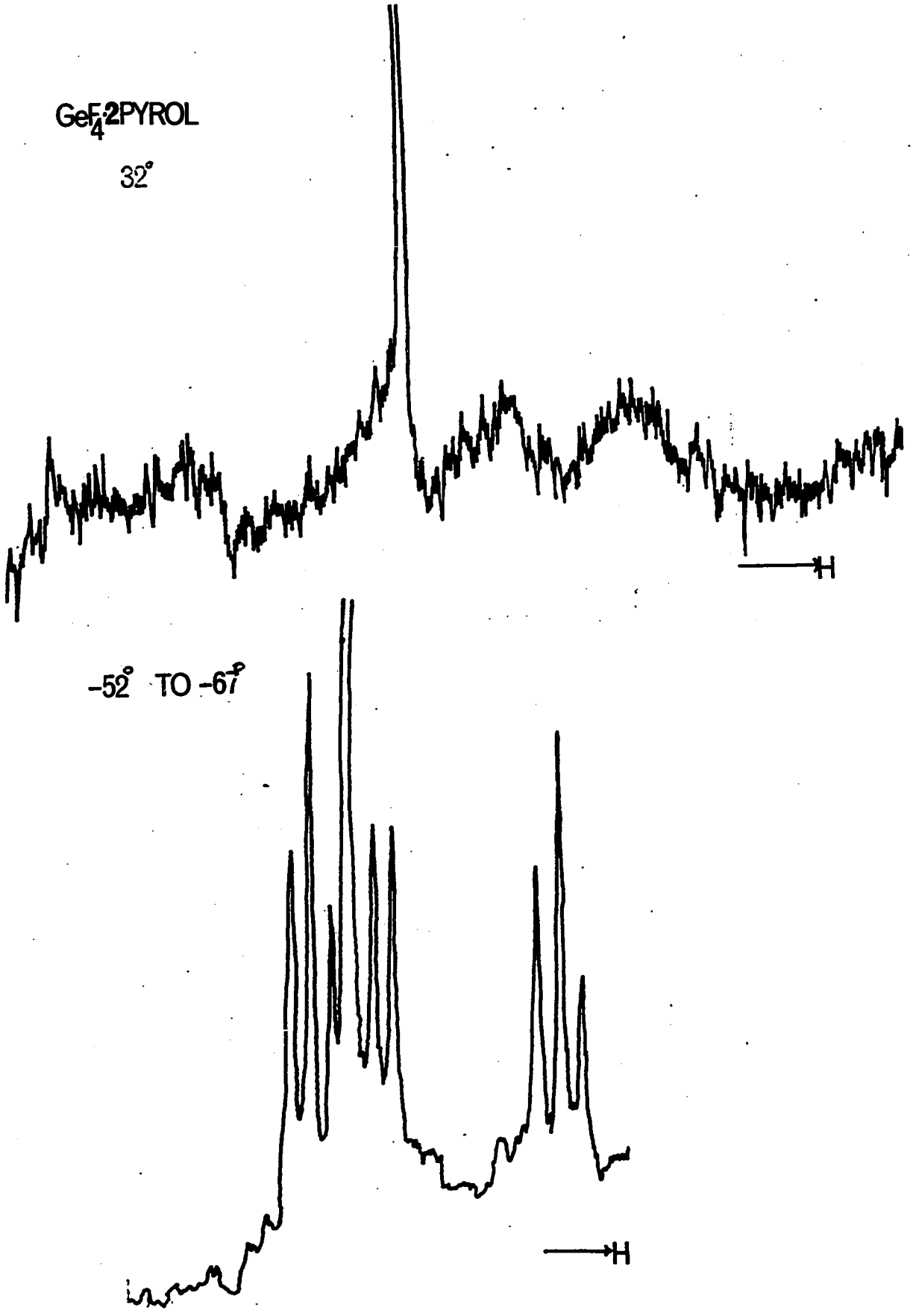

Figure 100. ^{19}F NUCLEAR MAGNETIC RESONANCE SPECTRUM IN $ClCH_2CN$

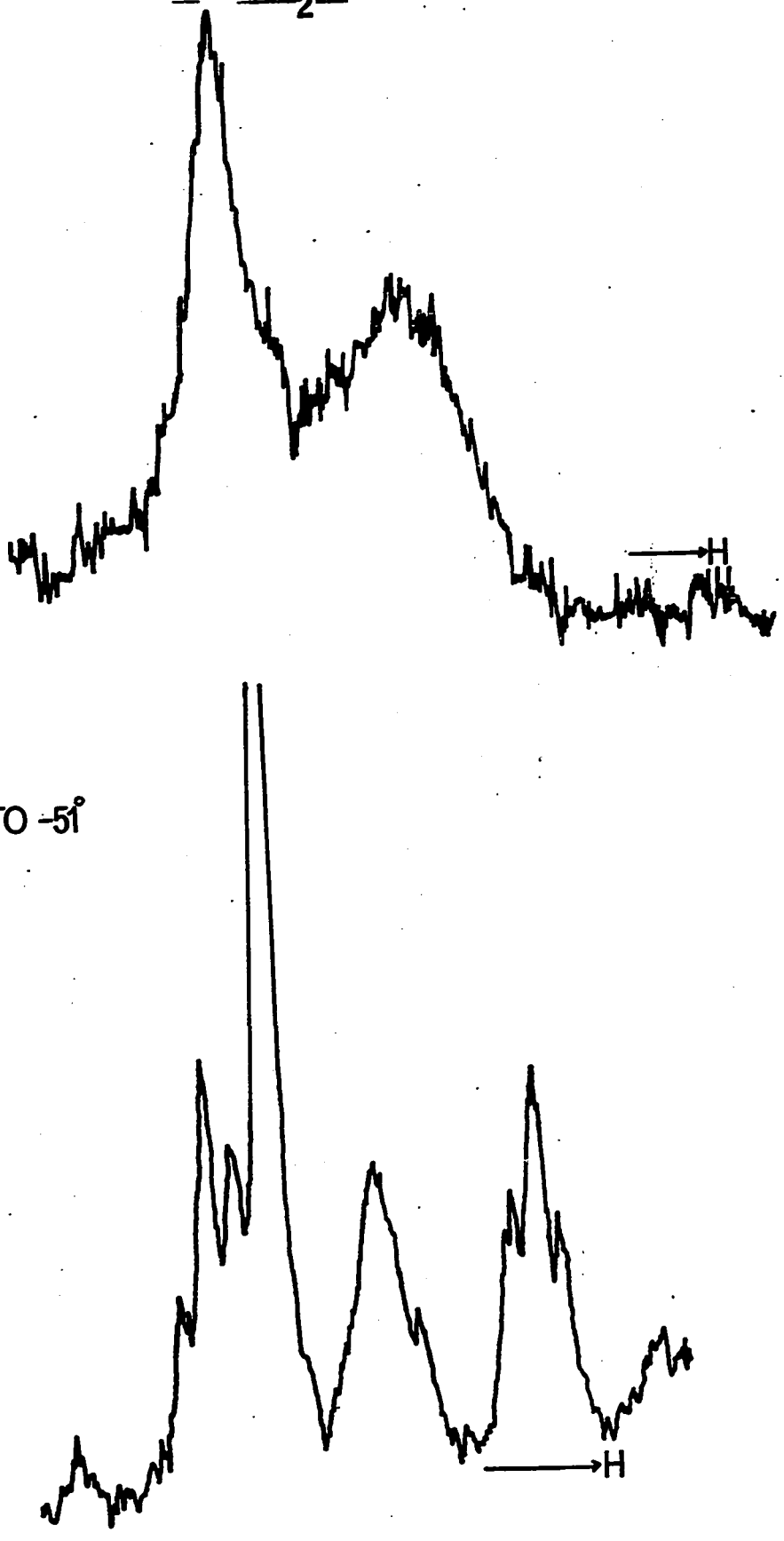

Figure 101. ^{19}F NUCLEAR MAGNETIC RESONANCE SPECTRUM IN $ClCH_2CN$

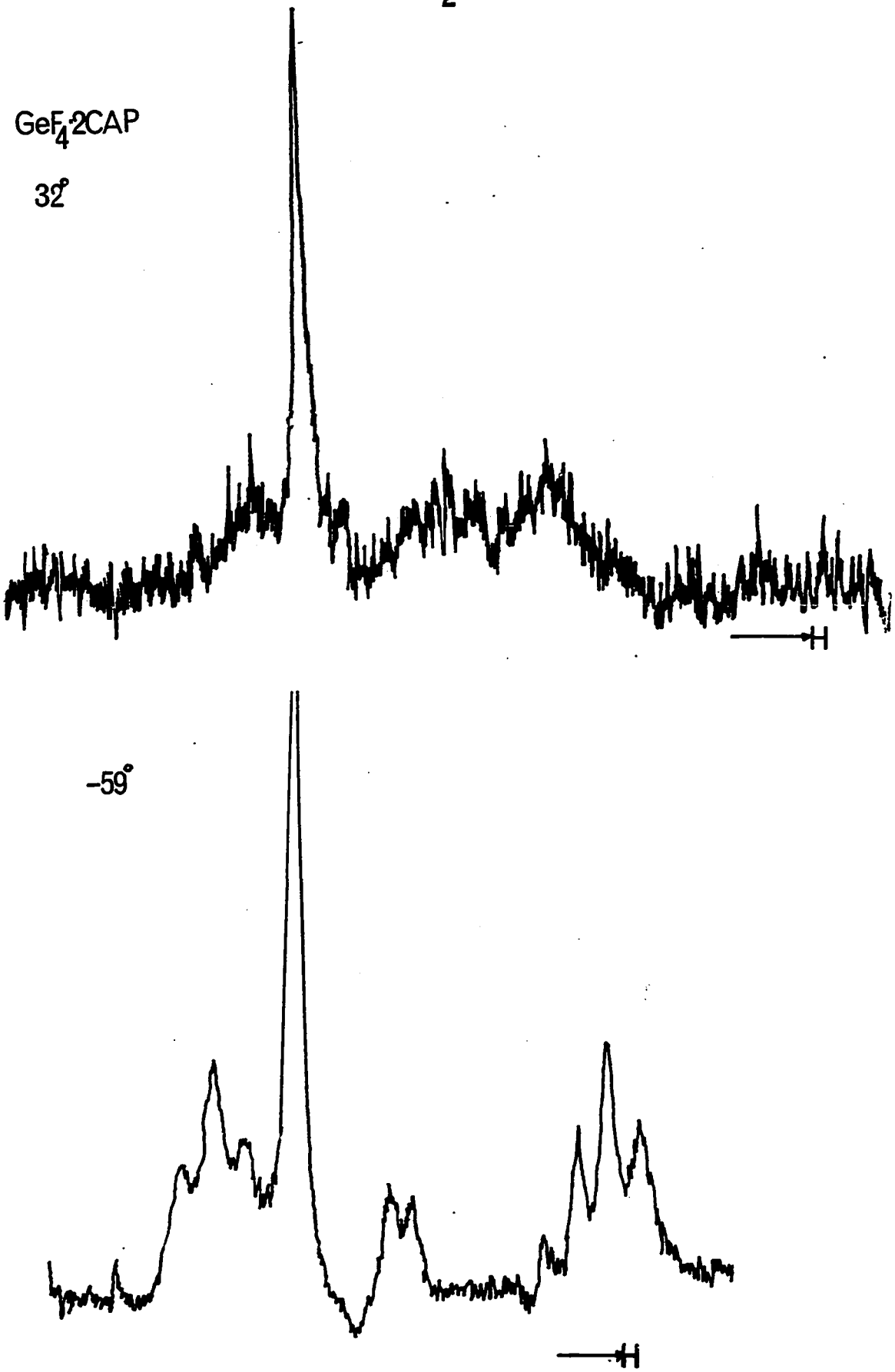

Figure 102. ^{19}F NUCLEAR MAGNETIC RESONANCE SPECTRUM IN $ClCH_2CN$

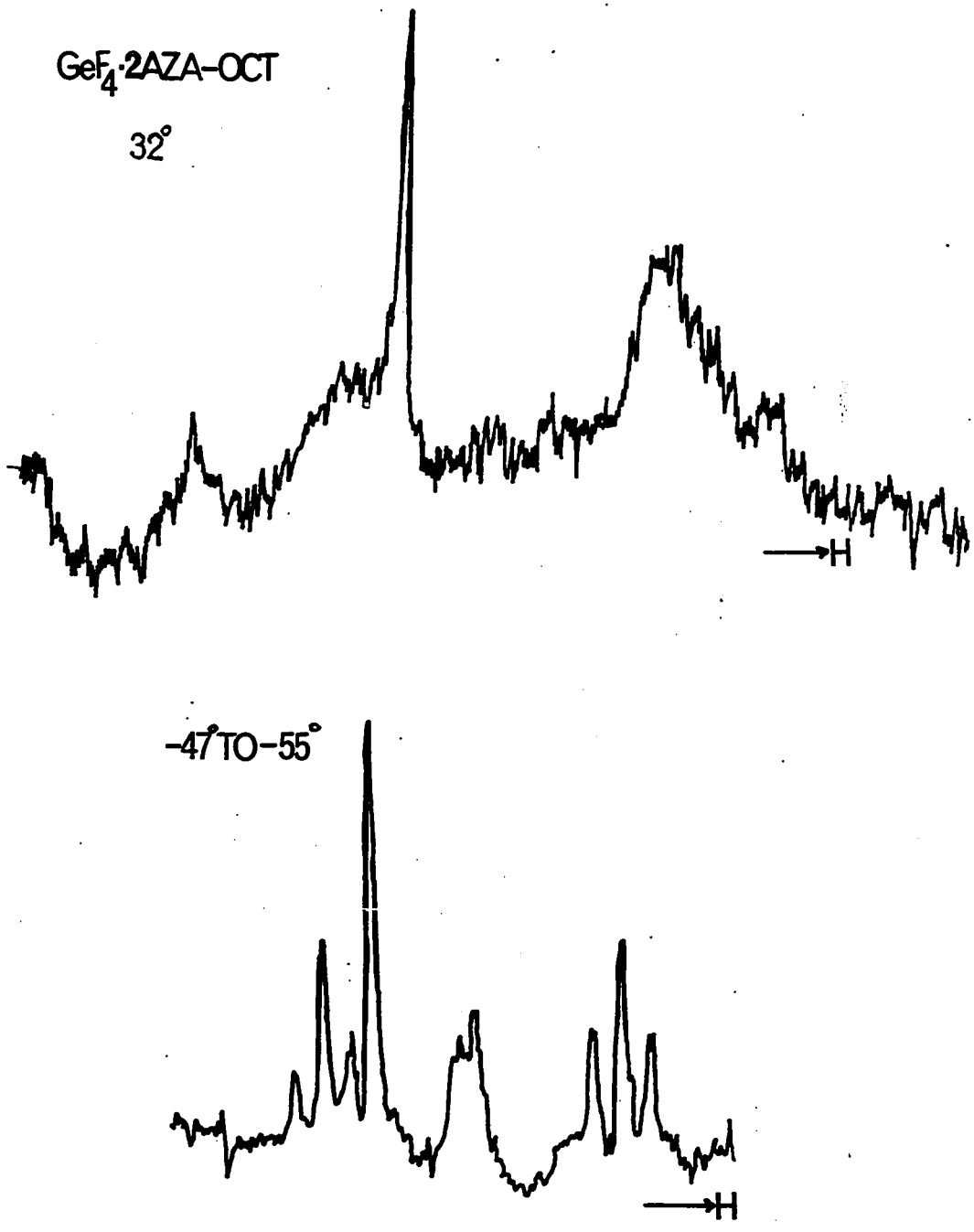

Figure 103. ^{19}F NUCLEAR MAGNETIC RESONANCE SPECTRUM IN $ClCH_2CN$

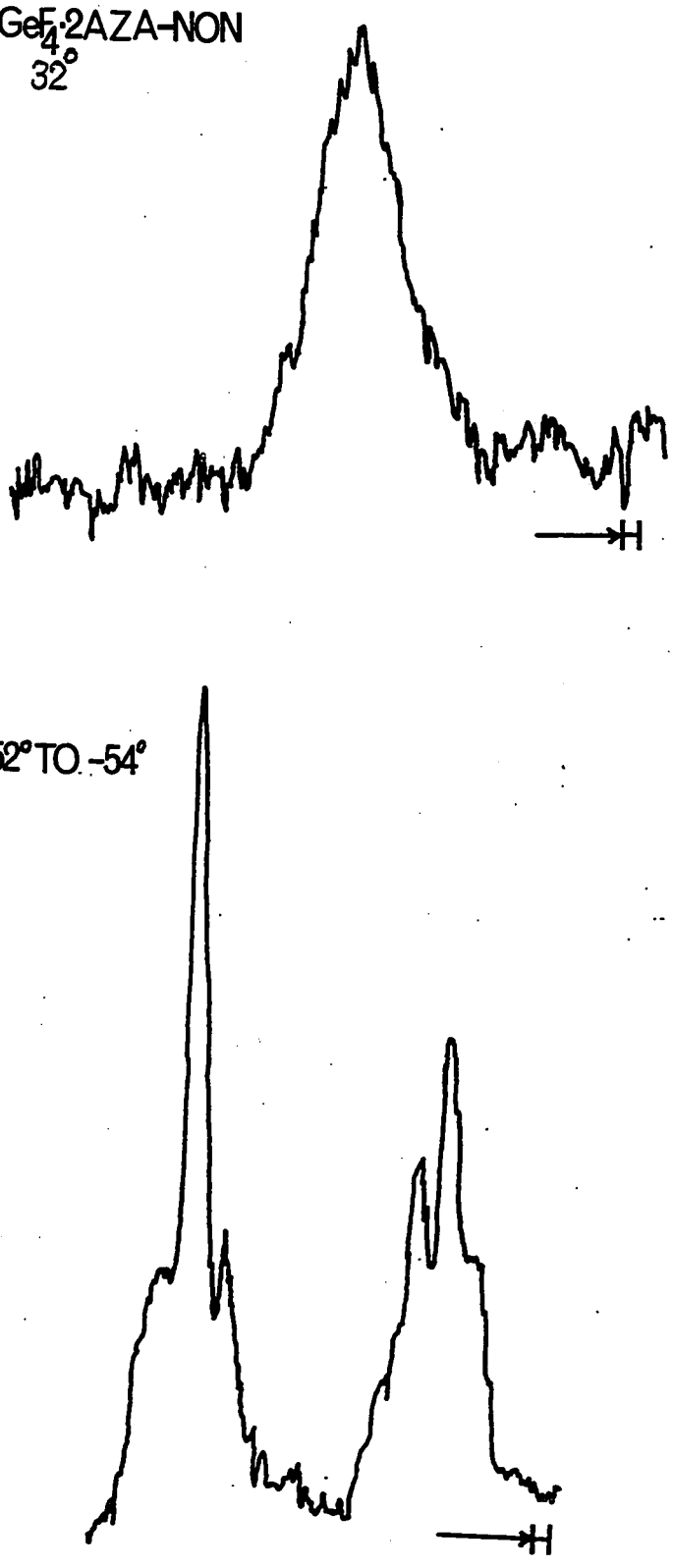

Figure 104. ^{19}F NUCLEAR MAGNETIC RESONANCE SPECTRUM IN $ClCH_2CN$

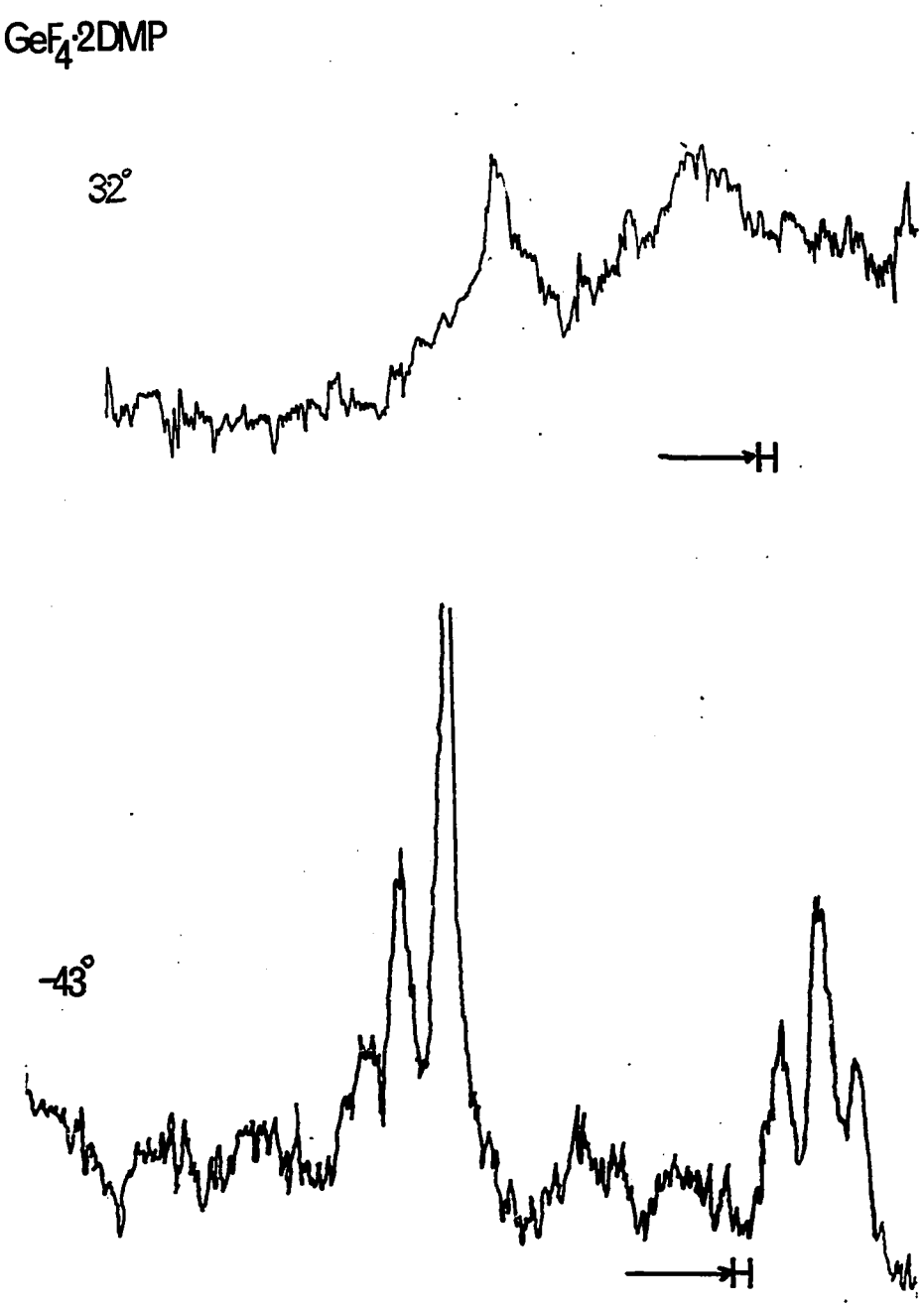

Figure 105. ^{19}F NUCLEAR MAGNETIC RESONANCE SPECTRUM IN $ClCH_2CN$

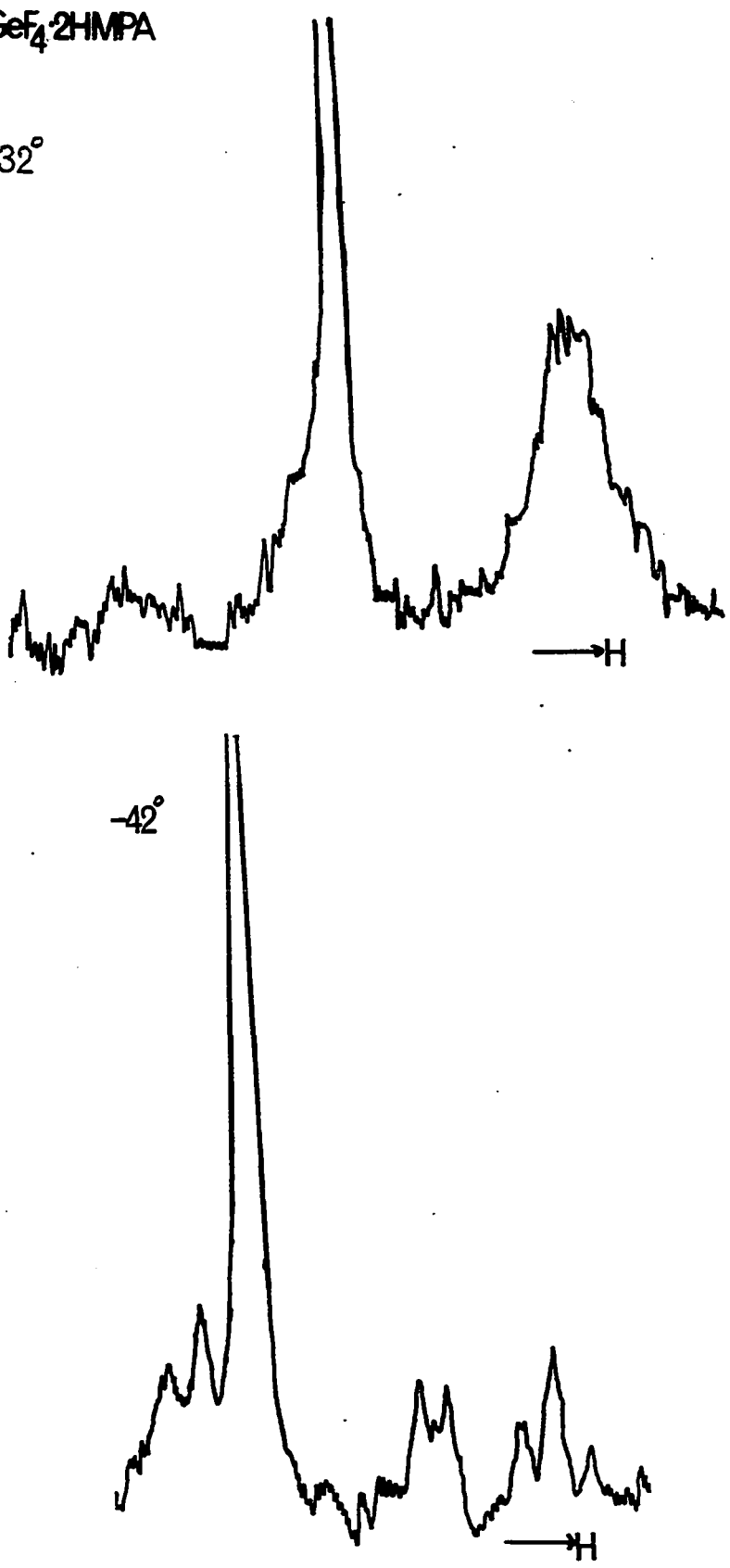

Figure 106. ^{19}F NUCLEAR MAGNETIC RESONANCE SPECTRUM IN $ClCH_2CN$

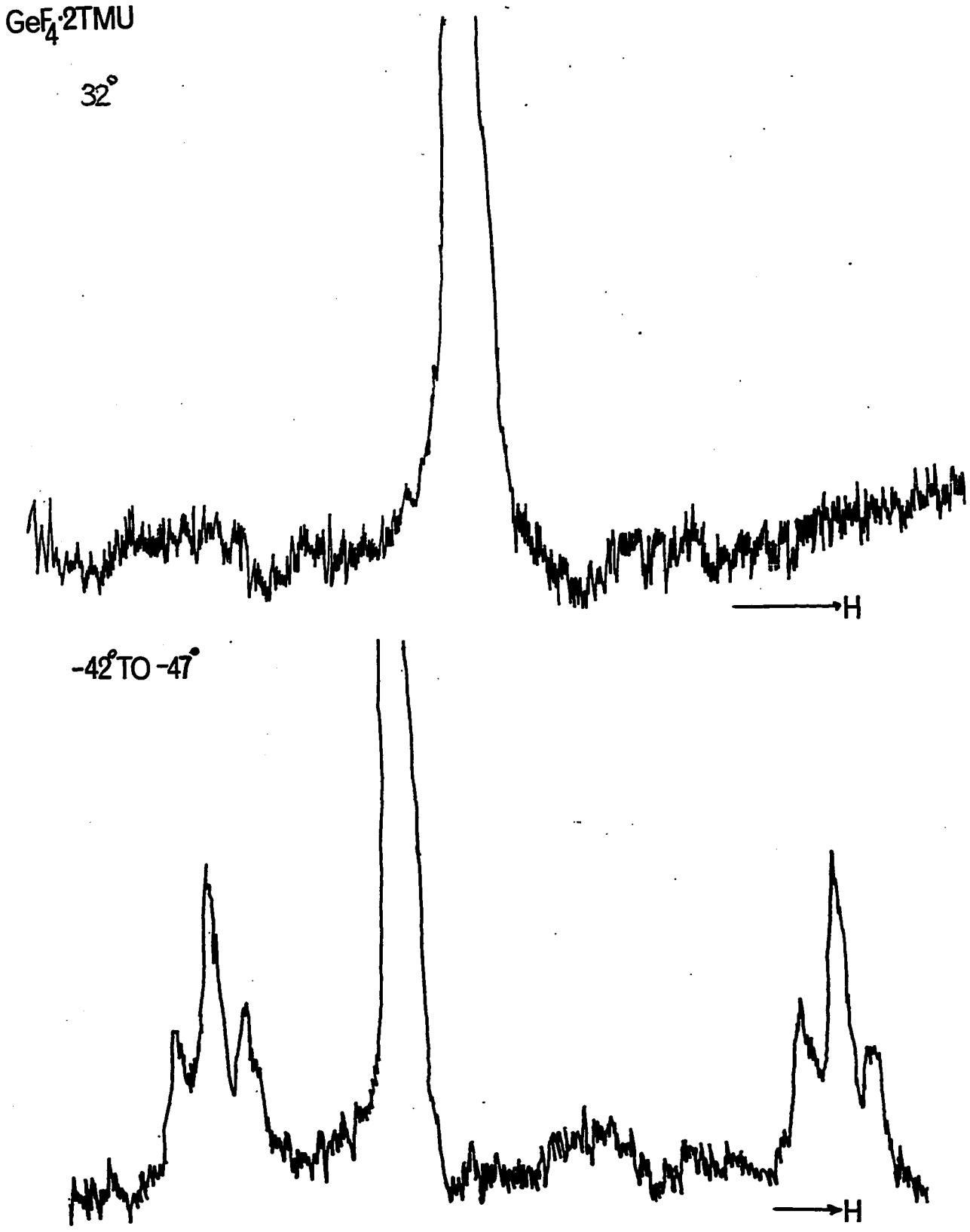

Figure 107. ^{19}F NUCLEAR MAGNETIC RESONANCE SPECTRUM IN $ClCH_2CN$

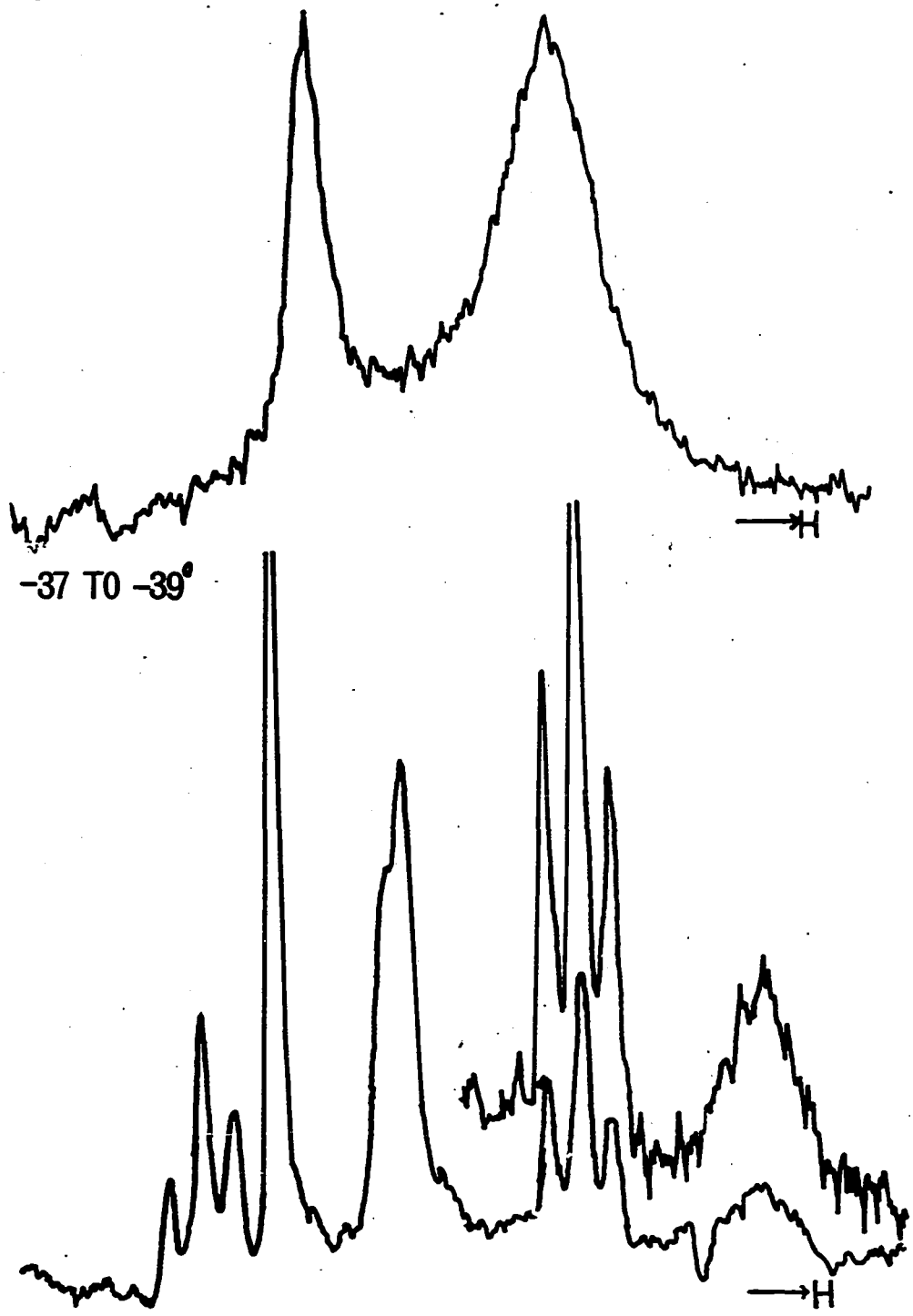

Figure 108. ^{19}F NUCLEAR MAGNETIC RESONANCE SPECTRUM IN WATER.

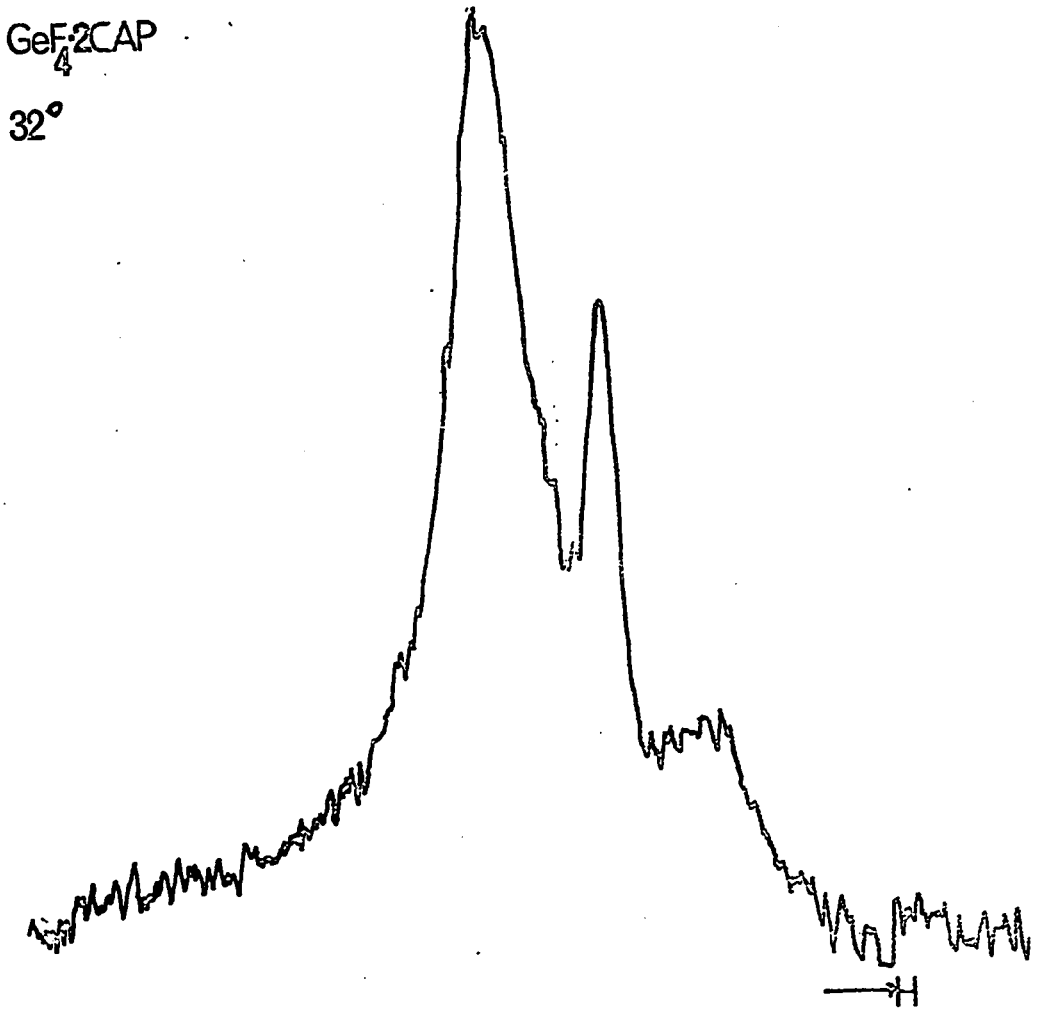

Figure 108. ^{19}F NUCLEAR MAGNETIC RESONANCE SPECTRUM IN WATER

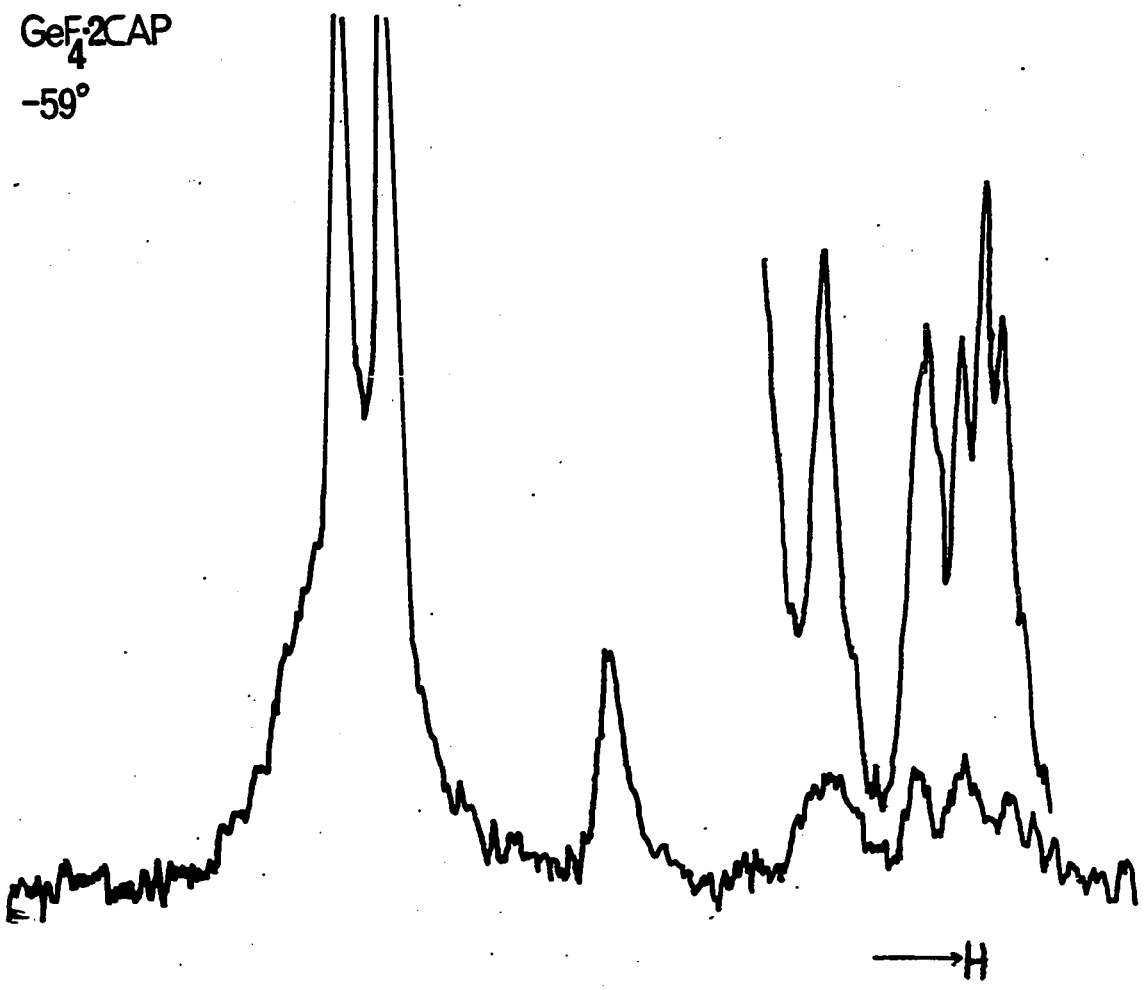

Figure 109. ^{19}F NUCLEAR MAGNETIC RESONANCE SPECTRUM IN $ClCH_2CN$

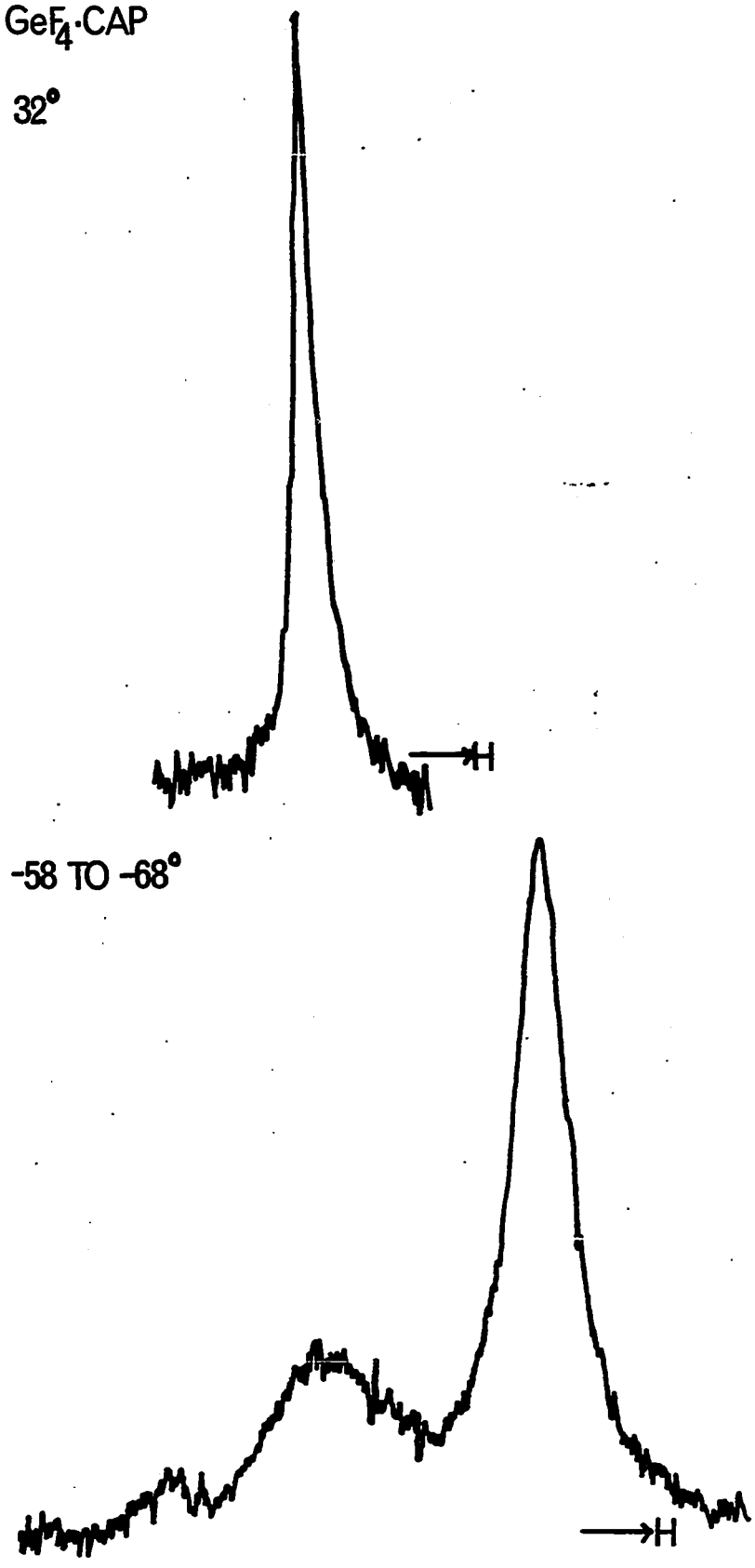

Figure 110. ^{19}F NUCLEAR MAGNETIC RESONANCE SPECTRUM IN $ClCH_2CN$

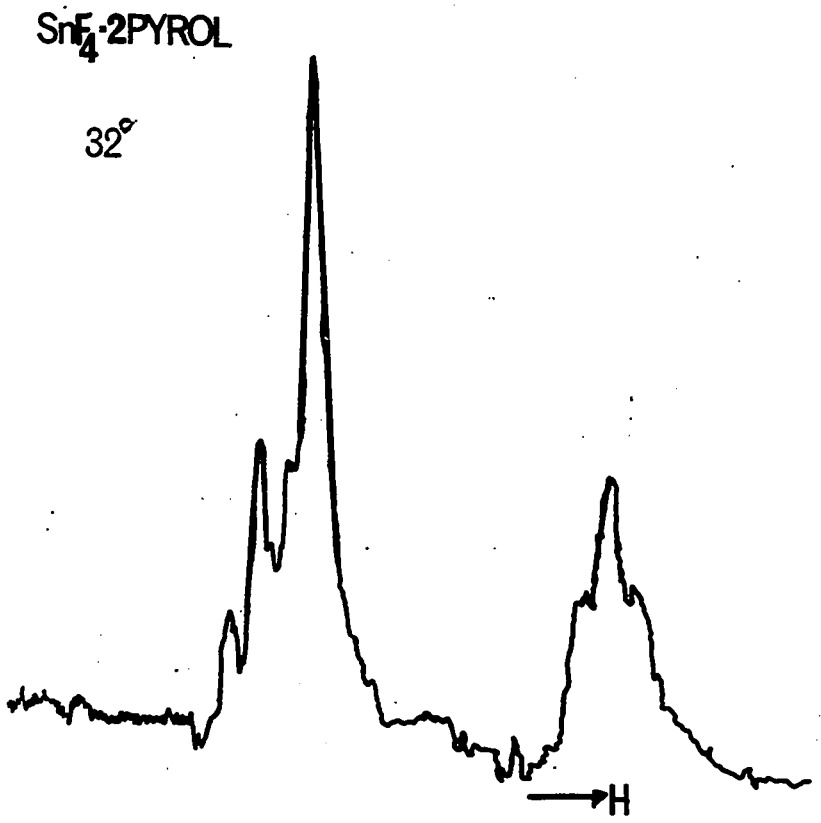

Figure 111. ^{19}F NUCLEAR MAGNETIC RESONANCE SPECTRUM IN $ClCH_2CN$

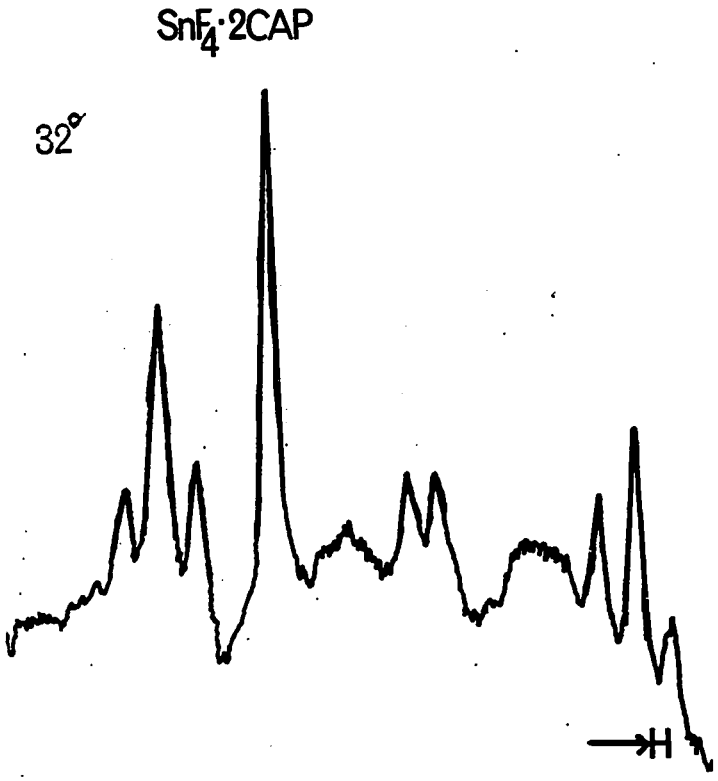

Figure 112. ^{19}F NUCLEAR MAGNETIC RESONANCE SPECTRUM IN $ClCH_2CN$

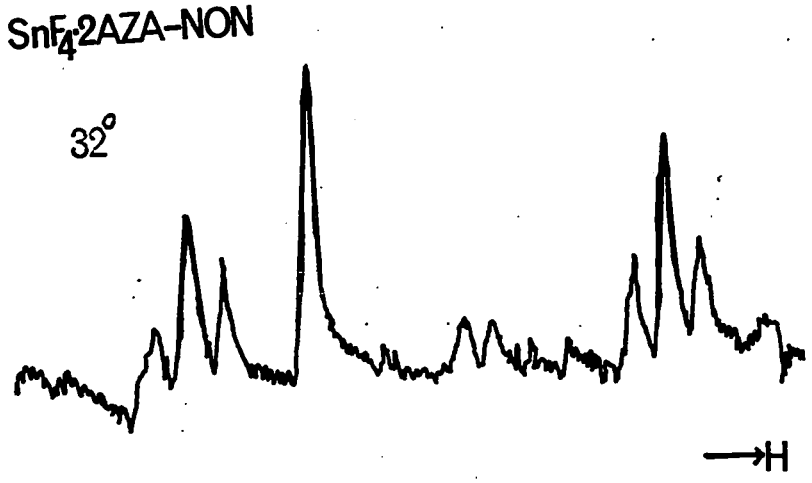

Figure 113. ^{19}F NUCLEAR MAGNETIC RESONANCE SPECTRUM IN $ClCH_2CN$

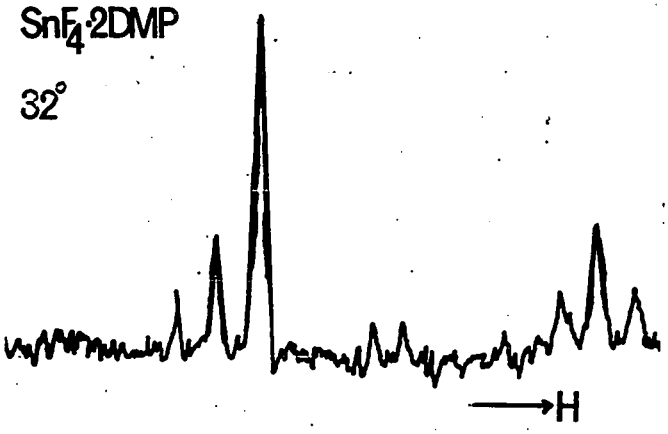

Figure 114. ^{19}F NUCLEAR MAGNETIC RESONANCE SPECTRUM IN $ClCH_2CN$

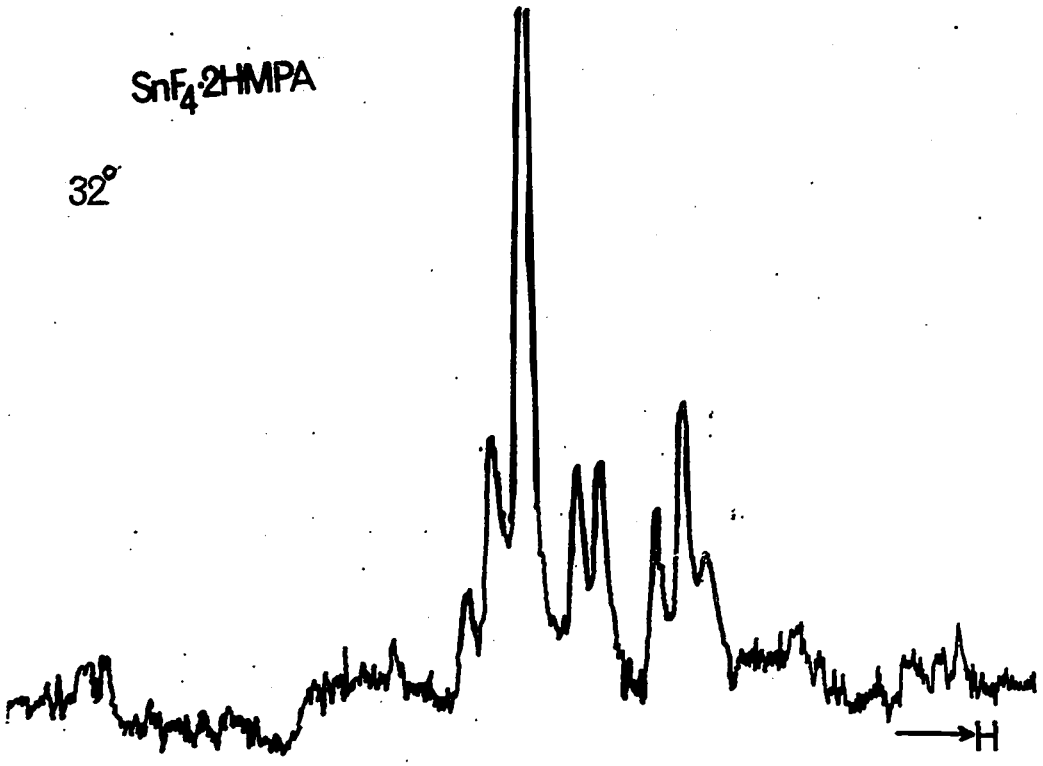

Figure 115. ^{19}F NUCLEAR MAGNETIC RESONANCE SPECTRUM IN $ClCH_2CN$

SnF_4 2AZA-NON + $((CH_3CH_2CH_2)_2NH_2)_2SnF_6$

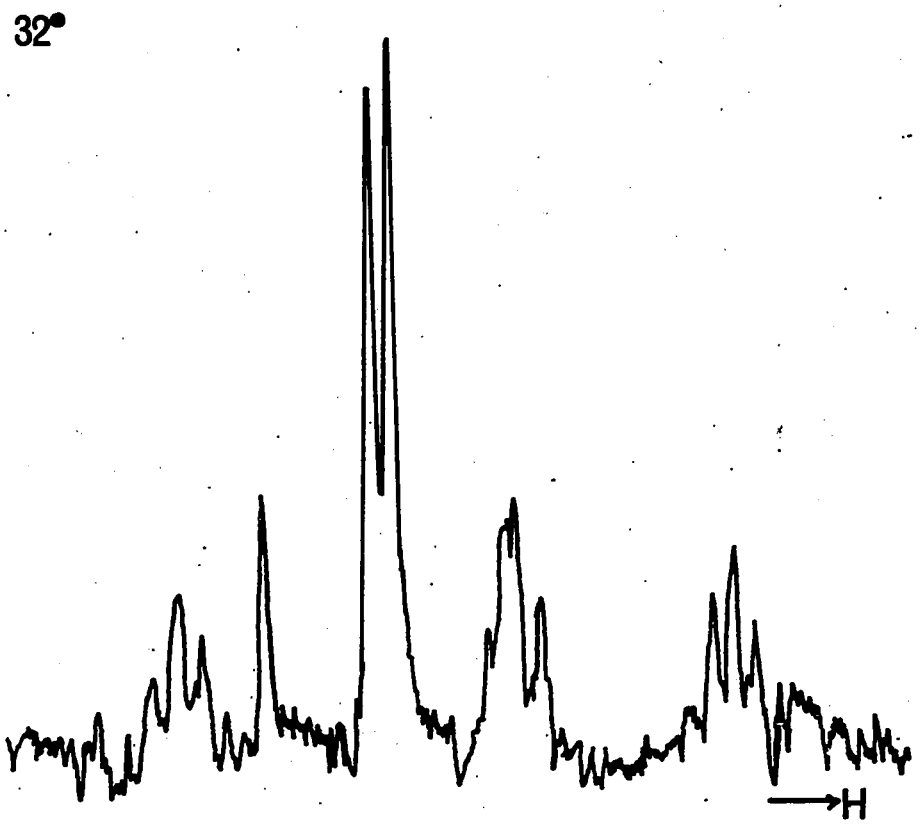

Figure 116. ^{19}F NUCLEAR MAGNETIC RESONANCE SPECTRUM IN WATER.

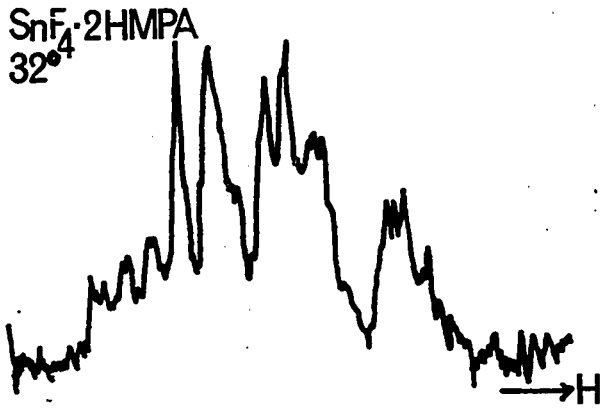

Figure 117. ^{19}F NUCLEAR MAGNETIC RESONANCE SPECTRUM IN $ClCH_2CN$

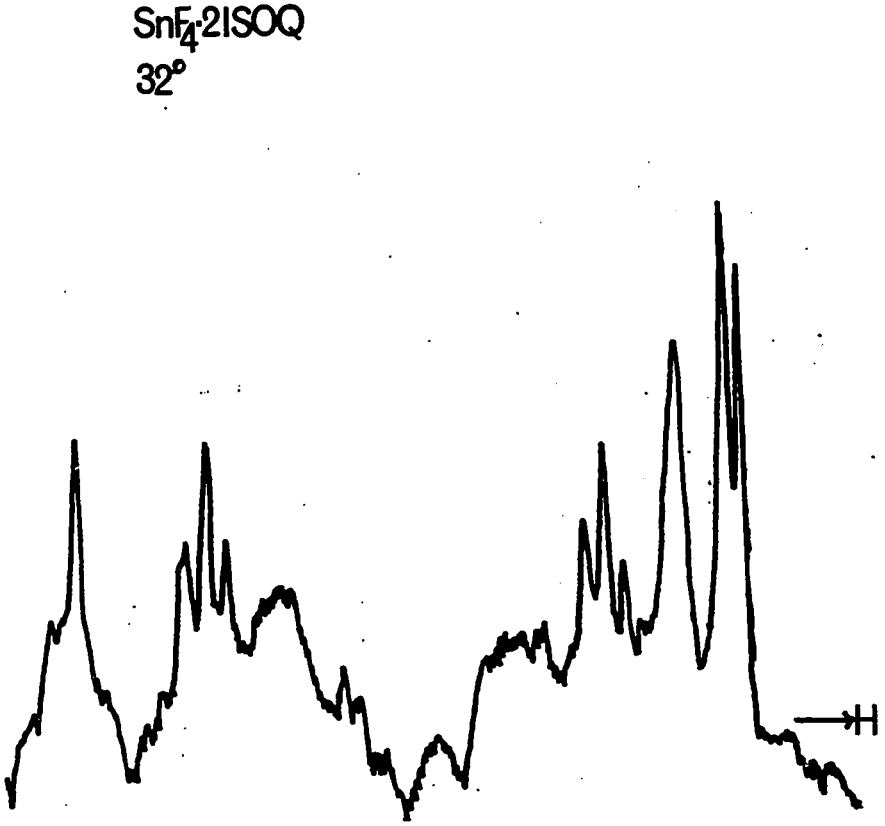

Figure 118 ^1H NUCLEAR MAGNETIC RESONANCE SPECTRUM IN $ClCH_2CN$

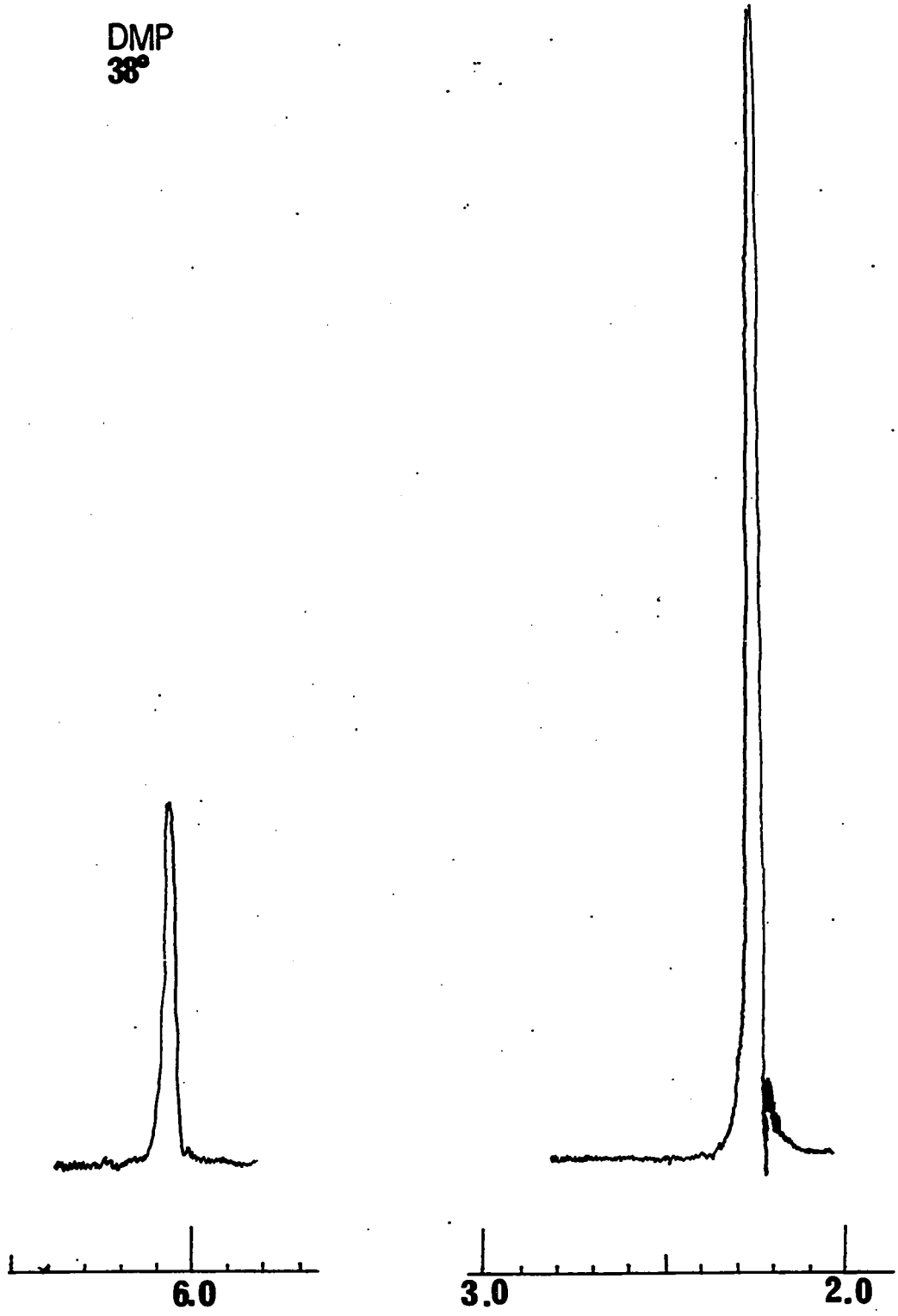

Figure 119. ^1H NUCLEAR MAGNETIC RESONANCE SPECTRUM IN $ClCH_2CN$

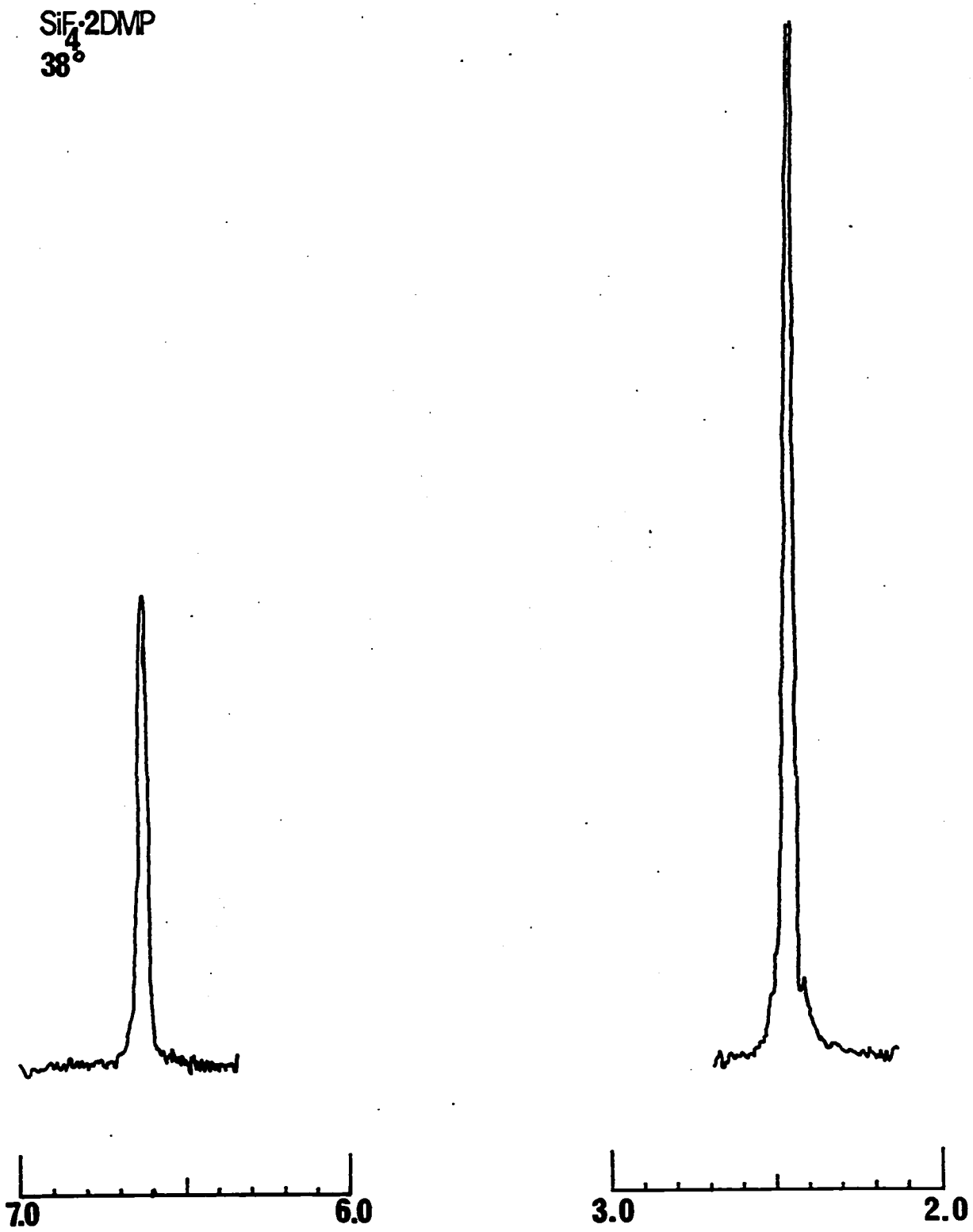

Figure 119. ^1H NUCLEAR MAGNETIC RESONANCE SPECTRUM IN $ClCH_2CN$

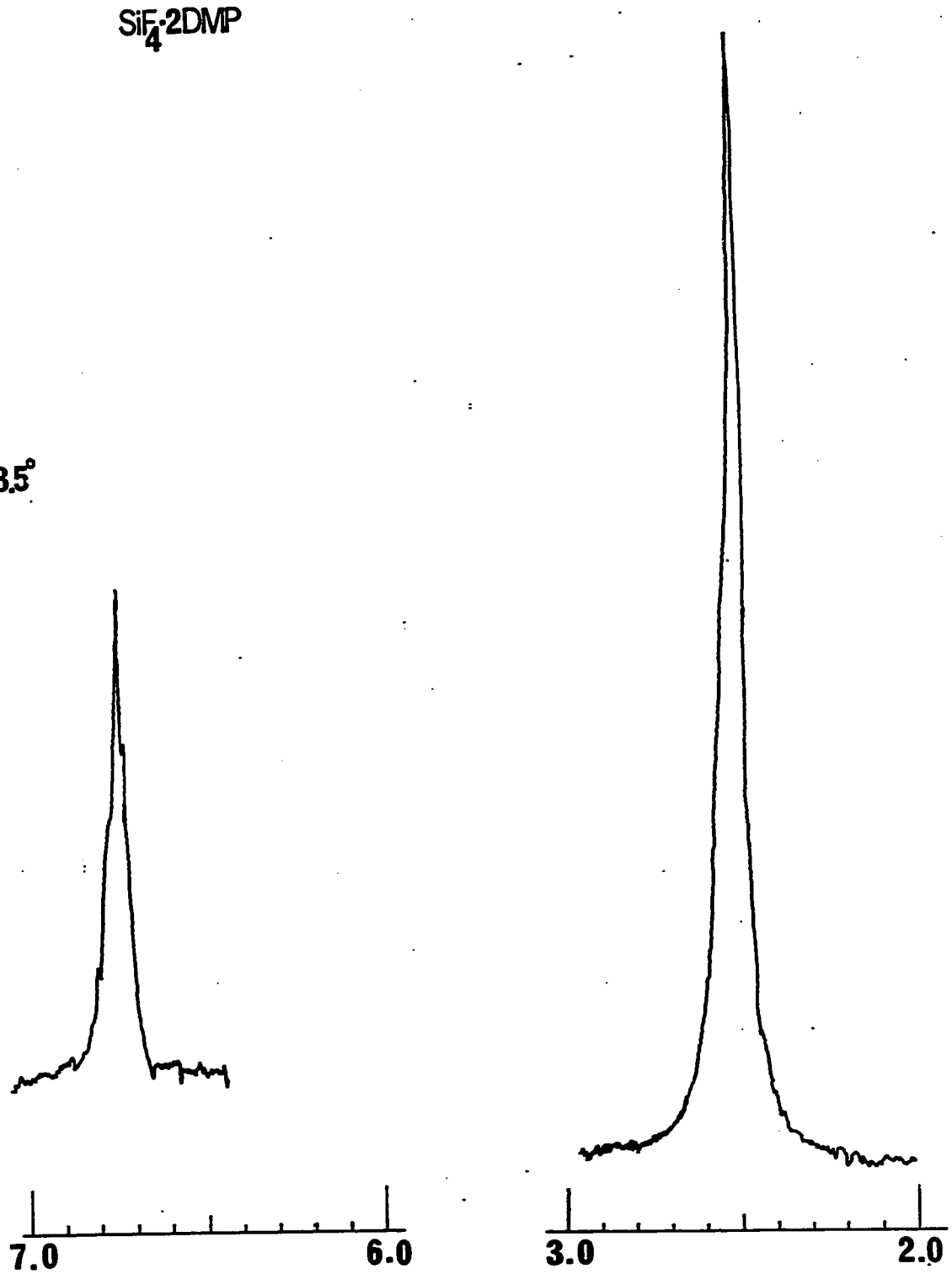

Figure 120. ^1H NUCLEAR MAGNETIC RESONANCE SPECTRUM IN $ClCH_2CN$

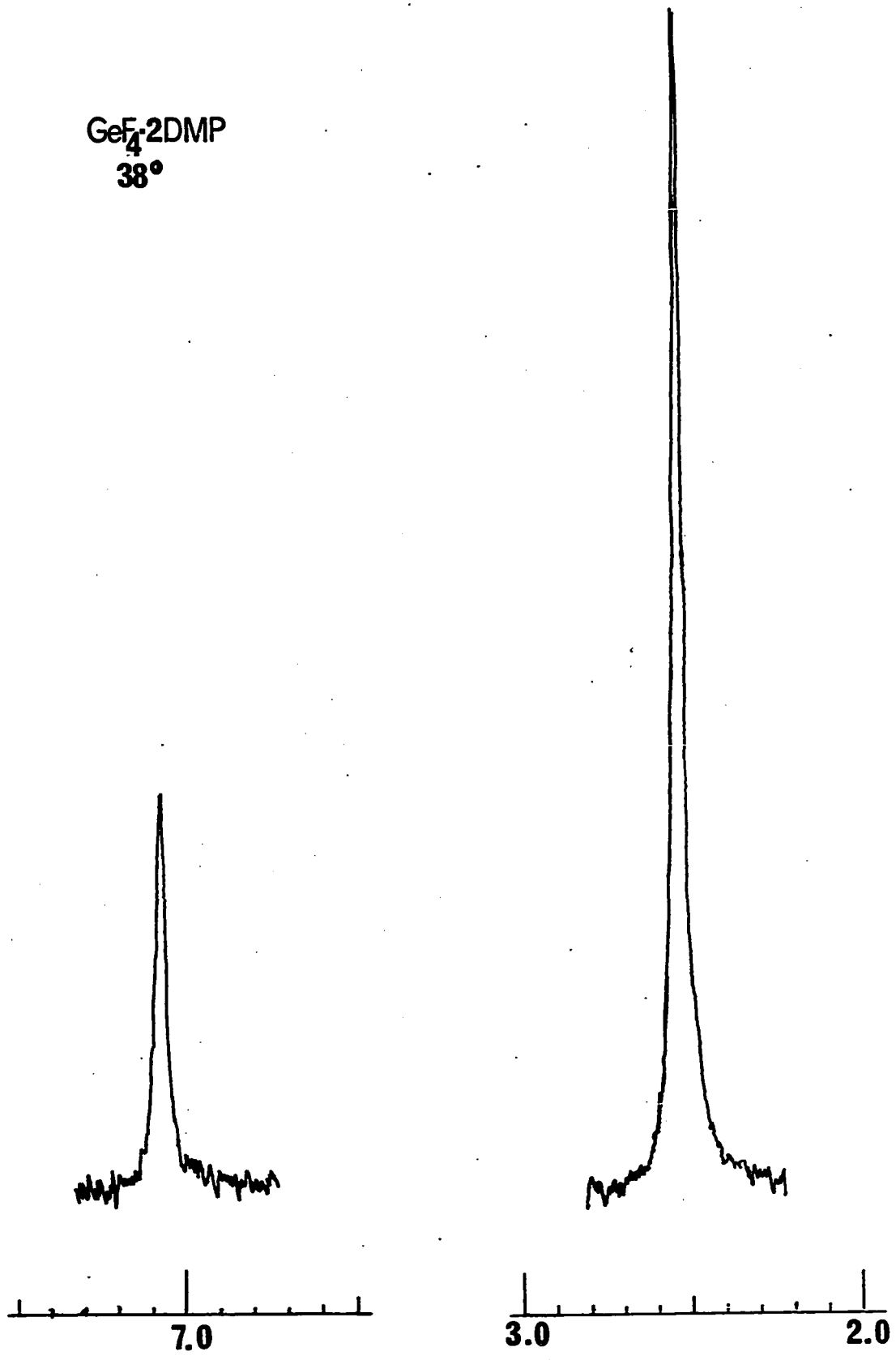

Figure 120. ^1H NUCLEAR MAGNETIC RESONANCE SPECTRUM IN $ClCH_2CN$

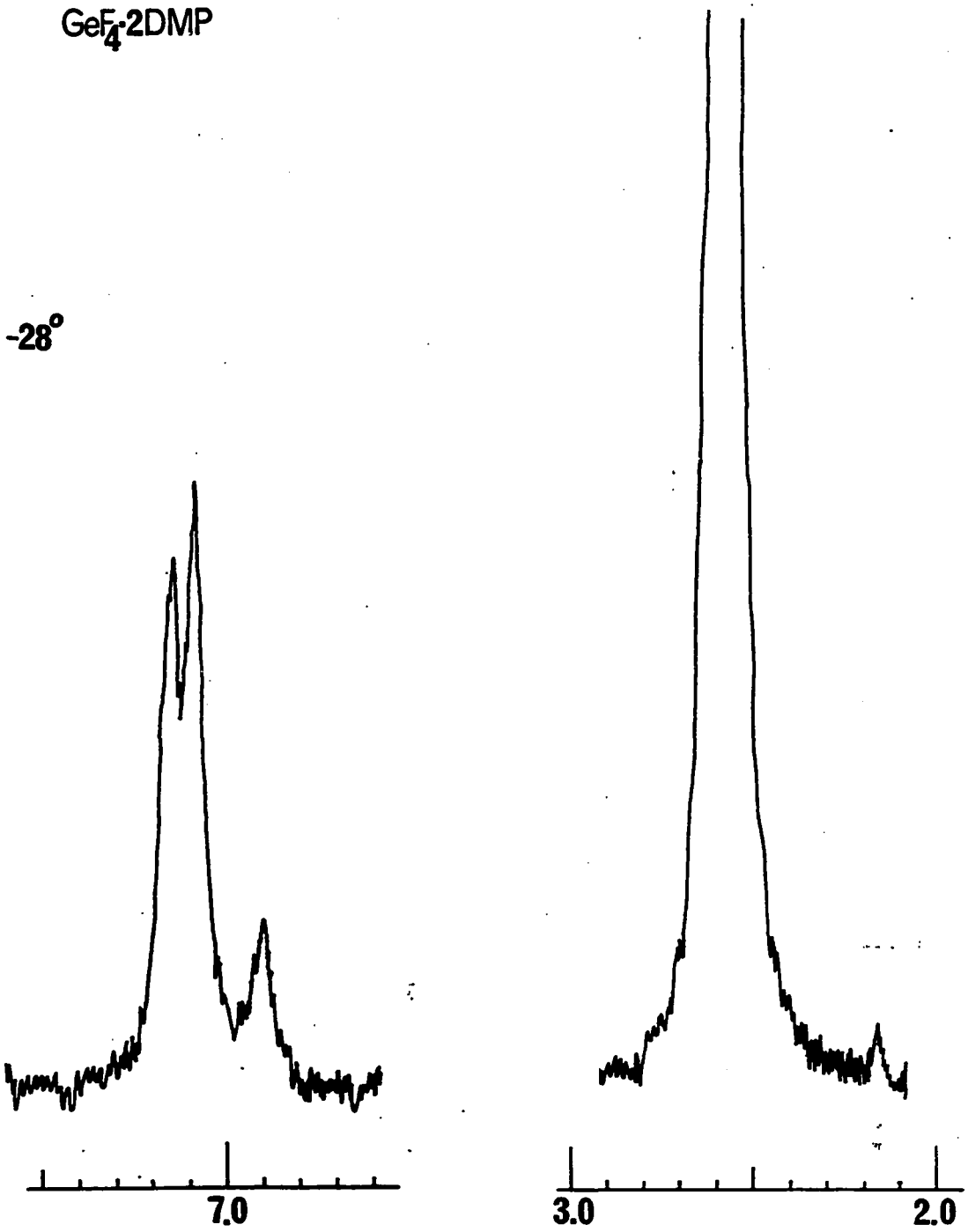

Figure 121. ^1H NUCLEAR MAGNETIC RESONANCE SPECTRUM IN $ClCH_2CN$

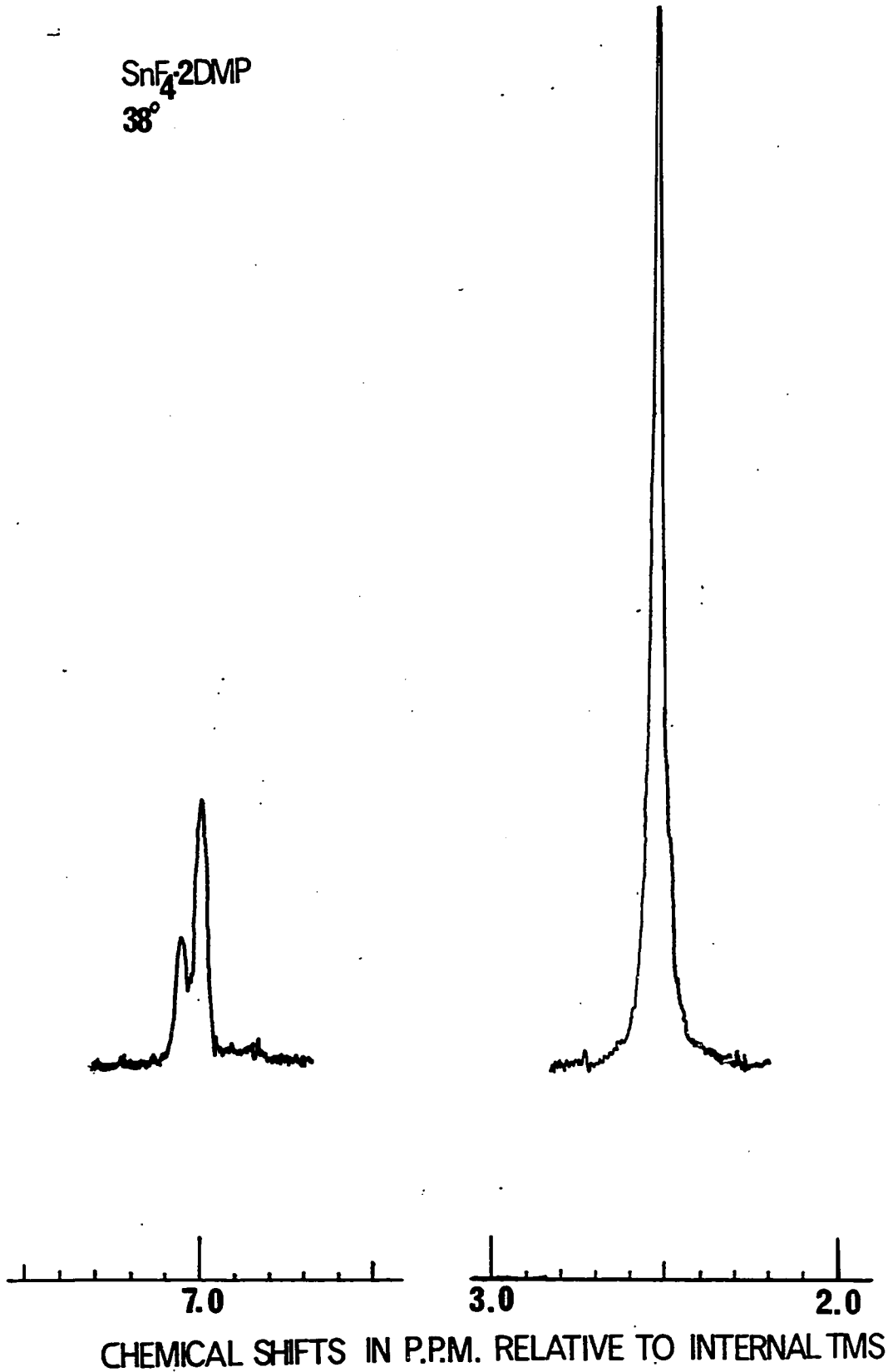

Figure 122. ^1H NUCLEAR MAGNETIC RESONANCE SPECTRUM IN $ClCH_2CN$

$GeF_4 \cdot 2DMP$ + EXCESS DMP

38°

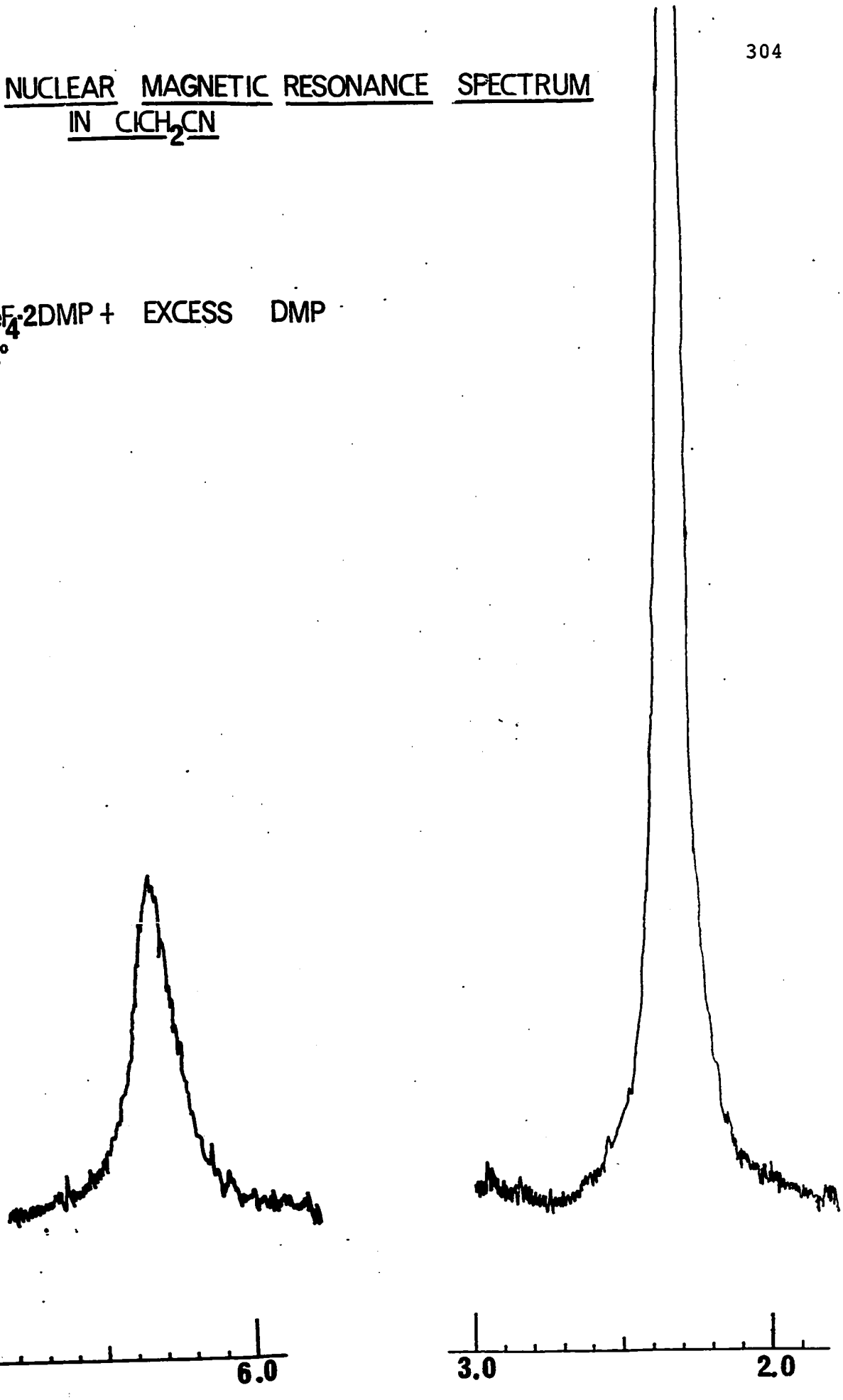

Figure 122. ^1H NUCLEAR MAGNETIC RESONANCE SPECTRUM IN $ClCH_2CN$

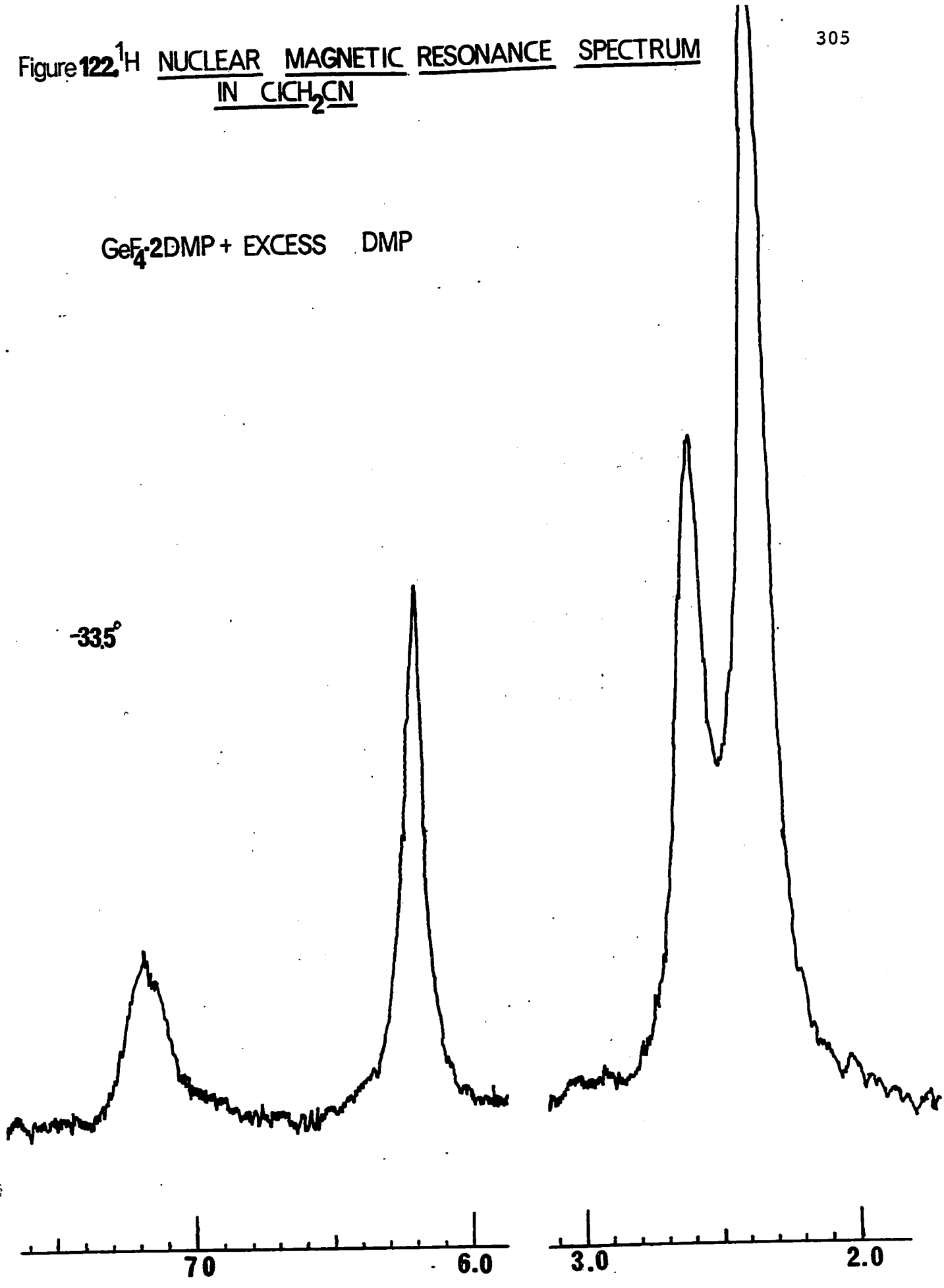

Figure 123. ^1H NUCLEAR MAGNETIC RESONANCE SPECTRUM IN $ClCH_2CN$

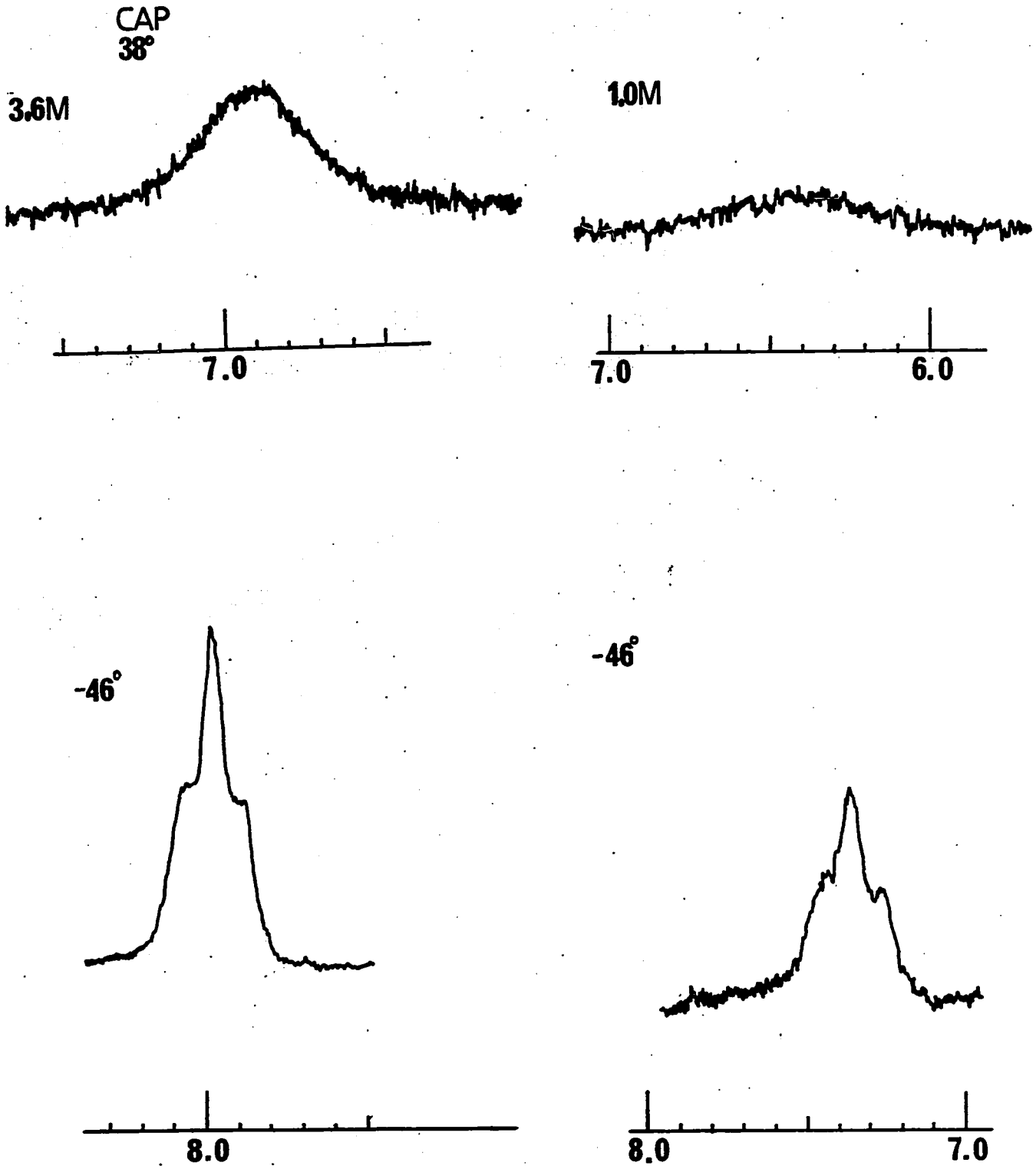

CHEMICAL SHIFTS IN P.P.M. RELATIVE TO INTERNAL TMS

Figure 124. ^1H NUCLEAR MAGNETIC RESONANCE SPECTRUM IN $ClCH_2CN$

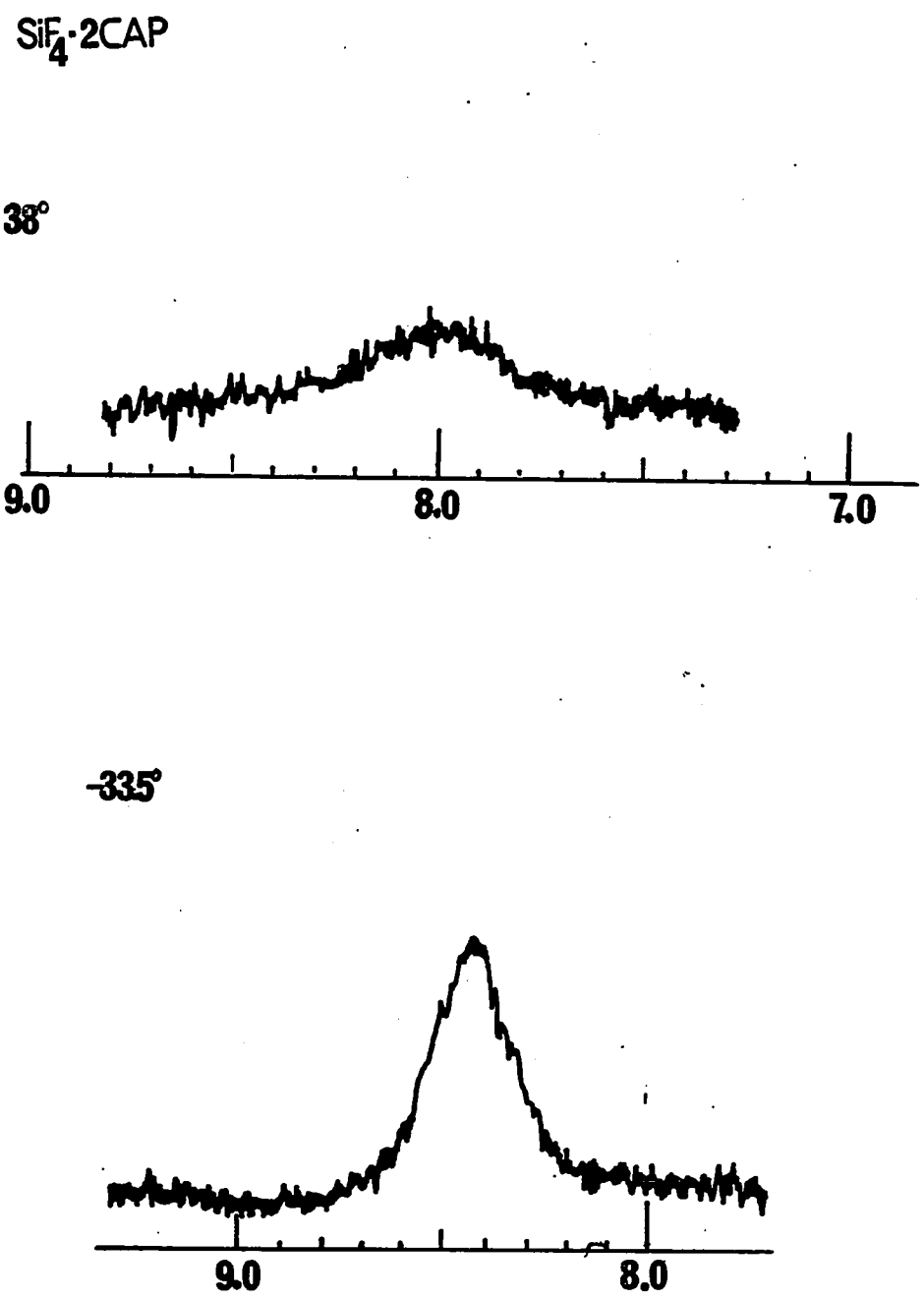

Figure 125. ^1H NUCLEAR MAGNETIC RESONANCE SPECTRUM IN $ClCH_2CN$

GeF_4:2CAP

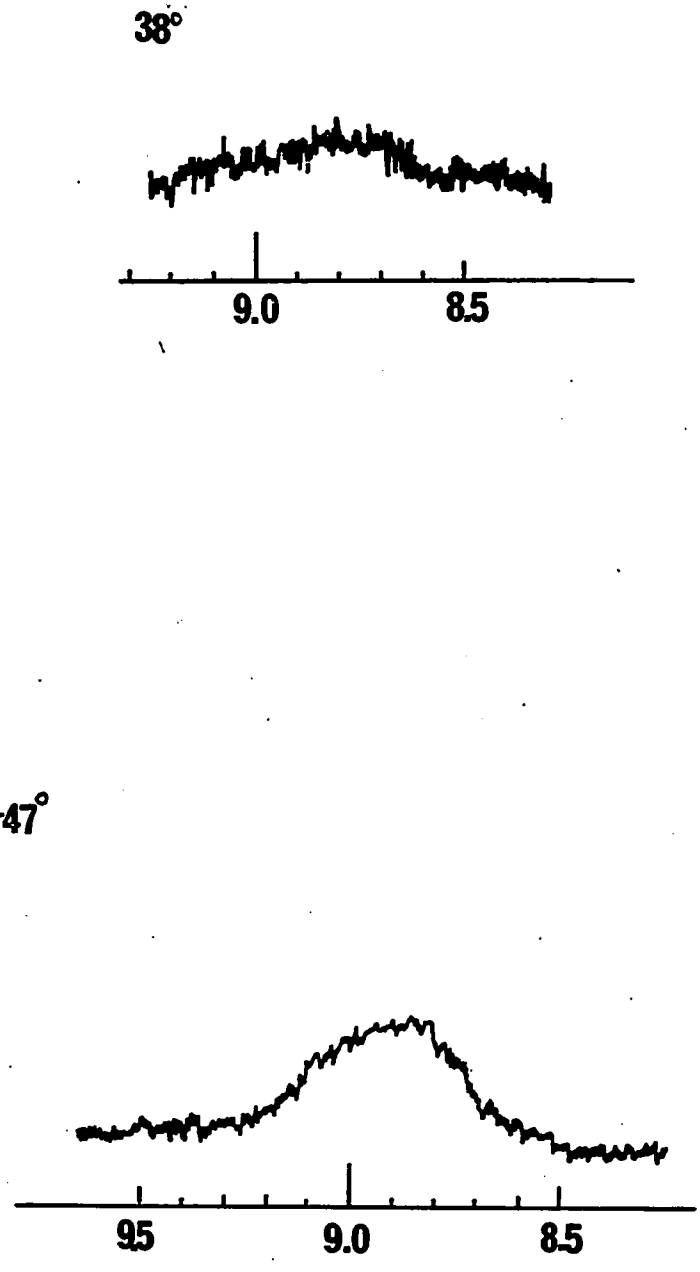

CHEMICAL SHIFTS IN P.P.M. RELATIVE TO INTERNAL TMS

Figure 126. ^1H NUCLEAR MAGNETIC RESONANCE SPECTRUM IN $ClCH_2CN$

$SnF_4$2CAP

38°

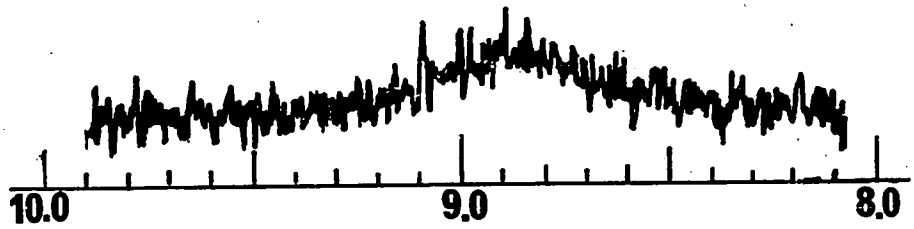

-46°

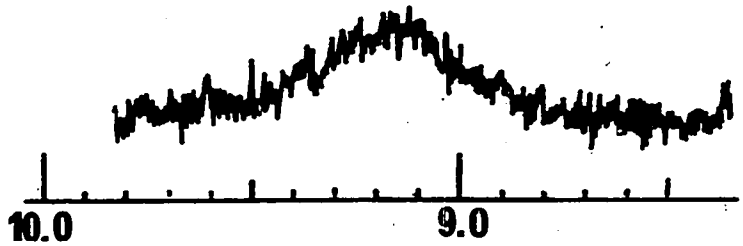

CHEMICAL SHIFTS IN P.P.M. RELATIVE TO INTERNAL TMS

Figure 127. ^1H NUCLEAR MAGNETIC RESONANCE SPECTRUM IN $ClCH_2CN$

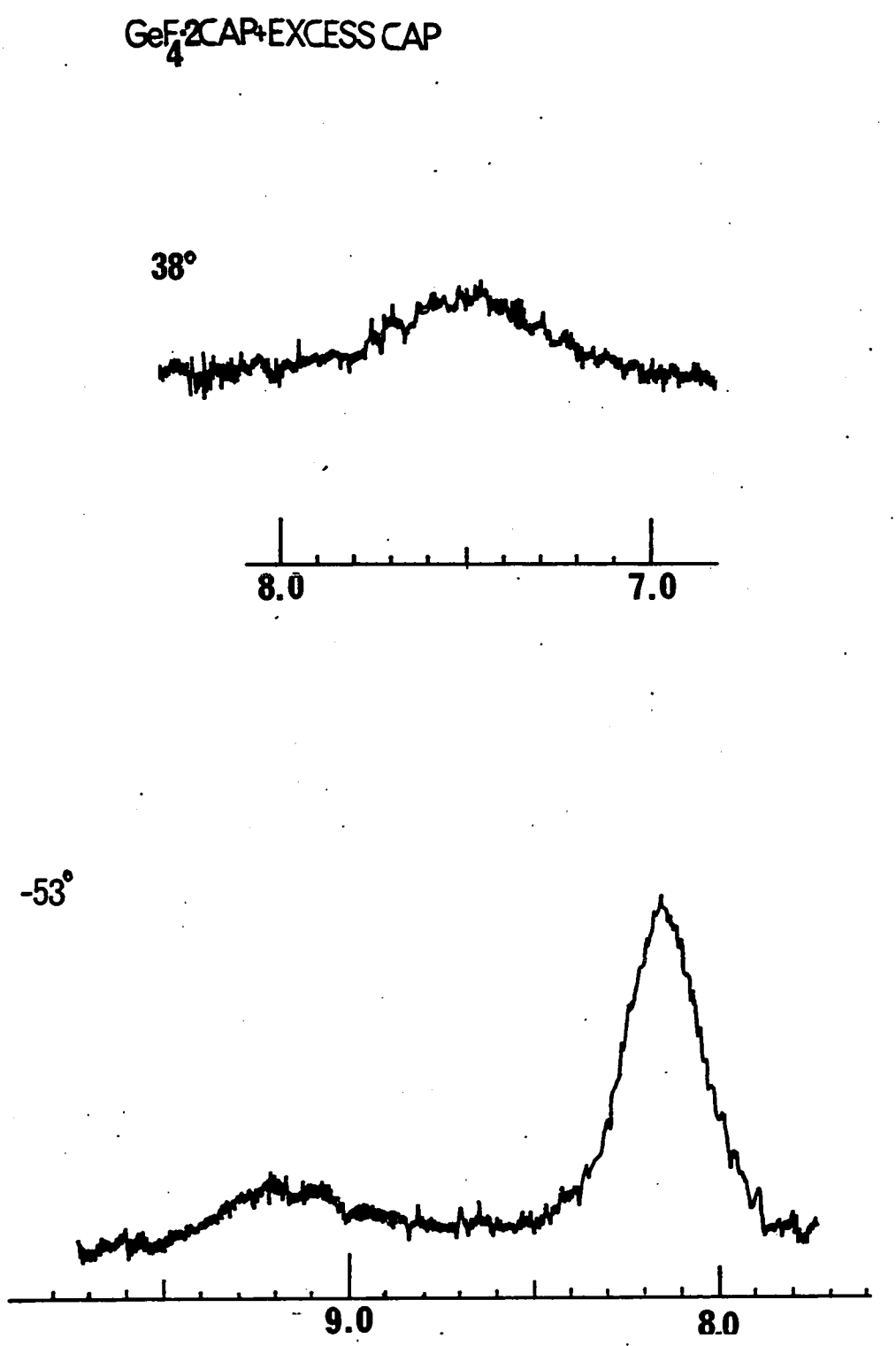

Figure 128. ^1H NUCLEAR MAGNETIC RESONANCE SPECTRUM IN $ClCH_2CN$

$SnF_4$2CAP + EXCESS CAP

38°

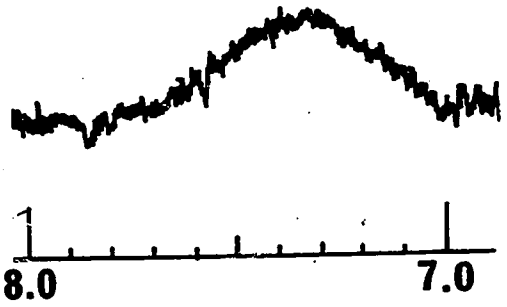

-53°

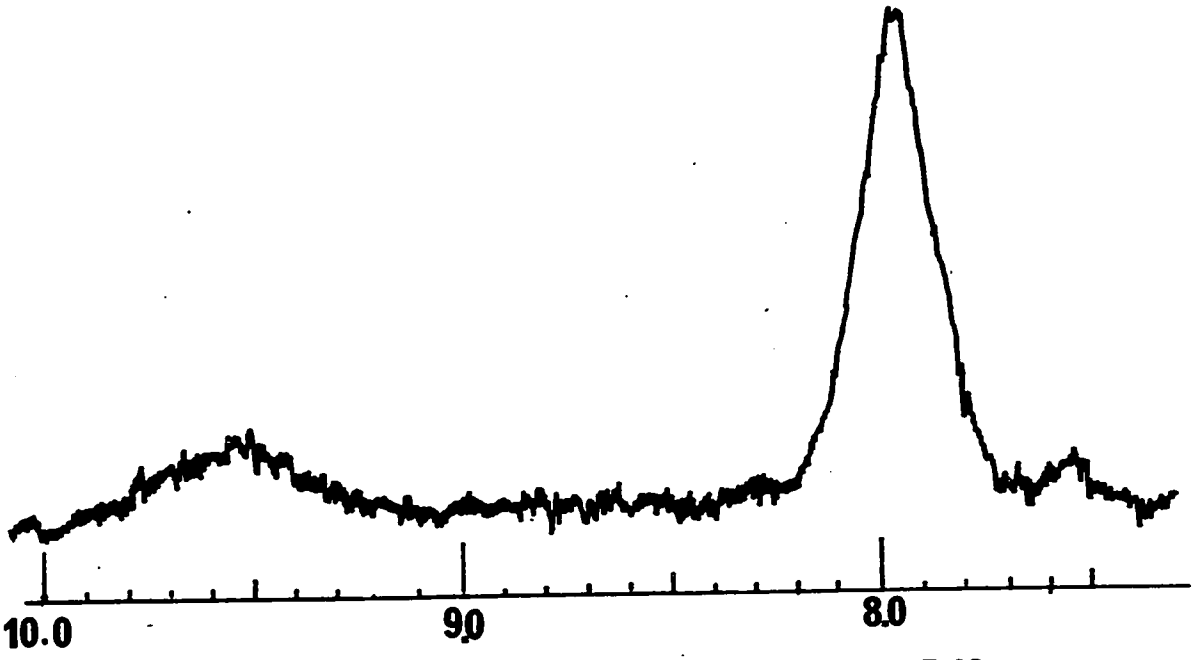

CHEMICAL SHIFTS IN P.P.M. RELATIVE TO INTERNAL TMS